Measurement and characterisation of microvesicles and nanovesicles in pregnancy and pre-eclampsia

Rebecca Dragovic

Mansfield College

Michaelmas Term 2011

Abstract

Measurement and characterisation of microvesicles and nanovesicles in pregnancy and pre-eclampsia

Rebecca Dragovic, Mansfield College

A thesis submitted in partial fulfilment of the requirements for the degree of Doctor of Philosophy at the University of Oxford, Michaelmas Term 2011

Excessive release of syncytiotrophoblast vesicles (STBM) from the placenta into the maternal circulation may cause the inflammatory response, endothelial dysfunction and activation of the coagulation system characteristic of pre-eclampsia (PE). Consequently, other cell types including platelets, leukocytes, red blood cells (RBC) and endothelium may be activated to release cellular vesicles which exacerbate the disease. This thesis aimed to develop methodology for enumerating and phenotyping STBM and the other vesicle types to determine whether they could be used as biomarkers for PE.

In vitro derived STBM and vesicles from the other cells of the vascular compartment were examined to select a suitable panel of antibodies to analyse these same vesicle types in plasma samples from non-pregnant (NonP), normal pregnant (NormP) and PE women.

Our flow cytometer was shown to detect microvesicles ≥290nm, hence smaller nanovesicles and exosomes could not be detected by this method. Therefore, a novel technique for analysing both microvesicles and nanovesicles, Nanoparticle Tracking Analysis (NTA), was explored and was found to be able to detect vesicles as small as 70nm.

The origins of the vesicles that change in pregnancy are not yet known. Flow cytometry and NTA were used in parallel to determine the size, number and phenotype of STBM and other cellular vesicles in NonP, NormP and PE women. Flow cytometry showed that majority of vesicles were derived from platelets, followed by RBC vesicles, leukocyte vesicles and STBM. NTA showed that the total number of vesicles in plasma was significantly elevated in NormP and late-onset PE women compared to NonP controls, and the vesicles were smaller in size. Similarly, flow cytometry showed differences in the composition of vesicles between pregnant and non-pregnant women, demonstrating that pregnancy affects vesicle release. However, no differences were found between NormP and PE women. This was probably due to the majority of samples studied being from late rather than early-onset PE. Thus, although this is the most comprehensive analysis of circulating vesicles in pregnancy to date, their use as biomarkers for PE remains an open question.

Acknowledgements

I must first offer my sincere thanks to my supervisor, Prof. Ian Sargent, for allowing me the opportunity to undertake a D.Phil at the University of Oxford. This project has been challenging and at times a little frustrating, but ultimately it has been a very enjoyable and rewarding experience. Many thanks for your support, guidance and enthusiasm. You are truly a great mentor.

I would also like to thank Prof. Chris Redman for additional support and guidance throughout this D.Phil project. It has been a privilege to have access to your expertise in this area and I thank you for all the help you have given me. Thanks also to Prof. Stephen Kennedy for allowing me to undertake this D.Phil in the department whilst also carrying out my departmental flow cytometer operator duties.

I am hugely grateful to Dr. Jen Southcombe for absolutely everything. Thank you for your wealth of flow cytometry knowledge, your support, both practical and emotional, and for all your helpful advice. Thanks also for sharing the necessary “closed door, blind down” situations and for all the much needed coffee breaks. You are a great colleague and an even better friend.

To all the past and present members of the Sargent/Redman group, a big thank you. A special mention should be made to Dr. Dionne Tannetta and Dr. Gavin Collett for all their help in the laboratory. Thank you also to Dr. Chris Gardiner for carrying out the experiments using the NanoSight NS500 instrument. Thank you to the team of research midwives who recruited all the patients to the Oxford Pregnancy Biobank, especially Carol Simms whose hard work is much appreciated. Also, thank you to the Biobank Ladies for processing the samples, in particular to Jacqui Marks. To my two flow cytometry pals Dr. Ingrid Granne and Dr. Katie May. I guess you’re both not too bad, considering you’re medics! Thanks for being such great colleagues and for all your help in the laboratory. Thanks to Dr. Leanne Hodson from OCDEM for carrying out lipoprotein and triglyceride measurements on some of the samples and thanks to Dr. Patrick Hole for all your valuable help and expertise with the NanoSight instrument.

To my family: Mum, Dad, Matt and Shanna, despite the fact that you are thousands of miles away I could not have done this without your constant encouragement, support, belief and love. Thank you.

There are many friends that have helped me throughout this project, but in particular I must thank Elizabeth and Ross, who have always been there for me, to make me laugh and provide support when I needed it. I am incredibly fortunate to have friends like you.

Finally, I must thank my very supportive partner Rob. Thank you for everything, especially in these last few months. I can't begin to tell you how much I appreciate all the encouragement you have given me. I honestly could not have done this without you.

Contents

Abbreviations

4-MUP	4-Methylumbelliferyl Phosphate
A-23187	Calcium Ionophore A-23187
AFM	Atomic Force Microscopy
ANOVA	Analysis of Variance
APC	Allophycocyanin
APC-Cy7	Allophycocyanin-cyanine 7
APOB	Apolipoprotein B
Bio-Maleimide	BODIPY FL N-(2aminoethyl) maleimide
BSA	Bovine Serum Albumin
CD	Cluster of Differentiation
CPT	Camptothecin
DLS	Dynamic Light Scattering
DMSO	Dimethyl sulfoxide
EDTA	Ethylenediaminetetraacetic Acid
ELISA	Enzyme-Linked Immunosorbant Assay
eSTBM	explants Syncytiotrophoblast Vesicles
FcR	Fragment-crystallisable receptor
FBS	Fetal Bovine Serum
FCS	Forward Scatter
FITC	Fluorescein isothiocyanate
FMO	Fluorescence Minus One
HELLP	Haemolytic anaemia Elevated Liver Enzymes Low Platelets
HDL	High Density Lipoprotein
HLA	Human Leukocyte Antigen
HUVEC	Human Umbilical Vein Endothelial Cell
IgG	Immunoglobulin G
IL	Interleukin
IL-1α	Interleukin-1α
IUGR	Intrauterine Growth Restriction
LDL	Low Density Lipoprotein
LPS	Lipopolysaccharide
MHC	Major Histocompatibility Complex
miRNA	Micro Ribonucleic Acid
mSTBM	mechanical Syncytiotrophoblast Vesicles
NDOG2	Anti-placental alkaline phosphatase antibody
NonP	Non-pregnant
NormP	Normal pregnant
NTA	Nanoparticle Tracking Analysis
PBMC	Peripheral Blood Mononuclear Cell
PBS	Phosphate Buffered Saline
PE	Phycoerythrin
PE	Pre-eclampsia
PECy5	Phycoerythrin Cyanine 5
PECy7	Phycoerythrin Cyanine 7
PFP	Platelet Free Plasma
PLAP	Placental Alkaline Phosphatase
PLGF	Placental Growth Factor
PMA	Phorbol Myristate Acetate

PRP	Platelet Rich Plasma
pSTBM	perfused Syncytiotrophoblast Vesicles
Qdot	Quantum Dot
RBC	Red Blood Cell
RPE	R-Phycoerythrin
SD	Standard Deviation
SE	Standard Error
sFlt-1	Fms-like tyrosine kinase-1
SSC	Side Scatter
SN	Supernatant
STBM	Syncytiotrophoblast Vesicles
STS	Staurosporine
TG	Triglyceride
TNFα	Tumour Necrosis Factor-α
TRAP	Thrombin Receptor Activating Peptide
VEGF	Vascular Endothelial Growth Factor
VLDL	Very Low Density Lipoprotein

Chapter 1

Introduction

1.1 Pre-eclampsia

Pre-eclampsia (PE) is a multi-system disorder of pregnancy that can be life threatening to both mother and fetus. The condition is relatively common and affects about 3.0% of pregnancies. PE may develop at anytime during pregnancy after 20 weeks gestation and the maternal syndrome is characterised by the onset of clinical symptoms such as hypertension and proteinuria. The maternal complications of PE include: renal failure, pulmonary oedema, impaired liver function, cerebral oedema and stroke, HELLP syndrome (haemolysis, elevated liver enzymes and low platelets) and disseminated intravascular coagulation. The condition can be divided into two distinct entities: early-onset PE which develops at ≤34 weeks gestation and late-onset PE which develops ≥34 weeks The gestational age chosen to distinguish the two is arbitrary (Eastabrook *et al.*, 2011, Raymond and Peterson 2011) and both are related to poor pregnancy outcomes, but evidence suggests that they are different with regard to biochemical markers, heritability and clinical features (von Dadelszen *et al.*, 2003, Vatten and Skjaerven 2004, Raymond and Peterson 2011). Early on-set PE is commonly associated with incomplete placentation and the fetus is at increased risk of intrauterine growth restriction (IUGR), whereas late-onset PE is more associated with adequate placentation and normal fetal growth (Eastabrook *et al.*, 2011, Raymond and Peterson 2011). There is no predictive test available, nor can PE be prevented and the condition will only resolve after delivery of the baby and placenta. The fetal complications of PE that arise are most commonly associated with inducing pre-term delivery. Very severe early on-set PE can result in fetal intrauterine or perinatal death.

Risk factors for PE include: a personal or family history of the condition, nulliparity, multiple pregnancy, increased maternal age, obesity, new paternity and a history of certain

medical conditions such as hypertension, diabetes, kidney disease or antiphospholipid syndrome (Duckitt and Harrington 2005).

1.2 Placental Pre-eclampsia

The general consensus is that PE originates in the placenta (Redman 1991). PE is typically referred to as a "two stage disease" (Figure 1). The first (pre-clinical) stage results from poor placentation in early pregnancy (8-18 weeks). In normal pregnancy, extravillious cytotrophoblast cells invade the decidua to mediate spiral artery remodelling which increases maternal blood flow to the placenta (Pijnenborg *et al*., 1983, Moffett-King 2002) (Red-Horse *et al.,* 2004). In PE, cytotrophoblast invasion is restricted and remodelling of the spiral arteries is impaired, resulting in inadequate uteroplacental circulation causing areas of the placenta to become hypoxic. Insufficient spiral artery remodelling may not only reduce the volume of blood flow, but retention of their smooth muscle may also cause periodic vasoconstriction of the spiral arteries resulting in intermittent blood flow, triggering placental oxidative stress through ischemia/reperfusion injury (Hung and Burton 2006, Burton *et al.,* 2009, Redman and Sargent 2009).

The reduced blood flow and generation of oxidative stress has consequences for both the mother and fetus (second stage). The fetus may not receive adequate oxygen and nutrients which can result in IUGR. The mother is affected by various pro-inflammatory and anti-angiogenic factors released from the oxidatively stressed placenta into the maternal circulation. These cause endothelial dysfunction (Roberts *et al.,* 1989) and systemic inflammation (Redman and Sargent 2003) both of which contribute to the maternal clinical symptoms and signs of PE.

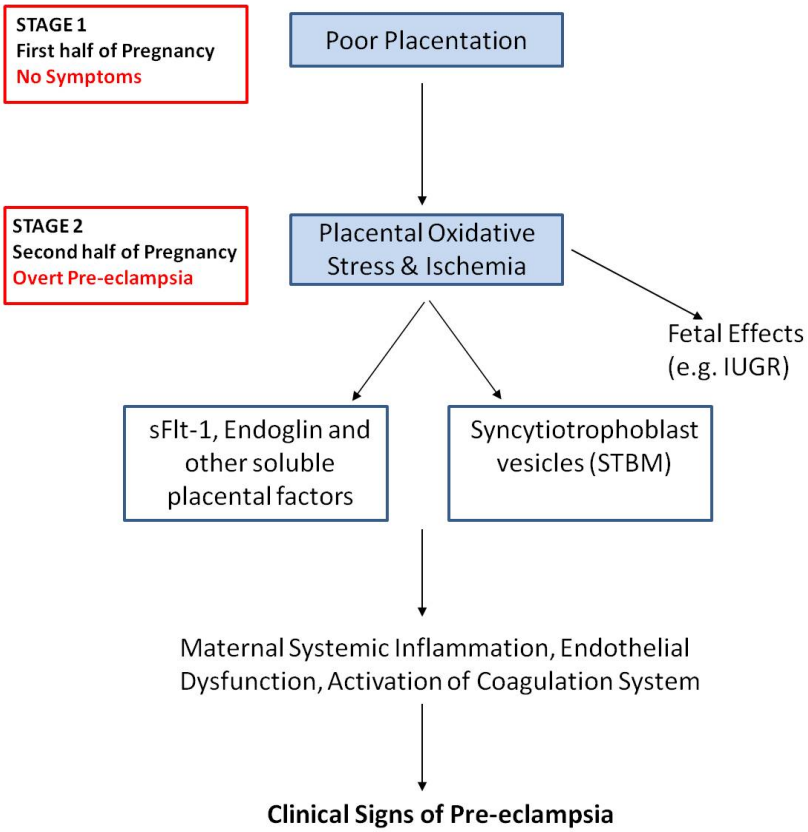

Figure 1. The two-stage model of pre-eclampsia. Stage 1 of the condition develops in the first half of pregnancy and is asymptomatic. Impaired cytotrophoblast invasion of the decidua results in poor placentation leading to placental oxidative stress and ischemia. In stage 2 of the disorder the oxidatively stressed placenta can affect both the mother and fetus. Placental soluble factors (e.g. sFlt-1 and Endoglin) and syncytiotrophoblast vesicles (STBM) are released and lead to maternal systemic inflammation, endothelial dysfunction and activation of the coagulation system. In turn this leads to the clinical signs of pre-eclampsia. Adapted and modified from (Redman and Sargent 2009).

A mild systemic inflammatory response is also apparent in the third trimester of normal pregnancy (Sacks *et al.*, 1998, Redman *et al.*, 1999). As pregnancy advances, systemic oxidative stress increases (Gratacos *et al.*, 1998, Morris *et al.*, 1998) and there is evidence showing activation of granulocytes (Rebelo *et al.*, 1995, Sacks *et al.*, 1998) and monocytes (Sacks *et al.*, 1998). In PE the inflammatory response is more exaggerated and this is thought to be due to a plethora of placental derived factors.

1.3 The Role of Placental Derived Factors in Pre-eclampsia

It is unlikely that the maternal syndrome of PE is caused by one sole factor. The syncytiotrophoblast layer of the placenta is in direct contact with the maternal circulation and has been shown to secrete many different factors, including corticotrophin releasing hormone (CRH) (Perkins *et al.,* 1995), activin-A (Muttukrishna *et al.*, 1997), inhibin-A (Muttukrishna *et al.,* 1997), leptin (Mise *et al.,* 1998), placental growth factor (PLGF) (Torry *et al.,* 1998, Thadhani *et al.,* 2004) and free heme (Olsson *et al.,* 2010), all of which are altered in PE and potentially contribute to maternal systemic inflammation and endothelial dysfunction. Of major interest is the anti-angiogenic factor Fms-like tyrosine kinase-1 (sFlt-1). sFlt-1 is the soluble receptor for vascular endothelial growth factor (VEGF) -1 and PLGF and its release is stimulated by hypoxia (Nevo *et al.,* 2006). In PE sFlt-1 levels are raised and it is thought to bind to and inactivate VEGF and PLGF, both of which are essential factors for the maintenance of the endothelium (Maynard *et al.,* 2003, Levine *et al.,* 2004). Hence, deprivation of VEGF and PLGF may induce systemic endothelial dysfunction (Bdolah *et al.,* 2004, Karumanchi and Bdolah 2004). Another anti-angiogenic factor also shown to be elevated in PE is soluble endoglin, the co-receptor for transforming growth factor β (TGFβ) (Levine *et al.,* 2006, Venkatesha *et al.,* 2006). Together these placental factors may play a role in the pathogenesis of PE. However it is not just soluble molecules that are released from the placenta and these factors alone cannot account for the diversity of the maternal features. Other factors must be involved that contribute to the systemic inflammatory response and disseminated intravascular coagulation.

There is a range of debris shed from the placenta, including deported trophoblast (20 - 100μm). Autopsies carried out on pregnant women who died for various reasons showed

deported trophoblast trapped within the lungs and this was most commonly observed in women with PE or eclampsia (Attwood and Park 1961). Syncytiotrophoblast vesicles (abbreviated in this thesis to STBM) are also shed from the placenta (Jones and Fox 1980, Jones and Fox 1991, Redman *et al.*, 2012) and are thought to be a product of normal turnover and renewal of the syncytial surface of the placenta by apoptosis (Huppertz *et al.*, 1998). Unlike deported trophoblast which are filtered out in the lungs, STBM will reach the maternal peripheral circulation. STBM have previously been shown to be elevated in the maternal circulation in PE (Knight *et al.*, 1998) and these are a major focus of this thesis.

1.4 Syncytiotrophoblast Vesicles (STBM) in Normal Pregnancy and Pre-eclampsia

STBM can be detected in plasma from normal pregnant women in increasing amounts from late in the first trimester onwards and levels are significantly increased in PE (Knight *et al.*, 1998, Germain *et al.*, 2007). However, vesicle shedding is not unique to the syncytiotrophoblast. Many if not all cells shed or secrete vesicles from their surface.

1.4.1 Formation and Composition of Cellular Derived Vesicles

There are three types of vesicles: microvesicles, exosomes and apoptotic bodies, all which differ with respect to size, protein content and mode of production. Microvesicles range in size from 100nm - 1μm and are released in response to cell activation or apoptosis. Microvesicles are generated by direct budding or shedding of the plasma membrane (Figure 2). They are also sometimes referred to as microparticles or ectosomes. Microvesicles are released in response to stimuli which lead to an increase in intracellular

calcium levels, causing remodelling of the plasma membrane and the release of vesicles (Hugel *et al.,* 2005). Exosomes are smaller, their size is 30 – 100nm. These vesicles are generated by invagination within the cell to form a structure called the endosome. Reverse budding of the endosome membrane results in multivesicular bodies which fuse with the plasma membrane of the cell and are released by exocytosis (Figure 2). Exosome release is dependent on the cell type and can be released constitutively by cells or in response to cellular activation (Théry *et al.,* 2009). Apoptotic bodies are released from blebbing cells undergoing apoptosis (Figure 2). They can be much larger, up to 4µm in diameter but may overlap in size with apoptotic microvesicles (Hristov *et al.,* 2004). Shedding of large apoptotic and necrotic trophoblast debris has been demonstrated *in vitro* (Chen *et al.,* 2009a, Chen *et al.,* 2009b, Chen *et al.,* 2010a, Chen *et al.,* 2010b).

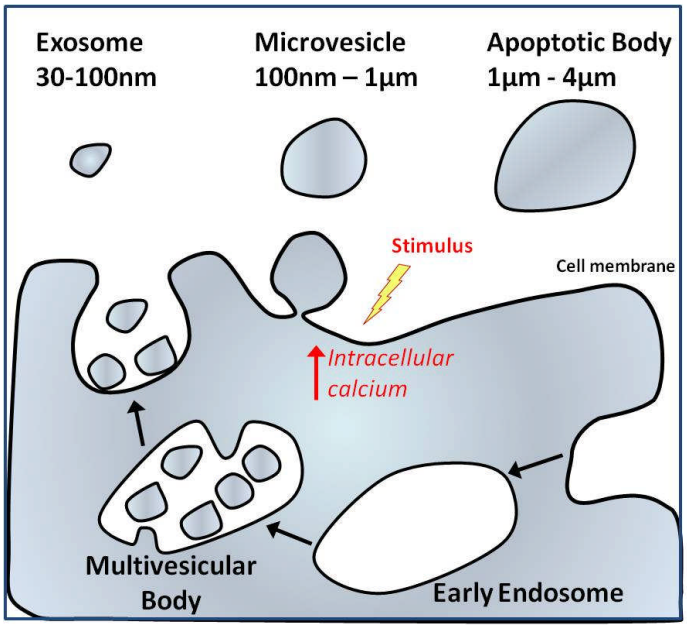

Figure 2. Three vesicle subtypes: Exosomes, Microvesicles and Apoptotic bodies. Exosomes (30-100nm) are generated from reverse budding of the endosome membrane, resulting in a multivesicular body which fuses with the plasma membrane of the cell and exosomes are released by exocytosis. Microvesicles (100nm - 1µm) are produced by direct budding or shedding of the plasma membrane. They are released in response to stimuli causing an increase in intracellular calcium levels and remodelling of the plasma cell membrane. Apoptotic bodies (1 - 4µm) are released from cells undergoing apoptosis. Figure adapted and modified from (Cocucci *et al.,* 2009).

Microvesicles and exosomes are rich in lipid rafts and generally express phosphatidylserine on their surface (Théry *et al.,* 2009). They have been described as "miniature versions" of their parent cell as the orientation of the membrane is the same and they also retain molecules expressed on the cell of origin (Théry *et al.,* 2009). For example, microvesicles released from platelets strongly express the integrin β3 subunit (CD61) (Abid Hussein *et al.,* 2003), and exosomes secreted from B-Cells or dendritic cells are enriched with Major Histocompatibility Complex (MHC) Class I and Class II molecules (Raposo *et al.,* 1996, Zitvogel *et al.,* 1998). Microvesicle phenotype may also be influenced by the stimuli used to trigger their release (Jimenez *et al.,* 2003). Moreover, both vesicle subtypes contain mRNA, micro RNAs (miRNAs) and DNA (Valadi *et al.,* 2007, Pisetsky *et al.,* 2011). Exosomes contain various cytoskeletal proteins, but do not contain mitochondrial, golgi or endoplasmic reticulum proteins, indicative that their mode of formation is different to microvesicles (Smalheiser 2007). Exosome formation has been shown to involve protein sorting, for example during reticulocyte maturation the transferrin receptors and GPI-anchored proteins CD55 and CD59 are incorporated into exosomes (Denzer *et al.,* 2000). Although there is not one particular cellular protein that clearly distinguishes a microvesicle from an exosome, there are certain proteins that are enriched in exosomes. These include: MHC Class I and Class II in exosomes secreted from many different antigen presenting cells, heat shock proteins HSP70 and HSP90, the cytoskeletal proteins actin and tubulin, and the tetraspanin protein family CD9, CD37, CD53, CD63, CD81 and CD82 (reviewed in Denzer *et al.,* 2000, Thery *et al.,* 2002, Théry *et al.,* 2009). In this thesis the term "vesicles" will refer to both microvesicles and exosomes unless otherwise stated. The composition of STBM in terms of microvesicles and exosomes is not yet known.

1.4.2 Function and Role of Cellular Derived Vesicles

Circulating vesicles may play a role in normal physiological processes including, stress responses, inflammation and tissue regeneration (Simak and Gelderman 2006). Vesicles are involved in cell to cell communication and cell signalling, possibly by transferring functional molecules to the target cell. Upon release vesicles will deliver their cargo to their target cell by one of three ways: 1) binding via a receptor, 2) direct fusion with the target cell membrane, 3) internalisation by endocytosis (Cocucci *et al.,* 2009) (Figure 3). Interaction of vesicles with their target cell is a highly regulated process as vesicles will only interact with certain types of recipient cells. For example, platelet vesicles have been shown to interact with monocytes, but not neutrophils (Losche *et al.*, 2004). Vesicles have been shown to function in a variety of different ways including: 1) transferring of receptors between cells, 2) delivering mRNAs and miRNAs to recipient cells, 3) transmission of infectious particles including HIV and prions and 4) transferring organelles (e.g. mitochondria between cells) (all reviewed in Ratajczak *et al.,* 2006). Furthermore, vesicle interaction has been shown to induce functional and phenotypic changes in the target cell; with vesicles released from neutrophils modulating maturation of monocyte-derived dendritic cells (Eken *et al.,* 2008) and tumour cell derived vesicles interacting with monocytes to alter their phenotype and biological function (Baj-Krzyworzeka *et al.,* 2006).

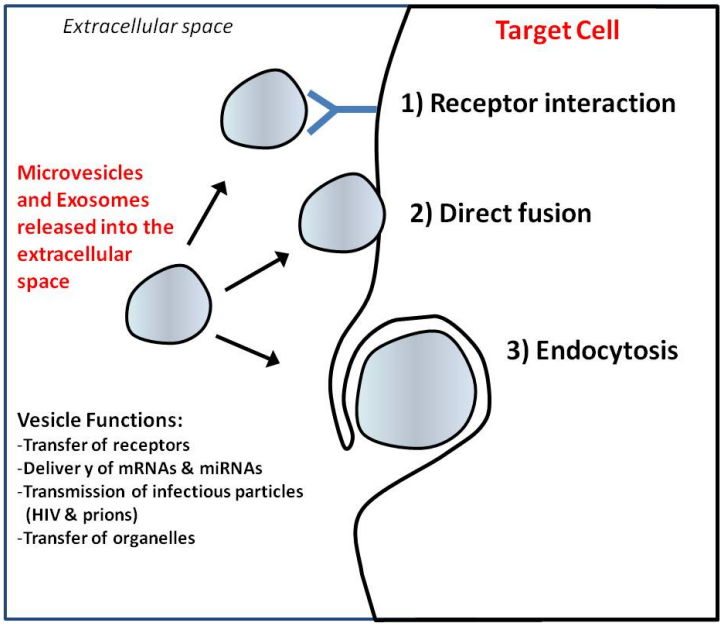

Figure 3. Interactions of vesicles with their target cell. Vesicles are released into the extracellular space and can interact with their target cell via three different ways: 1) bind via a receptor, 2) direct fusion, 3) internalisation via endocytosis. Vesicle interaction with its target cell is a highly regulated process and vesicles have been shown to function in a variety of different ways. Figure adapted and modified from (Cocucci *et al.*, 2009).

Vesicles have been implicated in a large number of vascular pathologies where they have been found to be elevated, including cardiovascular diseases (VanWijk *et al.*, 2003), rheumatoid arthritis (Distler and Distler 2010), haematological diseases (Ardoin *et al.*, 2007), inflammatory diseases (Ardoin *et al.*, 2007) and cancer (Mostefai *et al.*, 2008). Cardiovascular diseases such as atherosclerosis and acute coronary syndrome are typically associated with endothelial activation, vascular inflammation and coagulation, and in these conditions endothelial, leukocyte and platelet vesicles are elevated (VanWijk *et al.*, 2003, Enjeti *et al.*, 2008b). In rheumatoid arthritis there is evidence showing that elevated leukocyte and platelet vesicles are related to the clinical features of the condition including increased inflammation and tissue damage (Distler and Distler 2010). Measurement of circulating vesicles in plasma raises the possibility of their use as potential prognostic and diagnostic biomarkers for a range of clinical diseases, including PE.

1.4.3 Syncytiotrophoblast Vesicles (STBM)

Endothelial dysfunction is central to the pathophysiology of PE and STBM have been shown to interact with the endothelium causing dysfunction to cultured human umbilical vein endothelial cells (HUVEC) (Smarason *et al.,* 1993, Gupta *et al.,* 2005b) and ex vivo preparations of subcutaneous arteries (Cockell *et al.,* 1997). STBM carry potent anti-endothelial activity suppressing HUVEC proliferation and disrupting the cell monolayer to give a honeycomb like pattern (Smarason *et al.,* 1993). Endothelial damage is one component of the systemic inflammatory response in PE. STBM also interact with immune cells which are the major contributors to systemic maternal inflammation. This was first shown by co-culture of STBM with HUVECs *in vitro* and the subsequent activation of neutrophils (von Dadelszen *et al.,* 1999). This observation was later followed up by showing that STBM can directly activate neutrophils to stimulate superoxide production (Aly *et al.,* 2004).

To study the functional properties of STBM *in vitro* it is possible to prepare vesicles in a variety of ways. STBM can be produced by; 1) mechanical dissection of the placenta (mSTBM), 2) shedding from placental explants in culture (eSTBM) and 3) perfusion of the maternal side of a placenta lobe (pSTBM). All of the early studies used mSTBM (Smarason *et al.,* 1993, von Dadelszen *et al.,* 1999, Aly *et al.,* 2004), which may not be as representative of the *in vivo* material as eSTBM or pSTBM (Gupta *et al.,* 2005b).

Flow cytometry analysis has shown that monocytes will bind STBM *in vivo* (Germain *et al.,* 2007). This observation has recently been extended by a study in our laboratory showing that pSTBM *in vitro* will bind both monocytes and B cells (Southcombe *et al.,* 2011). Furthermore pSTBM, but not mSTBM have been shown to stimulate pro-

inflammatory cytokine (tumour necrosis factor-α (TNF-α), interleukin (IL)-18, IL-12 and interferon γ (IFNγ) release from cultured peripheral blood mononuclear cells (PMBC) (Gupta *et al.,* 2005a, Germain *et al.,* 2007). Three separate studies have shown that it is specifically the monocytes that are stimulated to produce pro-inflammatory cytokines (TNF-α, IL-1a, IL-1b, IL-6 and IL-8) in response to pSTBM (Morelli 2006, Messerli *et al.,* 2010, Southcombe *et al.,* 2011). More recently, an up-regulation of PBMC secretion of many cytokines and chemokines was observed in response to eSTBM from pre-eclamptic placentas opposed to eSTBM from normal term placentas (Holder *et al.*, 2012).

The first study to measure STBM *in vivo* from plasma was carried out in our laboratory using an in house ELISA with an anti-placental alkaline phosphatase antibody (NDOG2) used to capture the STBM. STBM were detected in the third trimester of normal pregnancy and in significantly higher concentrations in PE (Knight *et al.,* 1998). In a subsequent study, circulating STBM were detected as early as the late first trimester of normal pregnancy and were shown to increase throughout normal pregnancy gestation (Germain *et al.,* 2007). Moreover, the significant elevation of STBM in PE compared to normal pregnancy seen in the original study (Knight *et al.,* 1998) was confirmed (Germain *et al.,* 2007). In a further study the differences in STBM levels between normal pregnancy and PE was found to be greater in early-onset PE (≤ 34 weeks gestation) compared to late-onset PE (≥34 weeks gestation) (Goswami *et al.,* 2006). However there was no difference in STBM levels in women with normotensive IUGR compared to controls (Goswami *et al.,* 2006). STBM levels have also been examined during labour (Reddy *et al.,* 2008). Significantly more STBM were detected in the maternal circulation in PE women during labour compared to pre-labour, however no difference was detected in normal pregnant women (Reddy *et al.,* 2008). The enhanced STBM shedding in labour may be a cause of

post-partum worsening of PE. By measuring changes in STBM levels in the maternal circulation prior to the onset of the disorder, STBM have the potential to be used as a biomarker for PE.

1.5 Measurement of Cellular Derived Vesicles

Cellular vesicles can be isolated and measured in cell-culture supernatants, blood, urine and saliva (Théry *et al.*, 2006). To date, much of the research investigating *in vivo* derived cellular vesicles has been carried out using plasma. Many different detection methods are available, all of which have advantages and disadvantages associated with them. There are three main methodologies: 1) flow cytometry, 2) capture based ELISA and, 3) transmission electron microscopy. The advantages and disadvantages of these techniques are outlined in Table 1.

Method of Detection	Advantage(s)	Disadvantage(s)
Flow Cytometry	Quantitative Biological samples can be analysed directly (although sometimes preliminary concentration of the sample may be required) Simultaneous analysis of multiple antigens	Expensive Experienced operator required Size limitation (sensitivity of standard flow cytometers is ~500nm and digital flow cytometers ~300nm)
Capture Based ELISA	Quantitative	Detects only a single antigen at a time Detects soluble antigens No information on cellular vesicle size
Transmission Electron Microscopy	Measure all vesicle sizes Immunolabelling of vesicles Analyse internal structure	Expensive Experienced operator required Vesicle undersizing (due to fixation and shrinkage) Not quantitative

Table 1. The three main methodologies used to analyse vesicles. The advantages and disadvantages associated with all methods. Table adapted and modified from (Harrison and Gardiner 2010).

The most widely used method to investigate vesicles is flow cytometry. This technique is typically used to analyse cells, but when analysing much smaller sized vesicles it is

associated with a number of technical limitations and standardisation issues (Gelderman and Simak 2008). One of the major limiting factors is resolving vesicles from the instrument electronic noise and this can be highly variable between instruments. Analogue flow cytometers can only resolve vesicles down to ~500nm whereas newer digital instruments are reported to analyse vesicles of ≥300nm (Perez-Pujol *et al.*, 2007), but both are probably only analysing a fraction of the total vesicles. Most studies use the phosphatidylserine probe Annexin V to define vesicles, however it is now evident that not all vesicles expose phosphatidylserine on their surface (Shet *et al.*, 2003, Perez-Pujol *et al.*, 2007). Immunophenotyping of vesicles is used to identify their origin, using either direct or indirect conjugated antibodies. Most studies investigating *in vivo* derived cellular vesicles from plasma phenotype vesicles using single- or double-antibody labelling.

1.6 Hypothesis for the Pathogenesis of Pre-eclampsia

It is hypothesised that the release of STBM into the maternal circulation may cause the inflammatory response, endothelial dysfunction and activation of the coagulation system characteristic of PE. This in turn leads to the activation and release of cellular vesicles from other cell types, including the endothelium, platelets, red blood cells (RBC) and leukocytes to further exacerbate the disease (Figure 4). By measuring STBM (the cause) in parallel with other circulating derived vesicles (the consequence) the prediction and monitoring of the condition may be improved. STBM thus may have the potential to be used as predictive biomarkers of the maternal disorder, whereas the other circulating vesicles may be used diagnostically when the disorder is underway. The populations of vesicles present in the maternal circulation are incompletely characterised. There is an absolute requirement for improved approaches to address this issue.

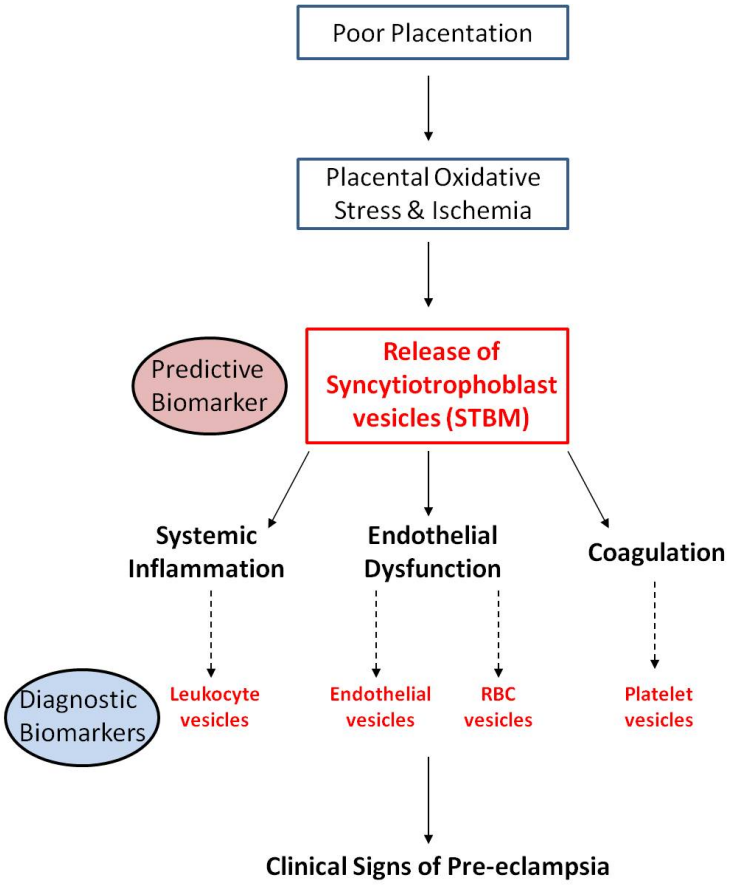

Figure 4. Hypothesis for the pathogenesis of pre-eclampsia. Poor placentation results in placental oxidative stress and ischemia. This triggers the release of STBM into the maternal circulation leading to systemic inflammation, endothelial dysfunction and activation of the coagulation system, which in turn results in the release of vesicles from leukocytes, endothelium, RBC and platelets. STBM has potential to be used as a predictive marker, whereas the other cellular derived vesicles could be used as diagnostic markers. Measuring these vesicles together may improve the prediction and monitoring of the condition.

1.7 Aims and Hypotheses of this Thesis

In the introduction to this thesis, previous work in our laboratory has been described showing that STBM are shed from the placenta during pregnancy and using an ELISA these STBM were shown to be significantly elevated in PE compared to normal pregnancy (Knight *et al.*, 1998, Germain *et al.*, 2007). Furthermore, STBM have been shown to interact with the maternal immune and endothelial cells. The hypothesis for the pathogenesis of PE is presented above in Section 1.6. The analyses of vesicles released from the placenta and from other cells of the vascular compartment have been limited by

the detection methods available and by an inability to address issues such as differences in vesicle size and composition. For example, the levels of STBM measured using an ELISA measures the entire population of vesicles (microvesicles, nanovesicles and vesicles >1μm) and cannot discriminate vesicles of different sizes or the level of surface PLAP. New technological advances in instrumentation and methodologies have become available for improved characterisation of STBM and other circulating derived vesicles.

Hypotheses

- Vesicles are present in the maternal circulation at a size too small previously to have been detected and individually characterised.
- Circulating STBM released in the maternal circulation is altered in PE compared to normal pregnancy.
- STBM triggers the release of other cellular vesicles from the vascular compartment (platelets, RBC, endothelium and leukocytes) and these too are altered in PE compared to normal pregnancy and non-pregnancy.

Aims

The overall aim of the thesis was to develop methodology for counting and phenotyping STBM and other cellular vesicles to determine whether they could be used as biomarkers for PE. Previous studies using flow cytometry to investigate cellular derived vesicles in plasma from normal pregnant and PE women have produced conflicting data. Differences in flow cytometry instrumentation and methodologies, including their isolation from plasma, antibody choice and labelling procedures, probably account for the variation between studies.

Chapter 2 describes the optimisation of our digital flow cytometer for the detection and enumeration of vesicles. Following this, panels of antibodies were tested on *in vitro* derived vesicles from a variety of cell types found in plasma to examine antibody specificity. These data were used to select a suitable panel of antibodies to analyse vesicles *in vivo* in plasma samples in non-pregnant (NonP), normal pregnant (NormP) and PE women (presented in Chapter 4).

During the course of chapter 2, it became apparent that there are large numbers of vesicles present that are undetectable by flow cytometry due to their small size. This led me to investigate an alternative method for analysis of vesicles, Nanoparticle Tracking Analysis (NTA), and its use is explored in Chapter 3.

The final aim of this thesis was to use flow cytometry and NTA to determine the number, size and phenotype of STBM and other cellular derived vesicles in normal pregnancy and PE. This is investigated in Chapter 4.

Chapter 2

Measurement of *in vitro* cellular derived vesicles using flow cytometry

2.1 Introduction

2.1.1 Flow Cytometry Instrument Set-up for Vesicle Analysis

Flow cytometry is the method most used to analyse cellular derived vesicles from culture supernatants or blood. This technique measures the size and granularity of vesicles from the laser light they scatter at 180° (forward light scatter - FSC) and 90° (side scatter – SSC) respectively. Flow cytometry is quantitative in that the number of vesicles in a sample can be determined using reference beads. Its major advantage is that vesicles can be phenotyped using fluorescent antibodies, ligands or dyes.

Typically, flow cytometers are set-up to visualise cells. However, vesicles cannot be analysed using the standard instrument settings for cells as they are too small to be detected at these settings. It is therefore necessary to adjust the voltages of the FSC and SSC detectors so that they can detect particles in the size range of cellular vesicles. This is done using size calibration beads (Aras *et al.*, 2004, Enjeti *et al.*, 2007, Perez-Pujol *et al.*, 2007, Ayers *et al.*, 2011). It is important to note that the ability of a flow cytometer to detect vesicles varies greatly between instruments. Most reports in the literature use older analogue instruments which have a sensitivity of ~500nm, whereas the newer digital cytometers can analyse vesicles down to ~300nm (Perez-Pujol *et al.*, 2007). The first aim of this chapter was therefore to investigate the sensitivity of our laboratory's digital flow cytometer to determine its ability to size, quantify and phenotype cellular vesicles.

2.1.1.1 Measuring STBM and Other Cellular Vesicles Using Flow Cytometry

One of the primary aims of this thesis was to develop a flow cytometry method to count and phenotype STBM in plasma from normal pregnant and PE women and distinguish

these from other types of vesicles that are also released into the maternal circulation including those derived from platelets, RBC, endothelial cells and leukocytes (lymphocytes, monocytes and granulocytes). To do this requires a panel of markers which can be used in parallel to distinguish the specific populations of vesicles released from the different cell types.

To determine which markers should be included in this panel, vesicles were derived from pure populations of the different cell types *in vitro*. This was done in different ways depending on the cell type. STBM were prepared simply by perfusing the maternal side of a placental lobe (pSTBM). However, other cell types need to be activated to shed vesicles *in vitro*. There are many studies using a variety of agonists to stimulate vesicles from different cell types. For example, calcium ionophore A-23187 (A-23187) is a common agonist used to generate vesicles from platelets (Abid Hussein *et al.,* 2003, Perez-Pujol *et al.,* 2007, Trummer *et al.,* 2008) and RBC (Hugel *et al.,* 1999, Salzer *et al.,* 2002, Trummer *et al.,* 2008, Nantakomol *et al.,* 2011) whereas endothelial cells can be stimulated to release vesicles using TNF-α (Combes *et al.,* 1999, Jimenez *et al.,* 2001, Sabatier *et al.,* 2002).

With respect to vesicle markers, Annexin V is the most widely used. However its binding is dependent on the availability of phosphatidylserine on the cell membrane and it is evident that not all vesicles expose sufficient phosphatidylserine on their surface to be detected by Annexin V (Shet *et al.,* 2003, Perez-Pujol *et al.,* 2007). Other markers such as Lactadherin can be used as an alternative to Annexin V as it has a higher affinity for phosphatidylserine (Shi *et al.,* 2004). Alternative markers which label cell membranes independent of phosphatidylserine are now being explored to better define the total

number of vesicles present. These include calcein acetoxymethyl ester (calcein AM) (Bernimoulin *et al.,* 2009), phalloidin (Mobarrez *et al.,* 2010), SYTO 13 (Ullal *et al.,* 2010) and Bio-Maleimide (Enjeti *et al.,* 2008a), the use of which has been investigated in this thesis. The antibodies used to phenotype the vesicles were chosen based on literature searches, whereby positive staining was evident for the cell type of interest.

In vitro derived vesicles provide the ideal platform to test and verify whether cell specific antibodies that recognise and bind surface antigens on cells can also bind the vesicles derived from them. Once suitable vesicle markers and specific antibodies are identified they could be used in a multi-colour flow cytometry assay to analyse *in vivo* derived vesicles in plasma.

2.2 Aims

1. To optimise our digital flow cytometer for the detection of STBM and other cellular derived vesicles using standard size calibration beads.
2. To generate *in vitro* derived vesicles from placenta and a variety of cell types found in the plasma pool to examine antibody specificity.
3. To define a suitable panel of antibodies that could subsequently be used to analyse STBM and other types of cellular vesicles in plasma samples in non-pregnant, normal pregnant and PE women.

2.3 Materials and Methods

2.3.1 Flow Cytometry Instrument Set-up for Vesicle Analysis

A BD LSRII Flow Cytometer (BD Biosciences, Oxford UK) equipped with a 488nm (blue) and 633nm (red) laser was used for vesicle analysis. Logarithmic voltages were used for all channels and a side scatter (SSC) threshold of 200 (arbitrary units) was set. To help obtain optimal flow cytometry settings for measuring vesicles, fluorescent 1μm Fluoresbrite YG microspheres (Polysciences Europe GmbH, Eppelheim, Germany) and NIST polystyrene YG microspheres; 200nm, 290nm, 390nm, 590nm (Thermo Scientific, Fremont, CA) were used. Beads were diluted to achieve a flow rate of ~170-250 events/sec (see Materials and Methods Section 2.3.4.1) in phosphate buffered saline (PBS) which had been filtered through a Whatman Anotop 0.1μm filter to remove particulate debris (Scientific Laboratory Supplies, Nottingham, UK). Data were analysed using BD Diva 5.03 software.

2.3.2 Preparation of *In vitro* Derived Vesicles

2.3.2.1 Placenta

Placental syncytiotrophoblast vesicles (pSTBM) were prepared in the laboratory by Dr Dionne Tannetta using a dual placental perfusion system (Southcombe *et al.*, 2011). Placentas were obtained after caesarean section from normal healthy women with informed consent. In brief, an individual placental lobule was isolated and the fetal circulation was perfused at a rate of 5 mL/min with 0.1μm filtered medium (Medium 199 with L-glutamine and Earle's salts, supplemented with 0.8% (w/v) Dextran 20, 0.5% (w/v) bovine serum albumin (BSA), 5000 U/L sodium heparin and 2.75g/L $NaHCO_3$, pH 7.4) containing a 20ml bolus of 100,000 IU streptokinase, to prevent blood clots. The whole

placenta was turned upside down and laid inside a Perspex water jacket maintained at 37°C. The maternal circulation was then perfused with oxygenated (95% O_2, 5% CO_2) medium (Medium 199 with l-glutamine and Earle's salts, supplemented with 0.5% (w/v) BSA, 5000 U/L sodium heparin and 2.75g/L $NaHCO_3$, pH 7.4) at a rate of 20 mL/min for three hours. Following this, the maternal perfusate was centrifuged in a Beckman J6-M centrifuge at 600 × g for 10 min at 4°C. The remaining supernatant was centrifuged at 150,000 × g (max) for 1 hour at 4°C in a Beckman L8-80M ultracentrifuge. The resultant pellets were pooled and washed in PBS and then resuspended in PBS to a final total protein concentration of 5mg/ml. Protein content was determined by using a Pierce BCA protein assay kit (Thermo Scientific, Illinois, USA). pSTBM were stored in aliquots at -80°C until use. These studies were approved by the Oxfordshire Research Ethics Committee C.

2.3.2.2 Platelet Vesicles

Blood was taken from three healthy volunteers after obtaining informed consent (this study approved by the Oxfordshire Research Ethics Committee C). Platelet vesicles were derived as previously described (Abid Hussein *et al.*, 2003), but with slight modification. Blood was drawn through a 20-gauge needle into 4.5ml 0.105M buffered sodium citrate vacutainers (BD Biosciences) and processed immediately. Blood was centrifuged at 200 × g for 15min at room temperature to generate platelet rich plasma (PRP). PRP was centrifuged at 1000 × g for 20min at room temperature, the supernatant was discarded and the platelet pellet was resuspended in 10ml of Tyrode buffer (136.9 mmol/L NaCl, 11.9mmol/L $NaHCO_3$, 5.6mmol/L glucose, 2.7mmol/L KCl, 1.0mmol/L $MgCl_2H_2O$ and 0.36mmol/L $NaHPO_42H_2O$ (all from Sigma-Aldrich, Dorset, UK)) pH 6.5 containing

0.25% w/v BSA and 2mmol/L Ethylenediaminetetraacetic acid (EDTA) (both from Sigma-Aldrich). The platelet suspension was then washed by centrifugation at 1000 × g for 20min at room temperature. The supernatant was discarded and the platelet pellet was resuspended in 0.5ml Tyrode buffer (pH 7.4) containing 2mmol/L $CaCl_2$ (Sigma-Aldrich). Platelets were counted by flow cytometry using Trucount Beads (BD Biosciences) following the manufacturer's instructions and adjusted to $5x10^7$/ml. Platelets were then analysed by flow cytometry (using various markers of interest described below in Materials and Methods 2.3.3) and 200µl aliquots containing $1x10^7$ platelets were used to generate vesicles. These were activated using 2.5µmol/L calcium ionophore A-23187 (A-23187) (Sigma-Aldrich) and incubated at 37°C for 20min. After 20min 5mmol/L EDTA (Sigma-Aldrich) was added to each tube to stop the activation process and the platelets were pelleted by centrifugation at 1000 × g for 20min at room temperature. The supernatant containing the platelet vesicle population was analysed using flow cytometry.

2.3.2.3 Red Blood Cell (RBC) Vesicles

Blood from healthy volunteers was taken after obtaining informed consent. RBC vesicles were derived with slight modification as previously described (Hugel *et al.,* 1999). Blood was drawn through a 20-gauge needle into a 4.5ml 0.105M buffered sodium citrate vacutainer. Blood was centrifuged at 200 × g for 15min. The PRP was discarded and the pelleted RBCs were washed twice with PBS. RBCs were resuspended in PBS containing 2mmol/L $CaCl_2$. Aliquots of RBCs (~$1x10^7$/ml) were stimulated with 5µmol/L A-23187 for 30min at 37°C. After incubation, 5mmol/L EDTA was added to each aliquot to stop the activation process and the stimulated RBCs were centrifuged for 30sec at 12,000 × g to pellet RBCs and the vesicle containing supernatant was collected and analysed by flow cytometry.

2.3.2.4 Human Umbilical Vein Endothelial Cells (HUVEC) Vesicles

HUVEC were prepared from human umbilical cords by Dr Dionne Tannetta using a previously described method (Jaffe *et al.,* 1973). Three HUVEC preparations from different cords were used. HUVEC ($2x10^6$) stored in liquid N_2 were thawed, washed free of Dimethyl sulfoxide (DMSO; Sigma Aldrich) and cultured in M199 medium supplemented with 0.03mg/ml endothelial growth supplement, 90μg/ml heparin, 50 IU/ml penicillin-streptomycin, 2mmol/L l-glutamine (all from Sigma-Aldrich) and 10% (v/v) fetal bovine serum (FBS; PAA Laboratories, GmbH, Austria), in a $175cm^2$ flask pre-coated with 1% (v/v) gelatin (Sigma-Aldrich). Upon confluency HUVEC were seeded into 6 well plates coated with 1% gelatin at a density of $1x10^5$ per well. HUVEC at passage 3, 8 and 6 were used in three experiments. Confluent HUVEC were washed in PBS and cultured in 0.1μm filtered medium ± treatment (six wells/per treatment) as follows; media alone, 5ng/ml IL-1α (Invitrogen Ltd, Paisley, UK) for 12 hours, 5μmol/L Camptothecin (CPT; Sigma-Aldrich) for 24 hours to induce apoptosis and 0.5% DMSO (vehicle control for CPT) for 24 hours. These agonists were chosen based on previous reports in the literature (Simak *et al.,* 2002, Hussein *et al.,* 2003). After incubation, culture supernatants were collected and cells were removed by centrifugation at 1000 × g for 3min. The supernatant containing the endothelial vesicles was centrifuged at 150,000 × g (max) for 1 hour at 4°C in a Beckman L8-80M ultracentrifuge. As a control, 0.1μm filtered medium was also centrifuged under the same conditions. The pellets were resuspended in PBS and analysed by flow cytometry. Any background events/contaminating particles found in the control 0.1μm filtered medium pellet were subtracted from the final flow cytometry analysis.

2.3.2.5 Monocyte and Lymphocyte Vesicles

Blood samples (30-40ml) from three healthy volunteers were obtained after informed consent. Blood was collected into sodium heparin anti-coagulant (10U/ml) and peripheral blood mononuclear cells (PBMC) were prepared by density gradient centrifugation over lymphoprep (Axis Shield Diagnostics, Cambridgeshire, UK). Cells were washed once in PBS containing 1% (v/v) FBS at 2000 × g for 10min and a second time in 1% (v/v) FBS/PBS at 1200 × g for 10min. PBMC were counted and separated into monocytes and lymphocytes using immunomagnetic anti-CD14 MicroBeads, according to the manufacturer's instructions (Miltenyi Biotec GmbH, Bergisch Gladbach, Germany). Monocyte and lymphocyte purity was determined using flow cytometry (~95%). Monocytes and lymphocytes were cultured in 0.1μm filtered RPMI medium (Sigma-Aldrich), supplemented with 10% FBS, 50 IU/ml penicillin-streptomycin and 2mmol/L l-glutamine. Monocytes ($5x10^5$) were cultured in 12 well plates alone or treated with 1μg/ml Lipopolysaccharide (LPS; Sigma-Aldrich) to induce activation for 5 hours and 10 μmol/L A-23187 was added at the end of the culture for 15 min. This stimulus was chosen based on data showing vesicle generation from the monocytic cell line THP-1 (Aharon *et al.*, 2008).

Lymphocytes ($1x10^6$) were seeded into 12 well plates and were cultured with the following treatments; untreated (4 and 20 hours), + 10ng/ml phorbol myristate acetate (PMA) (Sigma-Aldrich) to induce activation, + 2μmol/L ionomycin (Sigma-Aldrich) for 4 hours, or 1μmol/L staurosporine (STS; Sigma-Aldrich), an apoptosis-inducing reagent, for 20 hours. Treatment with PMA/ionomycin is a common method used to induce T Cell activation and has been used previously to stimulate vesicle release from Jurkat cells (Distler *et al.*, 2005). STS treatment has also been shown to stimulate vesicle release from

Jurkat cells and peripheral blood lymphocytes (Reich and Pisetsky 2009, Kornek *et al.*, 2011).

After incubation at the various time intervals, culture supernatants were removed and cells pelleted by centrifugation at 400 × g for 5min. The remaining supernatant containing the monocyte/lymphocyte vesicles was centrifuged at 150,000 × g (max) for 1 hour at 4°C in a Beckman L8-80M ultracentrifuge. As a control, 0.1μm filtered medium was also centrifuged under the same conditions. The resultant pellets were resuspended in PBS and analysed by flow cytometry.

2.3.2.6 Granulocyte Vesicles

Blood samples (20ml) were obtained from three healthy volunteers after informed consent. Blood was collected into sodium heparin anti-coagulant (10U/ml) and granulocytes were prepared by step density gradient centrifugation over Percoll (GE Healthcare Life Sciences, Little Chalfont, UK). Stock isotonic Percoll was prepared by dissolving 9 parts Percoll (density 1.13g/ml) with 1 part 1.5 Mol/L NaCl (Sigma Aldrich). Isotonic Percoll was diluted with 0.15mol/L NaCl to a density of 1.0776g/ml and 1.090g/ml. A discontinuous gradient using isotonic Percoll was prepared as follows: 1.090g/ml isotonic Percoll was overlaid with 1.0776g/ml isotonic Percoll and blood was then carefully pipetted onto the top of the gradient and the tube was centrifuged at 350 × g for 20min. After centrifugation the granulocytes were removed and washed once in PBS containing 1% (v/v) FBS at 2000 × g for 10min and a second time in 1% (v/v) FBS/PBS at 1200 × g for 10min. Granulocytes were counted and further enriched using immunomagnetic anti-CD15 MicroBeads, according to the manufacturer's instructions (Miltenyi Biotec). Granulocyte purity was determined using flow cytometry. Granulocytes were cultured in

0.1μm filtered RPMI medium (Sigma-Aldrich), supplemented with 10% FBS, 50 IU/ml penicillin-streptomycin and 2mmol/L l-glutamine. Granulocytes ($1x10^6$) were cultured in 12 well plates for 18 hours. Granulocytes cultured *in vitro* will undergo apoptosis after 18 hours in culture (Pletz *et al.*, 2004).

After incubation, culture supernatants were removed and cells pelleted by centrifugation at 400 × g for 5min. The remaining supernatant containing the granulocyte vesicles was centrifuged at 150,000 × g (max) for 1 hour at 4°C in a Beckman L8-80M ultracentrifuge. As a control, 0.1μm filtered medium was also centrifuged under the same conditions. The resultant pellets were resuspended in PBS and analysed by flow cytometry.

2.3.3 Flow Cytometry of Platelets, RBCs, HUVEC, Monocytes, Lymphocytes and Granulocytes

2.3.3.1 Fluorescent Cell Membrane Dye and Monoclonal Antibodies

Table 2 shows the fluorescent cell membrane dye, antibodies and matching isotype control antibodies that were employed in this study. The choice of antibodies used in this study to identify a panel of markers that would discriminate each vesicle population derived from the different cells in the vascular compartment and the syncytiotrophoblast was based on: 1) literature searches of previous studies demonstrating positive labelling for the cell type of interest and, 2) referring to The Human Protein Atlas (http://www.proteinatlas.org/) showing the distribution of proteins for each cell type. Table 2 shows that certain antigens are expressed on more than one cell type. For example Endoglin, or CD105 is typically used as an endothelial cell marker, however it is also known to be expressed on the syncytiotrophoblast layer of the placenta (Gougos *et al*., 1992). Also, Glycoprotein IIIa, or

CD61 is commonly used as a platelet marker, but CD61 antigen is also found on endothelial cells and the syncytiotrophoblast layer of the placenta (Bowen *et al.*, 2000). Therefore it was important to test each parent cell and the vesicles derived from it with each panel shown in Table 3 and also test antibodies for cross reactivity to evaluate cell specificity. Ultimately this would help to identify a suitable panel of antibodies that could be used to analyse *in vivo* derived vesicles in plasma.

Fluorescent Label, Antibody/Isotype Control	Clone	Final Concentration	Specificity
Bio-Maleimide (BODIPY FL N-(2aminoethyl) maleimide)[a]	Not Applicable	0.25μM	Thiol reactive dye. General Cell membrane marker.
IgG1-PE[b]	MOPC-21	2.5μg/ml	
CD3-PE[b]	UCHT1	2.5μg/ml	T cells, NK-T cells
IgG1-APCCy7[b]	MOPC-21	5μg/ml	
CD4-APCCy7[b]	RPA-T4	5μg/ml	Thymocytes, subset of T cells, macrophages (low levels), dendritic cells (low levels)
IgG1-Alexa-647[c]	MOPC-21	2.5μg/ml	
CD14-Alexa-647[c]	HCD14	2.5μg/ml	Monocytes, Macrophages, Granulocytes (low levels)
IgG1-PECy7[d]	679.1Mc7	0.25μg/ml	
CD41 (Glycoprotein IIb) PECy7[d]	P2	0.25μg/ml	Platelets, Megakaryocytes, early embryonic hematopoietic stem cells.
CD45-APCCy7[b]	2D1	5μg/ml	Hematopoietic cells except platelets and mature erythrocytes
IgG1-PECy7[b]	MOPC-21	2.5μg/ml	
CD45-PECy7[b]	HI30	2.5μg/ml	Hematopoietic cells except platelets and mature erythrocytes
CD61 (Glycoprotein IIIa) PECy7[d]	SZ21	0.25μg/ml	Platelets, Megakaryocytes, Syncytiotrophoblast, Osteoclasts, Endothelial cells.
IgG1-APC[b]	MOPC-21	2.5μg/ml	
CD62-E (E-selectin) APC[b]	68-5H11	2.5μg/ml	Activated endothelial cells, bone marrow, placenta.
IgG1-FITC[c]		2.5μg/ml	
CD66b-FITC[c]	80H3	2.5μg/ml	Mature granulocytes

Fluorescent Label, Antibody/Isotype Control	Clone	Final Concentration	Specificity
IgG1-PE[e]	11711	0.5µg/ml	
CD105 (Endoglin) PE[e]	166707	0.5µg/ml	Vascular endothelial cells, Activated monocytes, Tissue macrophages, Stromal fibroblasts (low levels), Syncytiotrophoblast
IgG1-APC[f]	P3	2.5µg/ml	
CD144 (VE-cadherin) APC[f]	16B1	2.5µg/ml	Endothelial cells
IgG1-Alexa-647[g]	MOPC-21	0.125µg/ml 2.5µg/ml	
CD146 (MUC18, Mel-CAM) Alexa-647[g]	OJ79c	0.125µg/ml	Endothelial cells, Melanoma cells, Epithelial cells, Fibroblasts, Activated T cells, Mesenchymal stromal cells, Activated keratinocytes
IgG2b-PECy5[g]	MPC-11	0.05.µg/ml	
CD235a/b (Glycophorin A and Glycophorin B) PECy5[g]	HIR2	0.05µg/ml	Red blood cells, Erythroid precursors
IgG2a-Alexa-647[c]	MRC OX-34	2.5µg/ml	
HLA (Human Leukocyte Antigen) Class I (W6/32)-Alexa-647[c]	W6/32	2.5µg/ml	All hematopoietic cells, but not red blood cells. Platelets and endothelial cells
IgG1-PE [e] (conjugated using RPE Lightning Link kit)[h]	11711	3µg/ml	
NDOG2-PE (conjugated using RPE Lightning Link kit) [h]	Not Applicable	3µg/ml	Syncytiotrophoblast
IgG1-FITC [e] (conjugated using FITC Lightning Link kit)[h]	11711	3µg/ml	
NDOG2-FITC (conjugated using FITC Lightning Link kit)[h]	Not Applicable	3µg/ml	Syncytiotrophoblast

Table 2. Fluorescent labels, antibodies and isotype controls used in experiments. [a] Molecular Probes; Invitrogen, Paisley, UK. [b] BD Biosciences, Oxford, UK. [c] AbD Serotec, Kidlington, UK. [d] Beckman Coulter, High Wycombe, UK. [e] R&D Systems Europe Ltd, Abington, UK. [f] eBioscience, Ltd, Hatfield, UK. [g] Biolegend UK Ltd, Cambridge, UK. [h] Innova Biosciences Ltd, Cambridge, UK.

Cell Type	Antibodies					
Platelets	CD61	CD41	W632			
RBC	CD235a/b					
HUVEC	CD61	CD62E	CD105	CD144	CD146	W6/32
Monocytes	CD14	CD45	W6/32			
Lymphocytes	CD3	CD4	CD45	W6/32		
Granulocytes	CD45	CD66b	W6/32			
Syncytiotrophoblast	NDOG2					

Table 3. Antibody panels used to label cell types of interest.

All of the antibodies were mouse monoclonals and were purchased directly conjugated to the appropriate fluorochrome, with the exception of NDOG2 antibody and corresponding IgG1 isotype control antibody. NDOG2 is a trophoblast specific antibody that recognises placental alkaline phosphatase (PLAP) (Sunderland *et al.*, 1981). NDOG2 and the appropriate IgG control antibodies were conjugated to R-Phycoerythrin (RPE) or Fluorescein isothiocyanate (FITC) using a Lightning Link kit (Innova Biosciences, Cambridge, UK) according to the manufacturer's instructions.

2.3.3.2 Antibody Labelling and Flow Cytometry Analysis

Platelets and RBCs

Isolated platelets and RBCs were incubated for 15min in the dark at room temperature with a single-colour antibody and the matched isotype control. Platelets and RBCs were labelled individually with markers outlined in Table 4 and appropriately matched isotype control antibodies. Following incubation, platelets and RBCs were diluted with PBS and analysed collecting 10,000 events in total.

HUVEC

Confluent HUVEC at the same passage used for generating vesicles were washed with PBS and harvested with Accutase (PAA Laboratories) according to the manufacturer's instructions. HUVEC were centrifuged at 1500 × g for 3min and resuspended in 1% (v/v) FBS/PBS. $2.5x10^5$ HUVEC were incubated with 10μl of Fc receptor (FcR) blocking reagent (Miltenyi Biotec) for 10min at 4°C and then incubated in the dark at room temperature for 15min with a single-colour antibody and respective matched isotype control. HUVEC were labelled with the markers outlined in Table 4 and appropriately matched isotype control antibodies. Following incubation, HUVEC were washed at 1700 × g for 3min and resuspended in 300μl of 1% (v/v) FBS/PBS. A total of 10,000 events were analysed by flow cytometry.

Lymphocytes, Monocytes and Granulocytes

Isolated lymphocytes, monocytes and granulocytes were centrifuged at 1500 × g for 3min and resuspended in 1% (v/v) FBS/PBS. $2.5x10^5$ lymphocytes, $2.5x10^5$ monocytes and 5 x 10^5 granulocytes were incubated with 10μl of FcR blocking reagent for 10min at 4°C followed by incubation with single colour antibody and respective matched isotype control antibody for 15min at room temperature in the dark. Lymphocytes, monocytes and granulocytes were incubated with markers outlined in Table 4 and appropriately matched isotype control antibodies. After incubation, cells were washed at 1700 × g for 3min, resuspended in 300μl of 1% (v/v) FBS/PBS and analysed by flow cytometry collecting 10,000 total events.

All flow cytometry gates were set at 1% using isotype controls.

2.3.4 Flow Cytometry of *In vitro* Derived Vesicles Isolated from the Placenta, Platelets, RBCs, HUVEC, Monocytes, Lymphocytes and Granulocytes

2.3.4.1 Antibody Labelling and Flow Cytometry Analysis

Prior to use, all antibodies, FcR blocking reagent and Bio-Maleimide were filtered through Nanosep 0.2μm centrifugal devices (Pall Life Sciences, Portsmouth, UK). PBS was filtered through Whatman Anotop 0.1μm filters (Scientific Laboratory Supplies).

Prior to running vesicle samples, filtered PBS was analysed for two minutes to assess the level of background contaminating events (typically <5%) and these were subtracted from total vesicle counts. In order to label the same number of vesicles per sample, all *in vitro* derived vesicle preparations were firstly diluted with PBS and analysed by flow cytometry. Samples were diluted with a given volume of PBS whereby 20,000-30,000 total events (~170-250 events/sec) were collected within two minutes. 50μl of vesicle sample was incubated with 10μl of FcR blocking reagent for 10min at 4°C. Next, samples were single labelled with a panel of antibodies and respective isotype controls for 15min at room temperature in the dark. Vesicles were labelled with the following antibodies and respective isotype control antibodies as listed in Table 4. Following incubation, samples was diluted with PBS and analysed by flow cytometry. Each sample was acquired for two minutes.

Placental Vesicles
- Bio-Maleimide
- CD61-PECy7
- CD41-PECy7
- W6/32-Alexa-647
- CD235a/b-PECy5
- CD146-Alexa-647
- NDOG2-PE
- CD105-PE
- CD144-APC

Platelet and RBC Vesicles
- Bio-Maleimide
- CD61-PECy7
- CD41-PECy7
- W6/32-Alexa-647
- CD235a/b-PECy5
- CD146-Alexa-647
- NDOG2-PE

Lymphocyte Vesicles
- Bio-Maleimide
- CD61-PECy7
- CD41-PECy7
- W6/32-Alexa-647
- CD3-PE
- CD4-APCCy7
- CD45-APCCy7
- CD235a/b-PECy5
- CD146-Alexa-647
- NDOG2-PE

HUVEC Vesicles
- Bio-Maleimide
- CD61-PECy7
- CD41-PECy7
- W6/32-Alexa-647
- CD235a/b-PECy5
- CD146-Alexa-647
- NDOG2-PE
- CD144-APC
- CD105-PE
- CD62E-APC

Monocyte Vesicles
- Bio-Maleimide
- CD61-PECy7
- CD41-PECy7
- W6/32-Alexa-647
- CD14-Alexa-647
- CD45-APCCy7
- CD235a/b-PECy5
- CD146-Alexa-647
- NDOG2-PE

Granulocyte Vesicles
- Bio-Maleimide
- CD61-PECy7
- CD41-PECy7
- W6/32-Alexa-647
- CD66b-FITC
- CD45-PECy7
- CD235a/b-PECy7
- CD146-Alexa-647
- NDOG2-PE

Table 4. Fluorescent cell membrane dye and antibodies used to label *in vitro* derived vesicles.

Multi-colour flow cytometry was carried out on the pSTBM. The BD Biosciences Fluorescence Spectrum Viewer (http://www.bdbiosciences.com/research/multicolor/spectrum_viewer/index.jsp) was used to help select suitable combinations of fluorophores. Fluorochrome compensation was set-up using BD CompBeads (polystyrene beads that bind any mouse kappa light chain bearing immunoglobulin) (BD Biosciences) and a single stain using Bio-Maleimide labelled pSTBM. It was also necessary to perform fluorescence minus one (FMO) controls. FMO controls combine all reagents except the one of interest. For example, the FMO control for NDOG2-PE would combine all reagents in a single cocktail except for NDOG2-PE which would be replaced with the IgG1-PE isotype control

antibody. FMO controls are the only way to properly evaluate background fluorescence in a given channel and are a must in order to set gates. In a multi-colour experiment it is impossible to set accurate gates based solely on a single tube containing all isotype controls (Herzenberg *et al.*, 2006, Mahnke and Roederer 2007).

2.3.5 Immunogold Transmission Electron Microscopy of pSTBM

Immunogold Transmission Electron microscopy of pSTBM was carried out by Prof. David Ferguson (Nuffield Dept of Clinical and Laboratory Science, Oxford). In brief, formvar/carbon coated grids were floated on 50µl of pSTBM. Grids were washed on drops of PBS and immunogold labelling was performed as follows; pSTBM grids were labelled on a drop of NDOG2 (1:50) in PBS for 20 minutes and then washed in PBS. pSTBM grids were then placed on a drop of secondary goat anti-mouse (1:25) conjugated to 10nm colloidal gold and incubated for 20 minutes. Following incubation, grids were washed in PBS, fixed with glutaraldehyde, washed in distilled water and negatively stained with 1% methyl tungstenate. Grids were then examined in the electron microscope (Model JEOL 1200EX, JEOL Ltd UK).

2.3.6 Statistics

Each data set was first tested for a Guassian distribution by using a Shapiro-Wilk normality test and for equal variance using a Levene Median test. Data sets comparing two groups were analysed using a *t*-test. In data sets found to pass both the normality and equal variance test and that contained three or more treatment groups, a One Way ANOVA was performed. Whereby data were found to be significantly different, all pairwise multiple comparisons were made using a Holm-Sidak test. For non-parametric data a Kruskal-

Wallis One Way ANOVA on Ranks was performed and significant differences were identified using a multiple comparisons Tukey test. Values of $p<0.05$ were considered to be significant. SigmaPlot 12.0 (Systat Software, USA) was used for data analysis.

2.4 Results

2.4.1 Flow Cytometer Instrument Set-up for Vesicle Analysis

Experiments were carried out to evaluate the sensitivity of the BD LSRII flow cytometer for vesicle analysis. A range of fluorescent beads 200nm, 290nm, 390nm, 590nm and 1μm) were analysed on forward scatter (FSC) and side scatter (SSC) (Figure 5A). A SSC threshold of 200 (arbitrary units) was used as this is the lowest value possible on the LSRII. A high level of background instrument noise (determined by running 0.1μm filtered PBS) was present within the 200nm bead population at these settings, therefore the FSC and SSC voltages were lowered and a gate was set to include beads of only 300nm – 1μm (Figure 5B). Subsequently, minimal background noise was detectable.

To calculate vesicle concentrations we first investigated the use of BD Trucount Beads (3.0-3.4μm) following the manufacturer's instructions. Each BD Trucount tube contains a known number of fluorescent beads to provide a standard for calculating the absolute count of vesicles/ml of solution. Typically, the sample of interest is added directly to the BD Trucount tube and analysed by flow cytometry to determine an absolute cell count. However, we found that BD Trucount tubes contained many contaminating particles of a size which fell within the vesicle gate (Figure 5C) and could therefore not be used in the conventional way. We therefore developed an alternative method to determine absolute vesicle counts based on the instrument flow rate. 500μl of PBS was added to a BD

Trucount tube and acquired for two minutes on the "LO" flow rate (~12µl/min) setting. Two BD Trucount tubes were run at the beginning of each experiment and one at the end to monitor the flow rate. We have found this method to be very accurate and reliable for total vesicle counts (i.e. typical inter-assay CV of 3% and intra-assay CV of 4% over a one month period). Prior to each experiment a tube of 0.1µm filtered PBS was run for two minutes to assess the level of background contaminating events (Figure 5D). These results clearly demonstrate that by using a conventional flow cytometer only a portion of the total cellular vesicles (>300nm) can be detected. Hence, we can analyse a sub-population of microvesicles by flow cytometry, however nanovesicles are too small and cannot be measured using this method. Hence, the figures in this chapter only show microvesicle populations.

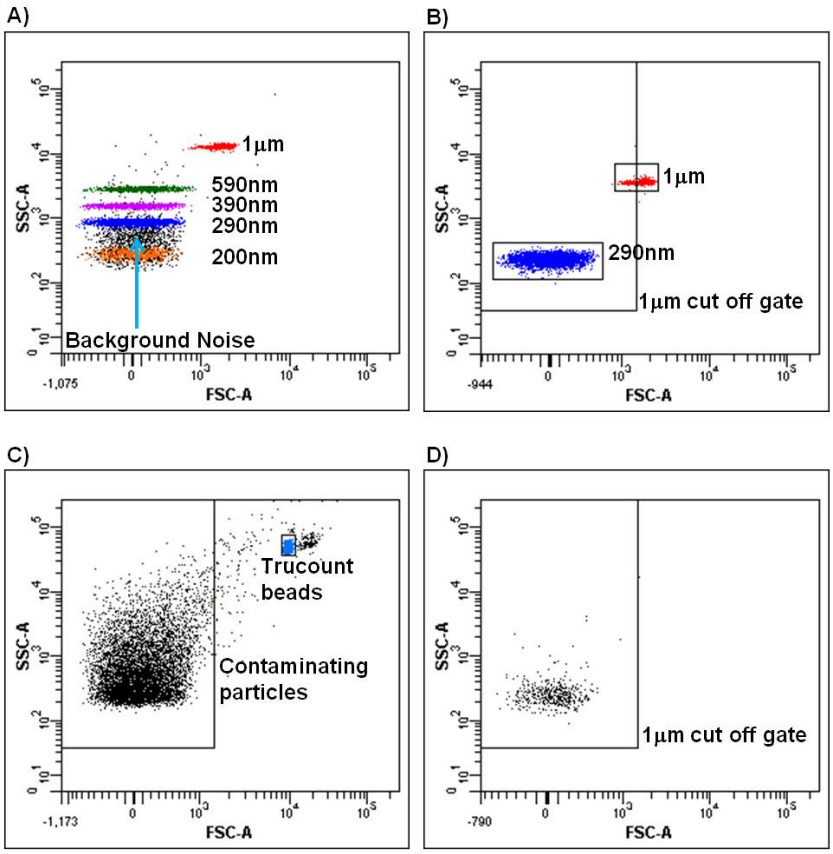

Figure 5. LSRII flow cytometry instrument set up. A) FSC vs. SSC dot plot of fluorescent microspheres (200nm – 1µm) and visualisation of instrument "background noise", **B)** SSC & FSC voltages adjusted to visualise microspheres at ≥290nm and establishment of ≤1µm gate at the lowest SSC threshold setting, **C)** Trucount beads analysed for two minutes and visualization of background particles present from the Trucount beads, **D)** Two minute analysis of 0.1µm filtered PBS using settings to visualise vesicles ≥ 290nm.

2.4.2 Flow Cytometric Analysis and Immunogold labelling of Placental Syncytiotrophoblast Vesicles (pSTBM)

Placental syncytiotrophoblast vesicles (pSTBM) from eight normal placentas were pooled and analysed using five-colour flow cytometry. It was essential to perform multi-colour analysis in order to establish the degree of purity of the pSTBM population. Using the dual placental perfusion system it is probable that vesicles from other cell types, such as those found in blood may also be included in the final pSTBM pellet. As the pSTBM preparations are not a homogenous population, two parameter histograms were used for the analysis. pSTBM were labelled with a five colour panel consisting of; Bio-Maleimide, NDOG2, CD61 or CD41, CD235a/b and W6/32. Gates were set using fluorescence minus one (FMO) with isotype controls. >90% of the pSTBM were <1μm (Figure 6A) and majority (~94%) labelled positive with Bio-Maleimide and the placental marker NDOG2 (Figure 6B). pSTBM were also found to label positive for the platelet markers CD61 and CD41, whereby >75% expressed CD61 (Figure 6C) and a subset (27.4%) expressed CD41 (Figure 6D). Only 1% of the pSTBM labelled with the RBC marker CD235a/b (Figure 6E) and ~3% with the MHC Class I marker W6/32 (Figure 6F). The NDOG2 antibody labelling of pSTBM was confirmed by immunogold transmission electron microscopy (Figure 7).

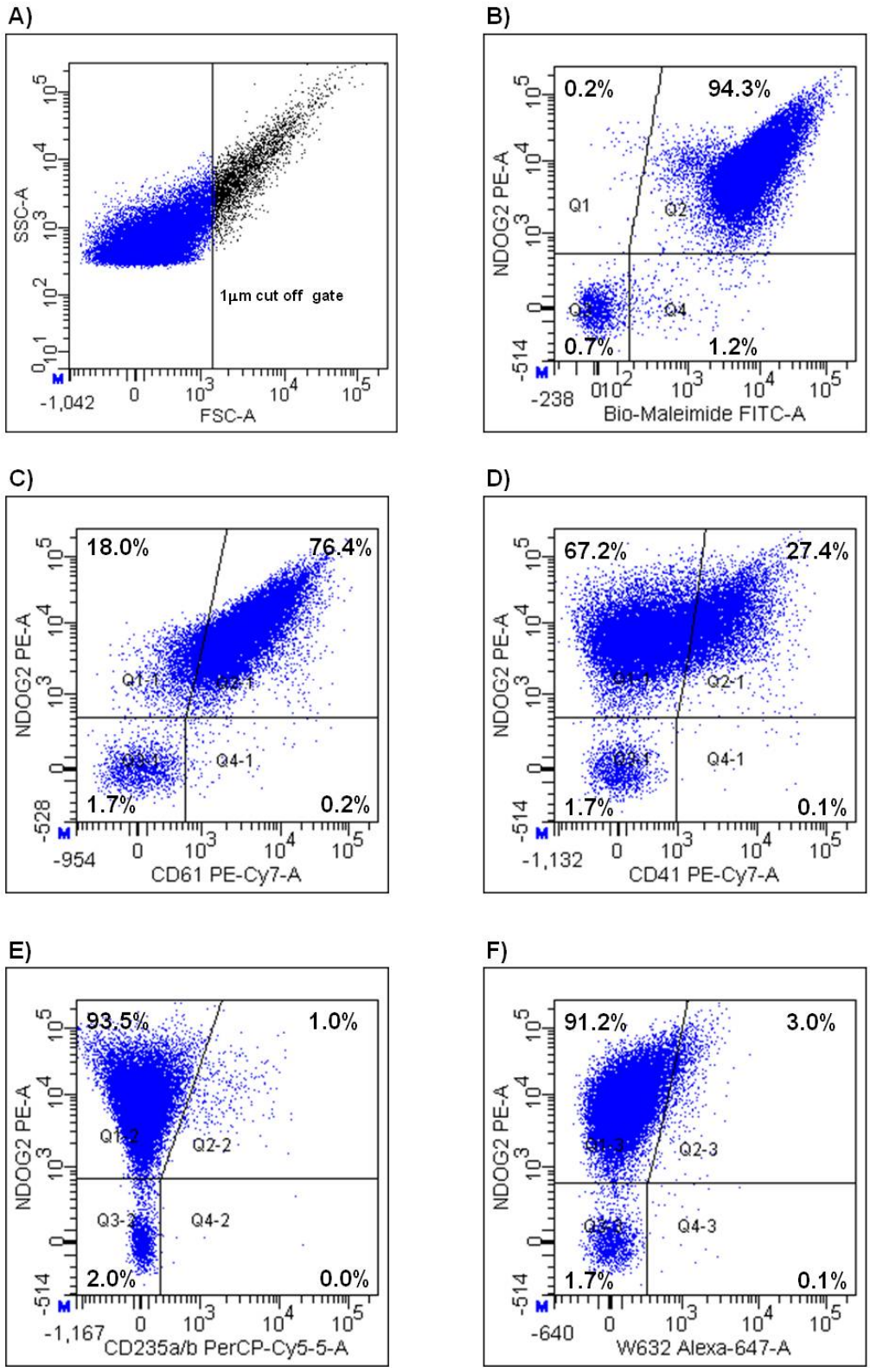

Figure 6. Flow cytometry analysis of pSTBM. A) FSC vs. SSC dot plot of pSTBM (>90% are <1µm). Double labelling of pSTBM, **B)** Bio-Maleimide vs. NDOG2, **C)** CD61 vs. NDOG2, **D)** CD41 vs. NDOG2. **E)** CD235a/b vs. NDOG2, **F)** W6/32 vs. NDOG2. Data show percentage positive pSTBM. Percentages have been adjusted to account for background contaminating particulates.

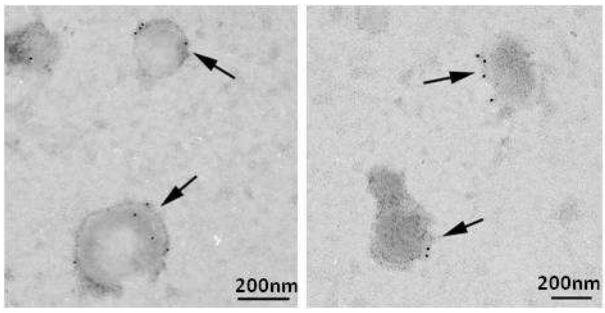

Figure 7. Immunogold labelling of pSTBM with NDOG2 antibody.

The endothelial cell-like characteristics of the syncytiotrophoblast have made it difficult to find an endothelial cell specific marker that does not cross react with the syncytiotrophoblast. pSTBM were double labelled with the placental marker NDOG2 and the endothelial cell markers CD146, CD144 or CD105. CD146 was not expressed on pSTBM (Figure 8A) and only a very small amount of pSTBM expressed CD144 (Figure 8B). In contrast, the vast majority of pSTBM expressed CD105 (Figure 8C).

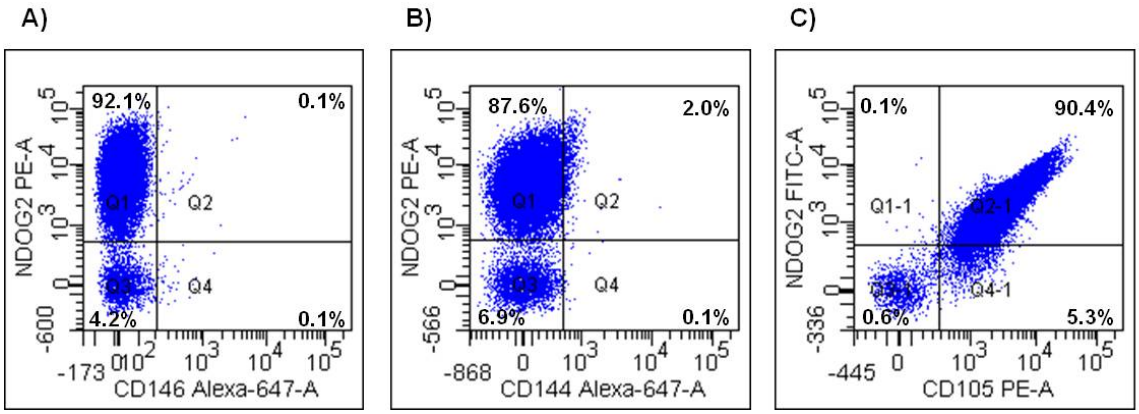

Figure 8. Flow cytometry analysis of endothelial cell markers on pSTBM. Double labelling of pSTBM **A)** NDOG2 vs. CD146, **B)** NDOG2 vs. CD144, **C)** NDOG2 vs. CD105. Data show percentage positive pSTBM. Percentages have been adjusted to account for background contaminating particulates.

2.4.3 Flow Cytometric Analysis of Platelets and *In vitro* Derived Platelet Vesicles

In this study platelet vesicles were generated from three healthy control subjects by activation with A-23187, as described in Materials and Methods Section 2.3.2.2. Platelets were identified by a FSC vs. SSC plot and by using a FSC threshold of 400 (arbitrary units) which allows analysis of platelets 1μm and above (Figure 9A). Phenotypic analysis was carried out by labelling with a panel of antibodies (as described above in Materials and Methods 2.3.3.1). In all three individuals platelets labelled with Bio-Maleimide (Figure 9B) and stained ~100% positive for CD41 (Figure 9C), CD61 (Figure 9D) and human leukocyte antigen (HLA) Class I (Figure 9E). No positive staining was detected when platelets were labelled with the endothelial cell marker CD146 (Figure 9F), placental marker NDOG2 (Figure 9G) or red blood cell marker CD235a/b (Figure 9H).

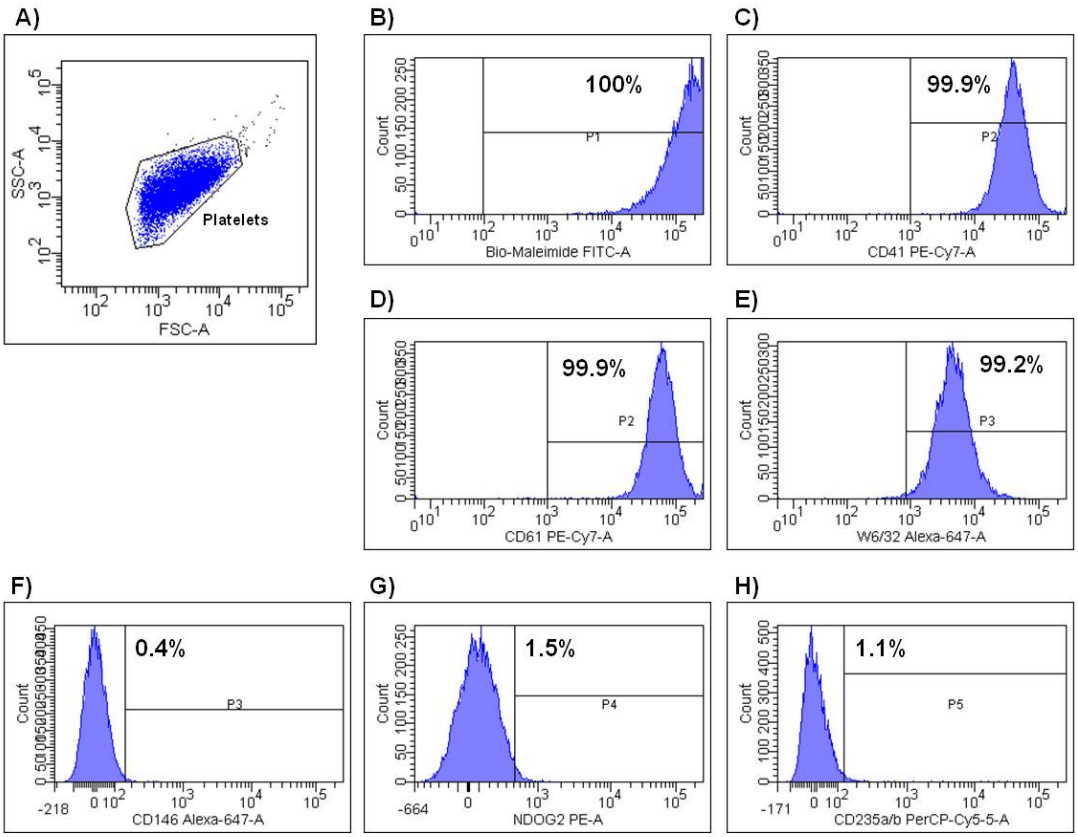

Figure 9. Flow Cytometry analysis of platelets. A) Representative FSC vs. SSC dot plot of isolated platelets. Representative histograms of platelets showing the percentage of positive labelling with **B)** Bio-Maleimide, **C)** CD41, **D)** CD61, **E)** W6/32, **F)** CD146, **G)** NDOG2, **H)** CD235a/b.

Using a SSC threshold of 200 and 300nm cut-off gate, platelet vesicles were then identified using a logarithmic FSC vs. SSC plot (Figure 10A). In all three individuals the majority (>97%) of platelet vesicles were <1µm. Representative histograms of the percentage positive labelling of platelet vesicles are shown for; Bio-Maleimide (Figure 10B), CD41 (Figure 10C), CD61 (Figure 10D), HLA Class I (Figure 10E), CD146 (Figure 10F), PLAP (Figure 10G) and CD235a/b (Figure 10H).

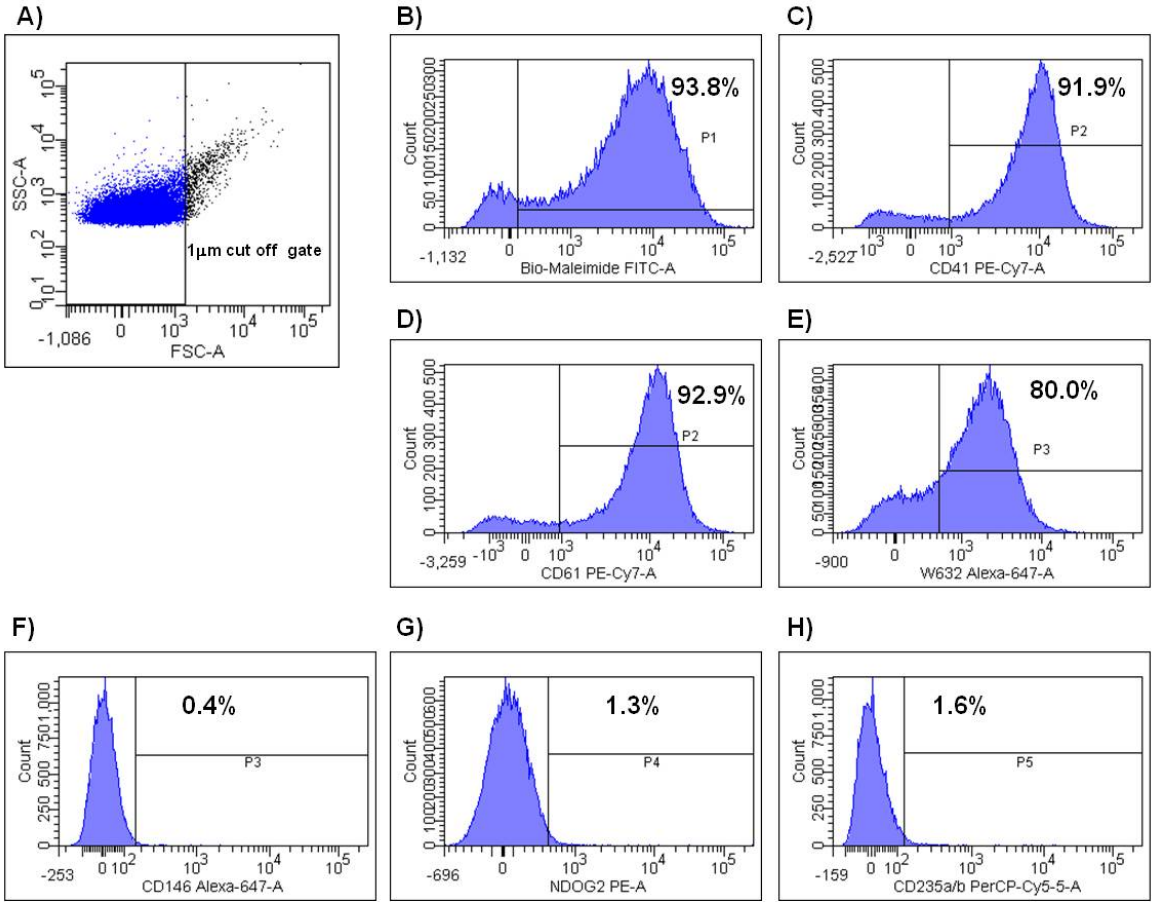

Figure 10. Flow Cytometry analysis of platelet vesicles. A) Representative FSC vs. SSC dot plot of platelet vesicles. Representative histograms of platelet vesicles showing the percentage of positive labelling with **B)** Bio-Maleimide, **C)** CD41, **D)** CD61, **E)** W6/32, **F)** CD146, **G)** NDOG2, **H)** CD235a/b. Percentages have been adjusted to account for background contaminating particulates.

Similar to the phenotyping of platelets, positive staining was detected on platelet vesicles labelled with Bio-Maleimide (Figure 11A), CD41 (Figure 11B) CD61 (Figure 11C) and HLA Class I using W6/32 (Figure 11D). The expression of Bio-Maleimide and all these

antigens was however significantly reduced as compared to platelets. Platelets and platelet vesicles expressed no CD146 (Figure 11E), PLAP (NDOG2) (Figure 11F) or CD235a/b (Figure 11G).

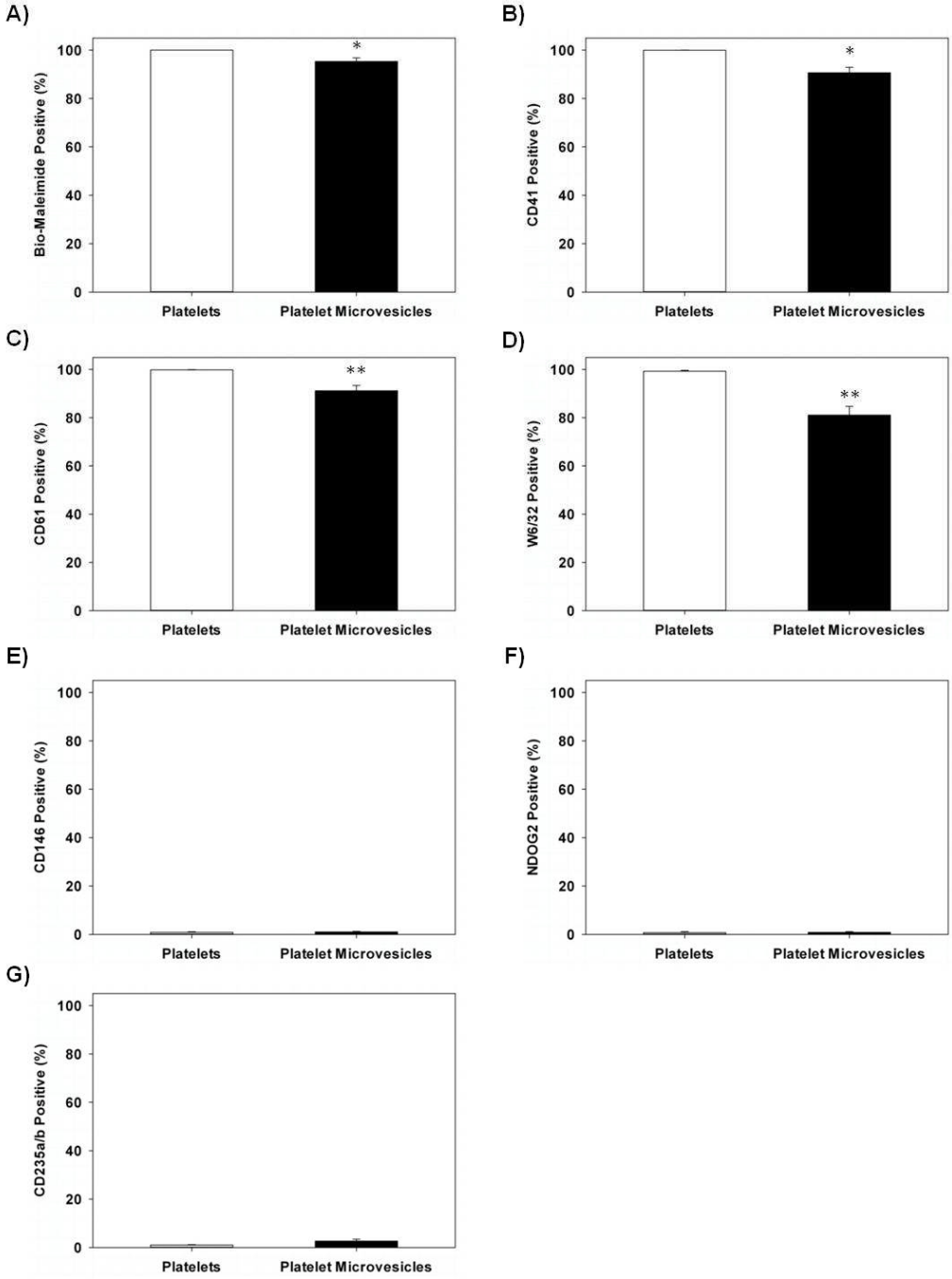

Figure 11. Flow cytometry analysis of antigen expression on platelets and platelet vesicles. Data are from three individual experiments showing the percentage of positive staining with **A)** Bio-Maleimide, **B)** CD41, **C)** CD61, **D)** W6/32, **E)** CD146, **F)** NDOG2 and **G)** CD235a/b on platelets (□) and platelet vesicles(■) stimulated with A-23187. Percentages have been adjusted to account for background contaminating particulates. Bars represent Mean ± SE. p values (*p<0.05. **p<0.01) compare platelets vs. platelet vesicles.

2.4.4 Flow Cytometric Analysis of Red Blood Cells (RBCs) and *In vitro* Derived RBC Vesicles

Isolated RBCs were identified by a logarithmic FSC vs. SSC plot and using a FSC threshold of 1000 (arbitrary units). Figure 12A shows a representative FSC vs SSC plot of RBCs. Phenotypic analysis of RBCs showed positive staining with Bio-Maleimide (Figure 12B) and the RBC marker CD235a/b (Figure 12C), which recognises the sialglycoproteins Glycophorin A and Glycophorin B. RBCs were tested for cross reactivity with other antibodies including; CD41 (Figure 12D) and CD61 (Figure 12E), W6/32 (Figure 12F), CD146 (Figure 12G) NDOG2 (Figure 12H), no positive staining was detected.

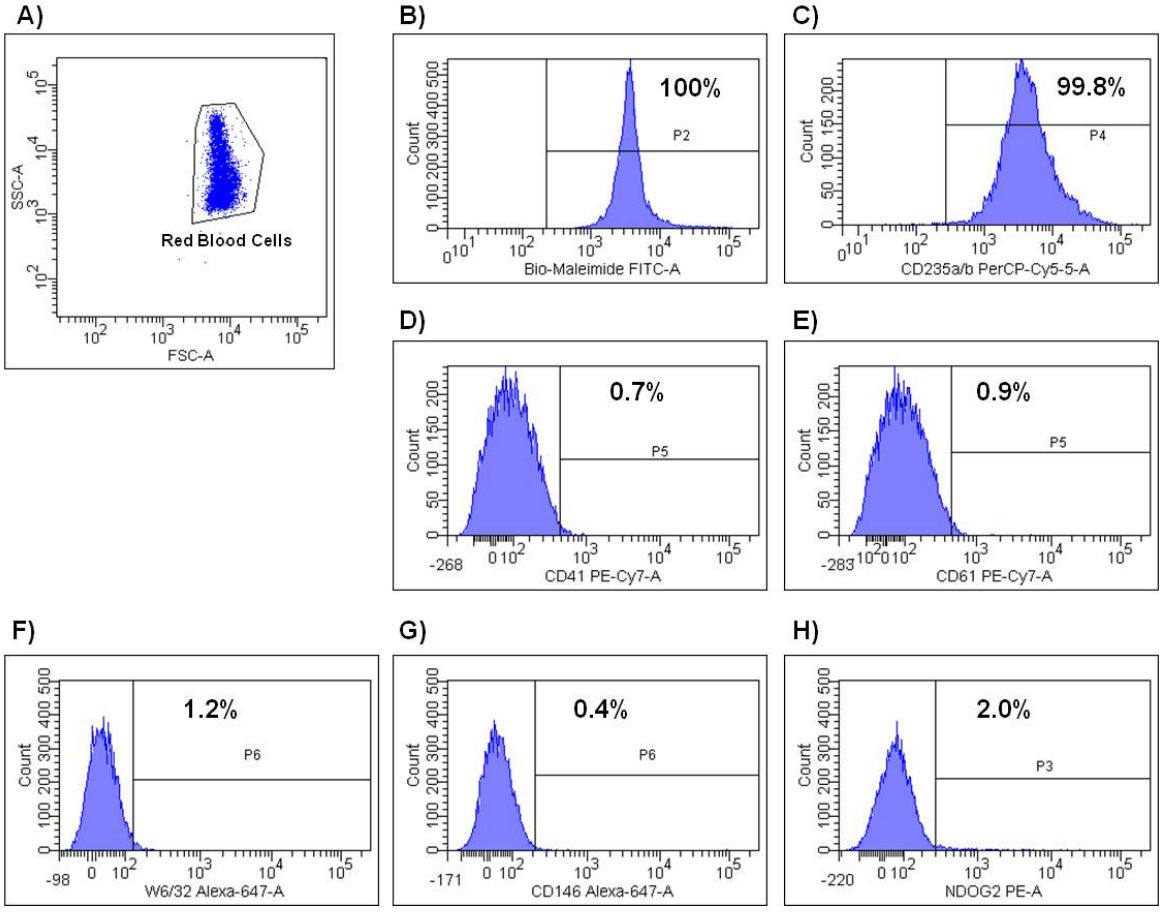

Figure 12. Flow Cytometry analysis of RBCs. A) Representative FSC vs. SSC dot plot of RBCs. Representative histograms of RBCs showing the percentage of positive labelling with **B)** Bio-maleimide, **C)** CD235a/b, **D)** CD41, **E)** CD61, **F)** W6/32, **G)** CD146, **H)** NDOG2.

Similar to platelets, RBCs were also stimulated with A-23187 to generate RBC vesicles. This resulted in two very distinct populations of vesicles when looking at the FSC vs. SSC plot (Figure 13A). Representative histograms are shown of RBC vesicle labelling with Bio-Maleimide (Figure 13B), CD235a/b (Figure 13C), CD41 (Figure 13D), CD61 (Figure 13E), HLA Class I as detected using W6/32 (Figure 13F), CD146 (Figure 13G) and PLAP using NDOG2 (Figure 13H).

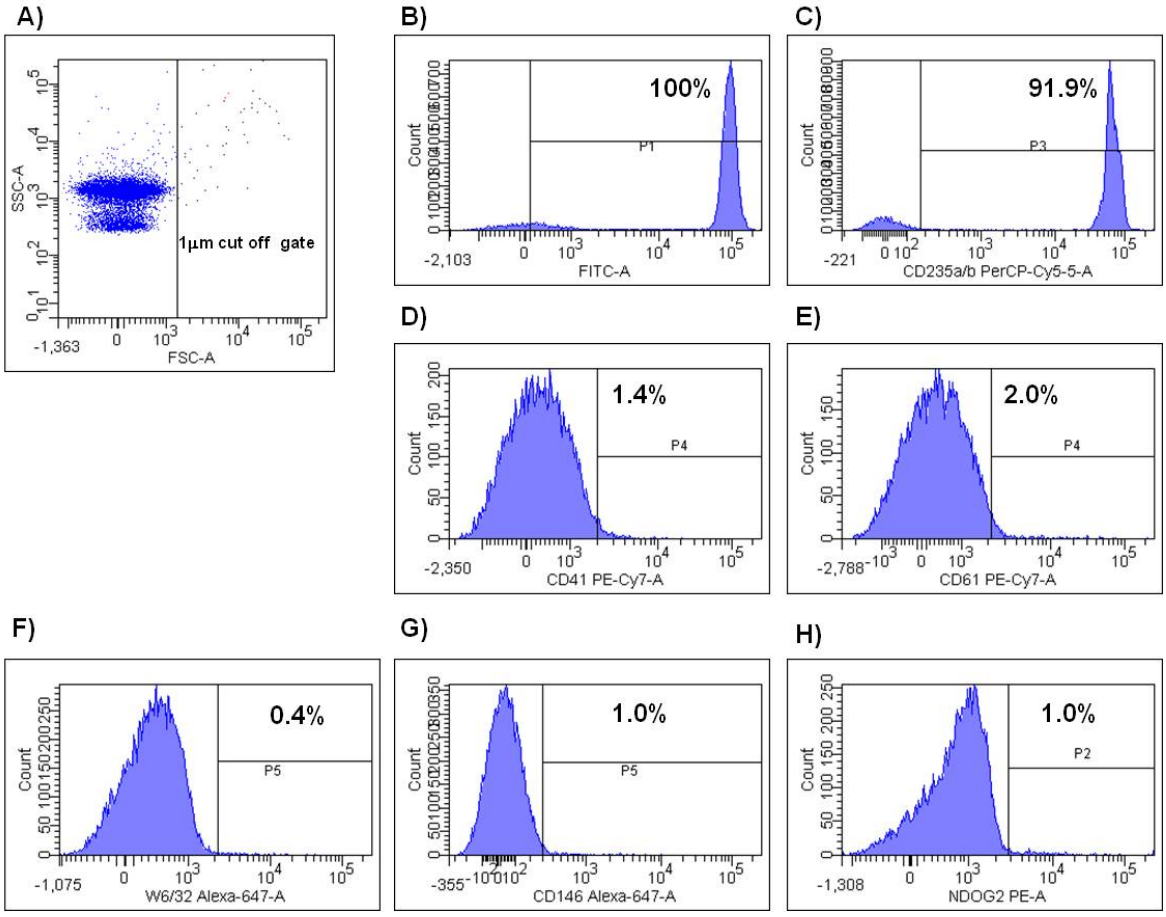

Figure 13. Flow Cytometry analysis of RBC vesicles. A) Representative FSC vs. SSC dot plot of RBC vesicles. Representative histograms of RBC vesicles showing the percentage of positive labelling with **B)** Bio-maleimide, **C)** CD235a/b, **D)** CD41, **E)** CD61, **F)** W6/32, **G)** CD146, **H)** NDOG2. Percentages have been adjusted to account for background contaminating particulates.

The same pattern of staining that was observed for RBCs was evident with the RBC derived vesicles. 100% of the RBC vesicles labelled positive with Bio-Maleimide (Figure 14A). >90% of the RBC vesicles labelled positive for CD235a/b but compared to RBCs,

the expression of CD235a/b on the vesicles was significantly reduced (Figure 14B). No expression of CD41 (Figure 14C), CD61 (Figure 14D), HLA Class I (Figure 14E), CD146 (Figure 14F) or PLAP (Figure 14G) was present on the RBC vesicles.

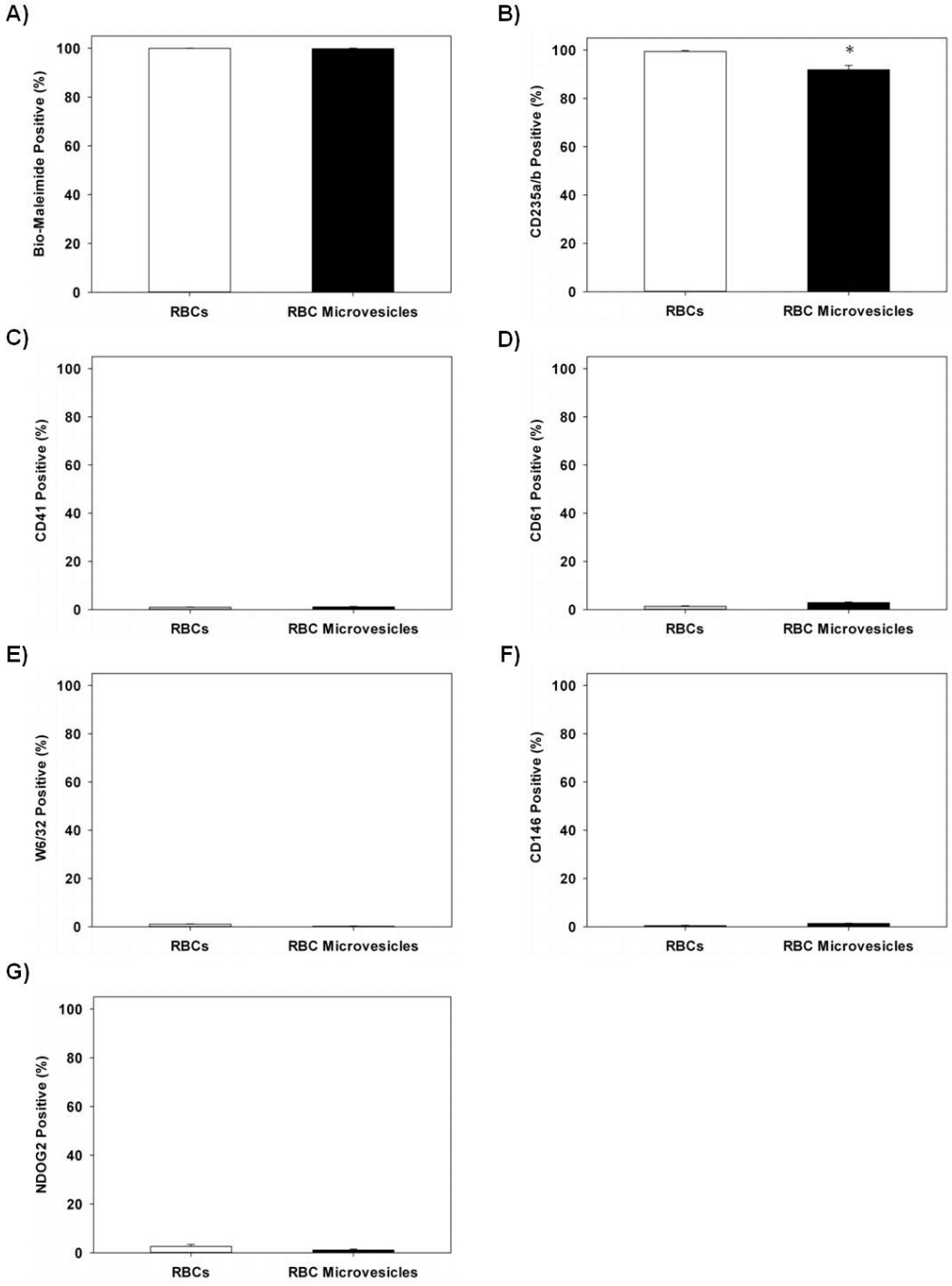

Figure 14. Flow cytometry analysis of antigen expression on RBCs and RBC vesicles. Data are from three individual experiments showing the percentage of positive staining with **A)** Bio-Maleimide, **B)** CD235a/b, **C)** CD41, **D)** CD61, **E)** W6/32, **F)** CD146 and **G)** NDOG2 on RBCs (□) and RBC vesicles(■) stimulated with A-23187. Percentages have been adjusted to account for background contaminating particulates. Bars represent Mean ± SE. p value (*p<0.05) compare RBCs vs. RBC vesicles.

2.4.5 Flow Cytometric Analysis of HUVEC and *In vitro* Derived HUVEC Vesicles

HUVEC isolated from three different cords were examined for expression of Bio-Maleimide and multiple surface antigens (as described in Materials and Methods 2.3.4.1) Representative histograms of staining are shown in Figure 15. A FSC threshold was set at 5000 (arbitrary units) and HUVEC were first identified by their scatter properties (Figure 15A). All HUVEC labelled positive with Bio-Maleimide (Figure 15B) and expressed CD61 (Figure 15C), HLA Class I (Figure 15D), CD146 (Figure 15E), CD144 (vascular endothelial cadherin; Figure 15F) and CD105 (Endoglin; Figure 15G). Low amounts of CD41 were expressed (Figure 15H) and no expression of CD62E (E-Selectin; Figure 15I), PLAP (Figure 15J) or CD235a/b (Figure 15 K) was detected.

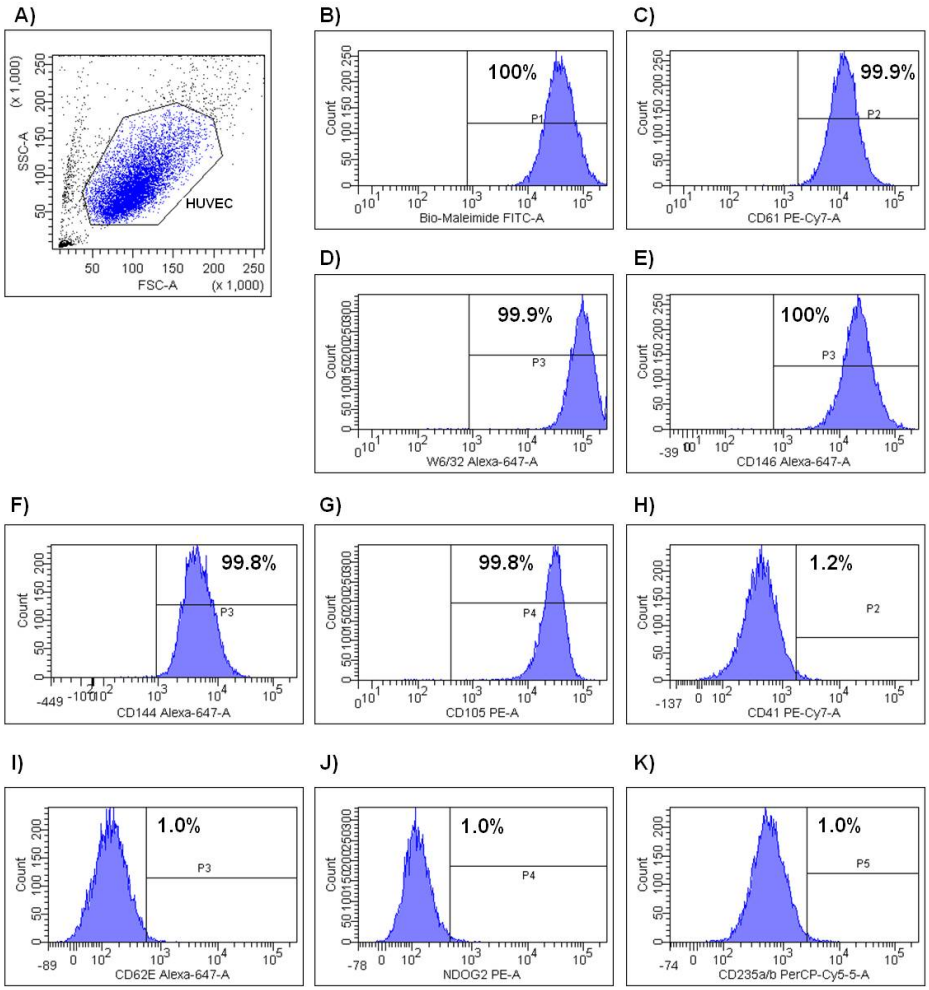

Figure 15. Flow cytometry analysis of HUVEC A) Representative FSC vs. SSC dot plot of HUVEC Representative histograms of HUVEC showing the percentage of positive labelling with **B)** Bio-maleimide, **C)** CD61, **D)** W6/32 **E)** CD146, **F)** CD144, **G)** CD105, **H)** CD41, **I)** CD62E, **J)** NDOG2, **K)** CD235a/b.

HUVEC vesicles were generated by stimulating HUVEC with the apoptosis inducing agent camptothecin (CPT) (Simak *et al.*, 2002) or with the pro-inflammatory cytokine interleukin 1 alpha (IL-1α) (Abid Hussein *et al.*, 2003). Total vesicle counts were significantly increased when HUVEC were cultured in the presence of CPT for 24 hours compared to the 0.5% DMSO culture medium control (Figure 16). However, no increase in HUVEC vesicle count was observed in the 12 hour IL-1α treated HUVEC as compared to the 12 hour culture media control (Figure 16).

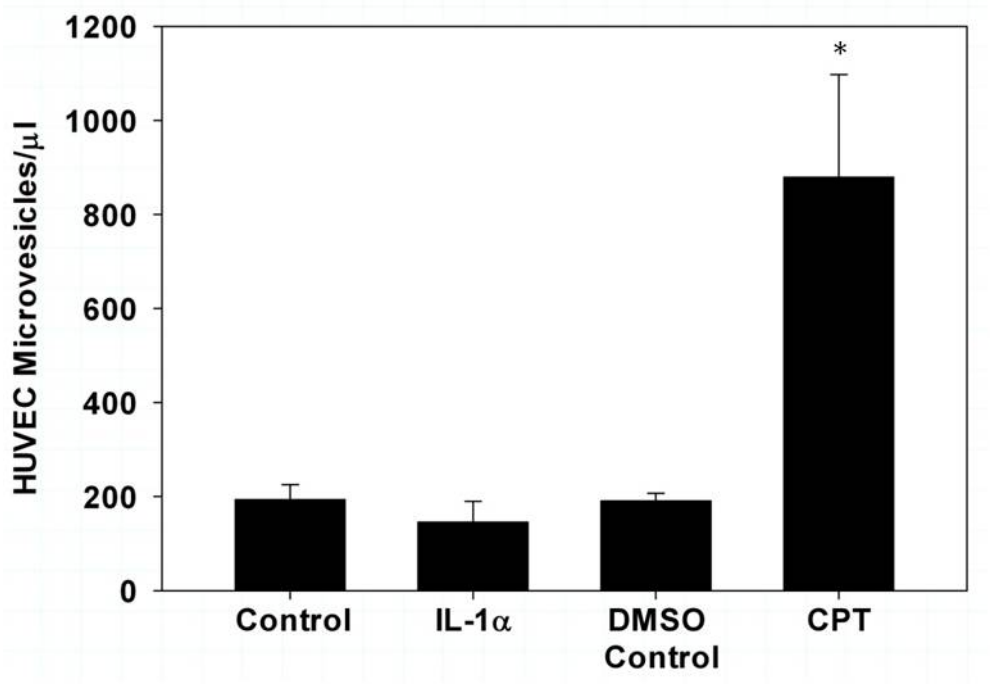

Figure 16. Total HUVEC vesicle counts as measured by flow cytometry. 12 hour stimulation of HUVEC vesicles measured in culture medium only (Control) or with IL-1α 5ng/ml (IL-1α). 24 hour stimulation of HUVEC vesicles measured in 0.5% DMSO culture medium (DMSO Control) or with CPT 5µM (CPT). Bars represent Mean ± SE. Results are of three independent experiments. * $p<0.05$ CPT vs. DMSO Control.

Representative histograms of CPT stimulated HUVEC vesicles are shown in Figure 17. Figure 17A shows the scatter profile (FSC vs. SSC) of the HUVEC vesicles. HUVEC vesicles were labelled with Bio-Maleimide (Figure 17B), CD61 (Figure 17C), W6/32

(Figure 17D), CD146 (Figure 17E), CD144 (Figure 17F) and CD105 (Figure 17G), CD41 (Figure 17H), CD62E (Figure 17I), NDOG2 (Figure 17J) or CD235a/b (Figure 17K).

No expression of the cell surface antigens CD41 (Figure 18A), PLAP (Figure 18B) or CD235a/b (Figure 18C) was detected on HUVEC vesicles. CD62E expression was not found on resting HUVEC, however IL-1α stimulated HUVEC did express CD62E (data not shown) as did vesicles from IL-1α stimulated HUVEC (Figure 18D). The percentage of positive staining with Bio-Maleimide (Figure 18E) and the expression of CD105 (Figure 18F), CD61 (Figure 18G), W6/32 (Figure 18H), CD146 (Figure 18I) and CD144 (Figure 18J) were all significantly reduced in the vesicles from IL-1α- and CPT-stimulated HUVEC as compared to HUVEC. No significant differences in Bio-Maleimide staining or antigenic phenotype were detected when comparing the two different activation methods (vesicles from IL-1α– or CPT-stimulated HUVEC) with their respective controls or to each other.

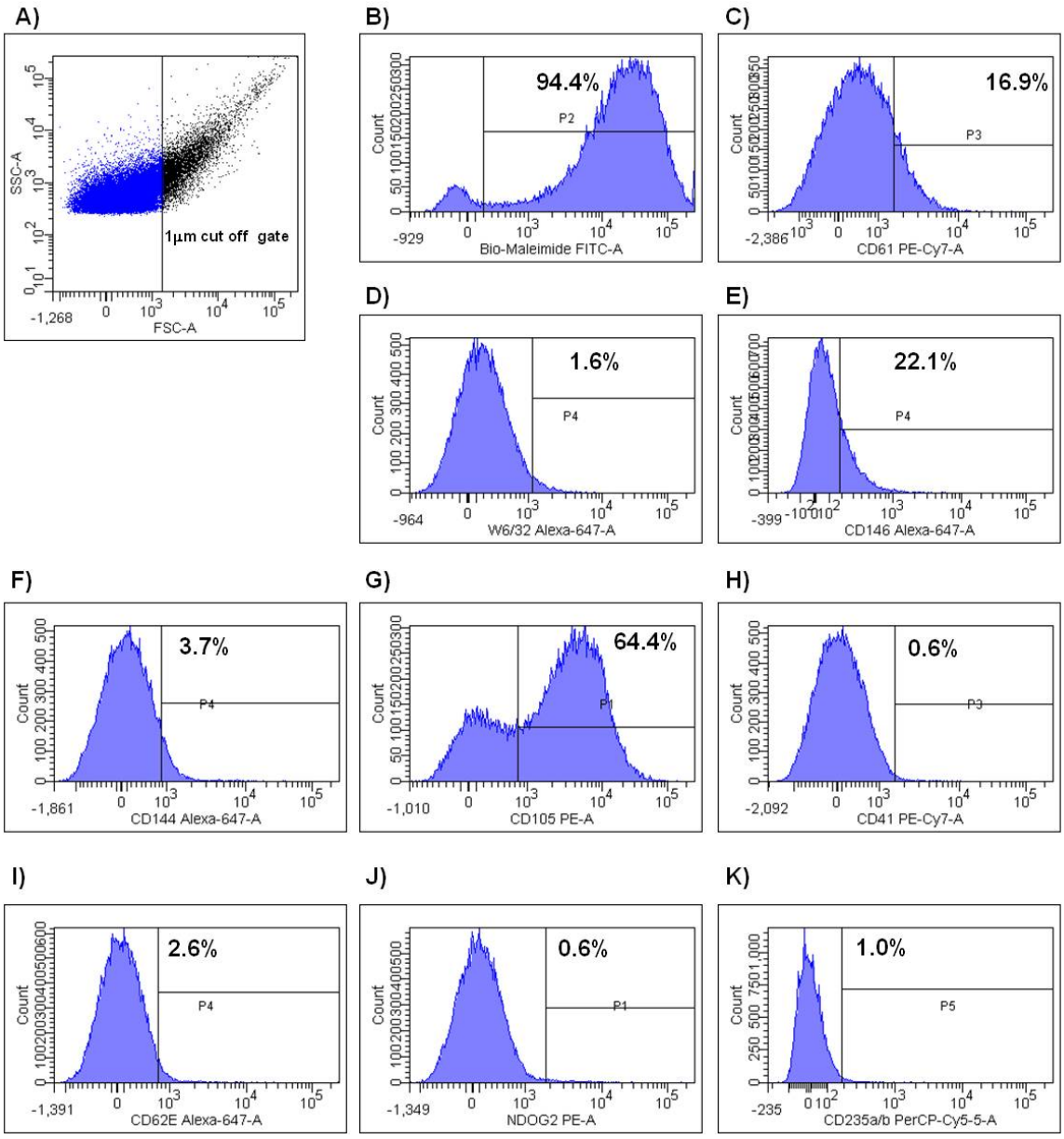

Figure 17. Flow cytometry of HUVEC vesicles from CPT stimulation. Representative flow cytometry histograms of CPT stimulated HUVEC vesicles. **A)** FSC vs. SSC profile of HUVEC vesicles. HUVEC vesicle labelling; **B)** Bio-Maleimide, **C)** CD61, **D)** W6/32, **E)** CD146, **F)** CD144, **G)** CD105, **H)** CD41, **I)** CD62E, **J)** NDOG2, **K)** CD235a/b. Percentages have been adjusted to account for background contaminating particulates.

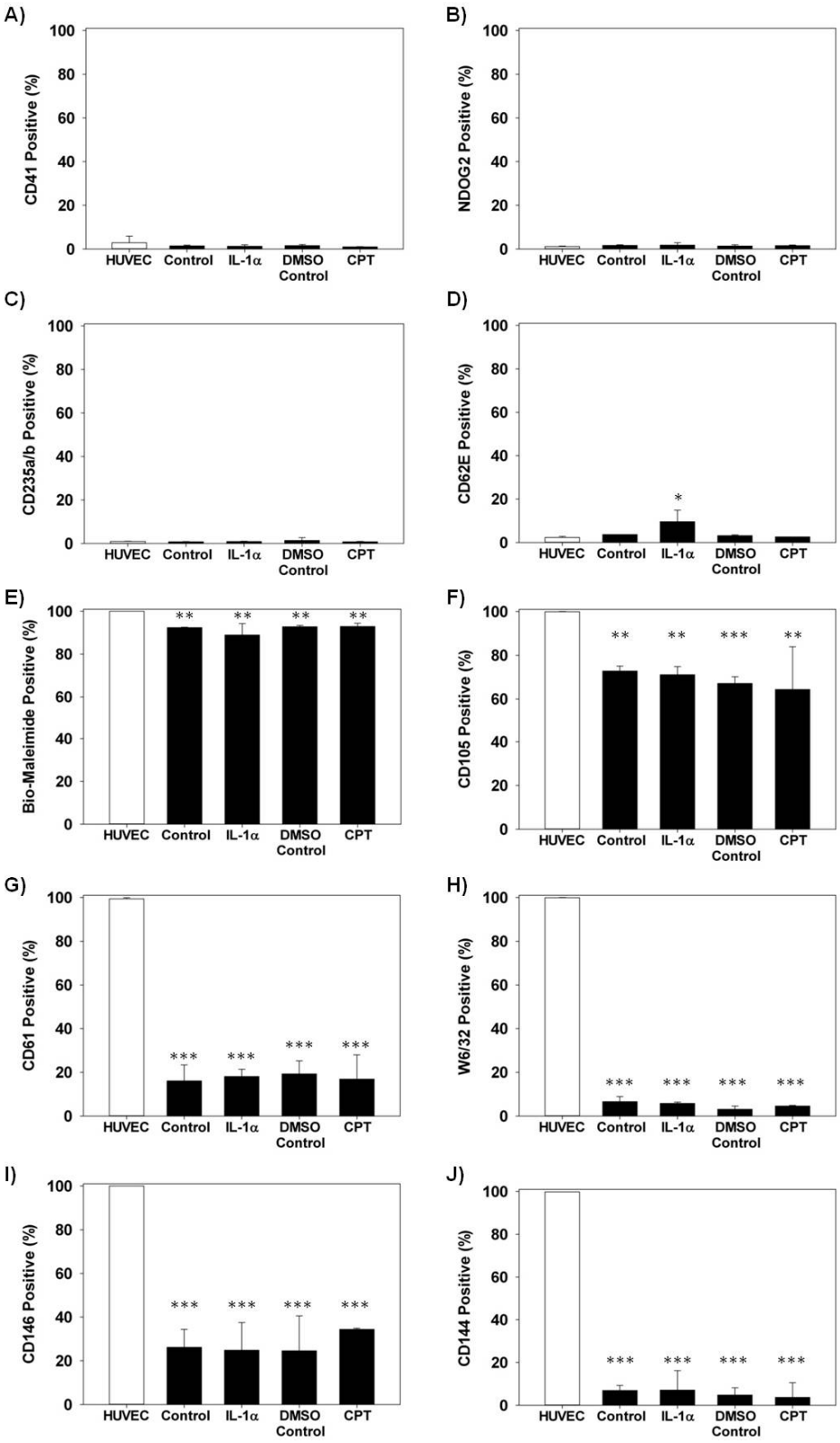

Figure 18. Flow cytometry analysis of antigen expression on HUVEC and HUVEC vesicles. Data are from three individual experiments showing the percentage of positive staining with **A)** CD41, **B)** NDOG2, **C)** CD235a/b, **D)** CD62E, **E)** Bio-Maleimide, **F)** CD105, **G)** CD61, **H)** W6/32, **I)** CD146 and **J)** CD144 on HUVEC (□) and HUVEC (■) vesicles stimulated with IL-1α, CPT and their respective controls. Percentages have been adjusted to account for background contaminating particulates. Bars represent median with the interquartile range. p values (*p<0.05. **p<0.01, ***p<0.001) compare HUVEC vs. Control, IL-1α, DMSO Control and CPT HUVEC vesicles.

2.4.6 Flow Cytometric Analysis of Monocytes and *In vitro* Derived Monocyte Vesicles

Monocytes were isolated from PBMCs using immunomagnetic anti-CD14 MicroBeads. The purity of the isolation method was first assessed by identifying and gating the monocyte population based on their FSC and SSC characteristics using a FSC threshold of 35,000 (arbitrary units). >90% of isolated cells were within the monocyte gate (Figure 19A). Secondly, monocytes were incubated with an antibody toward CD14, a monocyte marker, and in all three individuals CD14 expression was >99% (Figure 19B). Monocytes were also tested for antibody cross reactivity by labelling with a panel of antibodies (as described in Materials and Methods 2.3.3.2) and the membrane marker Bio-Maleimide. Representative histograms showing the percentage of positive staining with Bio-Maleimide and for each antibody in the panel is shown in Figure 19C-J.

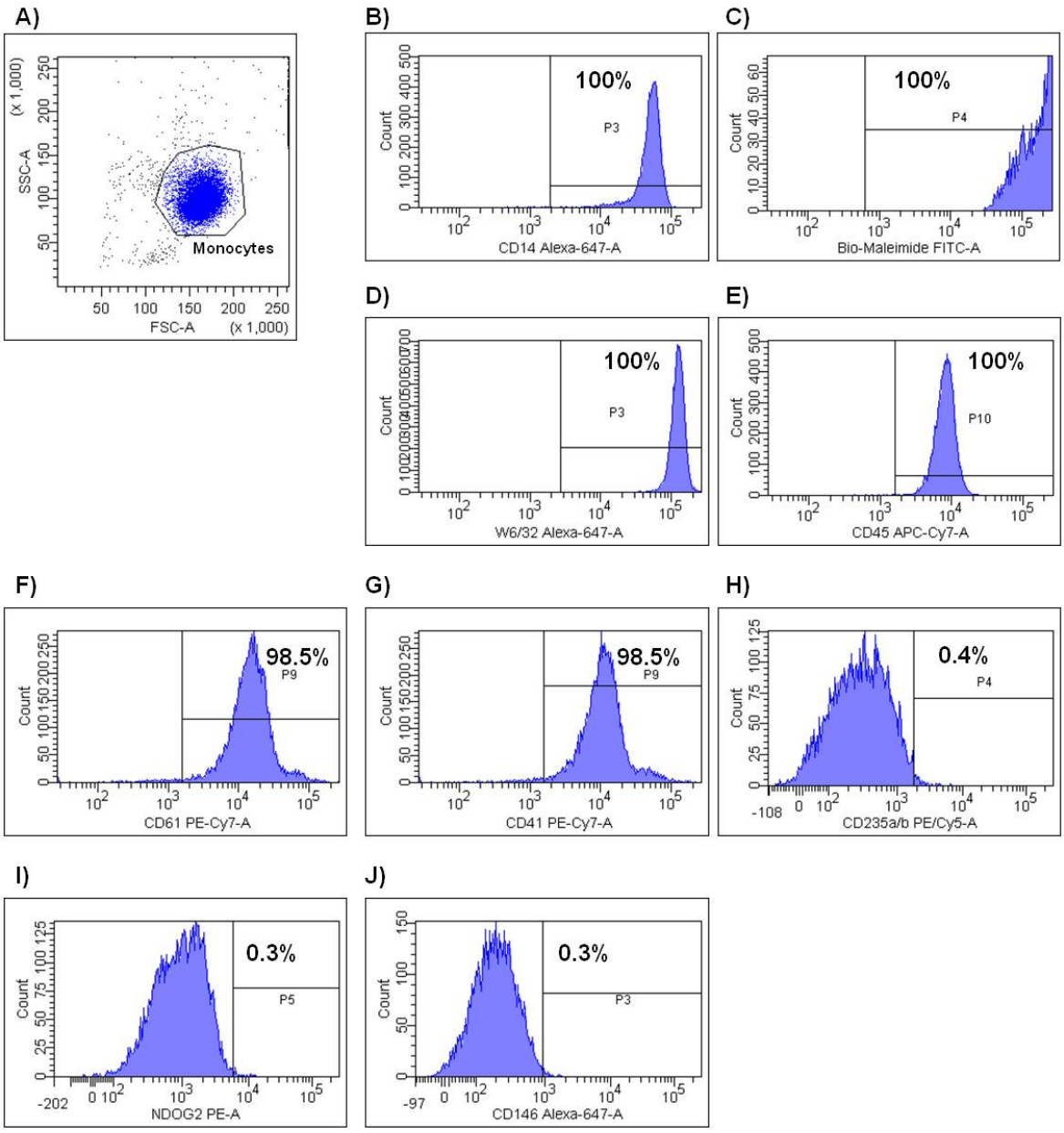

Figure 19. Flow cytometric analysis of monocytes after CD14 magnetic bead isolation. A) FSC vs. SSC profile of monocytes. Representative histograms showing the percentage of positive labelling with **B)** CD14, **C)** Bio-Maleimide, **D)** W6/32, **E)** CD45, **F)** CD61 **G)** CD41, **H)** CD235a/b, **I)** NDOG2 and **J)** CD146.

Monocytes were stimulated to produce vesicles using a combination of LPS and A-23187, following a previously described method (Aharon *et al.*, 2008) used to stimulate the release of vesicles from the monocyte cell line THP-1. A 2.7-fold increase (p=0.08) in monocyte vesicles was observed in the group stimulated with LPS + A-23187 as compared to the control (monocytes in culture medium) (Figure 20).

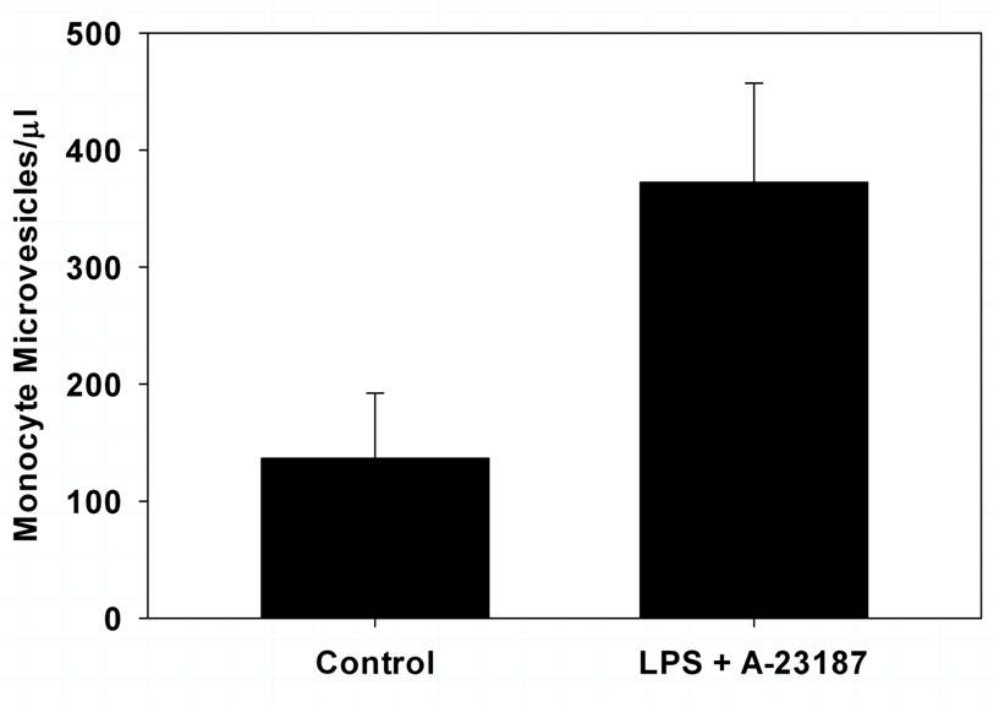

Figure 20. Flow Cytometric analysis of monocyte-derived vesicles stimulated using LPS + A-23187. 5 hour stimulation of monocyte vesicles measured in culture medium only (Control) or after treatment with 1µg/ml LPS + 10µmol/L A-23187. Bars represent Mean ± SE. Results are from three independent experiments.

Representative histograms of LPS + A-23187 vesicles are shown in Figure 21. A FSC vs. SSC profile of the monocyte vesicles after stimulation with LPS + A23187 is shown in Figure 21A. Monocyte vesicles stimulated using LPS + A-23187 were labelled with Bio-Maleimide, CD14, W6/32, CD45, CD61 and CD41 (Figure 21B-G). No expression of PLAP, CD235a/b or CD146 was observed on monocyte cells but due to the limited number of vesicles available it was not possible to test monocyte vesicles for the expression of these antigens.

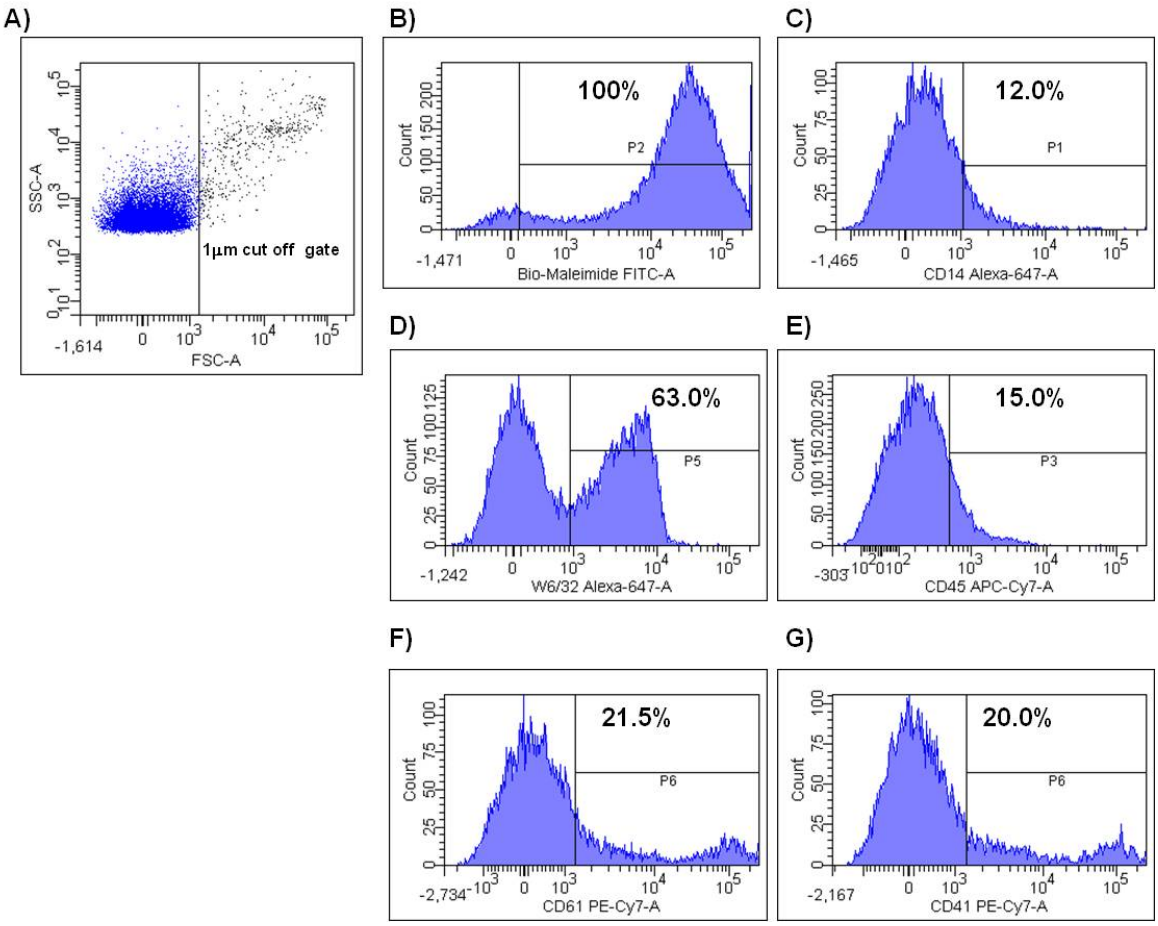

Figure 21. Flow cytometry of monocyte vesicles stimulated using LPS + A-23187. Representative histograms of monocyte derived vesicles stimulated using LPS + A-23187. **A)** FSC vs. SSC profile of monocyte vesicles. Percentage of positive labelling with **B)** Bio-Maleimide, **C)** CD14, **D)** W6/32, **E)** CD45, **F)** CD61 and **G)** CD41. Percentages have been adjusted to account for background contaminating particulates in culture media alone.

Greater than 95% of the control monocyte vesicles or those released after stimulation with LPS + A-23187 were Bio-Maleimide positive (Figure 22A). In comparison to monocyte cells, a significant decrease in the expression of CD14 (Figure 22B) and CD45 (Figure 22C) was observed in control and LPS + A-23187 stimulated monocyte vesicles. HLA Class I expression using the marker W6/32 (Figure 22D) was significantly lower on the control (50%) and LPS + A-23187 (60%) monocyte vesicles as compared to monocyte cells (100%). Similarly, CD61 (Figure 22E) expression was also significantly reduced on the control (39%) and LPS + A-23187 (34.5%) monocyte vesicles as compared to monocyte cells (99%). Due to sample size constraints, CD41 expression was examined

only on vesicles derived from LPS + A-23187 stimulation. Expression of CD41 (Figure 22F) was significantly reduced on vesicles in comparison to monocyte cells. Of all the antigens examined, HLA Class I was shown to be the most highly expressed antigen on the monocyte vesicles using the marker W6/32.

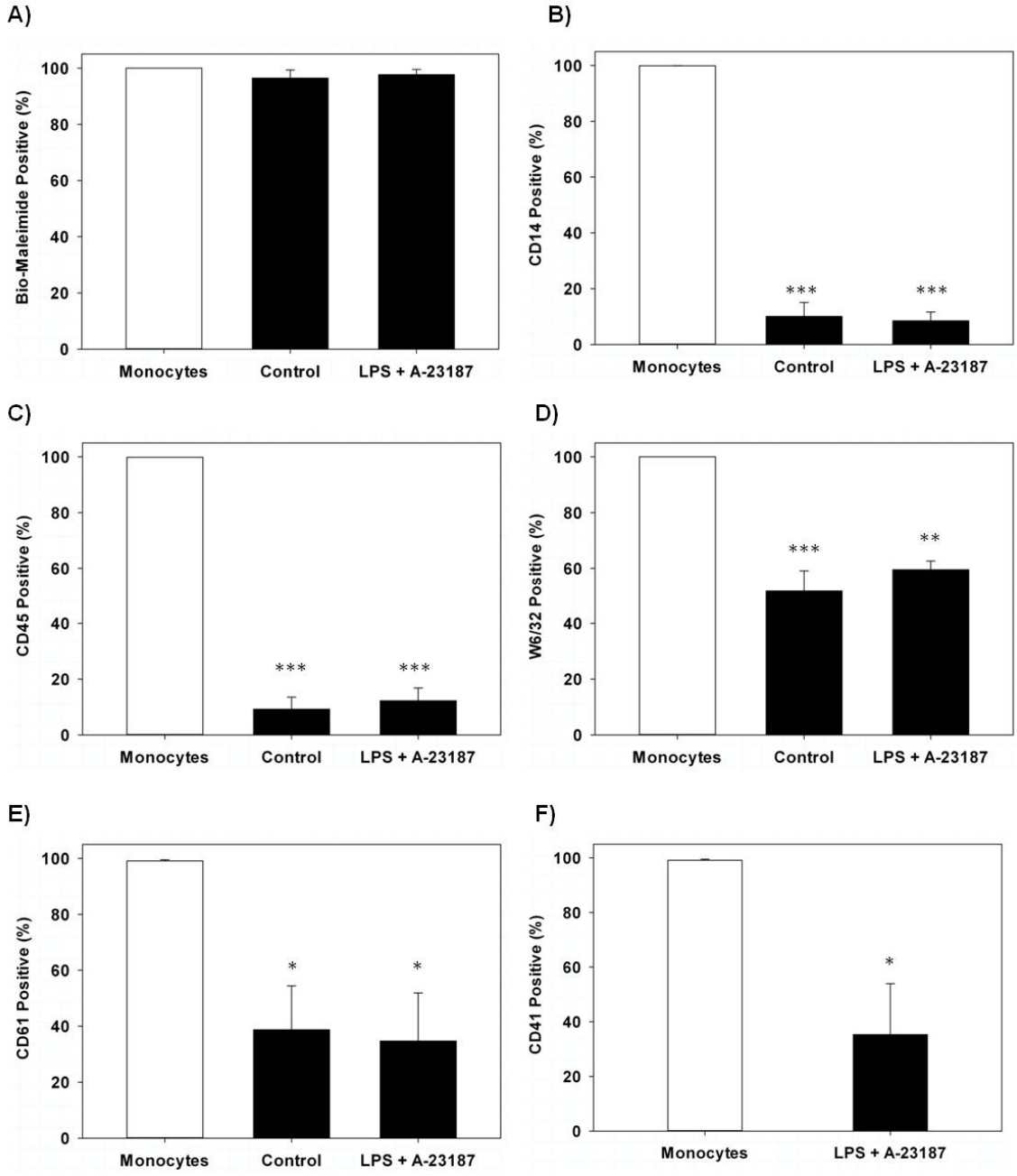

Figure 22. Flow cytometry analysis of antigen expression on monocyte and monocyte vesicles. Data are from three independent experiments showing the percentage of positive staining with **A)** Bio-Maleimide, **B)** CD14, **C)** CD45, **D)** W6/32, **E)** CD61 and **F)** CD41 on monocytes (□) and monocyte vesicles (■) stimulated ± LPS + A-23187. Percentages have been adjusted to account for background contaminating particulates in culture media alone. Bars represent Mean ± SE. p values (*p<0.05, **p<0.01 and ***p<0.001) compare monocytes vs. control and LPS + Calcium Ionophore A-23187 lymphocyte vesicles.

2.4.7 Flow Cytometric Analysis of Lymphocytes and *In vitro* Derived Lymphocyte Vesicles

To determine the most suitable marker to use for the detection of lymphocyte vesicles *in vivo* and to check for antibody cross reactivity we tested a panel of antibodies using *in vitro* derived lymphocyte vesicles. The antibody panel (as described in Materials and Methods 2.3.3.2) was first tested on lymphocytes which were isolated from PBMCs by negative selection using immunomagnetic anti-CD14 MicroBeads. The purity of the lymphocyte population was >90% as determined by their FSC and SSC characteristics (Figure 23A) and labelling with a lymphocyte marker anti-CD3. Representative histograms showing the percentage of lymphocyte positive labelling are shown in Figure 23B-K.

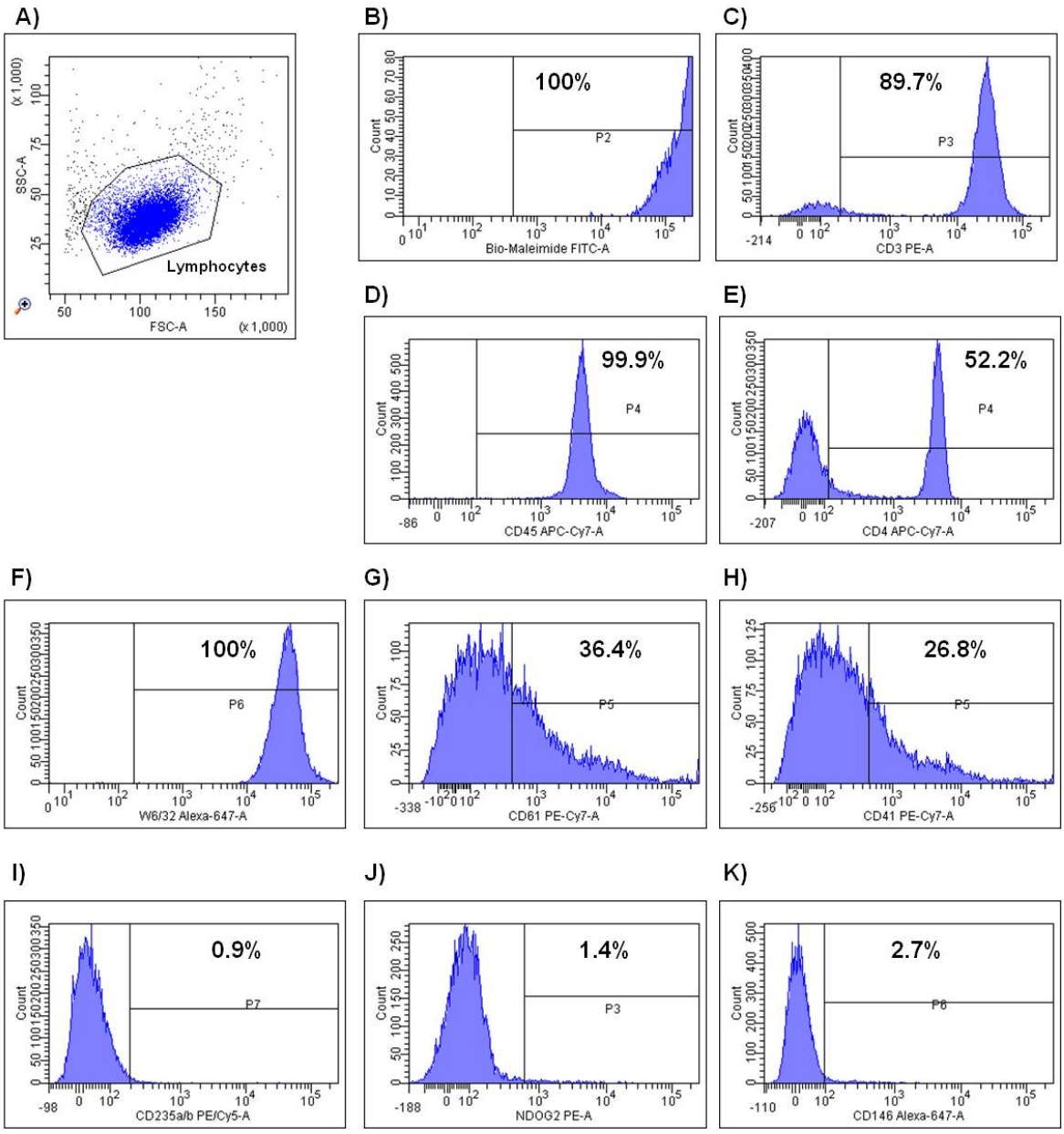

Figure 23. Flow cytometric analysis of lymphocytes. A) FSC vs. SSC profile of lymphocytes. Representative histograms showing the percentage of positive labelling with **B)** Bio-Maleimide, **C)** CD3, **D)** CD45, **E)** CD4, **F)** W6/32, **G)** CD61, **H)** CD41 **I)** CD235a/b, **J)** NDOG2 and **K)** CD146.

Lymphocytes were stimulated to produce vesicles using PMA + ionomycin, a common method used to activate T Cells *in vitro* or with the apoptosis-inducing reagent STS. Stimulation with PMA + ionomycin or STS resulted in a similar number of lymphocyte vesicles (Figure 24). The number of vesicles was elevated, but not significantly in the 20 hour control group compared to the 4 hour control group. This was probably a reflection of

the culture time period. The number of PMA + ionomycin vesicles was increased compared to the control group (lymphocytes in culture medium), however this was not significant (Figure 24). Vesicle number in the STS stimulated lymphocytes was not different to that of the control group (Figure 24).

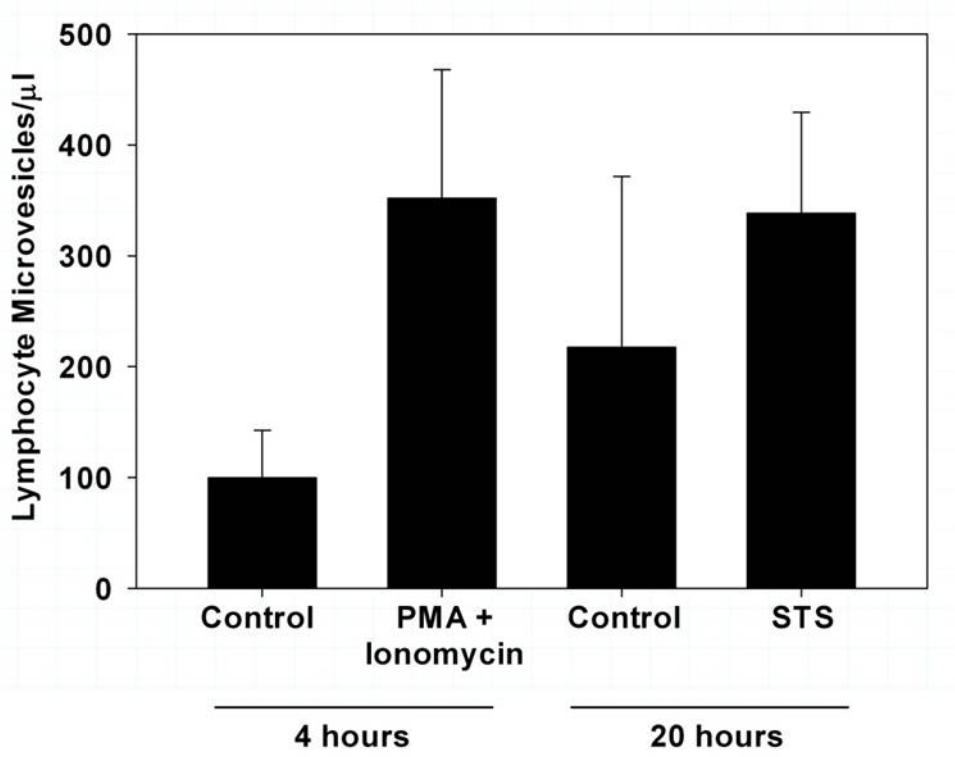

Figure 24. Flow cytometry total lymphocyte vesicle counts. 4 hour stimulation of lymphocyte vesicles measured in culture medium only (Control) or with 10ng/ml PMA + 2µmol/L Ionomycin. 20 hour stimulation of lymphocyte vesicles measured in culture medium only (Control) or with 10µmol/L staurosporine (STS). Bars represent Mean ± SE. Results are of 3 independent experiments.

Representative histograms of vesicles stimulated from lymphocytes using PMA + ionomycin or STS are shown in Figure 25 and Figure 26 respectively. A FSC vs. SSC profile of the vesicles from lymphocytes treated with PMA + ionomycin is displayed in Figure 25A. These vesicles were labelled with Bio-Maleimide (Figure 25B), CD3 (Figure 25C), W6/32 (Figure 25D), CD45 (Figure 25E), CD4 (Figure 25F) and CD61 (Figure 25G).

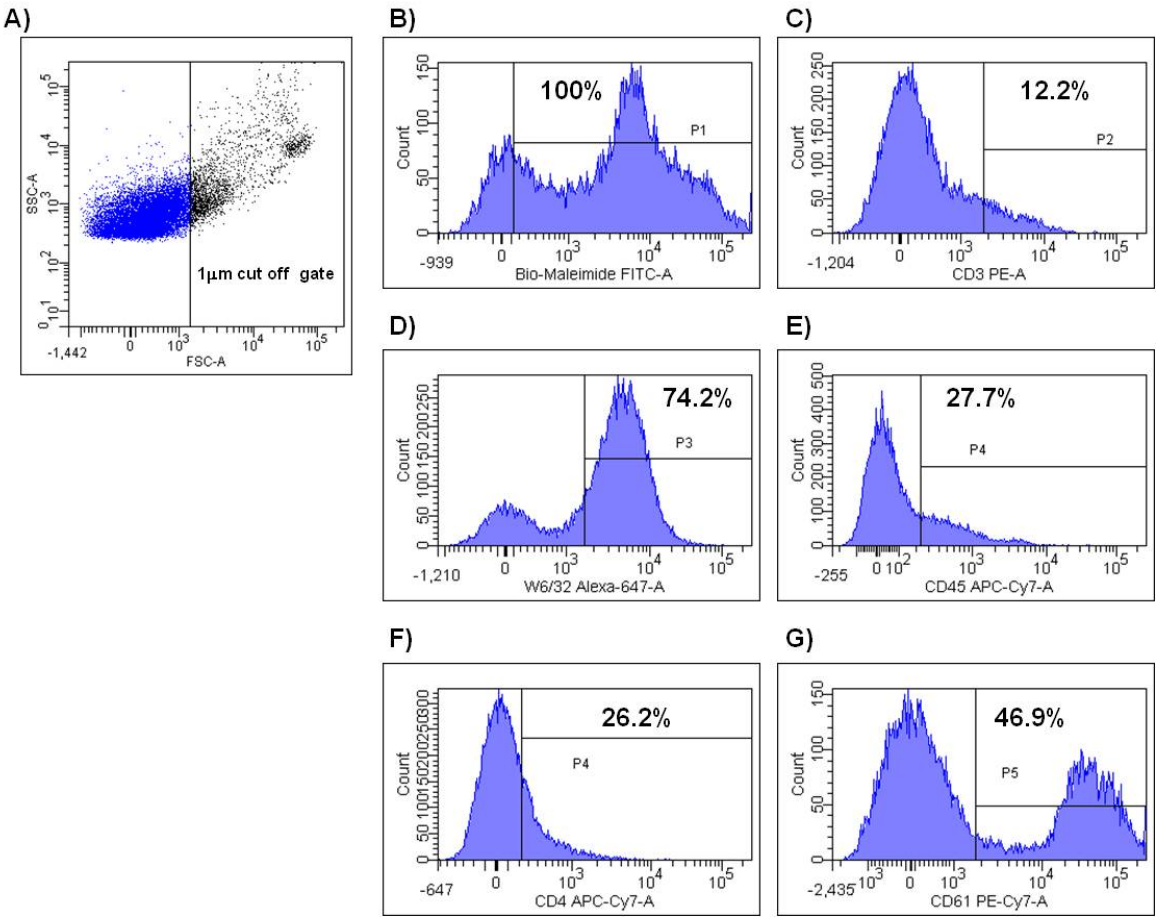

Figure 25. Flow cytometry of lymphocyte vesicles after stimulation using PMA + ionomycin. Representative histograms of PMA + Ionomycin stimulated lymphocyte vesicles. **A)** FSC vs. SSC profile of lymphocyte vesicles. Percentage of positive labelling with **B)** Bio-Maleimide, **C)** CD3, **D)** W6/32, **E)** CD45, **F)** CD4 and **G)** CD61. Percentages have been adjusted to account for background contaminating particulates in culture media alone.

Figure 26A shows a representative FSC vs. SSC profile of the vesicles from lymphocytes stimulated with STS. These vesicles were labelled with Bio-Maleimide (Figure 26B), CD3 (Figure 26C), W6/32 (Figure 26D), CD45 (Figure 26E), CD4 (Figure 26F) and CD61 (Figure 26G). No expression of PLAP, CD235a/b or CD146 was observed on lymphocyte cells and due to the limited number of vesicles available it was not possible to test lymphocyte vesicles for the expression of these antigens.

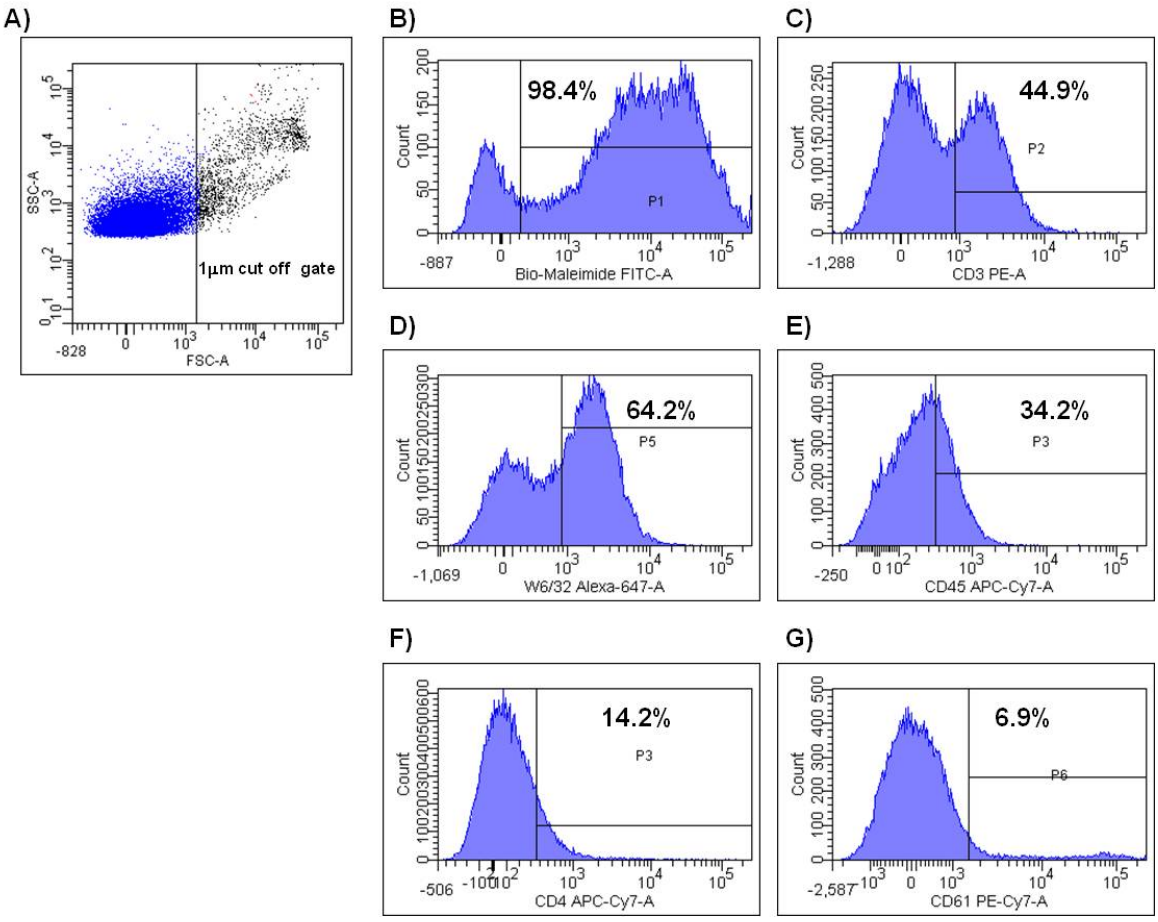

Figure 26. Flow cytometry of lymphocyte vesicles after stimulation using Staurosporine (STS). Representative histograms of STS stimulated lymphocyte vesicles. **A)** FSC vs. SSC profile of lymphocyte vesicles. Percentage of positive labelling with **B)** Bio-Maleimide, **C)** CD3, **D)** W6/32, **E)** CD45, **F)** CD4 and **G)** CD61. Percentages have been adjusted to account for background contaminating particulates in culture media alone.

More than 95% of the lymphocyte vesicles labelled with Bio-Maleimide (Figure 27A). Compared to lymphocyte cells a significant reduction in the expression of CD3 on vesicles was observed from the 4 hour control, PMA + ionomycin, 20 hour control and STS stimulated lymphocytes (Figure 27B). The decrease in CD3 expression on the vesicles derived from stimulation with PMA + ionomycin was significantly greater than that of the vesicles stimulated using STS (Figure 27B). Furthermore, the expression of CD45 (Figure 27C) and CD4 (Figure 27D) on lymphocyte vesicles in the 4 hour control, PMA + ionomycin, 20 hour control and STS treatment groups was significantly decreased compared to lymphocyte cells. Expression of HLA Class I on lymphocyte vesicles from all

the different treatment groups was lower as compared to lymphocyte cells, however this reduction was not significant (Figure 27E). Approximately one third of lymphocytes were found to express CD61 on their surface (Figure 27F). Greater than 60% of lymphocyte vesicles derived from the 4 hour control group and 75% derived from the PMA + ionomycin treatment group expressed CD61 (Figure 27F). Interestingly, significantly fewer lymphocyte vesicles were shown to express CD61 when lymphocytes were stimulated with STS compared to PMA + ionomycin (Figure 27F).

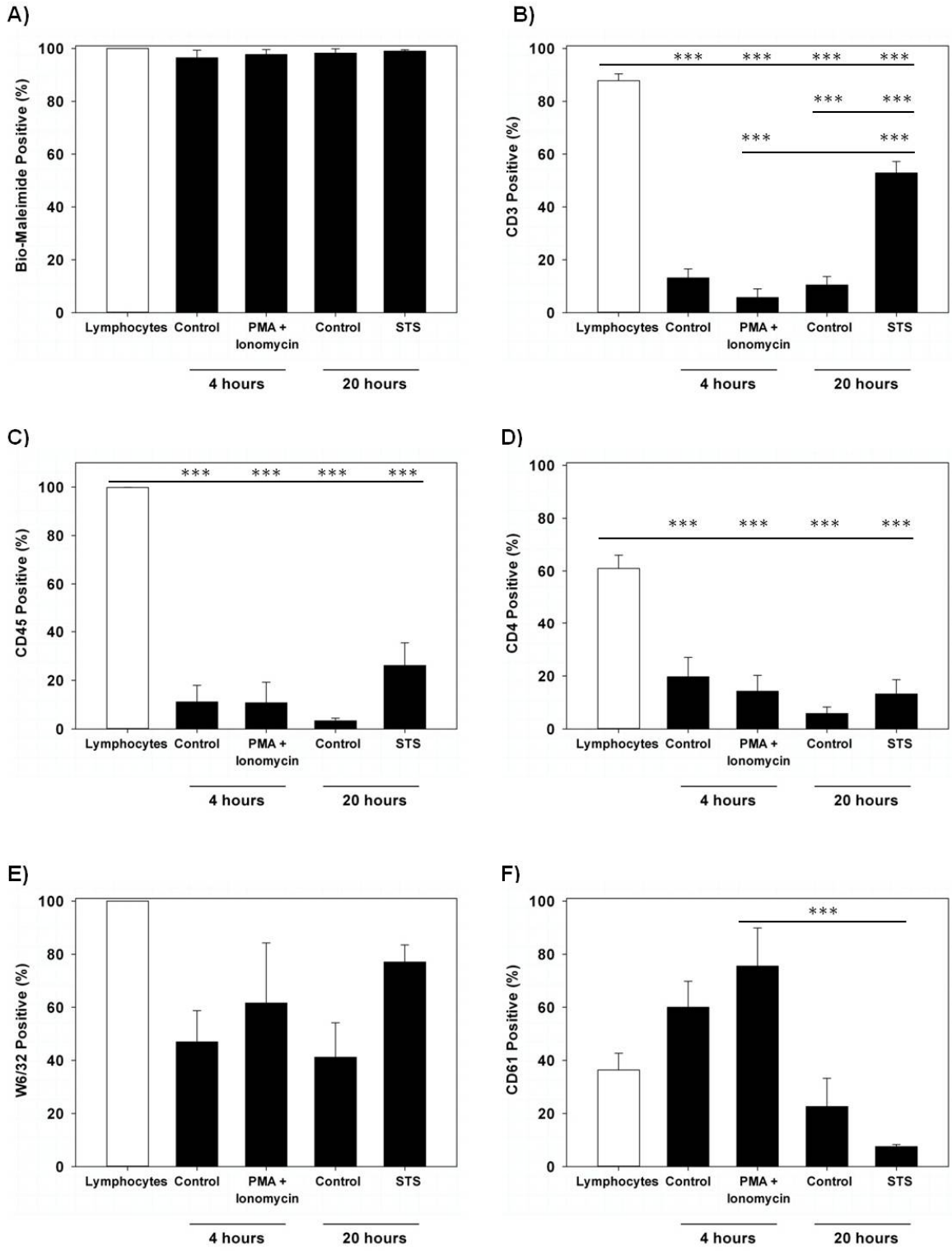

Figure 27. Flow cytometry analysis of antigen expression on lymphocytes and lymphocyte vesicles. Data are from three independent experiments showing the percentage of positive staining with **A)** Bio-Maleimide, **B)** CD3, **C)** CD45, **D)** CD4, **E)** W6/32 and **F)** CD61 on lymphocytes (□) and lymphocyte vesicles (■) stimulated ± PMA + ionomycin. Percentages have been adjusted to account for background contaminating particulates in culture media alone. Bars represent Mean ± SE. p values (**p<0.01 and ***p<0.001) compare lymphocytes vs. treatment groups and between treatment groups.

2.4.8 Flow Cytometric Analysis of Granulocyte Vesicles

Granulocytes were isolated using a step density Percoll gradient and further enriched using immunomagnetic anti-CD15 MicroBeads. The purity of the isolation method was first assessed by identifying and gating the granulocyte population based on their FSC and SSC characteristics using a FSC threshold of 35,000 (arbitrary units). >90% of isolated cells were within the granulocyte gate (Figure 28A). Granulocytes were labelled with an antibody against CD66b, a granulocyte marker, and expression was >99% in all three individuals (Figure 28B). Granulocytes were further tested for antibody cross reactivity by labelling with a panel of antibodies (as described in Materials and Methods 2.3.3.2) and the membrane marker Bio-Maleimide. Representative histograms showing the percentage of positive staining with Bio-Maleimide and for each antibody in the panel are shown in Figure 28C-J.

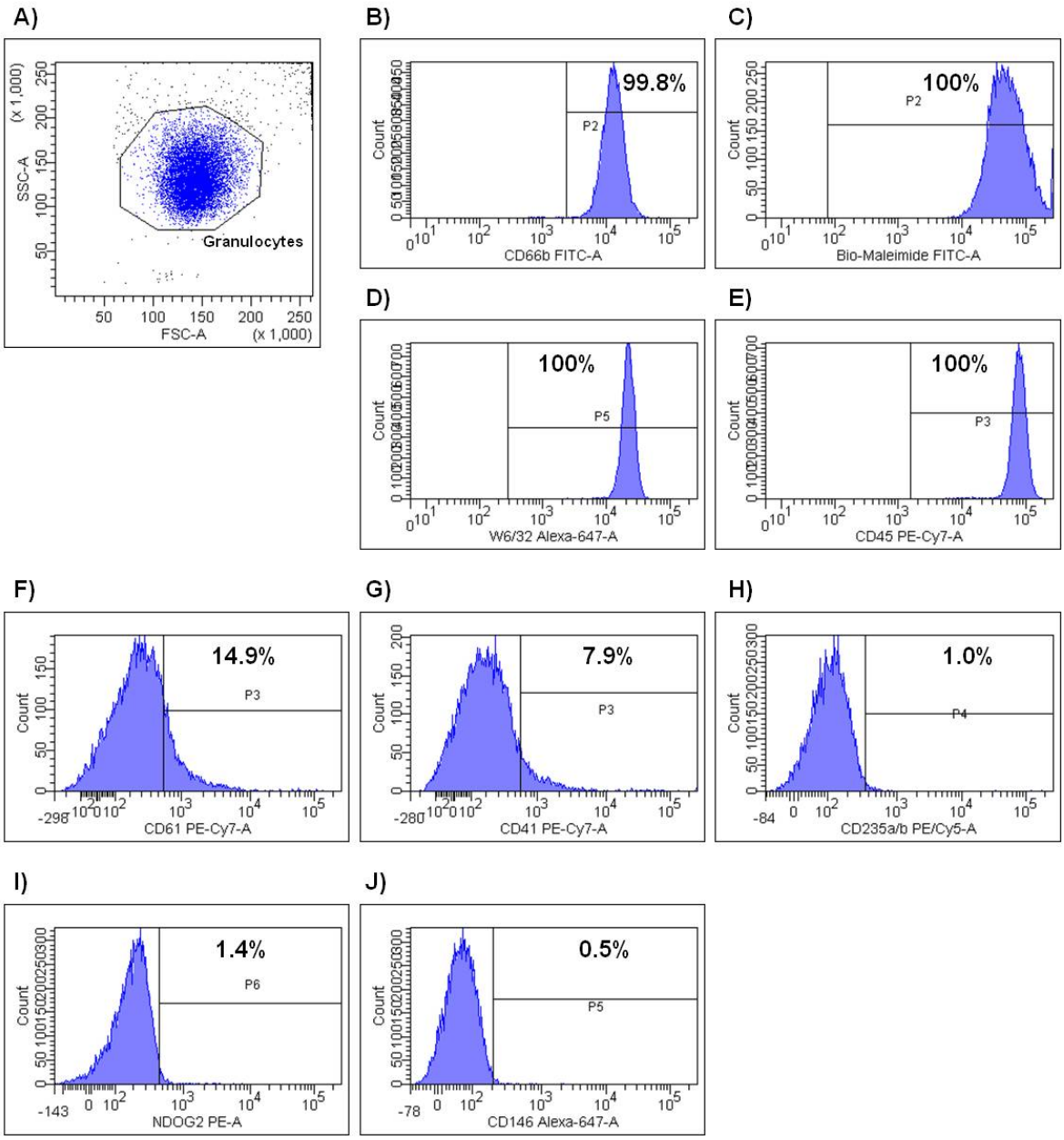

Figure 28. Flow cytometric analysis of granulocytes after CD15 magnetic bead isolation. A) FSC vs. SSC profile of granulocytes. Representative histograms showing the percentage of positive labelling with **B)** CD66b, **C)** Bio-Maleimide, **D)** W6/32, **E)** CD45, **F)** CD61 **G)** CD41, **H)** CD235a/b, **I)** NDOG2 and **J)** CD146.

Vesicle release was measured from granulocytes cultured *in vitro* for 18 hours. Unlike monocytes and lymphocytes, granulocytes were not stimulated with an agonist to induce vesicle production as granulocytes cultured alone for 18 hours undergo apoptosis (Pletz *et al.*, 2004) and hence will release large numbers of vesicles as shown in Figure 29.

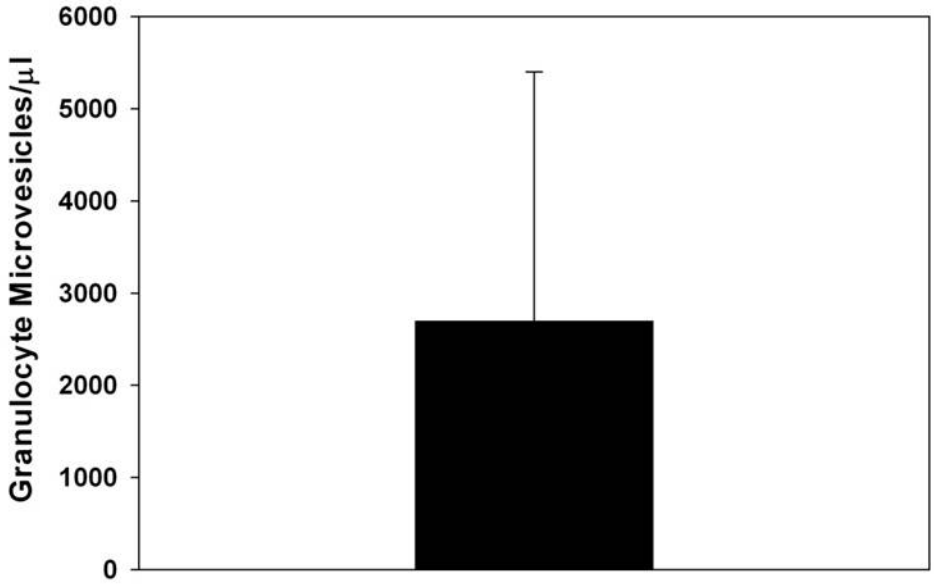

Figure 29. Flow cytometry total granulocyte vesicle counts. Granulocyte vesicles measured in culture medium after 18 hours. Bar shows Median with the interquartile range. Results are of 3 independent experiments.

Representative histograms of granulocyte vesicles are shown in Figure 30. A FSC vs. SSC profile of the granulocyte vesicles is displayed in Figure 30A. These vesicles were labelled with Bio-Maleimide (Figure 30B), CD66b (Figure 30C), W6/32 (Figure 30D), CD45 (Figure 30E), CD61 (Figure 30F) and CD41 (Figure 30G), CD235a/b (Figure 30H), NDOG2 (Figure 30I) and CD146 (Figure 30J).

The majority (>95%) of the granulocyte vesicles were Bio-Maleimide positive (Figure 31A). In comparison to granulocyte cells, a significant decrease in the expression of CD66b (Figure 31B), HLA Class I (using the marker W6/32) (Figure 31C) and CD45 (Figure 31D) was observed on granulocyte vesicles. Less than 20% of granulocyte cells expressed CD61 and expression was reduced on granulocyte vesicles, but not significantly (Figure 31E). CD41 expression on the surface of the granulocyte vesicles was significantly decreased in comparison to granulocyte cells (Figure 31F). No expression of CD235a/b

(Figure 31G), PLAP (Figure 31H) or CD146 (Figure 31I) was detected on granulocyte cells or granulocyte vesicles.

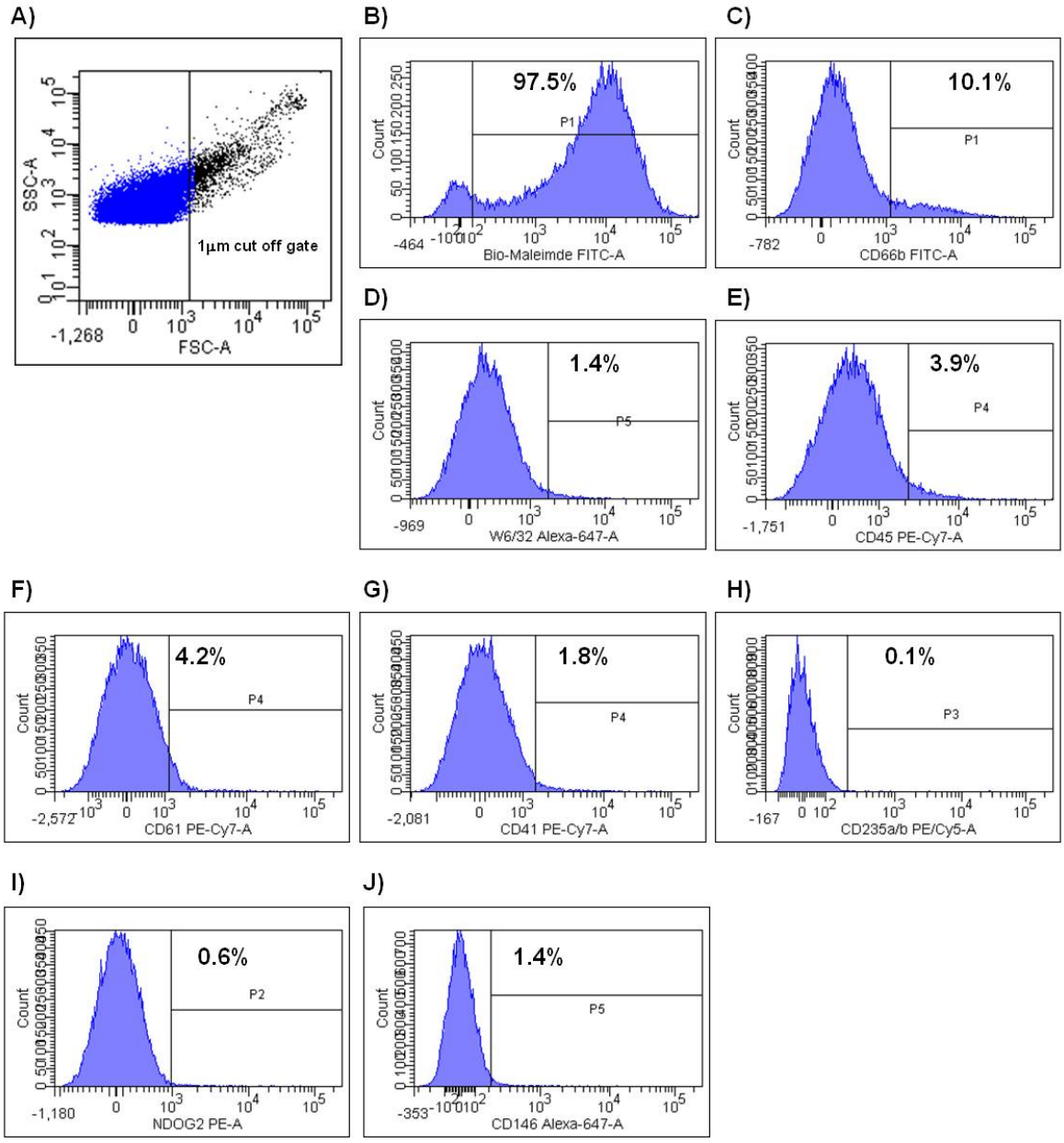

Figure 30. Flow cytometry of granulocyte vesicles. Representative histograms of granulocyte vesicles. **A)** FSC vs. SSC profile of granulocyte vesicles. Percentage of positive labelling with **B)** Bio-Maleimide, **C)** CD66b, **D)** W6/32, **E)** CD45, **F)** CD61, **G)** CD41, **H)** CD235a/b, **I)** NDOG2 and **J)** CD146. Percentages have been adjusted to account for background contaminating particulates in culture media alone.

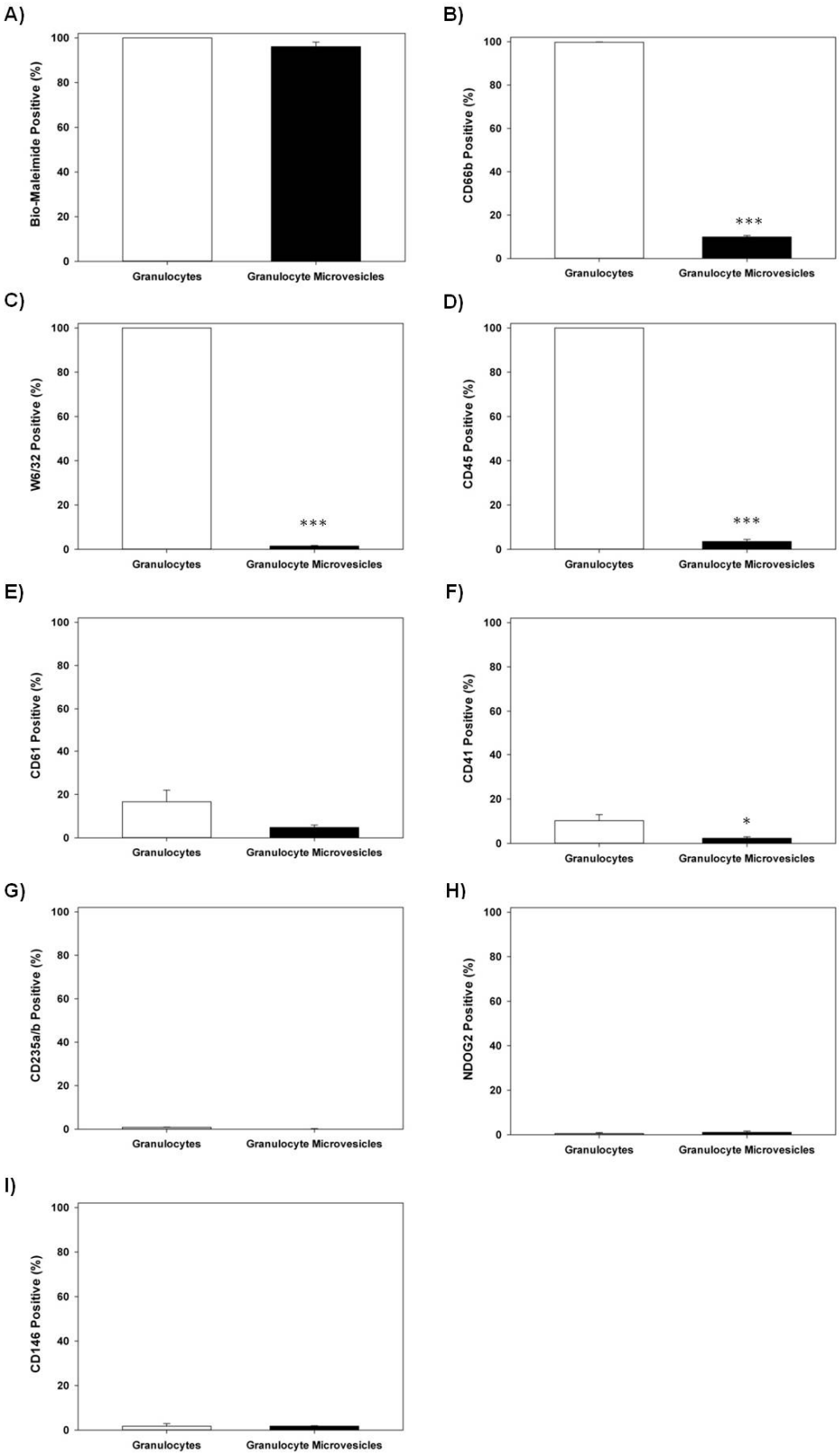

Figure 31. Flow cytometry analysis of antigen expression on granulocyte and granulocyte vesicles. Data are from three individual experiments showing the percentage of positive staining with **A)** Bio-Maleimide, **B)** CD66b, **C)** W6/32, **D)** CD45, **E)** CD61, **F)** CD41, **G)** CD235a/b, **H)** NDOG2 and **I)** CD146 on granulocytes (□) and granulocyte vesicles(■). Percentages have been adjusted to account for background contaminating particulates. Bars represent Mean ± SE. p values (*p<0.05. ***p<0.001) compare granulocytes vs. granulocyte vesicles.

2.5 Discussion

2.5.1 Flow Cytometry Set Up to Detect Vesicles

In this chapter the sensitivity of our BD LSRII flow cytometer for vesicle analysis was evaluated. The flow cytometer had no modifications made to the electronics, fluidics or optics. However, the instrument was carefully maintained by adhering to a rigorous cleaning regime to reduce the build-up of background debris in the tubing and flow cell which would impede the detection of vesicles.

A threshold parameter is used in flow cytometry to limit the number of events that the flow cytometer processes. Once a threshold value has been set, the flow cytometer will only process events that are equal to or greater than the set threshold. Conventionally, FSC thresholds are used when examining cells to eliminate events such as debris from being included in the analysis. Initial experiments were carried out on our flow cytometer to investigate using a FSC threshold for the analysis of vesicles. Fluorescent polystyrene beads ranging in size from 200nm - 1μm were used. It was clear that the FSC detector on our flow cytometer was sub-optimal for the detection of vesicles as a large amount of instrument "noise" was present, compromising the signal of the 200nm and 290nm beads (data not shown). Alternatively, the minimum SSC threshold of 200 (arbitrary units) for this instrument was set and tested for the analysis of vesicles. Using these settings the BD LSRII flow cytometer could detect 200nm beads, but similar to using a FSC threshold these appeared in the same region as the instrument "noise". On this basis, lowering the FSC and SSC voltages to give a 300nm cut off was a more realistic limit for the detection of vesicles and gave a far superior signal/noise ratio when compared to using a FSC threshold.

Another option is to use a fluorescence threshold, whereby cells/vesicles are pre-labelled with a fluorescent stain or fluorescent conjugated antibody. Each cell/vesicle will only be detected when the fluorescent signal rises above the threshold set. The advantage of using a fluorescence threshold compared to a SSC or FSC threshold is that non-fluorescent instrument "debris" that would normally be detected using light scatter would be excluded. This greatly improves the level of sensitivity of the instrument, therefore allowing the detection of vesicles <200nm. However, the major drawback to using a fluorescence threshold is that it assumes that all cells/vesicles label with the fluorescent marker of interest. Whilst this is true for fluorescent polystyrene beads, as they have a uniform distribution of fluorescence, the same assumption cannot be made when analysing biological vesicles and will result in vesicles negative for the fluorescent marker being excluded from the analysis.

During the course of this study a mixture of fluorescent beads (0.5μm, 0.9μm and 3.0μm) termed "Megamix beads" were released onto the market. One of the most extensive studies using these beads aimed to provide a reproducible flow cytometry method to analyse platelet vesicles >0.5μm (Robert *et al.,* 2009). A recent follow up study carried out by the International Society on Thrombosis and Haemostasis (ISTH) Scientific and Standardisation Comittee Working Group on Vascular Biology (Lacroix *et al.,* 2010b) aimed to standardise platelet vesicle measurement using Megamix beads. The same batch of Megamix beads, frozen platelet free plasma (PFP) (with three different concentrations of platelet vesicles) and platelet antibodies were provided to forty different laboratories across fourteen countries. The results showed that 33/49 (67%) of flow cytometers tested met the specified criteria and could therefore be used for vesicle detection. However, in use this gating strategy showed large discrepancies between cytometers when analysing

platelet vesicles. The fluorescent bead mix used in our study aimed to extend the analysis of vesicles below <0.5μm and to give a more accurate determination of size.

The defined upper size limit of a vesicle is arbitrarily considered to be 1.0μm. This is a general consensus in the field, but there is no solid evidence in the literature to prove this and it is probable that vesicles >1.0μm exist. Practically, however it is difficult to distinguish true vesicles >1.0μm from small platelets, apoptotic/necrotic bodies or aggregates of vesicles. For these reasons a 1μm size limit is considered to be the standard when analysing and enumerating vesicles and this size limit was used in the flow cytometry experiments described here.

2.5.2 *In vitro* Derived Vesicles

In this study *in vitro* derived vesicles were generated from a variety of cell types which are found in plasma. The primary aim was to test panels of antibodies on cellular derived vesicles to examine antibody specificity. In doing this, the results demonstrated that not all antigens found on the surface of the parent cell are present on the surface of the cellular derived vesicles. The antibody panels chosen by many researchers to investigate different cellular vesicles *in vivo* are based on the unproven assumption that the antigens expressed on the cell surface will also be present on the surface of the cellular derived vesicles. These experiments have helped identify a suitable panel of specific antibodies that can then be used to analyse these vesicles *in vivo* in plasma.

pSTBM

First, it was demonstrated that the placental vesicle (pSTBM) preparation was predominantly syncytiotrophoblast derived with the vast majority (>94%) of the vesicle

population labelling positive with the trophoblast marker NDOG2 (anti-PLAP antibody). NDOG2 antibody labelling of pSTBM was also confirmed by immunogold transmission electron microscopy. The syncytiotrophoblast is HLA Class I negative (Shorter *et al.*, 1993) and the purity of the pSTBM preparation was further confirmed by the negligible amounts of HLA Class I and CD235a/b expression. pSTBM also expressed high amounts of CD61 (76.4%) and to a lesser degree CD41 (27.4%). Hence, *in vivo* placental vesicles may be identified as $PLAP^+/CD61^+$ or $PLAP^+/CD41^+$. Endothelial cell markers including; CD146, CD144 and CD105 were examined for cross-reactivity with pSTBM and only CD105 was shown to be highly expressed.

Platelet vesicles

As previous studies have shown, vesicles can be produced from platelets *in vitro* using agonists such as thrombin receptor activating peptide (TRAP) and A-23187 (Abid Hussein *et al.*, 2003, Perez-Pujol *et al.*, 2007, Trummer *et al.*, 2008). Platelet vesicles were generated using A-23187 and it was found that this agonist produced a large number of vesicles of which >90% were <1.0μm in size. All platelets and most platelet vesicles stained positive with Bio-Maleimide and using a panel of antibodies were shown to express the antigens CD41, CD61 and HLA Class I. The percentage of vesicles labelled with Bio-Maleimide and stained positive for CD41, CD61 and HLA Class I were reduced as compared to platelets. 95% of the platelet vesicles labelled with the membrane marker Bio-Maleimide, indicative of the purity of the preparation. The 5% of platelet vesicles that did not label with Bio-Maleimide suggests that there were a very small number of contaminating particulates in the platelet vesicle preparation. Even though measures were taken to minimise background contaminating particles by filtering all buffers through a 0.1μm filter, it is possible that a small amount of particulate matter can pass through the

filter membrane. Also, some particles may have come from the A-23187 reagent. CD41 and CD61 were found to be expressed on >90% of the platelet vesicles and >80% expressed HLA Class I. These observations suggest that the majority of platelet vesicles express the same antigens as their parent cell. However, there were a small number of vesicles produced in which these antigens were not present at detectable levels and this was more pronounced with expression of HLA Class I compared to CD41 and CD61.

Various factors effecting vesicle release, which may help to explain these differences, include; the method used to isolate the platelets, the agonist and its concentration and the stimulation time. For example, three separate studies examined the expression of CD62-P (P-Selectin) on platelet vesicles stimulated using A-23187 (Abid Hussein *et al.,* 2003, Perez-Pujol *et al.,* 2007, Trummer *et al.,* 2008) and obtained different results. Two of the studies (Abid Hussein *et al.,* 2003, Perez-Pujol *et al.,* 2007) used very similar stimulation conditions (a preparation of washed platelets, comparable concentrations of agonist, yet slightly different stimulation times) and showed a high level of CD62P expression on the platelet vesicles. In contrast, a third study (Trummer *et al.,* 2008) found low levels of CD62P expression. In their experiments, platelets were stimulated for the same time, but a preparation of PRP rather than washed platelets was used and also the dose of agonist was much higher. These methodological variations between studies may account for the difference seen in antigen expression. Moreover, one study (Perez-Pujol *et al.,* 2007) showed that CD42b (Platelet Glycoprotein Ib) and CD61 were expressed at comparable levels on platelet vesicles produced by TRAP or A-23187, however the expression profile of CD62P was markedly reduced on TRAP vs. A-23187 stimulated vesicles. Therefore, it may be speculated that the observation made in the current study showing 80% expression

of HLA Class I, on platelet vesicles derived from A-23187 stimulation would be different in response to another agonist such as TRAP.

RBC vesicles

Vesicles were also generated from RBCs using A-23187, all of which labelled positive with Bio-Maleimide and >90% expressed CD235a/b. These RBC vesicles were screened with an antibody panel consisting of platelet, endothelial, MHC Class I and placental markers none of which were expressed. Stimulation of RBCs with A-23187 produced a population of vesicles in which >98% were <1μm in size. It is also interesting to note the scatter characteristics of the RBC vesicles. Two very distinct populations were evident in all three independent experiments (Figure 13A). It is impossible to know whether the larger of the two populations consist of genuinely larger vesicles or whether this is vesicle aggregation. Furthermore, this may be directly associated with the stimulation conditions, hence if the agonist or stimulation time was changed the scatter profile could also be altered.

The majority (>90%) of the RBC vesicles expressed CD235a/b, however when compared to the expression on RBCs (>99%) this was significantly reduced. In a previous study (Trummer *et al.,* 2008) describing RBC derived vesicles the expression of Glycophorin A, but not Glycophorin B was examined as the antibody used only recognised CD235a. The expression of CD235a on the RBC vesicles was ~50%, considerably lower compared to our results. These differences are likely to be explained by the purity of the starting RBC preparation from which the vesicles were derived. In our experiments an isolated population of RBCs was stimulated with A-23187, whereas the former study (Trummer *et al.,* 2008) also used A-23187, but stimulated whole blood. Other vesicles such as those

derived from platelets would have also been produced when stimulating whole blood. Hence, not all vesicles would have labelled CD235a positive. Our results suggest that during the formation of RBC vesicles from their parent cell some selection of the membrane antigens Glycophorin A and B must take place, otherwise the percentage of positive labelling on the vesicles would be equivalent to the RBCs. These results are in agreement with a previous study (Salzer *et al.,* 2002) who used gel electrophoresis/silver staining to show a reduction in Glycophorins and Band 3 (a membrane transport protein mediating the exchange of chloride for bicarbonate across the plasma membrane) in vesicles stimulated by A-23187 compared to RBCs.

Endothelial vesicles

A former study carried out on *in vitro* HUVEC and HUVEC vesicles examined the expression of ten different antigens in the presence or absence of IL-1α (Abid Hussein *et al.,* 2003). This study concluded that antigen expression on vesicles varied in comparison to HUVEC and antigen expression was dependent on the activation status of the parent cell (Abid Hussein *et al.,* 2003). Furthermore, another study (Simak *et al.,* 2002) saw differences in antigen expression on vesicles from CPT treated HUVEC vs. HUVEC when examining the expression of endothelial antigens CD59 and CD105. All CPT treated HUVEC vesicles expressed CD59, whereas only 50% expressed CD105. The current study has extended on both of these. The same agonists (IL-1α or CPT) were used to stimulate HUVEC vesicle production and antigen expression was examined on the parent cells and the HUVEC vesicles using a panel of markers, some of which had not previously been studied. In agreement with the latter study (Simak *et al.,* 2002) we found an increase in vesicle number from CPT stimulated HUVEC. No increase in vesicle number was apparent from IL-1α treated HUVEC.

In reference to the panel of markers examined in this study, no expression of PLAP or CD235a/b and very low amounts of CD41 on the surface of HUVEC or HUVEC vesicles were found. Thus, these antibodies have no cross reactivity with endothelial cells. In accordance with previous studies (Simak *et al.*, 2002, Abid Hussein *et al.*, 2003) a reduction in the percentage of positive labelling for antigens expressed on the surface of the HUVEC vesicles as compared to their parent cell was also found. All HUVEC labelled positive with Bio-Maleimide and for CD105, CD61, HLA Class I, CD146 and CD144, however the expression of Bio-Maleimide was slightly reduced, whereas all these antigens were significantly diminished on the surface of the vesicles, some to a greater extent than others. The small reduction in Bio-Maleimide positivity on the HUVEC vesicles suggests that a small amount of contaminating non-membrane particulate matter was present in the vesicle sample. This was probably due to the small number of particles that remained in the 0.1μm filtered culture media. CD105 was expressed on >60% of the vesicles from HUVEC stimulated using IL-1α and CPT, whereas only ~30% expressed CD146, ~20% expressed CD61 and <10% expressed HLA Class I or CD144.

CD62E expression was found on resting HUVEC and the percentage positive was increased by IL-1α stimulation (data not shown). Our results showed an increase in the percentage of vesicles expressing CD62E from IL-1α stimulated HUVEC, however the numbers are much lower than those previously reported (Abid Hussein *et al.*, 2003). Furthermore, in contrast to results previously described (Abid Hussein *et al.*, 2003) a higher number of CD61 and CD144 expressing vesicles from IL-1α treated HUVEC was observed. There are a number of possible reasons to explain these differences in the numbers of vesicles expressing these antigens. The first difference is the method used for vesicle isolation. The current study used high-speed ultracentrifugation at 150,000 × g

(max) for one hour, whereas the previous study (Abid Hussein *et al.,* 2003) used 2 x 30 min 17,570 × g centrifugations. The vesicles analysed in the present study are probably proportionally smaller as a centrifugation at 17,570 x g would not be expected to pellet the smaller vesicles. Secondly, different flow cytometers were used. In the current study a BD LSRII flow cytometer was used and followed a defined protocol with regard to instrument set-up, specifying the threshold set and size of vesicles examined. The previous study (Abid Hussein *et al.,* 2003) analysed vesicles using a BD FACSCalibur flow cytometer. No information regarding instrument threshold or an estimation as to the size of vesicles examined in this study was given. Furthermore, the BD FACSCalibur is an analogue instrument which cannot reliably discriminate vesicles below <0.5μm (Ayers *et al.,* 2011). Thirdly, the flow cytometry methodology differs between studies. The former study (Abid Hussein *et al.,* 2003) only analysed Annexin V positive vesicles and after antibody labelling the vesicles were washed by centrifugation at 17, 570 × g for 30 min. In this study all vesicles in the <1μm cut-off gate were analysed. A wash step of the vesicles after antibody labelling was not included as this would inevitably result in some vesicle loss. Taken together, all these factors impact on the final analysis of the vesicle population. Due to these methodological variations it is most likely that the vesicle populations in these two studies differ and thus may account for the observed variation in vesicle antigen expression.

Leukocyte vesicles

Many of the published studies of *in vitro* monocyte and lymphocyte derived vesicles have been performed using monocytic cell lines, including; THP-1 (Aharon *et al.*, 2008, Bernimoulin *et al.*, 2009) and HL60 (Trummer *et al.*, 2008, Reich and Pisetsky 2009) ,T Cell lines including: Jurkat T cells (Reich and Pisetsky 2009, Kornek *et al.*, 2011) and HUT-78 (Scanu *et al.*, 2008) and the pre-B leukemia cell line BV-173 (Trummer *et al.*, 2008). Cell lines provide an abundance of cells that can be stimulated to produce vesicles, but phenotypically may not be comparable to primary cells. We considered using HL-60, U937 and THP-1 cell lines to generate vesicles that would be representative of those derived from monocytes. However, initial experiments showed that none of these cell lines constitutively express CD14 (data not shown) and therefore may not be representative of primary blood monocytes. Therefore, in this study vesicles were generated from monocytes and lymphocytes isolated from peripheral blood.

Monocytes were stimulated with a combination of A-23187 and LPS to generate vesicles. Vesicle number was increased in response to the agonist, however this was not significant. Monocytes and vesicles were labelled with Bio-Maleimide and a panel of antibodies including; CD14, W6/32, CD45, CD61 and CD41. The number of monocytes expressing all these antigens exceeded 98%, whereas the numbers were significantly decreased for vesicles. Antigens were expressed on the vesicles at different levels. More than 50% of the vesicles expressed HLA Class I, ~40% expressed CD61 and CD41, and <20% expressed CD14 or CD45. As single labelling was carried out for each antibody, it is not clear from these data whether vesicles which are HLA Class I positive, shown by W6/32 expression also express CD61, CD41, CD14 or CD45. Further experiments would need to be carried out to obtain this information.

Isolated lymphocytes were stimulated with a combination of PMA + ionomycin or STS to induce vesicle shedding, however neither stimulation method generated a significant increase in vesicle number. Lymphocytes and lymphocyte vesicles were labelled with Bio-Maleimide and a panel of antibodies including; CD3, CD45, CD4, W6/32 and CD61. Labelling with antibodies to CD235a/b, PLAP and CD146 was also carried out on lymphocytes and was found to be negligible. For this reason and also due to sample constraints this was not done on the vesicles. CD41 was expressed at comparable levels to CD61 on lymphocytes and again due to sample size constraints was not tested on lymphocyte vesicles. Similar to the pattern observed with the monocytes and monocyte vesicles, the number of vesicles expressing some antigens was significantly reduced when compared to lymphocytes. This was apparent for CD3, CD45 and CD4. The percentage of vesicles expressing CD3 released from lymphocytes stimulated using STS was up-regulated five-fold in comparison to the percentage of CD3 expression on vesicles stimulated using PMA + ionomycin. This suggests that the expression of CD3 on vesicles is dependent upon the stimulus used for generation. HLA Class I was the most abundant antigen found on the surface of the lymphocyte vesicles and of all the antigens tested it was the only one found to be expressed at comparable levels to its parent cell.

The results of this study show that granulocytes cultured *in vitro* for 18 hours release large quantities of vesicles. Previous studies have shown that stimulating granulocytes with fMLP (N-formyl-methionine-leucine-phenylalanine) will also induce vesicle release (Gasser *et al.,* 2003, Gasser and Schifferli 2004, Gasser and Schifferli 2005). Greater than 99% of the granulocytes expressed CD66b, whereas its expression was significantly reduced by ~10-fold on the granulocyte vesicles. This is in contrast to previous results (Gasser *et al.,* 2003, Gasser and Schifferli 2005) showing that the majority of granulocyte

vesicles stimulated using fMLP expressed CD66b. There are many differences in the previous studies (Gasser *et al.,* 2003, Gasser and Schifferli 2005) that may account for the discrepancy in CD66b expression, including; the granulocyte fMLP stimulation, the methods used for isolation of the vesicles, indirect antibody labelling of the vesicles and the data were acquired using a FSC threshold. Similar to the results observed with the lymphocyte and monocyte vesicles, a significant reduction in the expression of CD45 was apparent on the granulocyte vesicles compared to the granulocytes from which they were derived. Data in this study has shown that unlike lymphocyte and monocyte vesicles which express HLA Class I, its expression was completely absent from the granulocyte vesicles. Furthermore, negligible amounts of CD235a/b, PLAP and CD146 were found on granulocytes or granulocyte vesicles. Both CD61 and CD41 were expressed on granulocytes and granulocyte vesicles, however not to the same degree when compared to lymphocytes or monocytes and their respective vesicles.

The positive CD61 and CD41 expression observed on monocytes, lymphocytes and granulocytes could possibly be due to platelet contamination in the preparations. It has been reported that activated platelets bind to leukocytes including lymphocytes, granulocytes and predominantly monocytes to form platelet-leukocyte aggregates (Jungi *et al.,* 1986, Rinder *et al.,* 1991, Harding *et al.,* 2007). The preparations of cells in this study may have included platelet-monocyte aggregates and platelet-lymphocyte aggregates, both of which have been subsequently cultured *in vitro*. Therefore, the *in vitro* derived monocyte and lymphocyte vesicle preparations may also contain platelet vesicles. The choice of anticoagulant can also effect the measurement of circulating platelet-monocyte aggregates, based on flow cytometric analysis of whole blood (Harding *et al.,* 2007, Bournazos *et al.,* 2008). Blood collected into tubes containing the anticoagulant sodium

citrate or EDTA had a lower percentage of platelet-monocyte aggregates compared to blood anticoagulated with heparin (Harding *et al.,* 2007, Bournazos *et al.,* 2008). The experiments in this study used blood anticoagulated with heparin as this is the preferred anticoagulant when analysing immune cell function. Furthermore, in this current study when platelet-monocyte and platelet-lymphocyte aggregates were measured using isolated PBMCs from blood collected into EDTA, sodium citrate or heparin no difference in the level of platelet-leukocyte aggregation using different anticoagulants was seen (data not shown). One study (Bournazos *et al.,* 2008) showed a reduction in platelet-monocyte aggregates after whole blood had been incubated with EDTA. In future experiments, EDTA could be added to the washing buffer to help minimise platelet-leukocyte aggregates.

2.5.3 Selecting Suitable Markers to Examine Plasma Vesicles

The results from these experiments have given an insight into the most abundantly expressed antigens on the surface of cells present in the blood and the vesicles derived from them. The data in this study has shown a significant reduction in the percentage of positively labelled vesicles using certain antibodies compared to the labelling of the parent cell. There are two possibilities that may be attributable to this reduction. Firstly, the antigens present on the surface of the parent cell may be selectively excluded from the surface of the vesicles, hence making these undetectable when labelling with a specific antibody. Secondly, it is also possible that the antigen copy number present on the surface of some vesicles is too low to be detected by flow cytometry. It is impossible to distinguish whether these two occurrences take place when vesicles are formed *in vivo,* however based on work presented in this study using *in vitro* derived vesicles from various

cell types, this may well happen. Hence, when choosing markers to examine cell types *in vivo* these points were taken into consideration.

The data from the *in vitro* derived vesicles was used to select a suitable six-colour panel to analyse vesicles *in vivo* in plasma samples from non-pregnant (NonP), normal pregnant (NormP) and pre-eclampsia (PE) women as shown in Chapter 4 of this thesis. This panel of markers is outlined in Table 5 and shows the percentage of antigen expression on cells and vesicles as well as any cross reactivity between markers.

The final panel was limited to six-colours and markers were chosen to identify vesicles derived from the syncytiotrophoblast, platelets, RBCs, endothelial cells, and leukocytes. Bio-Maleimide was also included in the final panel as a marker of vesicles. The panel consisted of: NDOG2 as a marker of STBM, CD41 to identify platelet derived vesicles, CD235a/b as a RBC marker, CD146 as an endothelial cell marker, W6/32 as a marker of all HLA Class I leukocyte vesicles. CD61 is also suitable as a platelet marker and was used in some experiments in Chapter 4 although it did show a higher percentage of cross-reactivity with STBM compared to CD41 and for this reason it was not used in the final six-colour panel. The percentage of CD105 expressed on the HUVEC vesicles was greater than that of CD146, but CD105 showed cross reactivity with STBM and therefore CD146 was chosen as the endothelial cell marker in the six-colour panel. HLA Class I, using the marker W6/32, was shown to be the most abundantly expressed antigen on the monocyte and lymphocyte vesicles, but did not label granulocyte vesicles. Although the expression of CD66b was reduced on granulocyte vesicles it was the most abundantly expressed antigen. However, there was no room to include this marker in the six colour panel and granulocyte vesicles were not studied further. Aware that W6/32 may not label granulocyte

vesicles *in vivo* it was chosen as a marker of leukocyte vesicles. W6/32 showed cross reactivity with platelet vesicles and endothelial vesicles, however using multi-parameter plots the leukocyte vesicles could still be positively identified.

	Percentage of positive labelling					
Cells/Vesicles	**Bio-Maleimide**	**CD41**	**CD235a/b**	**W6/32**	**CD146**	**NDOG2**
STBM	95.5	27.5	1.0	3.1	0.2	94.5
Platelets	100	99	ND	99	ND	ND
Platelet Vesicles	95.3	90.6	ND	81.1	ND	ND
RBCs	100%	ND	99	ND	ND	ND
RBC Vesicles	99.8	ND	92	ND	ND	ND
HUVEC	100	3.3	ND	99.9	100	ND
HUVEC Vesicles	92.3	ND	ND	3.7	30.5	ND
Monocytes	100	99.1	ND	100	ND	ND
Monocyte Vesicles	97.8	35.3	ND	59.6	ND	ND
Lymphocytes	100	27.2	ND	99.9	ND	ND
Lymphocyte Vesicles	99.0[a] 96.5[b]	DNT[a] DNT[b]	ND[a] DNT[b]	61.6[a] 77.1[b]	DNT[a] DNT[b]	DNT[a] DNT[b]
Granulocytes	100	10.2	0.9	100	1.7	0.5
Granulocyte Vesicles	96.1	2.3	0.1	1.5	1.8	1.1

Table 5. Final six-colour panel of selected markers used to analyse *in vivo* derived plasma vesicles. Table shows Bio-Maleimide expression and antigen expression on cells and *in vitro* derived vesicles. Antibodies include; Platelet marker; CD41, RBC marker; CD235a/b, HLA Class I Leukocyte marker; W6/32, endothelial cell marker; CD146 and syncytiotrophoblast marker; NDOG2. [a]lymphocyte vesicles = PMA + ionomycin stimulation and [b]lymphocyte vesicles = STS stimulation. ND = not detectable and DNT = did not test.

2.6 Summary

In this chapter the sensitivity of our flow cytometer was determined using fluorescent microspheres and shown to be 290nm. Vesicles were derived *in vitro* from the various cell types found in blood. Using these *in vitro* derived vesicles, antigen expression was examined using a panel of antibodies and the numbers of vesicles expressing a given antigen was compared to the parent cell. Results from these experiments have shown that many antigens are not expressed on all vesicles and the level of expression is highly variable between antigens. Some markers were shown to be more specific than others and the expression of some antigens on vesicles was also dependent on the stimulation method. All of these results have been taken into consideration when designing a panel of markers to examine *in vivo* derived vesicles in plasma.

As this study progressed it became more apparent from the literature that there are vesicles in plasma with sizes below the limit of flow cytometry (<290nm) that would have been excluded from this analyses. Therefore, an alternative method to flow cytometry to analyse this population was next explored. In Chapter 3 the use of Nanoparticle Tracking Analysis (NTA) to measure vesicles is described.

Chapter 3

Investigation of Nanoparticle Tracking Analysis as a novel method to analyse cellular derived vesicles

3.1 Introduction

In Chapter 2 of this thesis the sensitivity of our flow cytometer in terms of particle size measurement was evaluated using polystyrene beads and was shown to be ≥ 290nm. Thus flow cytometry can only analyse a portion of the total microvesicles present in a sample and completely excludes analysis of exosomes. Therefore, to analyse these smaller vesicles an alternative method is required. A number of techniques were considered and the advantages and disadvantages of each compared.

3.1.1 Methods for the Detection and Characterisation of Vesicles

3.1.1.1 Flow Cytometry Analysis of Vesicles Using Bead Capture

A number of studies have used flow cytometry to analyse vesicles that have been captured using magnetic beads coated with a specific antibody against the marker of interest (reviewed in Théry *et al.,* 2006). The vesicles bound to the beads are then labelled with a fluorescent antibody to give a semi-quantitative characterisation of their phenotype, similar to an ELISA. However, this technique gives no information about the size of the vesicles captured. It has been claimed that exosomes can be captured by using "exosome specific" antibodies (e.g. tetraspanin proteins such as CD63) (Théry *et al.,* 2006). However, experiments in our laboratory using flow cytometry showed that CD63 is highly expressed on pSTBM (i.e. analysis of vesicles ≥290nm), which casts doubt on its use as a specific marker for exosomes which are 30-100nm in size (Dragovic & Tannetta, unpublished observations).

3.1.1.2 Transmission Electron Microscopy

Apart from flow cytometry, transmission electron microscopy is probably the most commonly used method to detect cellular vesicles. Transmission electron microscopy can resolve objects down to the picometre level (Wang 2011) and can therefore demonstrate the presence of vesicles of all sizes. By using antibodies conjugated to gold particles it can also provide phenotypic information, but it is not quantitative and requires extensive sample preparation (Heijnen *et al.*, 1999, Aras *et al.*, 2004, Bernimoulin *et al.*, 2009). Furthermore, transmission electron microscopy requires fixation of the sample which can lead to vesicle under-sizing due to shrinkage (Jensen *et al.*, 1981, Théry *et al.*, 2006). Early experiments using transmission electron microscopy to size exosomes suggested they were "cup-shaped" (Théry *et al.*, 2006). However, by using cryo-electron microscopy which does not require fixation of the sample, this has now been shown to be an artefact of the fixation process (Gyorgy *et al.*, 2011).

3.1.1.3 Atomic Force Microsopy (AFM)

Atomic Force Microscopy (AFM) is another method to measure particle size and like transmission electron microscopy it also has a resolution down to the picometre level (Ricci and Braga 2004). It works by using a fine tip (<100 Å in diameter) attached to the free end of a cantilever which is used to scan the surface of the sample of interest. The interaction force generated between the tip and the sample surface is dependent on their proximity. Deflection of the cantilever is measured using a laser spot reflected at the top end of the cantilever which is collected into a detector, typically a photodiode. These deflections are measured and the scanning software creates a three-dimensional topographic image of the sample surface (Ricci and Braga 2004). Compared to transmission electron microscopy, AFM does not require sample fixation, therefore sizing

measurements are more accurate. AFM can analyse polydisperse samples (i.e. of various size and shape) with good sizing accuracy (Hoo *et al.,* 2008) and has been used to measure the size of platelet derived vesicles (Siedlecki *et al.,* 1999, Yuana *et al.,* 2010). AFM is only semi-quantitative as it dependent on how effectively the vesicles bind to a surface using a specific antibody. The data presented in Chapter 2 suggests that various types of vesicles generated from the same cell type may have different patterns of antigen expression and therefore some would not bind to a given antibody on the surface and would be excluded from the analysis. It has also been suggested that binding of vesicles to the surface may alter their morphology and in turn effect vesicle size measurements (van der Pol *et al.,* 2010). Furthermore, AFM instrumentation is extremely costly, it requires a highly experienced operator and is also very labour intensive.

3.1.1.4 Dynamic Light Scattering (DLS)

Dynamic Light Scattering (DLS), alternatively known as Photon Correlation Spectroscopy (PCS), is a more accessible technique widely used to determine particle size. DLS is reported to analyse particles in solution ranging in size from 1nm up to 6µm (van der Pol *et al.,* 2010). DLS determines size by light scattered from particles under Brownian motion, which is the random movement of particles in solution due to the bombardment by the solvent molecules that surround them. DLS measures scattered light from all the particles in solution and produces an average size. DLS is very accurate when analysing monodisperse particles (i.e. of the same size and shape) and has been used to measure cellular derived vesicles in plasma (Lawrie *et al.,* 2009). However, a major drawback of this technique is that it cannot resolve individual populations in polydisperse samples. Only an average particle size is given which is intensity biased toward the detection of larger particles (Lawrie *et al.,* 2009). Biological vesicles are highly likely to be

polydisperse as shown in Chapter 2 of this thesis and therefore DLS is not ideal for their analysis.

3.1.1.5 Nanoparticle Tracking Analysis (NTA)

Nanoparticle Tracking Analysis (NTA) is a unique system used for direct, real-time visualisation and analysis of particles in solution. It is a relatively new technique that was first marketed in 2006 and overcomes many of the problems associated with the methods described above (Carr *et al.*, 2009). NTA identifies each individual particle and then tracks its Brownian motion which is used to calculate particle size and estimate concentration. However, unlike DLS it can resolve different sized particles within a mixture, which is essential for analysing biological vesicles. This method is typically used to characterise particles for applications in engineering and material sciences and at the beginning of this part of my project its potential for analysing biological vesicles had not been tested.

3.2 Aims

The overall aim was to determine whether NTA can measure the size and concentration of cellular derived vesicles.

1. To optimise NTA instrument settings for cellular vesicle measurement using monodisperse beads and a polydisperse bead mixture to verify accurate particle sizing and concentration measurements.
2. To apply these instrument settings in the analysis of *in vitro* derived vesicles generated from pSTBM, platelets, RBC, HUVEC and PFP and to obtain vesicle size and concentration measurements.

3.3 Methods and Materials

3.3.1 NanoSight LM10 NTA Instrument

The NanoSight LM10 NTA instrument (NanoSight Ltd., Amesbury, UK) comprises a conventional optical microscope, a charged-coupled device (CCD) video camera and a sample analysis chamber (~0.5mm deep and volume ~0.25ml) into which a suspension of particles is introduced (Figure 32A). The instrument uses a finely focused laser beam which passes through the suspension of particles via a glass prism (Figure 32B). The beam refracts at a low angle as it passes through the sample, illuminating the particles and allowing their visualisation by the light they scatter. A video of typically 60 seconds is recorded of the light scattered by the moving particles at a frame rate of 30 frames per second and this is then analysed using the NTA software (Figure 32C). The NTA software firstly identifies each particle and then tracks its Brownian motion (Figure 32D and Figure 32E). The velocity of each particle is used to calculate particle size by applying the two dimensional Stokes Einstein equation:

$$< x, y >^2 = \frac{K_B T_{ts}}{3\pi\eta d_h}$$

Where $< x, y >^2$ is the mean square displacement, K_B is the Boltzmann's constant, T is the temperature of the solvent in Kelvin, ts is the sampling time (i.e., 1/30fpsec = 33msec), η is the viscosity, and d_h is the hydrodynamic diameter. The NTA software displays the data as a histogram of modal particle size (nm) vs. concentration [x10^6 particles/ml] (Figure 32F).

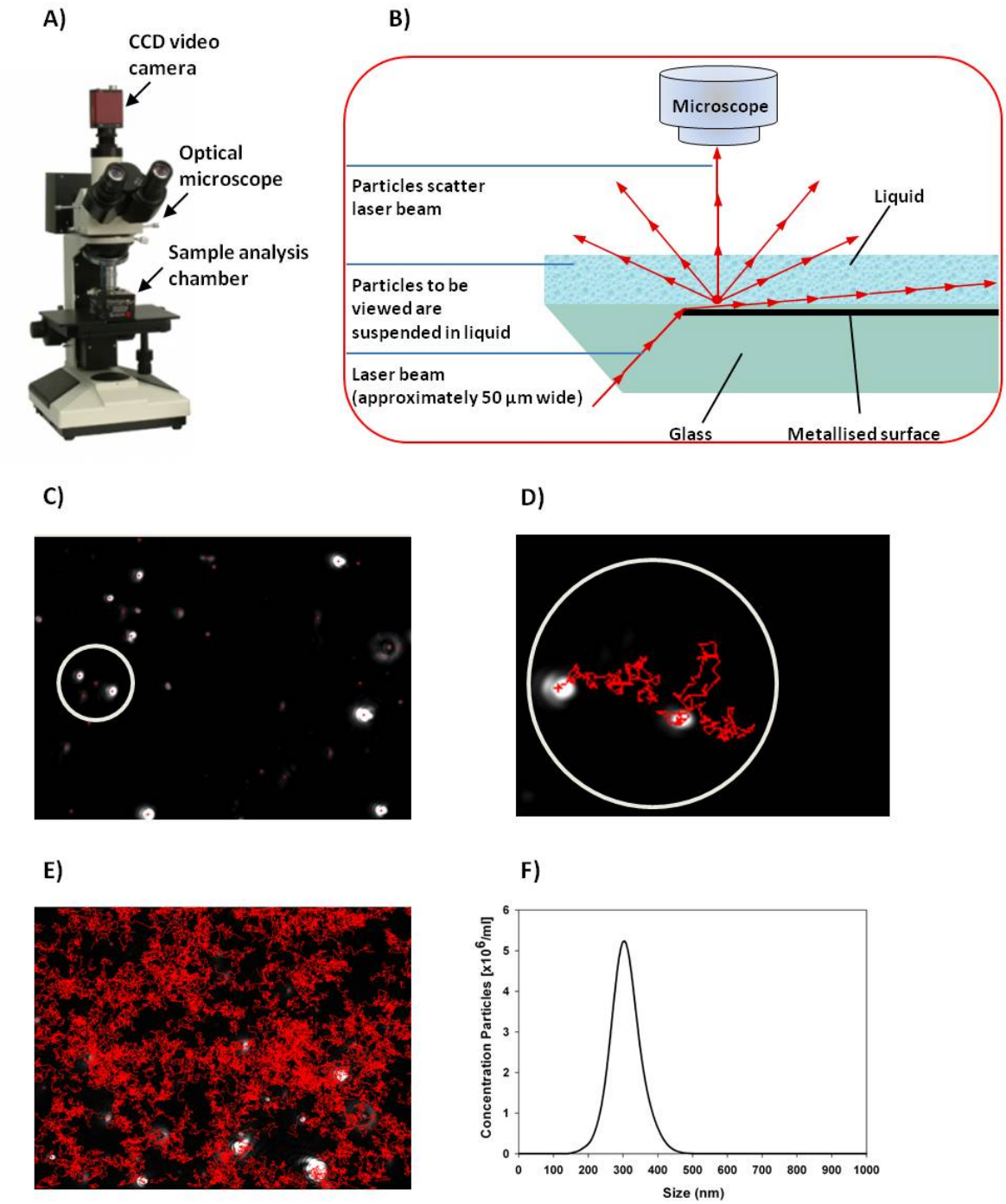

Figure 32. NanoSight LM10 Instrument and Operation of NTA. A) NanoSight LM10 NTA instrument, **B)** NanoSight LM10 sample analysis chamber configuration, **C)** Video capture of light scatter from particles moving under Brownian motion, **D)** Tracking of the two individual particles circled in C) using NTA; white spot = particle, red line = track of particle movement under Brownian motion, **E)** Thousands of particles are tracked on a frame-by-frame basis, **F)** NTA software displays the data of 300nm beads as a histogram profile of size (nm) vs. particle concentration [x10^6/ml].

A range of parameters can be adjusted both for video capture (i.e. shutter speed, camera gain, and capture duration) and analysis (i.e. brightness, gain, blur, detection threshold and minimum required track length) allowing optimisation of particle identification and tracking for any given sample. The software used for capture and analysis was NTA 2.0, Build 130. The flowchart illustrated below demonstrates a typical sequence of an NTA analysis experiment (Figure 33).

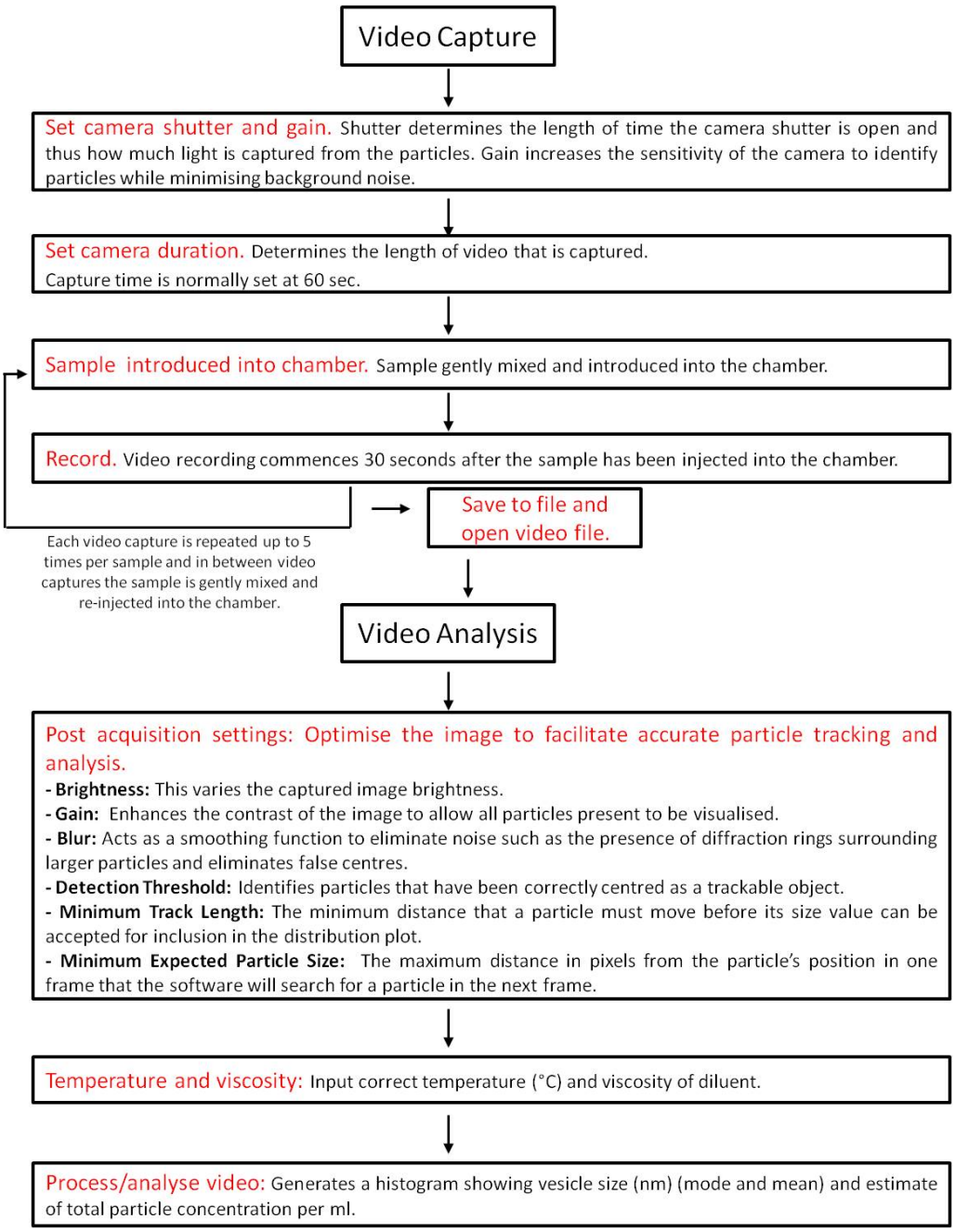

Figure 33. Flow chart illustrating a typical Nanoparticle Tracking Analysis (NTA) experiment using the NanoSight LM10 instrument.

The range of particle sizes that NTA can accurately measure is dependent on the refractive index of the particle. For example, gold has a very high refractive index and NTA can measure colloidal gold particles down to 20nm in size. However, a particle with a lower refractive index (e.g. silica particles) will scatter less light, reducing the signal to noise ratio of the image and therefore reducing the minimum detectable size. At the other end of the scale, particles > 1μm are unable to be tracked accurately by NTA as these particles move too slowly and therefore cannot be sized.

3.3.2 NTA Measurement of Particle Size and Concentration Using Polystyrene Bead Samples

Polystyrene beads with sizes of 50nm, 70nm, 100nm, 200nm, 300nm and 400nm (NIST beads; Thermo Scientific, Fremont, USA) were diluted in PBS at a range of concentrations [2 x 10^8/ml and 20 x 10^8/ml] and were analysed using the NanoSight LM10 instrument and NTA software version 2.0, Build 130. Bead samples were gently mixed before being introduced into the chamber and recording commenced after 30 seconds. Each sample was videoed for 60 seconds and between each recording the sample was mixed by sucking it out and re-injecting it into the chamber. Measurements were repeated 4-5 times per sample.

Different combinations of camera shutter and gain settings were tested and optimised for each bead size. A camera shutter speed of 1 equates to 20microseconds (i.e. shutter speed of 1000 = 20milliseconds). All beads were prepared at a concentration of 5 x 10^8/ml with the exception of 70nm beads, which were prepared at a concentration of 6 x 10^8/ml and 50nm beads were prepared at a concentration of 8 x 10^8/ml. The larger 300nm beads and 400nm beads were analysed using a camera shutter speed of 5-25 and a camera gain of 0.

200nm beads were analysed using camera shutter speeds ranging from 100-1500 and a camera gain of 0. 100nm beads were analysed at three camera shutter speeds; 500, 1000 and 1500 and a camera gain ranging from 0-650. The smaller 50nm and 70nm beads were analysed using the highest shutter speed of 1500 and highest gain setting of 650. 70 nm beads were also analysed using a shutter of 1000 and gain of 500. A polydisperse bead mixture of 100nm beads [5 x 10^8/ml] and increasing concentrations of 300nm beads [1-5 x 10^8ml] was analysed twice, first using the previously determined optimal camera shutter speed and gain settings for 100nm beads (camera shutter speed 1000, gain 500) and then repeated using the optimal setting for 300nm beads (camera shutter 20, gain 0).

The NTA post acquisition settings were based on the manufacturer's recommendations and were kept constant between samples and were as follows; Brightness = -10, gain = 1.50, blur = 5 x 5, automatic detection threshold = on, maximum blob size (pixel area) = 3000, automatic minimum track length = on and minimum expected particle size = 100nm. Each video was analysed to give the mode and mean vesicle size together with an estimate of particle concentration.

3.3.3 NTA Measurement of *In vitro* Derived Vesicles

pSTBM

The preparation of pSTBM is described in Chapter 2 Section 2.3.2.1. A single pSTBM preparation stored in PBS at -80°C was thawed at room temperature and diluted in PBS to give a range of concentrations between 2 x 10^8/ml – 10 x 10^8/ml when analysed by NTA.

Platelets

The preparation of platelet vesicles from three healthy volunteers is described in Chapter 2 Section 2.3.2.2. Platelet vesicles were diluted in PBS to obtain a concentration between 3 x 10^8/ml – 6 x 10^8ml when analysed by NTA. Data were from 3 independent experiments.

RBC

The preparation of RBC vesicles from three healthy volunteers is described in Chapter 2 Section 2.3.2.3. RBC vesicles were diluted in PBS to obtain a concentration between 3 x 10^8/ml – 5 x 10^8ml when analysed by NTA. Data were from 3 independent experiments.

HUVEC

The preparation of HUVEC vesicles by treatment with 5μmol/L Camptothecin (CPT) or 0.5% DMSO (vehicle control) is described in Chapter 2 Section 2.3.2.4. Samples were diluted in PBS to obtain a concentration between 3 x 10^8/ml – 6 x 10^8ml when analysed by NTA. The control pellet from 0.1μm filtered culture medium was analysed at the same dilution and the background was subtracted from the final analysis. Data were from two independent experiments.

In vitro derived vesicle samples were introduced into the chamber as described in Section 3.3.2. Each sample measurement was repeated 3-5 times. Post acquisition settings as stated in Section 3.3.2 were used for all samples. Each video was analysed to give the mode and mean vesicle size together with an estimate of vesicle concentration.

3.3.4 Preparation of Platelet Free Plasma (PFP)

Blood was taken from two healthy female volunteers after obtaining written informed consent. This study was approved by the Oxfordshire Research Ethics Committee C. Blood was drawn through a 20-gauge needle and the first 2ml was discarded to minimise

the risk of including activated platelets generated with the initial venepuncture. Blood was drawn into a 4.5ml 0.105M buffered sodium citrate vacutainer (BD Biosciences) and processed immediately. Platelet free plasma (PFP) was generated using a double centrifugation method; blood was centrifuged at 1500 × g for 15min to separate the plasma, the top 2/3 of the plasma layer was isolated and centrifuged at 13,000 × g for 2min to remove the platelets. PFP was then frozen in aliquots at -80°C until use.

3.3.5 Preparation of PFP Vesicles

3ml of frozen PFP was thawed at 37°C, made up to 11ml with PBS and centrifuged at 150,000 × g (max) for 1 hour at 4°C in a Beckman L8-80M ultracentrifuge. The supernatant was removed and the vesicle pellet was resuspended in PBS.

3.3.6 Transmission Electron Microscopy of pSTBM

Transmission electron microscopy of pSTBM was carried out by Prof. David Ferguson (Nuffield Dept of Clinical and Laboratory Science, Oxford). Formvar/carbon coated grids were floated on 50µl of pSTBM, washed in distilled water and negatively stained with 1% methyl tungstenate. The grids then underwent examination in the electron microscope (Model JEOL 1200EX, JEOL Ltd UK). Vesicle sizes were measured manually from the electron micrographs by Dr Chris Gardiner and Dr Alexandra Brooks (both from the Nuffield Dept Obstetrics & Gynaecology, University of Oxford).

3.3.7 Statistics

Each data set was first tested for a Guassian distribution by using a Shapiro-Wilk normality test and for equal variance using a Levene Median test. Data sets comparing

platelet, RBC and HUVEC *in vitro* derived vesicle counts measured by flow cytometry and NTA were log-transformed. These data sets all passed normality and equal variance and were compared using a student's *t*-test. SigmaPlot 12.0 was used for data analysis.

3.4 Results

3.4.1 Optimisation of NTA Measurement of Particle Size and Concentration Using Monodisperse Polystyrene Beads

The results in Chapter 2 Section 2.4.1 demonstrate that flow cytometry can analyse polystyrene beads ≥290nm, but the signal is compromised by instrument noise when trying to analyse smaller beads. Experiments were therefore carried out to optimise the NanoSight LM10 instrument settings using monodisperse polystyrene beads ranging in size from 50-400nm in order to verify the accuracy of NTA to size particles and estimate their concentration. Larger beads of 400nm and 300nm, which can also be visualised using flow cytometry were analysed first. This was then followed by analysis of smaller beads ranging in size from 200nm down to 50nm.

3.4.1.1 400nm Beads

400nm beads were prepared at a concentration of 5 x 10^8 beads/ml. A very low shutter speed setting (5) was used first to examine the 400nm beads as they can be visualised as single points of light at this setting. The sizing was relatively accurate (Figure 34A), however vesicle concentration was underestimated (Figure 34B). Increasing the shutter speed to 15 resulted in an accurate measurement of particle size (Figure 34A) and concentration (Figure 34B). Using higher shutter speeds of 20 or 25 also accurately sized the particles, but overestimated the concentration (Figure 34A and Figure 34B

respectively). A screenshot of the 400nm beads videoed using the optimal shutter speed of 15 is shown in Figure 34C. The beads are visualised as single points of light, which is ideal for sizing and quantification. Figure 34D shows a representative NTA size vs. concentration profile of 400nm beads using the optimal shutter speed of 15. The size distribution shows a distinct peak at 400nm, however the spread of data is due to the limitation of measuring Brownian motion by sampling for a finite time period (i.e. the time taken for each particle to be tracked). The NTA software can be adjusted to correct for this and produce tighter peaks, however when analysing biological samples no assumptions can be made regarding size distribution, therefore this correction was not used in any of the data analysis.

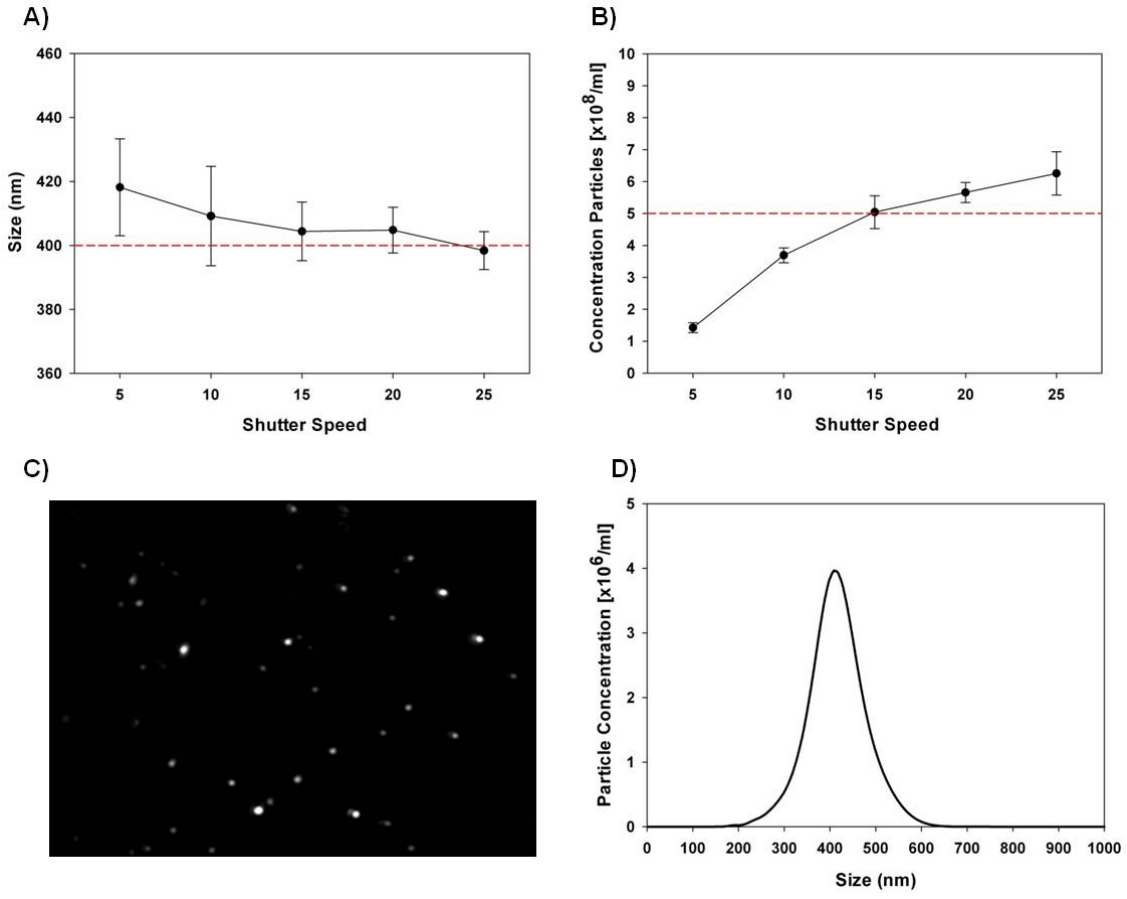

Figure 34. NTA of 400nm polystyrene beads. A) Modal particle size (Mean ± SD) measurement with increasing camera shutter speed settings. Red line denotes the actual size of beads, **B)** Measurement of particle concentration (Mean ± SD) with increasing camera shutter speed settings. Red line denotes the actual concentration of beads, **C)** Screenshot of 400nm beads using a shutter speed set at 15, **D)** NTA size vs. concentration profile. Values obtained for each camera shutter speed are the average of 4-5 separate video analyses.

3.4.1.2 300nm Beads

300nm beads were also used at a concentration of 5 x 10^8 beads/ml, and the shutter speed was first set at a very low speed of 5. Similar to the results shown with the 400nm beads, this shutter speed resulted in accurate particle sizing, but the particle concentration was underestimated. The optimal shutter speed for measuring particle size and concentration was obtained by increasing the value to 20 (Figure 35A and Figure 35B respectively). A shutter speed above 20 resulted in accurate particle sizing (Figure 35A), but an overestimation of the total concentration (Figure 35B). A screenshot of the 300nm beads videoed using the optimal shutter speed of 20 is shown in Figure 35C. A representative NTA size vs. concentration profile of 300nm beads using the optimal shutter speed of 20 is shown in Figure 35D.

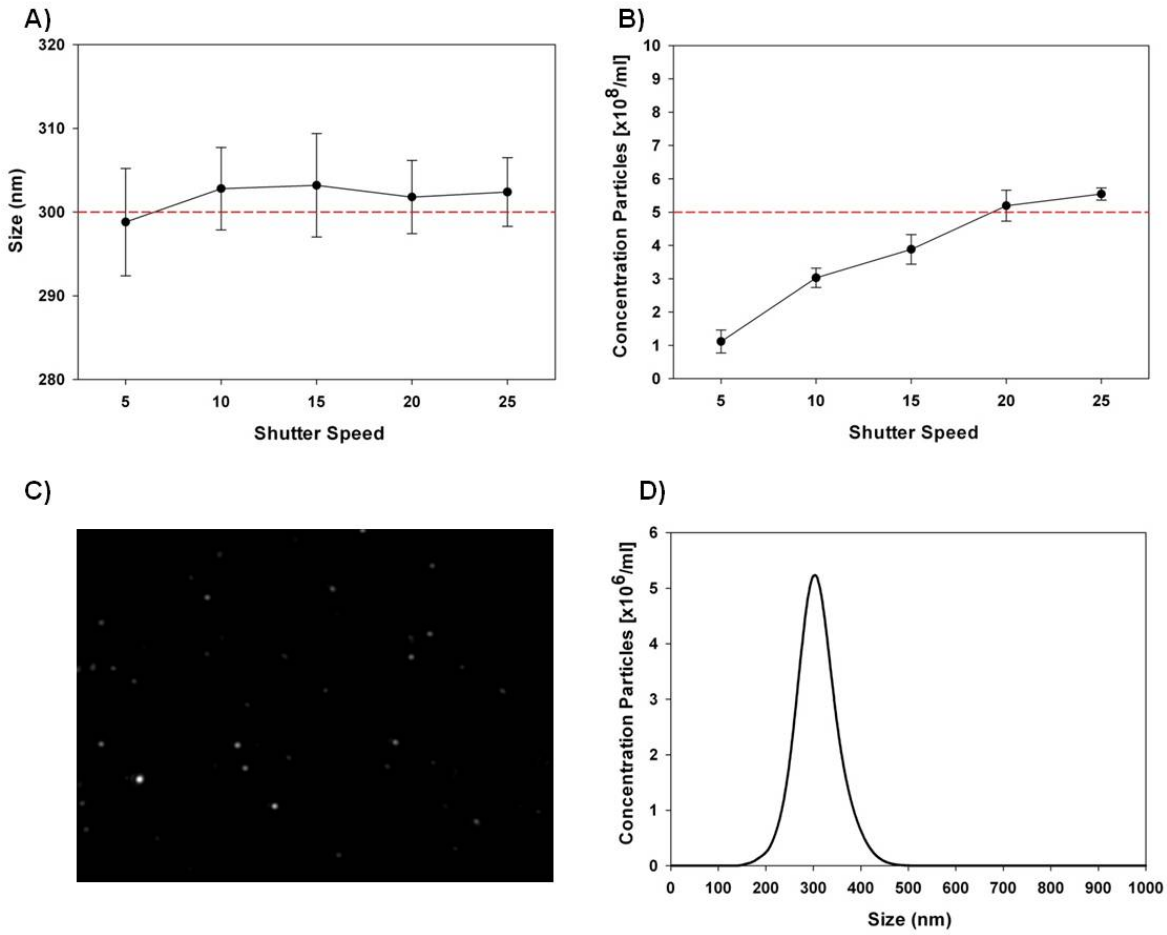

Figure 35. NanoSight NTA: 300nm polystyrene beads. A) Modal particle size (Mean ± SD) measurement with increasing camera shutter speed settings. Red line denotes the actual size of beads, **B)** Measurement of particle concentration (Mean ± SD) with increasing camera shutter speed settings. Red line denotes the actual concentration of beads, **C)** Screenshot of 300nm beads using a shutter speed set at 20, **D)** NTA size vs. concentration profile using the optimal shutter speed of 20.Values obtained for each camera shutter speed are the average of 4-5 separate video analyses.

Together, the NTA results from the larger 400nm and 300nm beads demonstrate that a very low shutter speed is required for optimal sizing and concentration measurements. The camera shutter speed can be varied up to a maximum value of 1500, NTA analysis was therefore carried out using smaller beads at higher shutter speeds to determine the sensitivity of the NanoSight LM10 instrument.

3.4.1.3 200nm Beads

The flow cytometry results in Chapter 2 Section 2.4.1 showed that 200nm beads could be visualised, but the signal was compromised by background instrument noise. A preparation of 200nm beads at a concentration of 5 x 10^8/ml was analysed using NTA. Optimal size and concentration settings for particles of 200nm were tested using shutter speeds ranging from 100-1500. These results show that too great an increase in shutter speed results in particle under sizing (Figure 36A) and an over-estimation of particle concentration (Figure 36B). Accurate particle sizing and concentration was observed when using a shutter speed of 225 and a screenshot of the beads at this shutter speed shows how these are visualised as single points of light (Figure 36C). In contrast, Figure 36D shows a screenshot of 200nm beads videoed using a maximum shutter speed of 1500. Here the 200nm beads appear as larger over-exposed objects with Newton's rings. Newton's rings are an interference pattern caused by the reflection of light between a spherical surface and an adjacent flat surface. These make the beads more difficult to track by NTA leading to inaccurate size and concentration measurements. A representative NTA size vs. concentration profile of 200nm beads videoed using the optimal shutter speed of 225 is shown in Figure 36E.

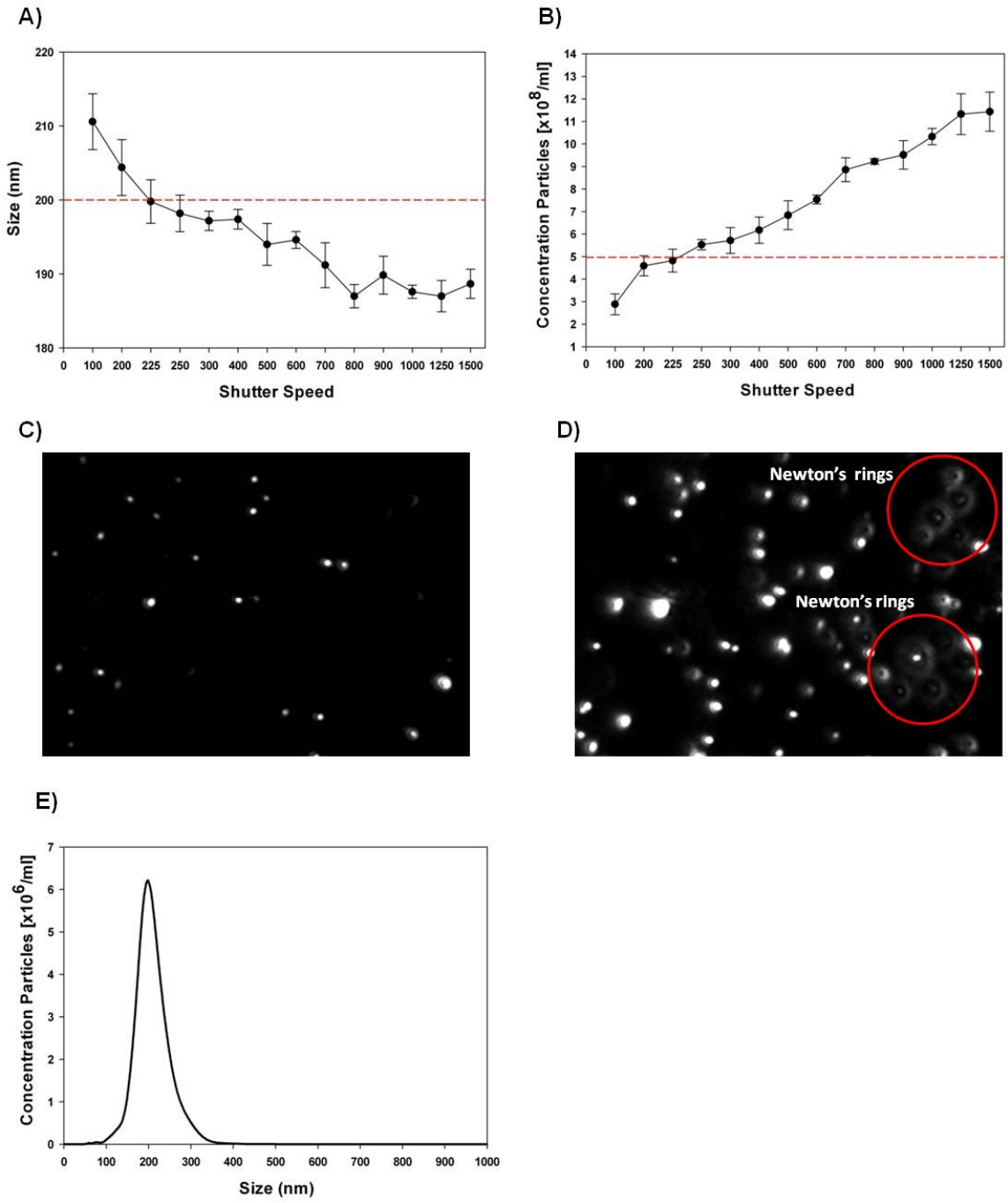

Figure 36. NanoSight NTA: 200nm polystyrene beads. A) Modal particle size (Mean ± SD) measurement with increasing camera shutter speed settings. Red line denotes the actual size of beads, **B)** Measurement of particle concentration (Mean ± SD) with increasing camera shutter speed settings. Red line denotes the actual concentration of beads, **C)** Screen shot image of 200nm beads videoed using the optimal shutter speed of 225, **D)** Screenshot of 200nm beads videoed using the maximum shutter speed of 1500 showing the presence of Newton's rings, **E)** NTA size vs. concentration histogram profile of 200nm beads videoed using the optimal shutter speed of 225. Values obtained for each camera shutter speed are the average of 4-5 separate video analyses.

3.4.1.4 100nm Beads

Next, a preparation of 100nm beads at a concentration of 5 x 10^8 beads/ml was analysed using NTA. Three different camera shutter speeds (500, 1000 and 1500) and camera gains ranging from 0-650 were used to determine the effect of these variables on particle measurement. This was the first time it was necessary to use the camera gain setting in order to visualise the light scatter from beads. Accurate particle sizing was observed with all three camera shutter speeds and 14 gain settings tested, however increased precision was obtained when using gains ≥ 150 (Figure 37A). Particle concentration was similarly evaluated using different camera shutter speeds and camera gains. The most accurate particle concentration measurements were obtained using three different combinations of camera shutter speed and gain settings: 1) camera shutter speed of 500 and gain 650; 2) camera shutter speed of 1000 and gain 500; and 3) camera shutter speed 1500 and gain 450 (Figure 37B). Figure 36C shows a representative NTA size vs. concentration profile of 100nm beads using a camera shutter of 1000 and gain of 500. Using the middle optimal shutter speed and gain combinations (shutter speed 1000 and gain 500) a range of concentrations of 100nm beads [2 x 10^8 – 20 x 10^8 beads/ml] was used to investigate the linearity of the instrument. Good linearity between the expected concentration and the observed concentration measured by NTA in the range of 1 x 10^8 – 8 x 10^8 beads/ml was observed (Figure 37D).

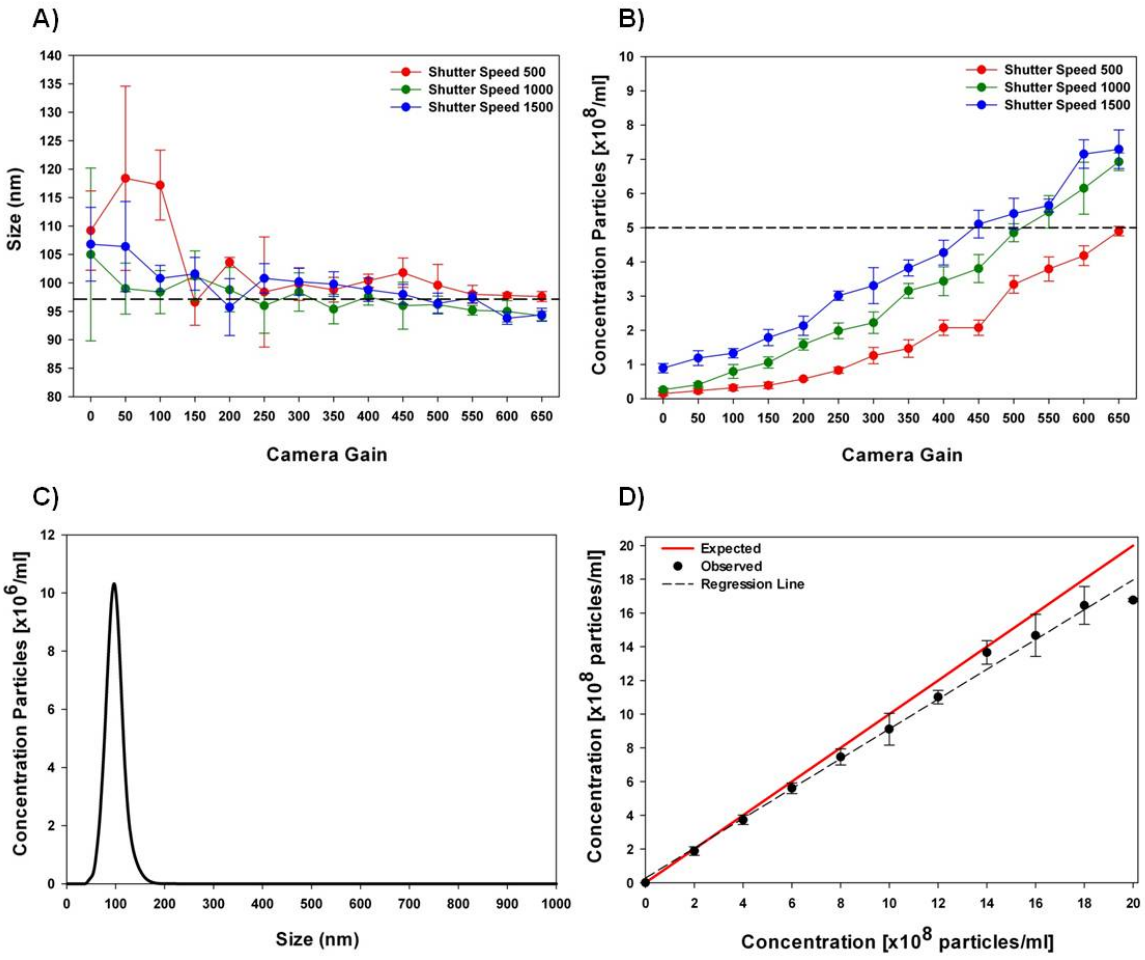

Figure 37. NTA of 100nm polystyrene beads. A) Modal particle size (Mean ± SD) measurement with increasing camera shutter speed and gain settings. Black line denotes the actual size of beads, **B)** Measurement of particle concentration (Mean ± SD) with increasing camera shutter speed and gain settings. Black line denotes the actual concentration of beads, **C)** NTA size vs. concentration profile of 100nm beads using a shutter speed of 1000 and camera setting of 500, **D)** Expected (red line) vs. observed concentration (black dotted line) (Mean ± SD) of particles using optimal camera shutter and gain settings. Values obtained for each camera shutter speed and camera gain setting are the average of 4-5 separate video analyses.

3.4.1.5 70nm and 50nm Beads

The optimal shutter speed setting of 1000 and gain setting of 500 for 100nm beads was then used to analyse even smaller beads. 70nm beads were prepared at a concentration of 6 x 10^8 beads/ml. These settings gave accurate sizing for the 70nm beads (76 ± 2.5 nm, Mode ± SD) (Figure 38A), however the concentration was underestimated by ~10-fold (0.69 x 10^8/ml) (Figure 38B). Increasing the shutter speed to a maximum of 1500 and maximum gain of 650 still underestimated particle concentration (2.23 x 10^8/ml) (Figure

38B), but sizing measurements remained accurate (76 ± 1.1 nm, Mode ± SD). Finally, 50nm beads were prepared at a concentration of 8 x 10^8 beads/ml and were evaluated using the maximum shutter speed of 1500 and maximum gain of 650. The beads were barely detectable and NTA was unable to accurately track these particles (data not shown). Thus, the lower limit of detection of the NanoSight LM10 instrument was between 50nm - 70nm.

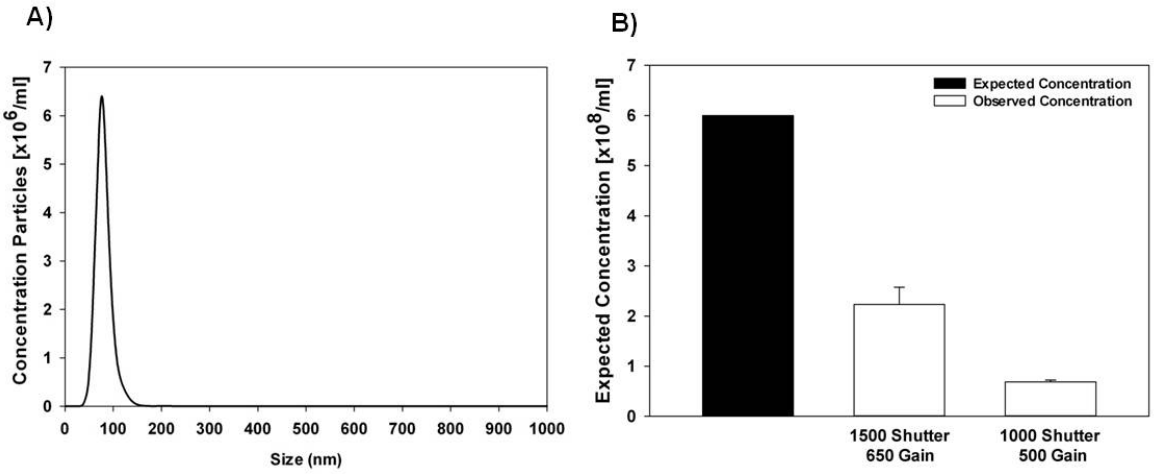

Figure 38. NTA of 70nm beads. A) Size vs. concentration profile using a shutter speed of 1000 and camera gain of 500, **B)** Expected vs. observed concentration (Mean ± SD) of particles using two different shutter speed and gain settings. Values obtained for each camera shutter speed are the average of 5 separate video analyses.

3.4.2 NTA Measurement of Particle Size and Concentration Using a Polydisperse Bead Mix of 100nm and 300nm Polystyrene Beads

Next a mixture of 100nm and 300nm beads was used to evaluate the ability of NTA to accurately size and quantitate a polydisperse bead mixture. As previously mentioned, this is an essential prerequisite for analysing cellular vesicles in biological fluids as it is likely that these will be polydisperse in nature. Using settings optimal for analysing 100nm beads (camera shutter speed 1000, gain 500), two distinct particle populations were observed with modal sizes of 94 ± 2.2 nm and 284 ± 5.7 nm (average mode ± SD) in Figure 39A.

Using these same camera settings, a constant concentration of 100nm beads [5 x 10^8 beads/ml] mixed with increasing concentrations of 300nm beads [1-5 x 10^8 beads/ml] was analysed and the particle size and concentration of the two bead populations were measured. Figure 39B shows that the 100nm bead population could be accurately sized at all particle concentrations, however as the 300nm bead concentration increased, the sizing precision for this population was compromised and the particles were under sized. An over-estimation of total particle concentration was observed in the presence of the 300nm beads when used at a concentration between [1-4 x 10^8 beads/ml] (Figure 39C). Figure 39D shows a screenshot of 100nm beads [5 x 10^8/ml] and 300nm beads [1 x 10^8/ml] analysed using a camera shutter speed of 1000 and camera gain of 500. The 100nm beads are visualised as single points of light, however the 300nm beads appear as larger over-exposed objects with Newton's rings. At these settings the 300nm beads may scatter multiple points of light, which are interpreted by the NTA software as individual particles, hence leading to an overestimation of their numbers.

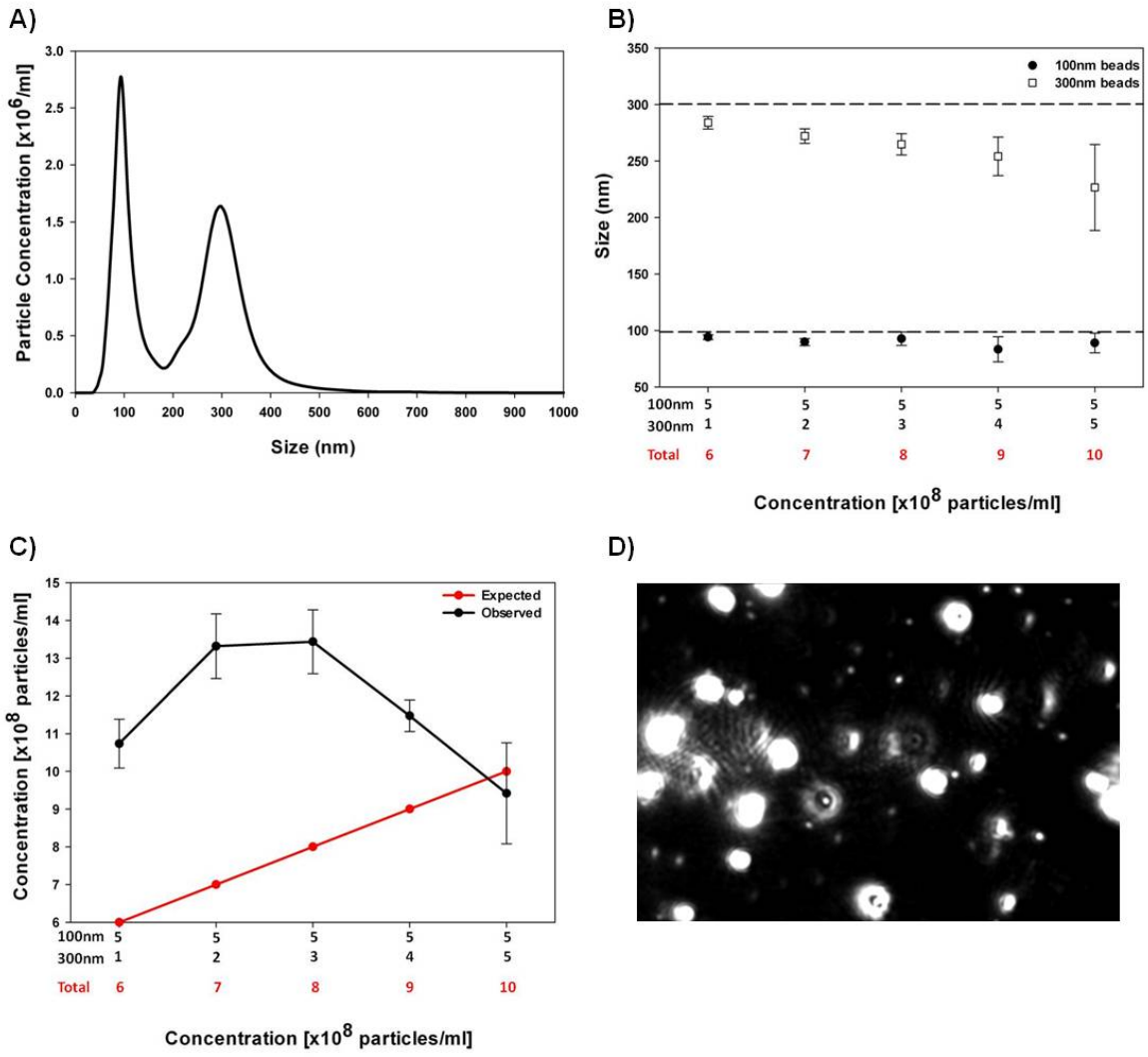

Figure 39. NTA using optimised settings for 100nm particles: 100nm and 300nm polystyrene bead mix. A) NTA size vs. concentration profile, **B)** Modal particle size (Mean ± SD) measurement with a constant concentration of 100nm beads [5 x 10^8/m] and an increasing concentration of 300nm beads [1-5 x10^8/ml]. Black dotted lines denote the actual size of beads, **C)** Expected vs. observed particle concentration (Mean ± SD) with a constant concentration of 100nm beads [5 x 10^8/m] and an increasing concentration of 300nm beads [1-5 x 10^8/ml], **D)** Screenshot of 100nm beads [5 x 10^8/ml] and 300nm beads [1 x 10^8/ml].Values obtained for each bead concentration are the average of 4-5 separate video analyses.

In contrast, using lower settings optimal for 300nm beads (camera shutter speed 20) only the 300nm bead population was observed as at this shutter speed the camera was unable to detect the 100nm beads (Figure 40A). The 300nm beads were accurately sized at all particle concentrations (Figure 40B), however due to the 100nm bead population being undetectable this resulted in an under-estimation of total particle concentration (Figure 40C). A screenshot of the 100nm beads [5 x 10^8/ml] and 300nm beads [5 x 10^8/ml] shows

the 300nm beads as single points of light, whereas at these camera settings the 100nm beads are undetectable (Figure 40D). From these results it can be concluded that NTA can analyse polydisperse samples, but sizing of the larger 300nm particles and total concentration measurements are less precise.

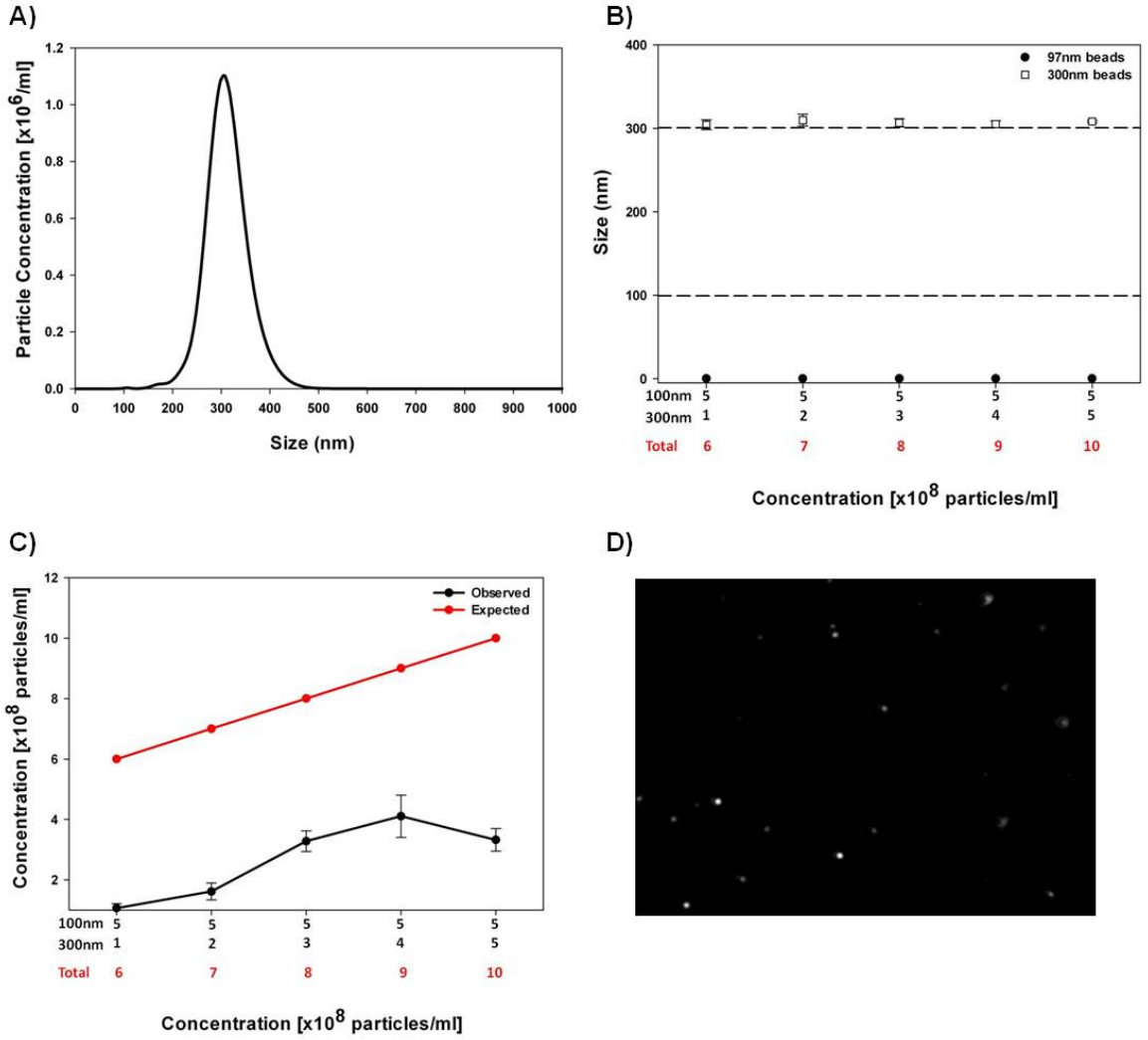

Figure 40. NanoSight NTA using optimised settings for 300nm particles: 100nm and 300nm polystyrene bead mix. A) NTA size vs. concentration profile, **B)** Modal particle size (Mean ± SD) measurement with a constant concentration of 100nm beads [5 x 10^8/m] and an increasing concentration of 300nm beads [1-5 x 10^8/ml]. Black dotted lines denote the actual size of beads, **C)** Expected vs. observed particle concentration (Mean ± SD) with a constant concentration of 100nm beads [5 x 10^8/m] and an increasing concentration of 300nm beads [1-5 x 10^8/ml], **D)** Screenshot of 100nm beads [5 x 10^8/ml] and 300nm beads [5x10^8/ml] showing light scatter from the 300nm beads only as at these settings the 100nm beads are undetectable. Values obtained for each bead concentration are the average of 4-5 separate video analyses.

3.4.3 NTA Measurement of *In vitro* Derived Cellular Vesicles

Prior to this study, the NanoSight LM10 instrument and NTA software had only been used to characterise particles for applications typically used in engineering and material sciences. This is the first study to evaluate NTA technology to analyse cellular microvesicles and nanovesicles. This included a preparation of pSTBM, platelet-derived vesicles, RBC-derived vesicles and HUVEC-derived vesicles, all described in Chapter 2. We also evaluated NTA for analysing vesicles in ultracentrifuge pellets of platelet free plasma (PFP). Based on the experiments carried out using polystyrene beads, and aware of the complexity involved in analysing polydisperse samples, a camera shutter speed of 1000 and camera gain of 500 was chosen. These are the settings optimal for measuring particles of 100nm and will also accurately measure the size of particles down to 70nm. Although these settings are sub-optimal for measuring larger particles (e.g., ≥300nm) by NTA, these larger vesicles are easily measured using flow cytometry.

3.4.3.1 Comparison of NTA, Flow Cytometry and Transmission Electron Microscopy of pSTBM

A serial dilution (1 in 400, 1 in 800 and 1 in 1600) of pSTBM was analysed using NTA. The mean vesicle size was comparable between all three dilutions (Mean ± SD: 1 in 400; 255 ± 113 nm, 1 in 800; 270 ± 106 nm and 1 in 1600; 288 ± 131 nm). The size distribution of vesicles showing the modal size for all three dilutions is illustrated in Figure 41A. Approximately 70% of the total vesicles measured using NTA were below the detection limit of flow cytometry (<290nm). A linear two-fold decrease in vesicle concentration was measured (Figure 41B) and the total vesicle concentration was 3.67×10^{11}/ml. When this same sample was analysed by flow cytometry as shown in Chapter 2 Section 2.4.2 the total vesicle count was 1.6×10^{9}/ml, a difference of two orders of magnitude (Figure 41C).

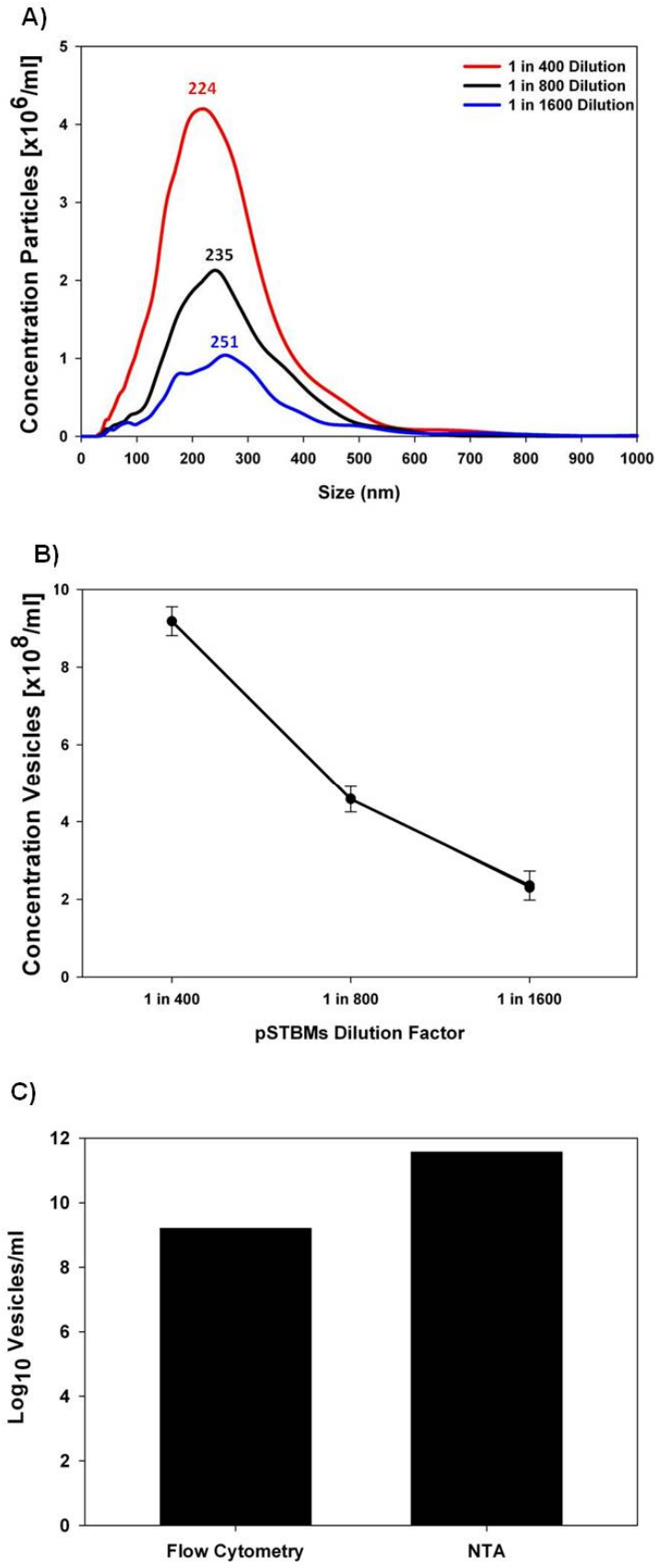

Figure 41. NTA Serial Dilution of pSTBM. A) Mode size vs. concentration of pSTBM serial dilution, **B)** Measured concentration (Mean ± SD) of pSTBM serial dilution. Each dilution factor is the average of 5 independent video analyses, **C)** Total vesicle counts as measured by flow cytometry vs. NTA.

The size distribution of pSTBM was also measured using transmission electron microscopy and directly compared to the NTA measurements. Electron micrographs of pSTBM are shown in Figure 42A, and Figure 42B is a screenshot of the same sample analysed by NTA. Electron microscopy showed a size distribution of vesicles ranging in size from 20nm to 600nm with a peak size between 40nm and 400nm. NTA gave a similar vesicle size distribution ranging from ~50nm-600nm with a peak around 250nm (Figure 42C). The peak of very small vesicles (20-60nm) observed by electron microscopy is absent in NTA profile. This is most likely to be due to the lack of sensitivity of the NanoSight instrument when analysing vesicles in this size range (as described in Section 3.4.1.5). Moreover, shrinkage artefacts during fixation for transmission electron microscopy may also lead to vesicle under sizing (Jensen *et al.*, 1981, Théry *et al.*, 2006).

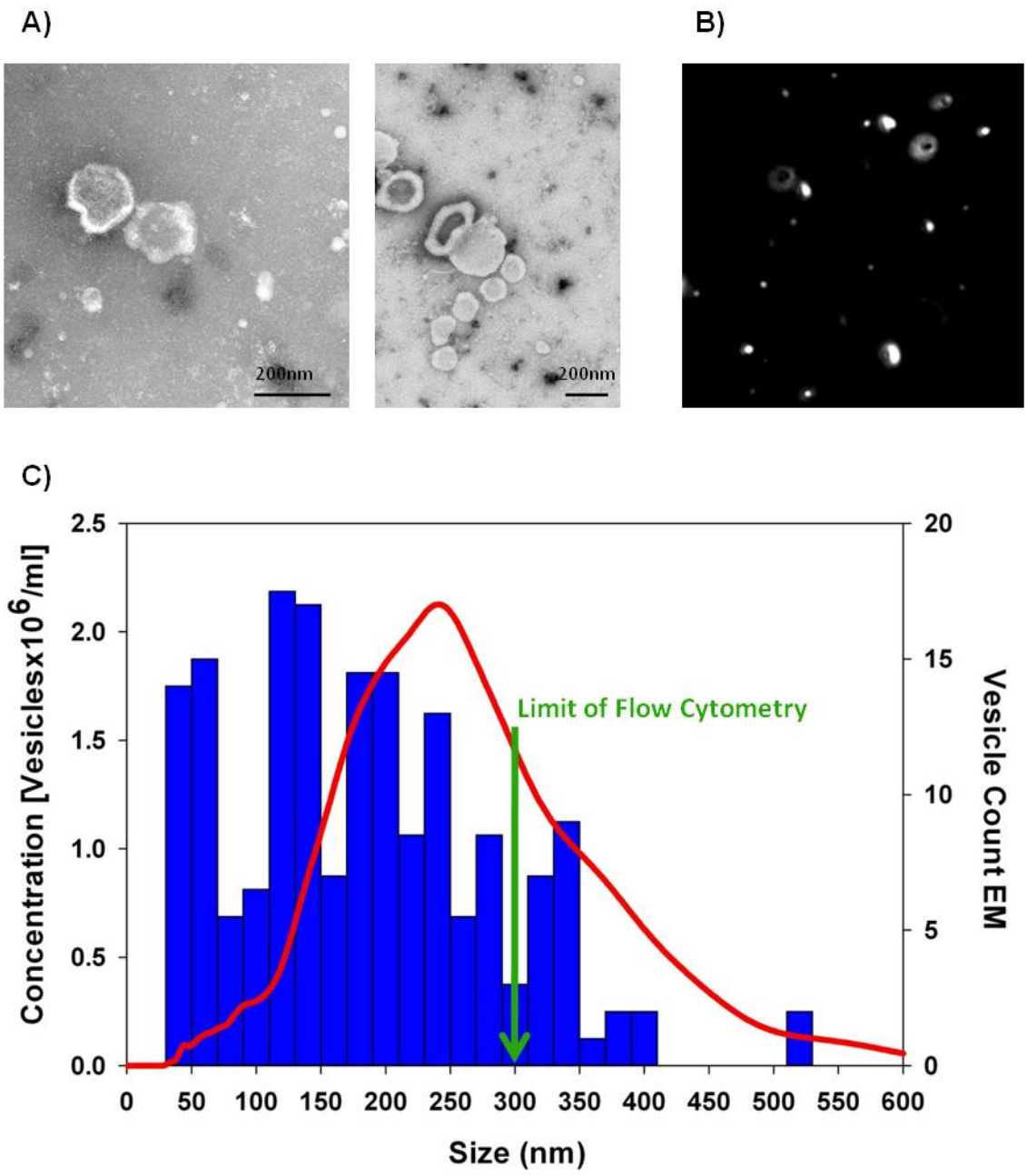

Figure 42. Comparison of NTA and electron microscopy of pSTBM. A) Electron micrograph of pSTBM, **B)** Screen shot image of NTA showing light scatter of pSTBM, **C)** Comparison of vesicle size as determined by NanoSight NTA (red line) vs. electron microscopy (blue bars).

3.4.3.2 NTA Measurement of *In vitro* Derived Platelet Vesicles

In vitro derived platelet vesicles from three healthy volunteers that were previously analysed using flow cytometry in Chapter 2 Section 2.4.3 were analysed using NTA. Figure 43A shows a NTA size vs. concentration profile of the vesicles from each volunteer

(colour dash lines) and the average of three (black line). The vesicles were highly polydisperse ranging in size from ~50-900nm with an average modal size of 219nm. The mean vesicle size was consistent between all three volunteers (Mean ± SD; 370 ± 207nm, 330 ± 163nm, 341 ± 161nm) and ~50% of the vesicles were smaller than those detectable using flow cytometry (<290nm). Total platelet vesicle concentration measured by NTA [2.92 x 10^9/ml] was significantly higher than that measured by flow cytometry FSC vs. SSC [3.87 x 10^7/ml] (Figure 43B).

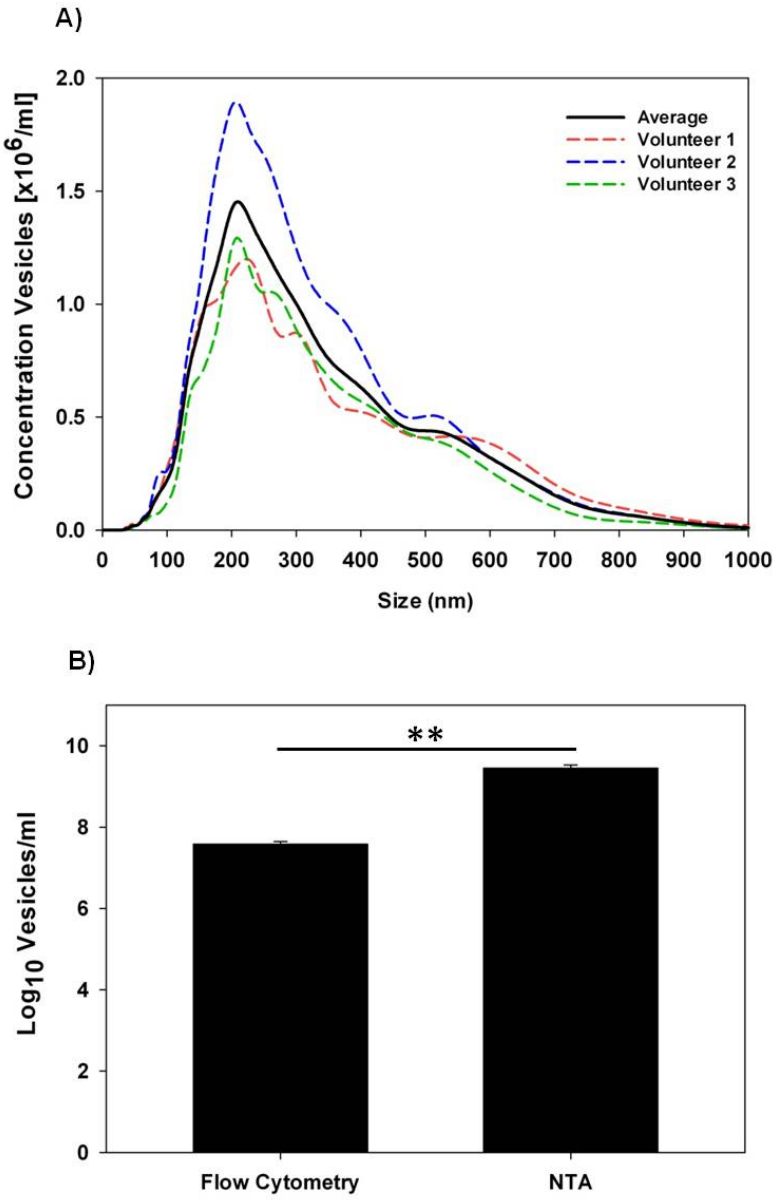

Figure 43. *In vitro* derived platelet vesicles. A) NTA size vs. concentration profile showing the distribution for each volunteer (dash colour lines) and the average (black line), **B)** Total vesicle counts as measured by flow cytometry and NTA. Bars represent Mean ± SE. **p<0.006.

3.4.3.3 NTA measurement of *In vitro* Derived RBC Vesicles

The *in vitro* derived RBC vesicles analysed by flow cytometry in Chapter 2 Section 2.4.4 were analysed using NTA. Unlike the pSTBM or *in vitro* derived platelet vesicles which were very polydisperse, the RBC vesicles were more uniform in size ranging from ~50-400nm with an average modal peak at 190nm (Figure 44A). The mean vesicle size was very consistent between samples from each volunteer (Mean ± SD; 212 ± 69nm, 208 ± 66nm, 201 ± 63nm). The vast majority (>90%) of vesicles were below the detection limit of flow cytometry (<290nm) and this was reflected in the concentration measurements as significantly more vesicles were analysed using NTA [2.19 x 10^9/ml] vs. flow cytometry [7.67 x 10^5/ml] (Figure 44B).

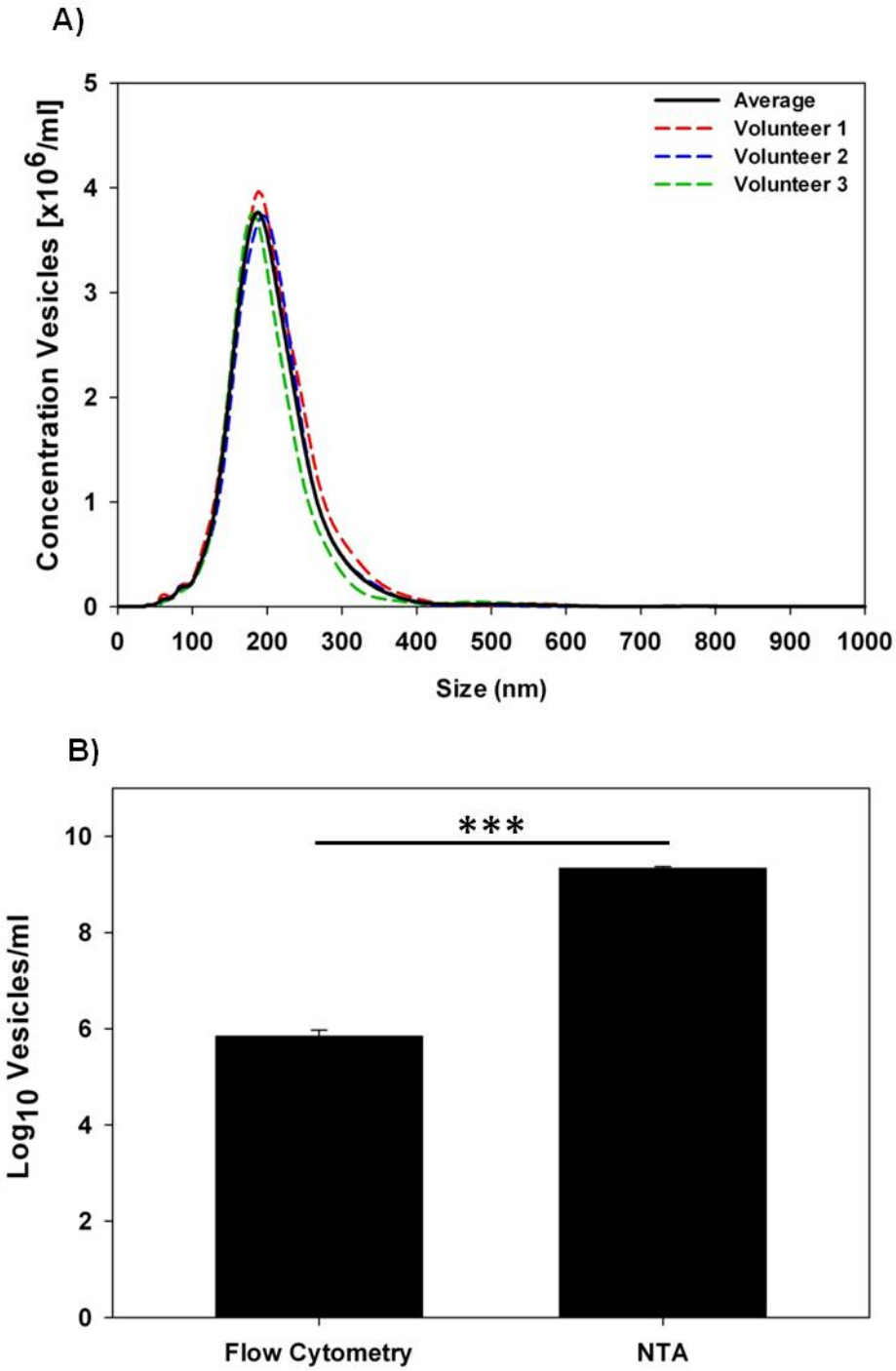

Figure 44. *In vitro* derived RBC vesicles. A) NTA size vs. concentration profile showing the distribution of each volunteer (dash colour lines) and the average (black line), **B)** Total vesicle counts as measured by flow cytometry and NTA. Bars represent Mean ± SE. **p<0.001.

3.4.3.4 NTA measurement of *In vitro* Derived HUVEC Vesicles

Two of the HUVEC *in vitro* derived vesicle preparations analysed by flow cytometry in Chapter 2 Section 2.4.5 were analysed using NTA. It was only possible to analyse two of

the three HUVEC vesicle preparations as one of the preparations was used up in the flow cytometry experiments. The flow cytometry data showed a significant elevation in vesicle counts in the camptothecin (CPT) stimulated HUVEC compared to the DMSO control, therefore we analysed these same samples using NTA. Very similar polydisperse size distributions ranging in size from ~50nm-650nm with a peak at ~200nm were measured in the DMSO control and CPT HUVEC vesicles (Figure 45A). The average mean vesicle size was 248 ± 115nm (mean ± SD) in the CPT HUVEC vesicles and 235 ± 106nm (mean ± SD) in the DMSO control HUVEC vesicles. Approximately 70-75% of the CPT and DMSO control HUVEC vesicles were smaller than 290nm, hence flow cytometry was only measuring 25-30% of the total vesicle population. HUVEC vesicle counts were elevated in the CPT treatment group vs. DMSO control group by ~2-fold in experiment 1 and >5-fold in experiment 2 (Figure 45B). Total HUVEC vesicle counts in the CPT treatment group as measured by NTA [9.48 x 10^9/ml] were higher compared to those measured using flow cytometry [8.79 x 10^5/ml] (Figure 45C).

Collectively, these data using the *in vitro* derived vesicle preparations demonstrate that NTA can measure the size and estimate the concentration of vesicles as small as ~50nm-70nm, exceeding the capabilities of flow cytometry.

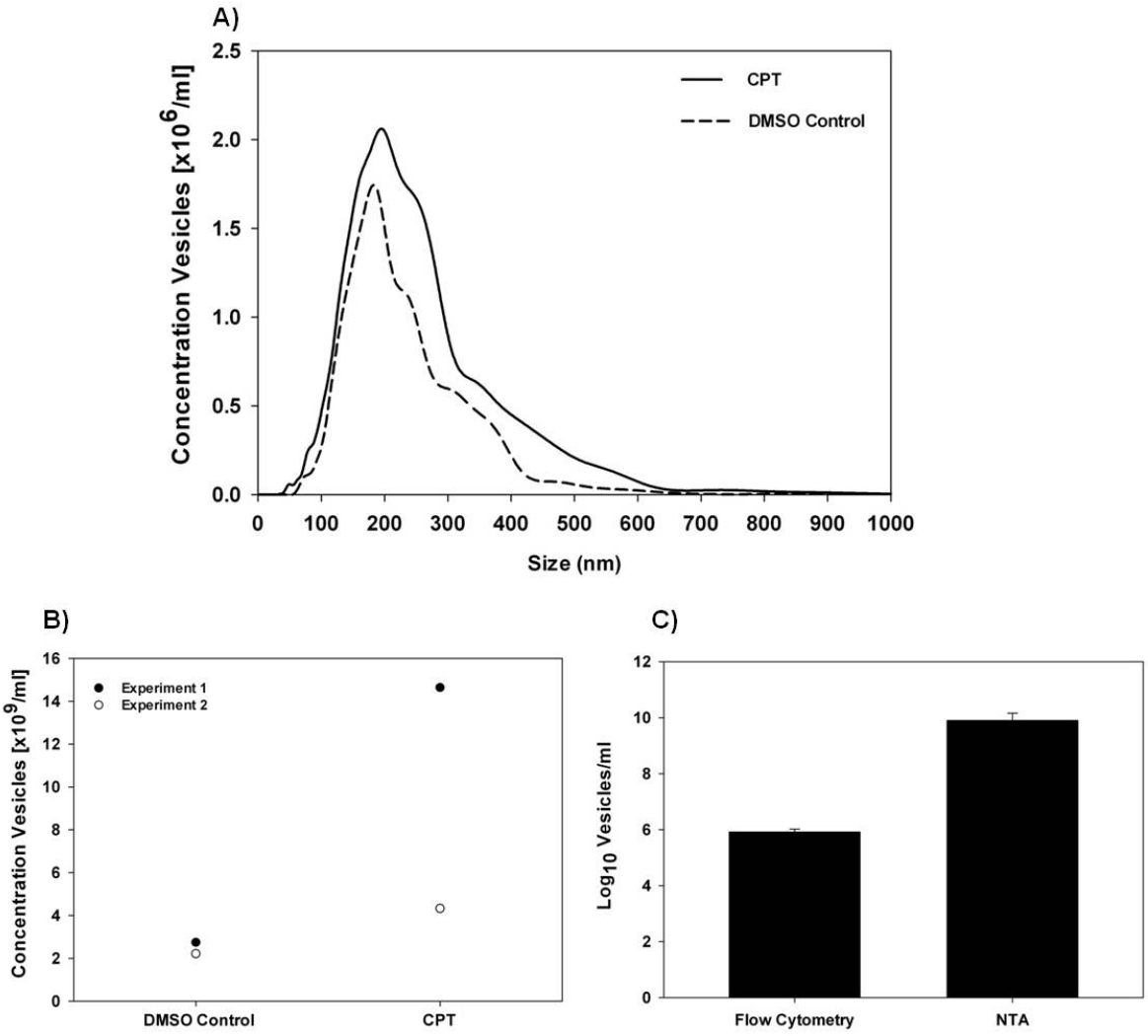

Figure 45. ***In vitro*** **derived HUVEC vesicles. A)** NTA size vs. concentration profile of HUVEC vesicles measured after stimulation for 24 hours with 5µM CPT or 0.5% DMSO, **B)** NTA total vesicle concentration measured in DMSO control and CPT, **C)** Total CPT vesicle counts measured by flow cytometry vs. NTA. Bars represent Mean ± SE. NTA; n = 2. Flow cytometry; n = 3.

3.4.4 NTA Measurement of PFP Vesicles

Having demonstrated the ability of NTA to measure *in vitro* derived vesicles from a number of different cell types, finally NTA was evaluated for its ability to measure vesicles in plasma. To determine whether NTA could accurately measure vesicle size and estimate the concentration in plasma, a two-fold dilution was performed using ultracentrifuge PFP pellets (resuspended in 250µl of PBS) from two single healthy female volunteers. A two-fold dilution (1 in 4 and 1 in 8) of the PFP vesicle pellet was analysed

using NTA. Figure 46A shows the modal size distribution vs. concentration profile for both dilutions in each volunteer. The total vesicle concentration (Figure 46B) and mean vesicle size (ranging from ~50nm-600nm) (Figure 46C) in each volunteer were shown to be highly consistent between dilutions. These data provide the proof of principle that NTA can analyse cellular derived vesicles in plasma. More detailed sets of experiments using NTA to analyse PFP are shown in Chapter 4.

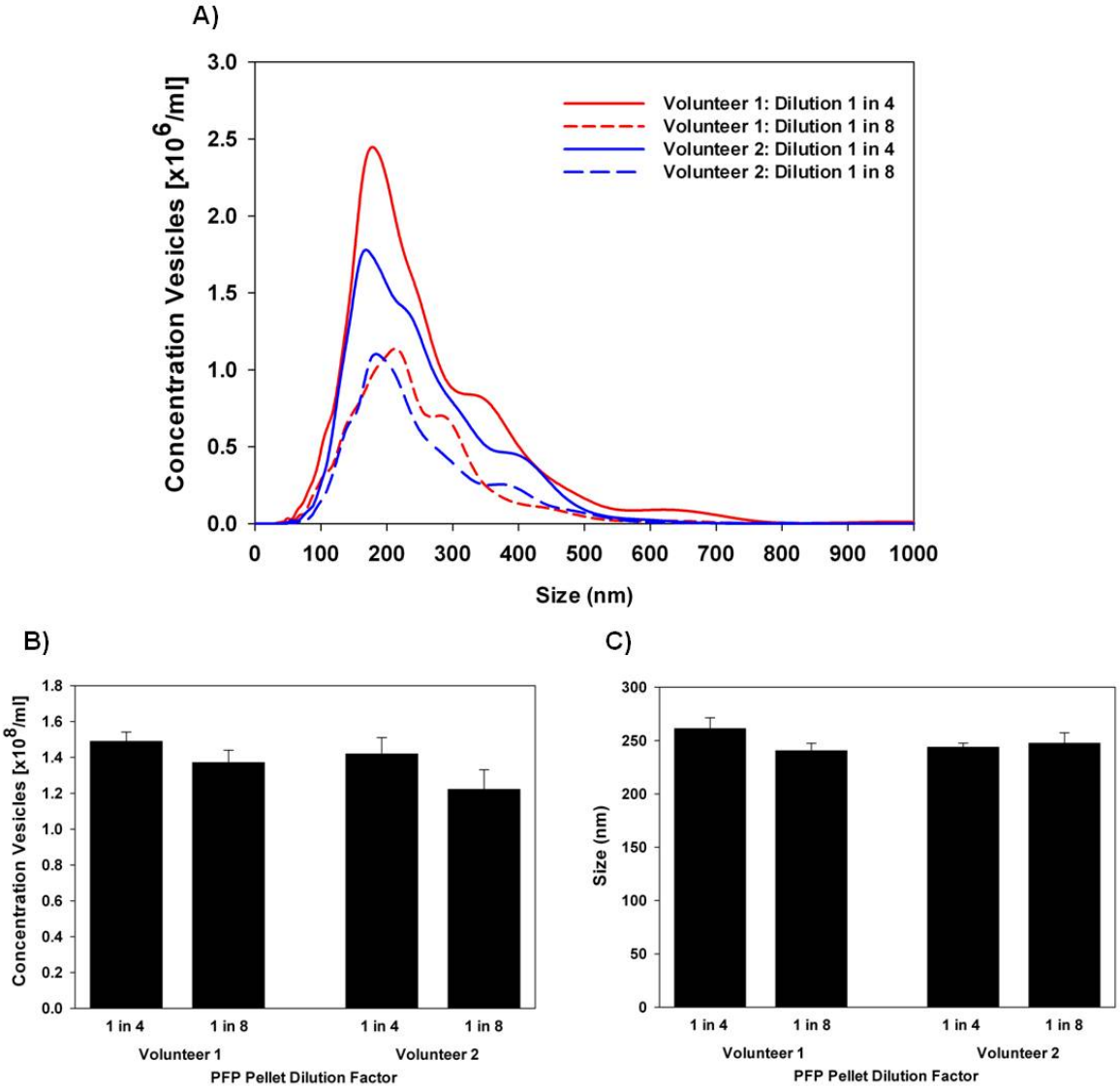

Figure 46. NTA dilution of PFP pellet. A) Modal size vs. concentration of PFP pellet two-fold dilution, **B)** Final Concentration (Mean ± SE) of vesicles in PFP pellet two-fold dilution, **C)** Vesicle size (Mean ± SE) of vesicles in PFP pellet two-fold dilution. Data is from two volunteers and is the average of 5 independent video analyses per dilution.

3.5 Discussion

3.5.1 Optimisation of the NanoSight LM10 Instrument

In this chapter NTA was evaluated as a novel method to analyse cellular derived vesicles. First, it was necessary to optimise the NanoSight LM10 instrument settings using monodisperse polystyrene beads ranging in size from 50-400nm. These experiments aimed to verify the accuracy of NTA to measure particle size and estimate concentration. The results showed that accurate NTA sizing and concentration measurements are made when the beads are visualised as single points of light and this is dependent on the camera shutter speed and gain settings. Larger particles (e.g. 200 - 400nm) required a very low camera shutter speed and no camera gain whereas a high camera shutter speed and high camera gain were required for the visualisation of smaller particles (e.g. 100nm). The lower limit of detection of the NanoSight instrument was in the order of 70nm, shown by accurate sizing measurements using maximum camera shutter speed and gain settings, however concentration measurement was vastly underestimated. Finally, monodisperse 100nm beads (using optimal camera shutter speed and gain settings) were used to determine the linearity of the NanoSight instrument and good linearity was observed in the range of $1 \times 10^8 – 8 \times 10^8$ beads/ml. Based on this result, all cellular vesicles were analysed at concentrations within this range.

The flow cytometry data presented in Chapter 2 illustrated that all the cellular vesicles were polydisperse and therefore it was essential to evaluate the ability of NTA to accurately size and quantitate a polydisperse sample using a mixture of 100nm and 300nm beads. Two distinct 100nm and 300nm bead populations were observed, however concentration measurements were largely overestimated due to using camera shutter and gain settings that were optimal for smaller (e.g. 100nm) particles. Increasing

concentrations of larger (e.g. 300nm) particles had no effect on the sizing accuracy of the smaller particles, however the larger particles were increasingly undersized. Hence, using optimal camera shutter and gain settings for smaller particles impacts negatively on the detection of the larger particles. Larger particles no longer appear as single points of light, but instead appear as large overexposed objects with Newton's rings that may scatter multiple points of light, which are interpreted by the NTA software as individual particles.

The results in this study are similar to those observed previously (Filipe *et al.*, 2010) whereby monodisperse and polydisperse mixtures of polystyrene beads were analysed using NTA and the results were directly compared to DLS. However, unlike our study, this study only evaluated NTA for measuring particle size and not for estimating particle concentration. Data from the previous study (Filipe *et al.*, 2010) showed that NTA was superior to DLS in accurately measuring the size distribution of monodisperse and polydisperse bead samples. DLS cannot accurately resolve polydisperse mixtures of particles because a single detection element simultaneously collects light from all the particles, meaning that the estimate of particle size and size distribution is biased to a larger particle size. This is in contrast to NTA which simultaneously measures particle size and scattering intensity on individual particles, therefore allowing polydisperse mixtures to be resolved. Moreover, NTA can estimate particle concentration by counting the observed number of particles within a known scattering volume. This information is unobtainable by DLS.

3.5.2 NTA Analysis of Cellular Vesicles

The data presented in this chapter demonstrates for the first time that NTA can be used to analyse cellular vesicles. Using pSTBM, a direct comparison of NTA, electron microscopy

and flow cytometry was made. NTA is far more rapid than electron microscopy allowing the detection of many more vesicles and, because the vesicles are analysed in suspension, they are not subject to shrinkage artefacts that are associated with fixation. NTA can detect vesicles much smaller than those detected by flow cytometry (≥290nm) and this was clearly reflected in the pSTBM total concentration measurements, whereby >200-fold more vesicles were analysed using NTA vs. flow cytometry. Furthermore, the mean vesicle size of pSTBM determined by NTA was smaller than that detectable by flow cytometry. This same pattern was reflected in the analysis of all the different types of cellular derived vesicles (platelet, RBC, HUVEC and PFP) analysed in this study. The size distribution of pSTBM, platelet derived-, HUVEC derived- and PFP derived-vesicles showed that each of these preparations were highly polydisperse. In contrast, the RBC derived vesicles showed a more monodisperse size distribution. The titration of pSTBM and PFP derived vesicles were both carried out within the linear range of the instrument and highly consistent vesicle size distributions and total concentration measurements between dilutions were observed. Together these data provide the proof of principle that NTA can be used to examine cellular derived vesicles.

Based on the data from the polydisperse beads, it is clear that the concentration measurements obtained using NTA for heterogeneous cellular derived vesicles do not give an absolute count and may be to some extent an overestimate. It is also probable that flow cytometry may underestimate the concentration of vesicles, as it is possible that coincident vesicles intercept the laser line and are therefore counted as a single vesicle, something which could also occur with aggregates of vesicles in NTA. The NTA polydisperse bead data show that the concentration can be overestimated by approximately double, whereas the difference in concentration observed in the cellular derived vesicles measured by NTA

compared to flow cytometry was shown to be increased by ~75-fold for the platelet derived vesicles and exceeding 10,000-fold for HUVEC derived vesicles. Hence, despite NTA overestimating vesicle concentration, this alone does not account for these huge fold differences when comparing NTA to flow cytometry. These data clearly demonstrate that NTA is more sensitive in analysing a population of vesicles not detectable by flow cytometry.

3.6 Summary

In this chapter the use of NTA was evaluated for the detection of cellular vesicles. The NanoSight instrument settings were optimised using polystyrene beads and the optimal settings were chosen based on accurate measurements of particle size and concentration. The sensitivity of the NanoSight LM10 instrument was in the order of 70nm thereby greatly exceeding that of flow cytometry (≥290nm). NTA was shown to analyse a polydisperse bead mix an essential requirement for the analysis of cellular derived vesicles. Limitations in the system were exposed whereby the concentration measurements and sizing of larger particles were less precise. Preparations of five different types of cellular derived vesicles were used to illustrate the ability of NTA to estimate vesicle size and concentration. The results clearly demonstrated that the vast majority of vesicles were smaller than those detectable by flow cytometry as reflected in the NTA mean vesicle size and concentration measurements. In summary, NTA extends the power of flow cytometry and can be used to analyse cellular derived vesicles. This technique was then used in parallel with flow cytometry to analyse PFP derived vesicles in NonP, NormP and PE women as presented in Chapter 4 of this thesis.

Chapter 4

Investigation of syncytiotrophoblast vesicles and other cellular derived vesicles in normal pregnancy and pre-eclampsia using flow cytometry and Nanoparticle Tracking Analysis

4.1 Introduction

4.1.1 Measurement of STBM in Plasma from NormP and PE Women Using Flow Cytometry

The working hypothesis presented in this thesis is outlined in Chapter 1 Section 1.6. To reiterate, it is hypothesised that STBM are the potential cause of the systemic inflammatory response, endothelial dysfunction and activation of the coagulation system, which accounts for many of the clinical signs of pre-eclampsia (PE) (Redman and Sargent 2005). By measuring STBM (the cause) in parallel with other circulating derived vesicles from platelets, RBCs, endothelium and leukocytes (the consequence) the prediction and monitoring of the condition may be improved.

Only four previous studies have used flow cytometry to examine circulating STBM in PE and NormP women (VanWijk *et al.,* 2002, Lok *et al.,* 2008a, Lok *et al.,* 2008b, Orozco *et al.,* 2009). In all these studies analogue flow cytometers (analysing vesicles ≥500nm) were used and, with the exception of one study (Orozco *et al.,* 2009) who analysed DNA-associated vesicles (i.e. those which labelled positive with PicoGreen DNA dye), only investigated Annexin V positive vesicles (VanWijk *et al.,* 2002, Lok *et al.,* 2008a, Lok *et al.,* 2008b). All studies used indirect antibody labelling (incubation with a primary antibody followed by incubation with a fluorescently conjugated secondary antibody) to identify circulating STBM in plasma which comprised 3-16% of the total vesicles in NormP and 5-10% in PE (Lok *et al.,* 2008b, Orozco *et al.,* 2009). One study also reported more circulating STBM in NonP controls vs. NormP and PE (VanWijk *et al.,* 2002). These variations may be accounted for by the specificity of antibodies used to detect STBM and it is also well known that indirect antibody labelling is more susceptible to non-specific

binding compared to direct antibody labelling and requires more thorough washing which is difficult to achieve when working with vesicles.

4.1.2 Measurement of Other Cellular Derived Vesicles in Plasma from NormP and PE Women Using Flow Cytometry

Aside from measuring circulating STBM, there have been fifteen studies (Harlow *et al.,* 2002, VanWijk *et al.,* 2002, Bretelle *et al.,* 2003, Gonzalez-Quintero *et al.,* 2003, Gonzalez-Quintero *et al.,* 2004, Holthe *et al.,* 2005, Meziani *et al.,* 2006, Biro *et al.,* 2007, Lok *et al.,* 2007, Lok *et al.,* 2008a, Lok *et al.,* 2008b, Lok *et al.,* 2009, Orozco *et al.,* 2009, Macey *et al.,* 2010, Alijotas-Reig *et al.,* 2011) that have used flow cytometry to measure cellular vesicles, including those derived from platelets, endothelial cells, RBCs and leukocytes in NormP and PE women. Four of these studies (Lok *et al.,* 2009, Orozco *et al.,* 2009, Macey *et al.,* 2010, Alijotas-Reig *et al.,* 2011) were published after commencing this current study. To date, the majority of studies have analysed Annexin V positive vesicles only, using analogue flow cytometry instrumentation. Similar to the studies examining circulating numbers of STBM, there are major inconsistencies in the numbers of the other circulating vesicles reported. For example, platelet vesicles have been identified using anti-CD41 or anti-CD61 and some studies have reported a decrease in circulating platelet derived vesicles in PE women vs. NormP women (Bretelle *et al.,* 2003), whereas others have reported an increase (Gonzalez-Quintero *et al.,* 2003, Alijotas-Reig *et al.,* 2011) or no difference at all (Lok *et al.,* 2008a). Moreover, circulating endothelial derived vesicles, identified using anti-CD51 were found to be comparable between PE and NormP women (Bretelle *et al.,* 2003), whereas when the endothelial marker anti-CD31 and platelet marker anti-CD42 were used in combination ($CD31^{+/}CD42^{-}$), numbers were found to be

significantly increased in PE vs. NormP women (Gonzalez-Quintero *et al.*, 2003, Gonzalez-Quintero *et al.*, 2004).

In Chapter 2 of this thesis it was demonstrated using *in vitro* derived vesicles that not all antigens from the parent cell are expressed on the surface of vesicles and the level of expression of those present is exceedingly variable. This may help to explain some of the observed differences in the studies described above. Moreover, the results from Chapter 2 showed that some markers are more specific for particular vesicle types than others. NDOG2 only labelled STBM and CD146 specifically labelled endothelial derived vesicles, whereas CD41 not only labelled platelet derived vesicles, but also labelled some STBM and monocyte vesicles. So far, all the studies that have analysed cellular derived vesicles in NormP and PE women have used single-antibody labelling, or at most double-antibody labelling to distinguish the cellular origin of the vesicles. This may have lead to some vesicles being incorrectly identified. To help overcome this problem, in this study a multi-colour flow cytometry assay was designed using the panel of directly conjugated antibodies that were tested on the *in vitro* derived vesicles shown in Chapter 2 of this thesis. In this chapter, these same antibodies were used to analyse *in vivo* circulating STBM, platelet, RBC, endothelial and leukocyte vesicles in plasma from NonP, NormP and PE women. These data have been expressed as vesicles/ml and as the percentage positive for each marker of interest. The vast majority of previous studies examining vesicles in plasma from NonP, NormP and PE women have only expressed the data as total circulating counts of vesicles and not as the percentage positive for the marker of interest. There may be a difference between the two and therefore in this study both have been reported.

Not only was this the first study to use a digital flow cytometer to investigate STBM and other cellular derived vesicles in plasma from NonP, NormP and PE women, but was also the first to use NTA in parallel. NTA enables the analysis of a sub-population of vesicles undetectable by flow cytometry and allows direct comparisons to be made between vesicle size and concentration measurements in all three groups. Vesicle size and concentration measurements may be altered in PE compared to NormP and NonP and therefore may be a direct reflection of the disorder. The STBM ELISA had not previously been used in conjunction with flow cytometry to measure circulating derived STBM in plasma. This allowed a direct comparison of the methodologies and established whether there was a correlation between the two. The use of the STBM ELISA, multi-colour flow cytometry assay and NTA aimed to provide the most comprehensive analysis of STBM and other cellular derived vesicles in NonP, NormP and PE to date.

4.2 Aims

To use flow cytometry and NTA to determine the number, size and phenotype of STBM and other cellular derived vesicles in NormP and PE.

4.3 Methods and Materials

4.3.1 Subjects

Blood from healthy male and female volunteers were used for methodology validation experiments, including investigating ultracentrifugation and the effect of freezing plasma. Blood samples were also taken from 10 non-pregnant (NonP), 10 normal pregnant (NormP) and 10 pre-eclamptic (PE) women, all recruited to the Oxford Pregnancy Biobank. PE was diagnosed as ≥90mmHg diastolic blood pressure on at least two

occasions within 24 hour and proteinuria ≥500mg in a 24 hour protein urine collection, 50mg/mmol protein/creatinine ratio or at least 2+ on dipstick testing on two consecutive measurements. PE women were matched to NonP women for age (± 4 years) and parity (0, 1-3, 4) and to NormP women for age, parity and gestational age (± 13 days) (Table 6). These studies were approved by the Oxfordshire Research Ethics Committee C and written informed consent was taken from all participants.

	Non-pregnant	Normal pregnant	Pre-eclampsia	p Value
Age (years)	33.6 (3.63)	33.4 (3.25)	33.6 (3.58)	n.s
Nulliparity	5/10 (50%)	5/10 (50%)	5/10 (50%)	n.s
Gestation (days)		254.4 (14.1)	259.1 (18.3)	n.s
Booking bp, mmHg		107/64 (6.86/6.80)	109/69 (10.00/10.39)	n.s
Max bp, mmHg		119/72 (11.20/5.65)	159/107 (14.30/11.21)	<0.001
Max proteinuria mg/24 h			3077.41 (4669.49) Range 585-15340	
Birthweight (g)		3564.1 (475.51)	2719(705.24)	<0.006

Table 6. Patient details for non-pregnant, normal pregnant and pre-eclamptic women (n=10). Data show Mean ± SD.

4.3.2 Preparation of PFP

PFP was prepared as described in Chapter 3 Section 3.3.4. PFP was then frozen in aliquots at -80°C until use.

4.3.3 Preparation of PFP Vesicles

2ml of frozen PFP was thawed at 37°C, made up to 11ml with PBS and centrifuged at 150,000 × g (max) for 1 hour at 4°C in a Beckman L8-80M ultracentrifuge. The supernatant (SN) was removed and the PFP pellet was resuspended in PBS.

4.3.4 Preparation of PFP Vesicles from Fresh vs. Frozen PFP

2ml of freshly isolated PFP from four healthy individuals were each made up to 11ml with PBS and centrifuged at 150,000 × g (max) for 1 hour at 4°C in a Beckman L8-80M ultracentrifuge. The SN was discarded, the PFP pellet was resuspended in 300µl of PBS and analysed immediately by flow cytometry. A separate aliquot of PFP was stored for ~1 month at -80°C and processed as above for flow cytometry analysis.

4.3.5 Flow Cytometry of PFP, PFP Ultracentrifuge Pellet and Supernatant

4.3.5.1 Fluorescent Stain and Antibody Labelling for Flow Cytometry Analysis

All reagents were filtered prior to use as described in Chapter 2 Section 2.3.4.1. Bovine Lactadherin–FITC was kindly provided by Dr Christian Heegaard (Protein Chemistry Laboratory, Milk Protein Research Consortium, Dept of Molecular Biology, University of Aarhus, Denmark). Lactadherin is a glycoprotein that binds externalised phosphatidylserine on the outer surface of the vesicle membrane via the C2 domain and can be used as an alternative to Annexin V for phosphatidylserine positive vesicle detection (Perez-Pujol *et al.*, 2007). PFP, ultracentrifuge pellet and SN were prepared from ten healthy individuals. PFP, ultracentrifuge pellet and SN (either neat or pre-diluted with PBS dependent on total vesicle concentrations) were labelled and analysed by flow cytometry as described in Chapter 2 Section 2.3.4.1. Samples were double-labelled with Lactadherin-FITC (5µg/ml) and a platelet marker CD61-PECy7 (0.25µg/ml; Beckman Coulter) or matching isotype control IgG1-PECy7 (0.25µg/ml; Beckman Coulter). Each sample was acquired for two minutes and the absolute count of vesicles/ml was established using BD Trucount tubes as described in Chapter 2 Section 2.4.1.

4.3.6 Measurement of Apolipoprotein B and Triglyceride Concentrations

Total Apolipoprotein (APOB) and triglyceride (TG) concentrations were measured by Dr Leanne Hodson (Oxford Centre for Diabetes Endocrinology and Metabolism (OCDEM), University of Oxford). Total APOB in PFP and SN were measured using a commercially available kit (Randox Laboratories Ltd., Crumlin, Co. Antrim). In brief, this is an antibody linked assay and measures turbitity of the sample excited at 340nm using an ILAB 600 analyser (Diamond Diagnostics, Holliston MA, USA). TG concentrations in PFP and SN were measured using a commercially available kit (Instrumentation Laboratory UK Ltd., Warrington, Cheshire). Absorbance measurements at 510nm were read using an ILAB 600 analyser (Diamond Diagnostics).

4.3.7 Flow Cytometry of PFP Vesicles: Fresh vs. Frozen PFP

4.3.7.1 Fluorescent Ligand and Antibody Labelling for Flow Cytometry Analysis

PFP derived vesicles in ultracentrifuge pellets were labelled and analysed by flow cytometry as described in Chapter 2 Section 2.3.4.1. Samples were triple labelled with Lactadherin FITC (5µg/ml), a platelet marker CD61-PECy7, RBC marker CD235a/b-PECy5 and matching isotype control antibodies as outlined in Chapter 2 Section 2.3.3.1 Table 2. Fluorochrome compensation was set-up using BD CompBeads and a single stain using Lactadherin-FITC labelled pSTBM. Gates were set using FMO with isotype controls. Samples were acquired for two minutes and enumeration of vesicles/ml was carried out as described in Chapter 2 Section 2.4.1.

4.3.8 Spiking pSTBM into Whole Blood for Flow Cytometry Analysis

Blood was taken from three healthy non-pregnant women as described in Section 3.3.4. pSTBM [1μg/ml] was added to whole blood and PFP was prepared as described in Section 4.3.2. PFP without pSTBM was used as a control. In addition a titration of pSTBM [0, 0.1, 0.5, 1μg/ml] was spiked into whole blood from one of the non-pregnant women. PFP derived vesicles were isolated by ultracentrifugation as described in Section 4.3.3 and resuspended in 400μl of PBS. Samples were labelled with NDOG2-FITC (3μg/ml) or matching isotype control at the same concentration. Samples were labelled and analysed using flow cytometry as described in Section 2.3.4.1. Samples were acquired for two minutes and vesicle enumeration was carried out as described in Chapter 2 Section 2.4.1.

4.3.9 Preparation of PFP Vesicles in NonP, NormP and PE Samples

Blood samples were taken from NonP, NormP and PE women and PFP was prepared as outlined in Section 4.3.2. 3ml of frozen PFP was thawed at 37°C and made up to 11ml with PBS and centrifuged at 150,000 × g (max) for 1 hour at 4°C in a Beckman L8-80M ultracentrifuge. The SN was discarded, the PFP pellet was resuspended in 750μl of PBS and analysed by flow cytometry and NTA.

4.3.10 Flow Cytometry of PFP Vesicles in NonP, NormP and PE Samples

PFP vesicles in ultracentrifuge pellets from NonP, NormP and PE samples were labelled and analysed by flow cytometry as described in Chapter 2 Section 2.3.4.1. Based on the findings of Chapter 2, samples were labelled with a panel of fluorescent stain/antibody combinations as outlined in Table 7. Previously, NDOG2 and the corresponding IgG1 isotype control were conjugated to PE or FITC using Lightning Link kits (Innova

Biosciences). However in this set of experiments, due to quality control issues with the Lightning Link kits, we used NDOG2-PE which was custom conjugated commercially by Biolegend. The BD Biosciences Fluorescence Spectrum Viewer was used to help select suitable combinations of fluorophores (http://www.bdbiosciences.com/research/multicolor/spectrum_viewer/index.jsp). Fluorochrome compensation was set-up using BD CompBeads and a single stain using pSTBM for Bio-Maleimide. Gates were set using FMO with isotype controls as explained in Chapter 2 Section 2.3.4.1. All samples were acquired for two minutes and the absolute count of vesicles/ml was carried out as described in Chapter 2 Section 2.4.1.

Fluorescent Label, Antibody/Isotype Control	Target Vesicle Cell Type	Clone	Final Concentration
Bio-Maleimide	**All vesicles**	Not Applicable	0.25μM
NDOG2-PE[b]	**Syncytiotrophoblast**	NDOG2	0.5μg/ml
IgG1-PE[b]		MOPC-21	0.5μg/ml
CD41-PECy7[c]	**Platelet**	P2	0.25μg/ml
IgG1-PECy7[c]		679.1Mc7	0.25μg/ml
HLA Class I (W6/32)-APCCy7[b]	**Leukocyte**	W6/32	2.5μg/ml
IgG2a-APCCy7[b]		MOPC-173	2.5μg/ml
CD235a/b-PECy5[b]	**Red Blood Cell**	HIR2	0.05μg/ml
IgG2b-PECy5[b]		MPC-11	0.05μg/ml
CD146-Alexa-647[b]	**Endothelial Cell**	OJ79c	0.125μg/ml
IgG1-Alexa-647[b]		MOPC-21	0.125μg/ml

Table 7. Fluorescent label, antibodies and isotype controls used. [a] Molecular Probes; Invitrogen. [b] Biolegend UK Ltd; [c] Beckman Coulter.

4.3.11 Measurement of STBM in PFP by ELISA

STBM in NonP, NormP and PE PFP samples were measured using an in-house ELISA as previously described (Goswami *et al.*, 2006) with modification. Frozen PFP samples were

thawed at 37°C and 2ml of PFP was made up to 11ml with PBS and centrifuged at 150,000 × g (max) for 1 hour at 4°C in a Beckman L8-80M ultracentrifuge. The SN was discarded and the PFP pellet was resuspended in 350µl of PBS containing 1% BSA (w/v) and 0.05% tween 20 (v/v; Sigma-Aldrich) and stored at -80°C until use.

A 96-well black maxisorp plate (Nunc; VWR International Ltd, Lutterworth, UK) was coated with 100µl of the anti-placental alkaline phosphatase NDOG2 antibody [10µg/ml] and incubated overnight at room temperature. Following incubation, the plate was washed five times with wash buffer (Tris-buffered saline containing 0.1% tween 20 (v/v)). 300µl of blocking buffer (5% BSA (w/v) in PBS) was added to each well and incubated for a further three hours. Following incubation, the plate was washed five times with wash buffer. A pooled preparation of pSTBM from eight normal placentas was used to prepare the standards (0-4000ng/ml of protein) for the ELISA. The PFP pellet was thawed at 37°C and 100µl was added per well and incubated overnight. The next day, the plate was washed ten times with wash buffer. An ELISA amplifier, 4-Methylumbelliferyl phosphate (4-MUP; Sigma-Aldrich) was used as a fluorescent substrate for the detection of endogenous alkaline phosphatase activity on the surface of the vesicles. 4-MUP was used at a final concentration of 0.2mg/ml and was prepared in an assay buffer of 100mmol/L diethanolamine and 21mmol/L $MgCl_2$ (both from Sigma-Aldrich) pH 10.0. The plate was read using a FLUOstar Optima (BMG Labtech) plate reader at excitation 355nm and emission 460nm at 1 hour. The pSTBM standard curve was used to determine the STBM concentration in each 350µl PFP sample in ng/ml. As samples had been concentrated by ultracentrifugation, this figure was divided by a concentration factor of x/y (where x = volume of original PFP sample in ml and y = volume in which the pellet was reconstituted

in ml. i.e. 2/.35=5.714) in order to calculate the STBM concentration in the original sample.

4.3.12 Nanoparticle Tracking Analysis (NTA)

4.3.12.1 Measurement of Vesicles in PFP, PFP Ultracentrifuge Pellet and Supernatant

PFP, PFP ultracentrifuge pellet and SN were diluted in PBS and were introduced into the sample chamber of the NanoSight LM10 instrument as described in Chapter 3 Section 3.3.2. Each sample measurement was repeated 3-5 times. Sample videos were captured using a camera shutter speed of 1000 and camera gain setting of 500. Post acquisition settings as stated in Chapter 3 Section 3.3.2 were used for all samples. Each video was analysed to give the mode and mean vesicle size, together with an estimate of vesicle concentration.

4.3.12.2 Measurement of PFP Vesicles from Fresh vs. Frozen PFP

Ultracentrifuge pellets from fresh vs. frozen PFP in two healthy subjects were analysed. Samples were diluted in PBS and analysed as described in Section 4.3.12.1.

4.3.12.3 Measurement of PFP Vesicles in NonP, NormP and PE Samples

PFP vesicles in ultracentrifuge pellets from NonP, NormP and PE samples were diluted in PBS. Samples were analysed as described above in Section 4.3.12.1.

4.3.13 Fluorescence NTA: NS500 Instrument

The NanoSight NS500 instrument is a development of the NanoSight LM10 system, incorporating the ability to phenotype vesicles by offering a fluorescence capability. The

NS500 is equipped with a 405nm (violet) laser and interchangeable 430nm long-pass filter. The upgraded camera system increases the sensitivity of the instrument, allowing the detection of smaller vesicles as small as 50nm. 200nm Nanosphere size standards (Thermo Scientific) and 100nm fluoresbrite YG microspheres (Polysciences) were diluted accordingly in PBS. These experiments were performed in our laboratory by Dr Chris Gardiner (Nuffield Dept Obstetrics and Gynaecology, University of Oxford). Settings were optimised and particles were measured using both the fluorescence (i.e. with the long-pass filter in place) and light scatter modes. Total vesicle numbers were measured and compared between the two modes.

4.3.13.1 pSTBM labelling with NDOG2 conjugated to Quantum Dots (Qdots)

Quantum dots (Qdots) were conjugated to NDOG2 antibody and the corresponding IgG1 isotype control antibody (R&D Systems) with a Qdot 605 Antibody Conjugation Kit (Invitrogen) according to the manufacturer's instructions. In brief, the polyethylene glycol amine (molecular weight 2000) coated Qdots were activated with the cross-linker 4-(maleimidomethyl)-1-cyclohexanecarboxylic acid *N*-hydroxysuccinimide ester (SMCC), yielding a maleimide-nanocrystal surface. Excess SMCC was removed by size exclusion chromatography. The antibody was then reduced by dithiothreitol to expose free sulfhydryl groups, and excess dithiothreitol was removed by size exclusion chromatography. The activated Qdots were covalently coupled with reduced antibody and the reaction quenched with mercaptoethanol. Conjugates were concentrated by ultrafiltration and purified by size exclusion chromatography. pSTBM were diluted 1:100 and NDOG2-Qdot605 or IgG1-Qdot605 was added to give a final Qdot concentration of 10nM. The molar ratio of antibody to Qdots was 3.5:1. Samples were incubated for 15 minutes at room temperature and then diluted with PBS and analysed by NTA.

4.3.14 Flow Cytometry of pSTBM Labelled With NDOG2 Conjugated to QDots

Antibodies were filtered prior to use as described in Chapter 2 Section 2.3.4.1. pSTBM were diluted in PBS and labelled with NDOG2-Qdot605 or IgG1-Qdot605 at 10μg/ml. Samples were made up to 1ml with PBS and analysed by flow cytometry as described in Chapter 2 Section 2.3.4.1.

4.3.15 Statistics

Each data set was first tested for a Guassian distribution by using a Shapiro-Wilk normality test and for equal variance using a Levene Median test. In data sets found to pass both the normality and equal variance test and those that compared two groups were analysed using a student's *t*-test. Non-Parametric data comparing two treatment groups were analysed using a Mann-Whitney Rank Sum Test. Data sets containing three treatment groups and those that passed normality and equal variance were analysed using a One Way ANOVA. When data were found to be significantly different, all pairwise multiple comparisons were made using a Holm-Sidak test. For non-parametric data a Kruskal-Wallis One Way ANOVA on Ranks was performed and significant differences were identified using a multiple comparisons Tukey test. Values of $p<0.05$ were considered to be significant. SigmaPlot 12.0 was used for the data analysis

4.4 Results

4.4.1 Flow Cytometric Analysis and NTA of PFP, PFP Ultracentrifuge Pellet and Supernatant

This study first examined if cellular vesicles could be analysed in PFP directly or whether ultracentrifugation was necessary to pellet and concentrate these vesicles. Flow cytometric analysis based on forward and side scatter measurements showed significantly more vesicles in the PFP and SN compared to that of the ultracentrifuge pellet (Figure 47A). In contrast, when PFP, PFP ultracentrifuge pellet and SN post ultracentrifugation were double labelled with Lactadherin (a positive marker of phosphatidylserine exposure on the surface of vesicles) and the platelet marker CD61, the numbers of vesicles were found to be significantly elevated in the PFP pellet compared to PFP or SN (Figure 47B and Figure 47C respectively) showing that they have been enriched by this process. Furthermore, the percentage of vesicles that labelled positive with Lactadherin and CD61 was significantly increased in the PFP pellet compared to that of the PFP or SN (Figure 47D). Figure 47E shows representative flow cytometry plots of Lactadherin/CD61 % positive vesicles in PFP, PFP pellet and SN.

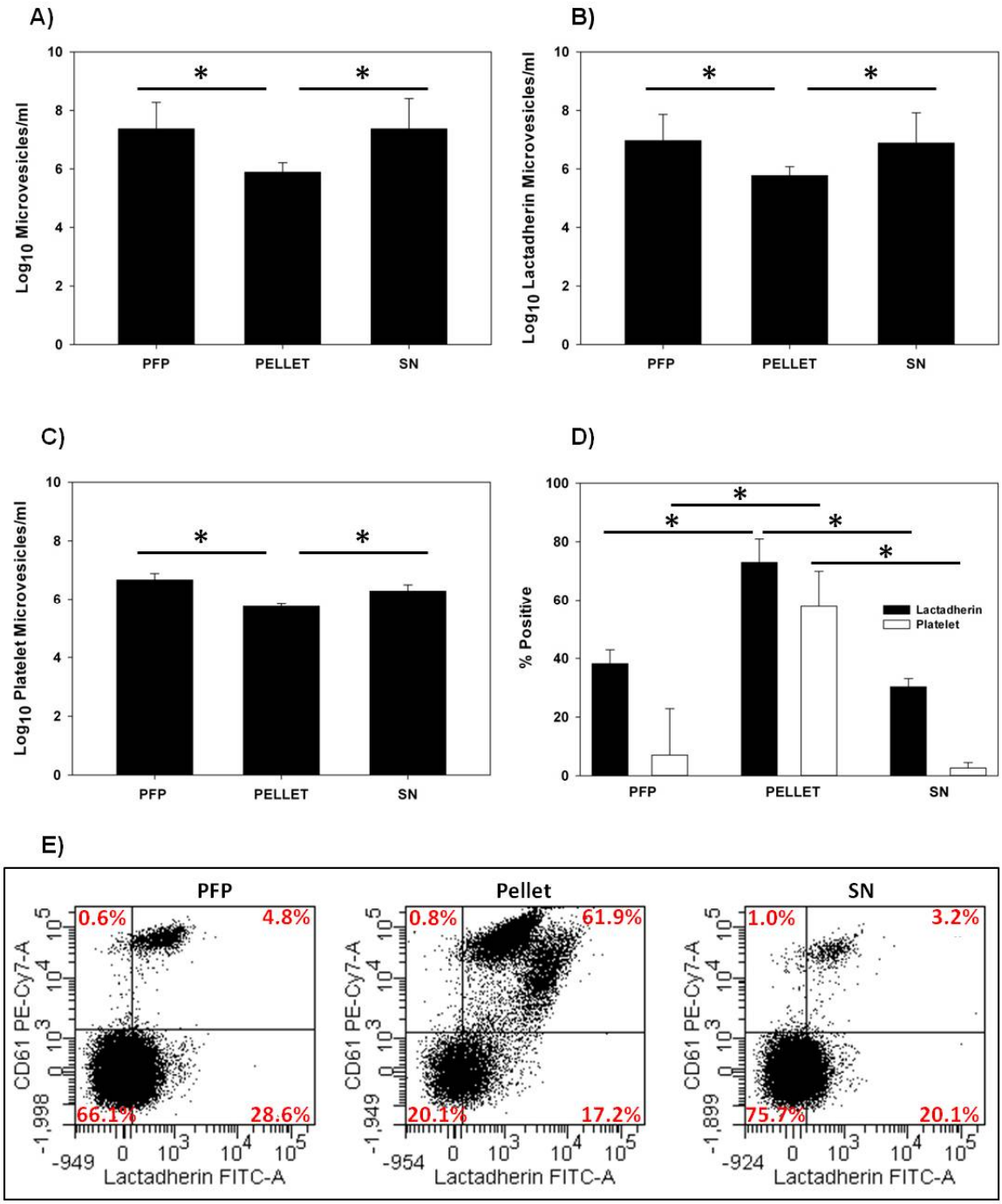

Figure 47. Flow Cytometry Analysis of PFP, PFP ultracentrifuge pellet and supernatant (SN). A) Total vesicle counts in PFP, pellet and SN, **B)** Total Lactadherin vesicles in PFP, pellet and SN, **C)** Total platelet vesicle count in PFP, pellet and SN, **D)** Percentage of positive Lactadherin and platelet vesicles in PFP, pellet and SN, **E)** Representative plots showing the percentage of positive labelling with Lactadherin and CD61 in PFP, pellet and SN. Bars represent median with interquartile range. n=10.

In agreement with the flow cytometry FSC vs. SSC data, NTA showed significantly more vesicles in the PFP and SN compared to the pellet (Figure 48A). Figure 48B shows the concentration of vesicles [x10^8/ml] vs. size (nm) in the PFP, pellet and SN. The vesicles

were polydisperse in size and ranged from 50nm to 500nm in the PFP and SN and from 50nm to 600nm in the pellet. The modal size of vesicles in the PFP, pellet and SN was; 142 ± 6.5nm, 195 ± 11.5nm and 134 ± 6.0nm (Mean ± SE) respectively. As might be expected, the mean size of vesicles in the pellet was found to be significantly larger than those in the PFP and SN (Figure 48C).

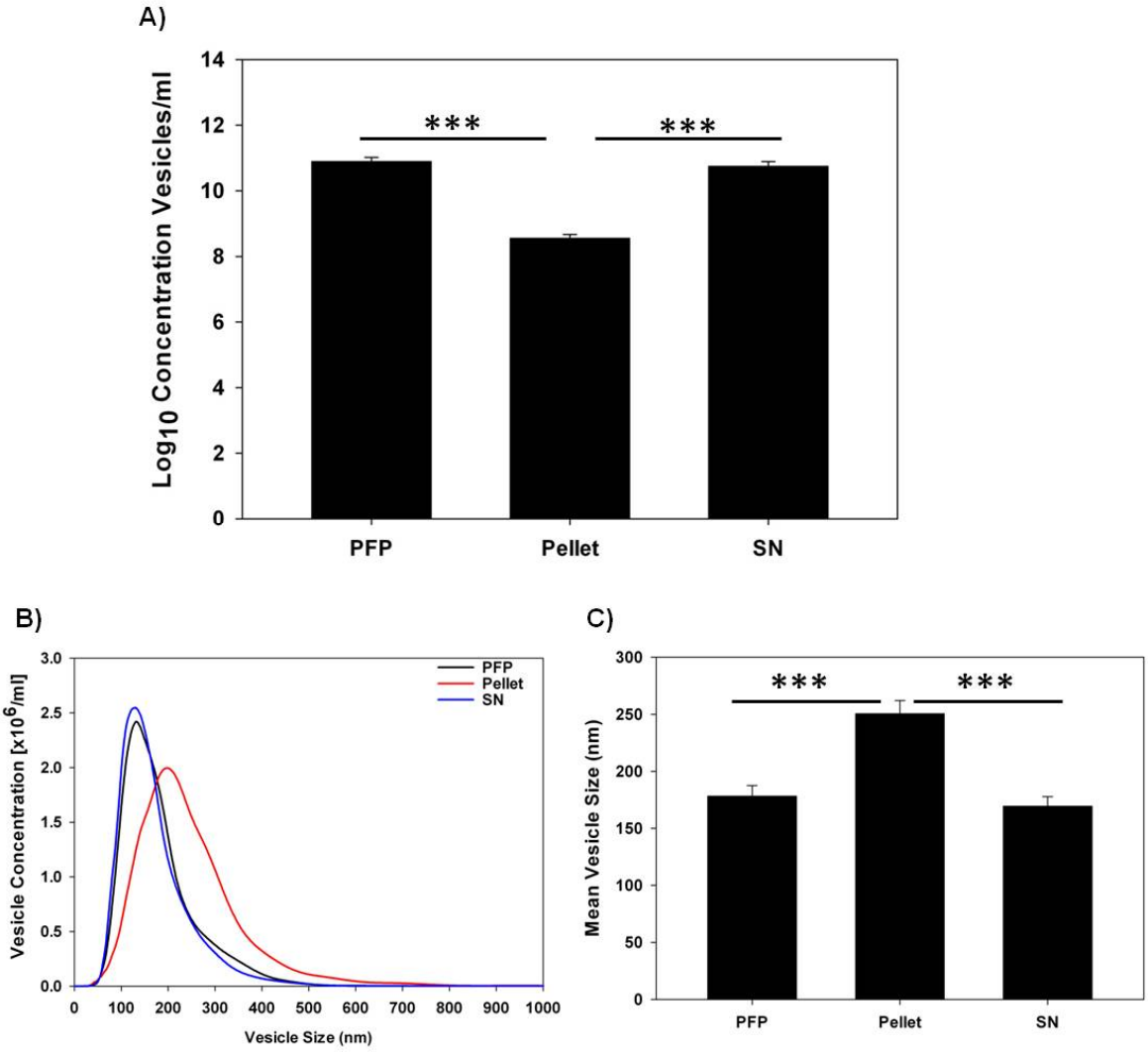

Figure 48. NTA measurement of vesicle concentration and size in PFP, ultracentrifuge pellet and SN. A) Concentration of vesicles/ml in the PFP, pellet and SN. Bars represent mean ± SE, **B)** Vesicle size vs. concentration profiles of PFP, pellet and SN, **C)** Mean vesicle size in PFP, pellet and SN. Bars represent Mean ± SE. n=10.

Measuring the concentration of vesicles in the PFP, pellet and SN using NTA vs. flow cytometry FSC vs. SSC, clearly demonstrated that significantly more vesicles were detected using NTA compared to flow cytometry (Figure 49).

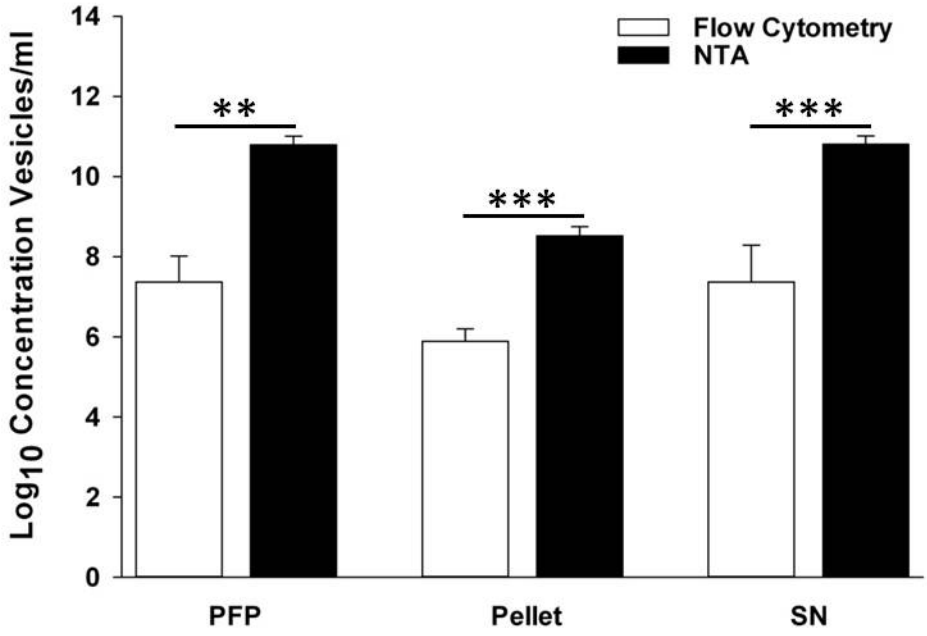

Figure 49. Comparison of vesicle concentration in PFP, PFP ultracentrifuge pellet and SN measured by flow cytometry and NTA. Bars represent median with interquartile range. p values (** $p<0.003$, ***$p<0.001$). n=10

Flow cytometry and NTA showed significantly elevated vesicle numbers in the PFP and SN compared to that of the pellet. Phenotypic analysis of the pellet showed that >70% of vesicles labelled with Lactadherin and >60% were platelet derived, in contrast to the PFP and SN in which the percentage of positive labelling with Lactadherin or the platelet marker was significantly lower. Furthermore, NTA illustrated that the vesicles in the pellet were significantly larger than those in the PFP and SN. Together these data suggest that the vesicles in the pellet were cellular in origin whereas those in the PFP and SN were different, as they appeared to have a lower density, not being pelleted by ultracentrifugation. Plasma contains four major groups of lipoproteins consisting of chylomicrons, very low density lipoproteins (VLDL), low density lipoproteins (LDL) and high density lipoproteins (HDL). Chylomicrons and VLDL are lipid vesicles and are similar in size to cellar vesicles (Frayn 2010) and can be detected by light scatter (Cantero *et al.*, 1998, Ruf and Gould 1999). Chylomicrons contain apolipoprotein B48 (APOB48),

whereas VLDL contains APOB100 and they are both rich in triglycerides (Frayn 2010). To determine whether the large numbers of vesicles in the PFP and SN were chylomicrons and VLDL, in collaboration with Dr. Leanne Hodson from the Oxford Centre for Diabetes Endocrinology and Metabolism (OCDEM), APOB (48 and 100) and triglyceride concentrations were measured in the PFP and SN and were found to be at comparable levels (Figure 50). It was not possible to measure APOB and triglycerides in the pellet due to the small sample available, but the fact that levels were the same pre- and post-ultracentrifugation suggests that the chylomicrons and VLDL were not pelleted by this process, emphasising the importance of centrifugation for cellular vesicle analysis.

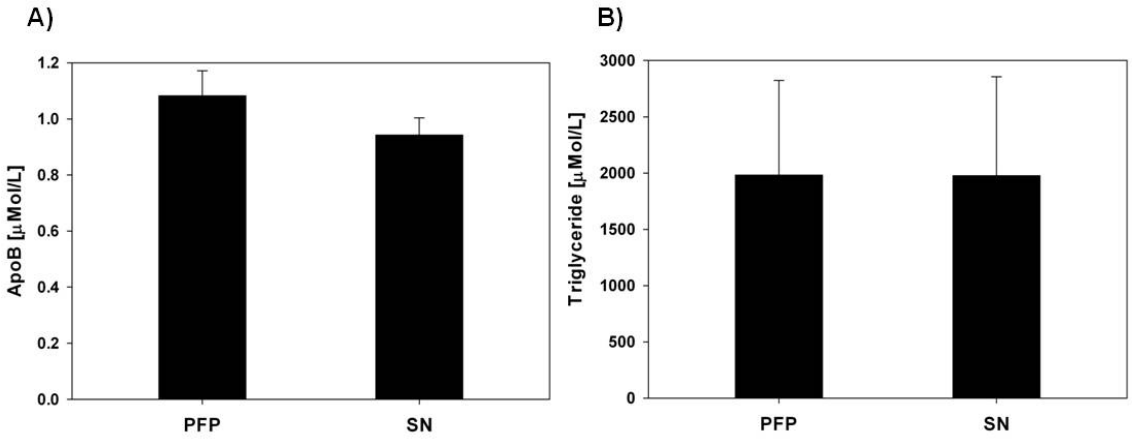

Figure 50. APOB and triglyceride concentrations in PFP and SN. A) APOB concentration in PFP and SN. Bars represent Mean ± SE, **B)** Triglyceride concentration in PFP and SN. Bars represent Median with interquartile range. n=18.

4.4.2 Flow Cytometric Analysis: Effect of Freezing PFP on Vesicle Quantification

A major concern with these studies is the possible effect of freezing and thawing on vesicle quantification. Flow cytometric analysis of ultracentrifuge pellets from fresh PFP compared to frozen PFP showed no significant difference in total counts of vesicles although there was a trend suggesting that the vesicle number was slightly reduced in pellets from frozen vs. fresh PFP (Figure 51A). Total Lactadherin positive vesicles were comparable between pellets from fresh PFP and frozen PFP (Figure 51B), however the percentage of vesicles that labelled positive for Lactadherin was significantly increased in the pellets from frozen PFP (Figure 51C), suggesting that phosphatidylserine exposure may be increased by freezing. There was a considerable increase in the number of vesicles measured by NTA as compared to flow cytometry (Figure 51D). However, NTA analysis of the pellets from fresh vs. frozen PFP was comparable and in the two subjects analysed no difference in modal vesicle size was detected when comparing pellets from fresh (Subject 1: 232nm, Subject 2: 208nm) and frozen (Subject 1: 209nm and Subject 2: 201nm) PFP.

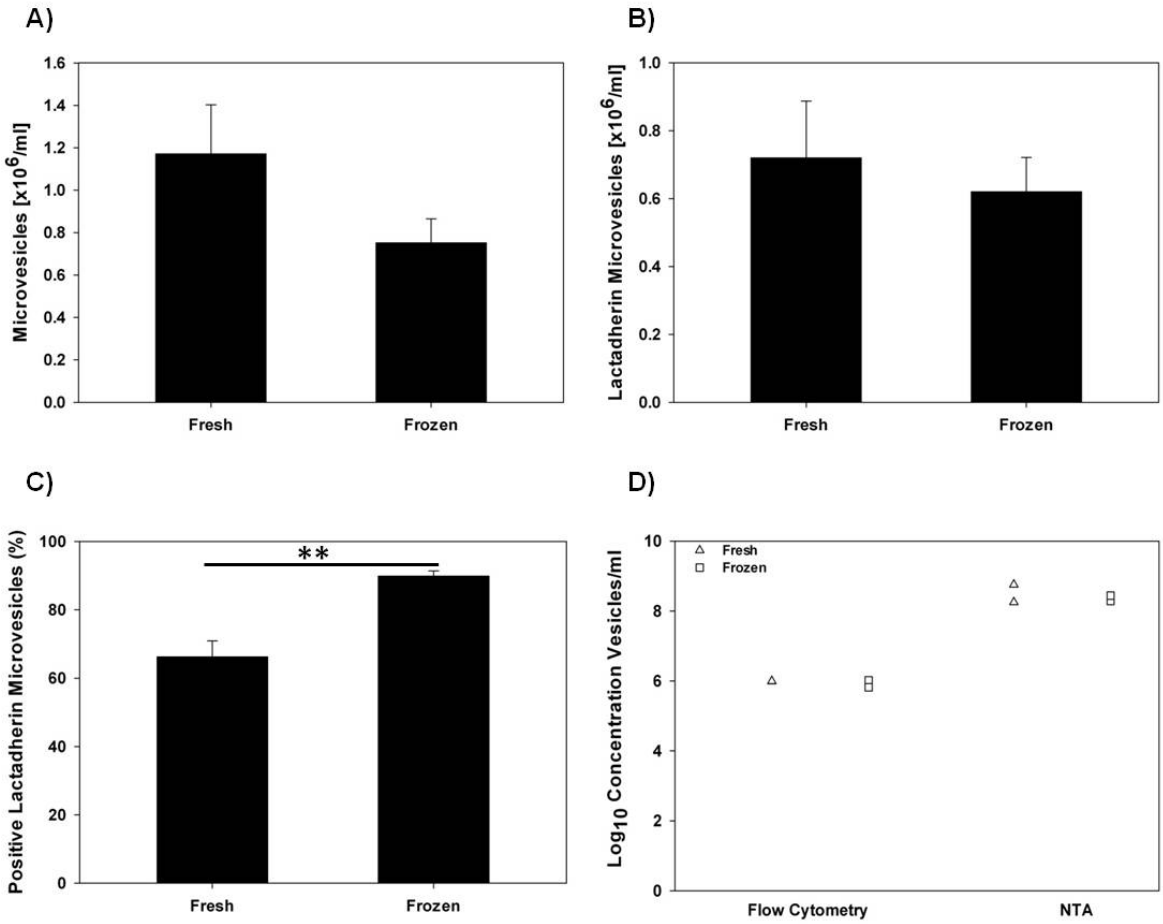

Figure 51. Flow Cytometry comparison of ultracentrifuge pellets from fresh vs. frozen PFP. A) Total vesicle counts, **B)** Total Lactadherin postitive vesicles, **C)** Percentage of vesicles labelling with Lactadherin, **D)** Total vesicle counts measured by flow cytometry and NTA. Flow cytometry n=4, NTA n=2. **p=0.003. Bars represent Mean ± SE.

Platelet vesicles were examined next, as these are known to be the most abundant population in plasma. Ultracentrifuge pellets from fresh and frozen PFP were double labelled with Lactadherin and an antibody to the platelet marker CD61 and analysed by flow cytometry. No difference was detected in CD61 (Figure 52A), $CD61^+$/$Lactadherin^+$ (Figure 52C) or $CD61^+$/$Lactadherin^-$ (Figure 52E) total vesicles in pellets from fresh or frozen PFP. The percentage of labelling for CD61 (Figure 52B), $CD61^+$/$Lactadherin^+$ (Figure 52D) and $CD61^+$/$Lactadherin^-$ (Figure 52F) vesicles was comparable in pellets from fresh and frozen PFP.

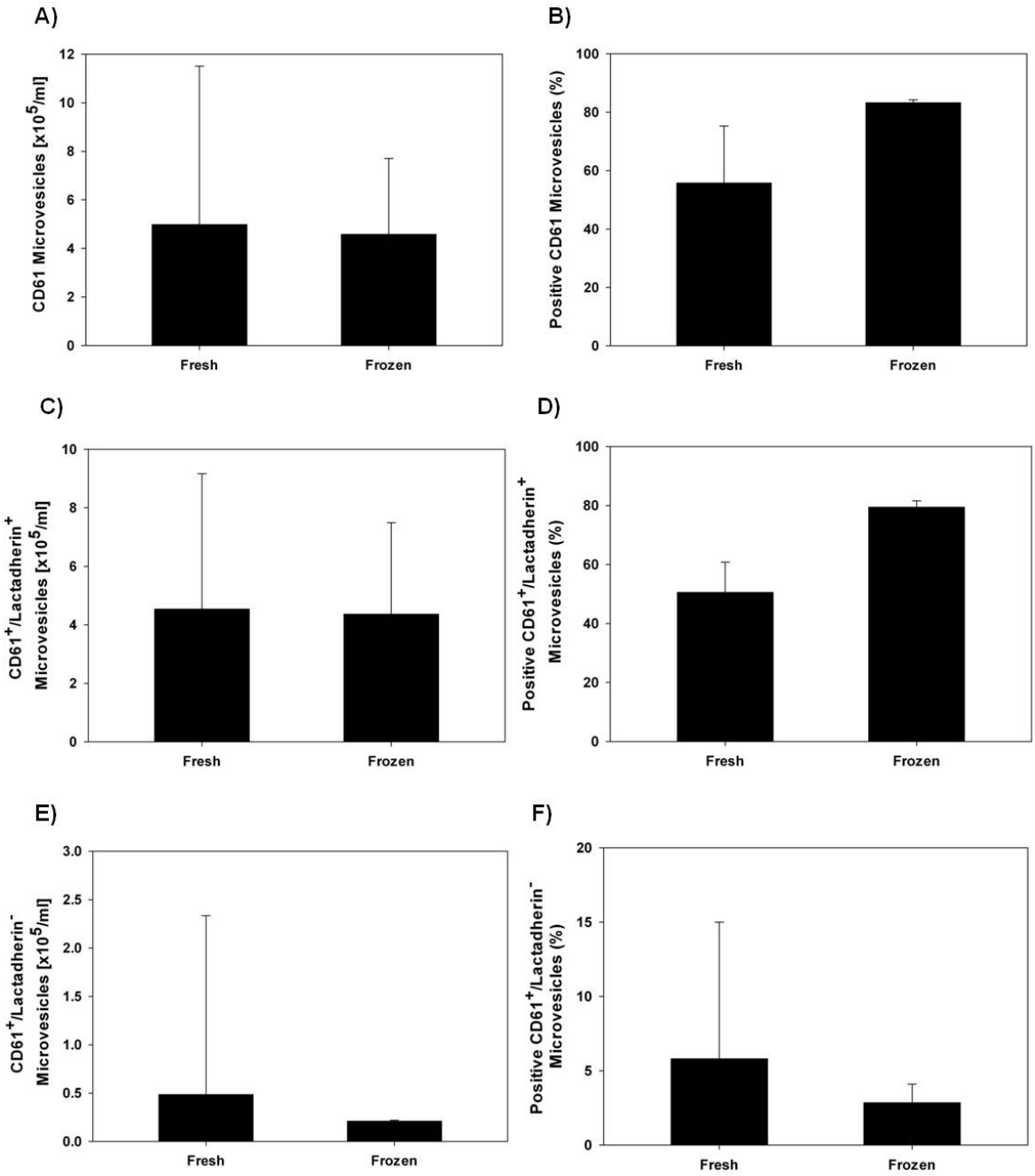

Figure 52. Flow cytometry analysis of ultracentrifuge pellets from fresh vs. frozen PFP: Platelet vesicles. A) Total CD61 vesicle counts, **B)** Percentage of CD61 positive vesicles, **C)** Total $CD61^+/Lactadherin^+$ vesicle counts, **D)** Percentage of $CD61^+/Lactadherin^+$ vesicles, **E)** Total $CD61^+/Lactadherin^-$ vesicle counts, **F)** Percentage of $CD61^+/Lactadherin^-$ vesicles. Bars represent median with the interquartile range. n=4.

Finally, RBC derived vesicles were examined and a significant reduction in total RBC derived vesicles labelled for CD235a/b in pellets from frozen PFP compared to fresh was shown (Figure 53A). The percentage of vesicles labelled for CD235a/b was comparable between pellets from fresh or frozen PFP (Figure 53B). No significant difference in total

CD235a/b^{+}/Lactadherin^{+} vesicles or the percentage positive was detected in pellets from fresh PFP compared to frozen PFP (Figure 53C and Figure 53D respectively). The number of CD235a/b^{+}/Lactadherin^{-} vesicles decreased by 12-fold in pellets from frozen compared to fresh PFP (Figure 53E). This was also reflected by a significant decrease in the percentage of vesicles labelled CD235a/b^{+}/Lactadherin^{-} in pellets from frozen PFP (Figure 53F).

These results showed that platelet vesicles were not susceptible to freezing, unlike RBC derived vesicles which were significantly decreased. Nonetheless, although total counts may be lower there is still a remaining population that can be analysed by flow cytometry.

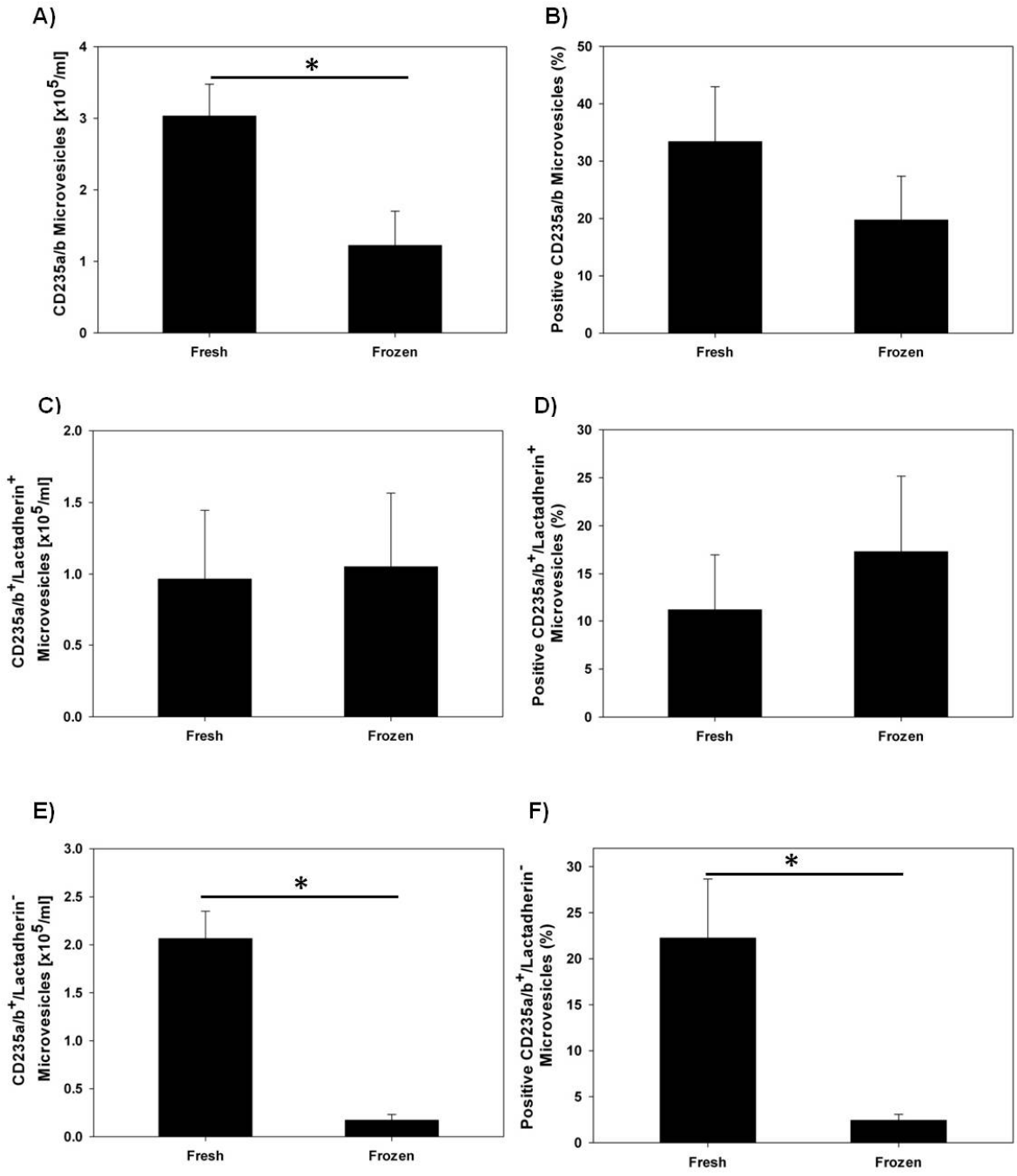

Figure 53. Flow cytometry analysis of ultracentrifuge pellets from fresh vs. frozen PFP: RBC vesicles. **A)** Total CD235a/b vesicle counts, **B)** Percentage of positive CD235a/b vesicles, **C)** Total CD235a/b$^+$/Lactadherin$^+$ vesicle counts, **D)** Percentage of CD235a/b$^+$/Lactadherin$^-$ vesicles, **E)** Total CD235a/b$^+$/Lactadherin$^-$ vesicle counts, **F)** Percentage of CD235a/b$^+$/Lactadherin$^-$ vesicles. Bars represent Mean ± SE * $p<0.05$. n=4.

4.4.3 Flow Cytometric Analysis of Spiking pSTBM into Whole Blood from NonP Women

To determine whether cellular vesicles can be recovered from the PFP pellet after ultracentrifugation, pSTBM were spiked into whole blood from NonP women. A representative FSC vs. SSC profile of vesicles in the PFP pellet containing 1μg/ml of pSTBM is shown in Figure 54A. A gate measuring 1% positive events was set by labelling the PFP pellet from the NonP control with the anti PLAP antibody NDOG2 (Figure 54B). NDOG2 labelling of the PFP pellet containing 1μg/ml of pSTBM detected a total of 8.6% PLAP positive vesicles (Figure 54C). A gate was drawn around the distinct pSTBM population and total vesicle counts were based around this gating strategy. Total PLAP vesicles and the percentage of positive labelling with NDOG2 in the pellet with and without 1μg/ml of pSTBM is shown in Figure 54D and Figure 54E respectively. A titration of pSTBM [0, 0.1, 0.5, 1μg/ml] illustrated that PLAP vesicles can be detected down to at least a concentration of 0.1μg/ml (Figure 54F).

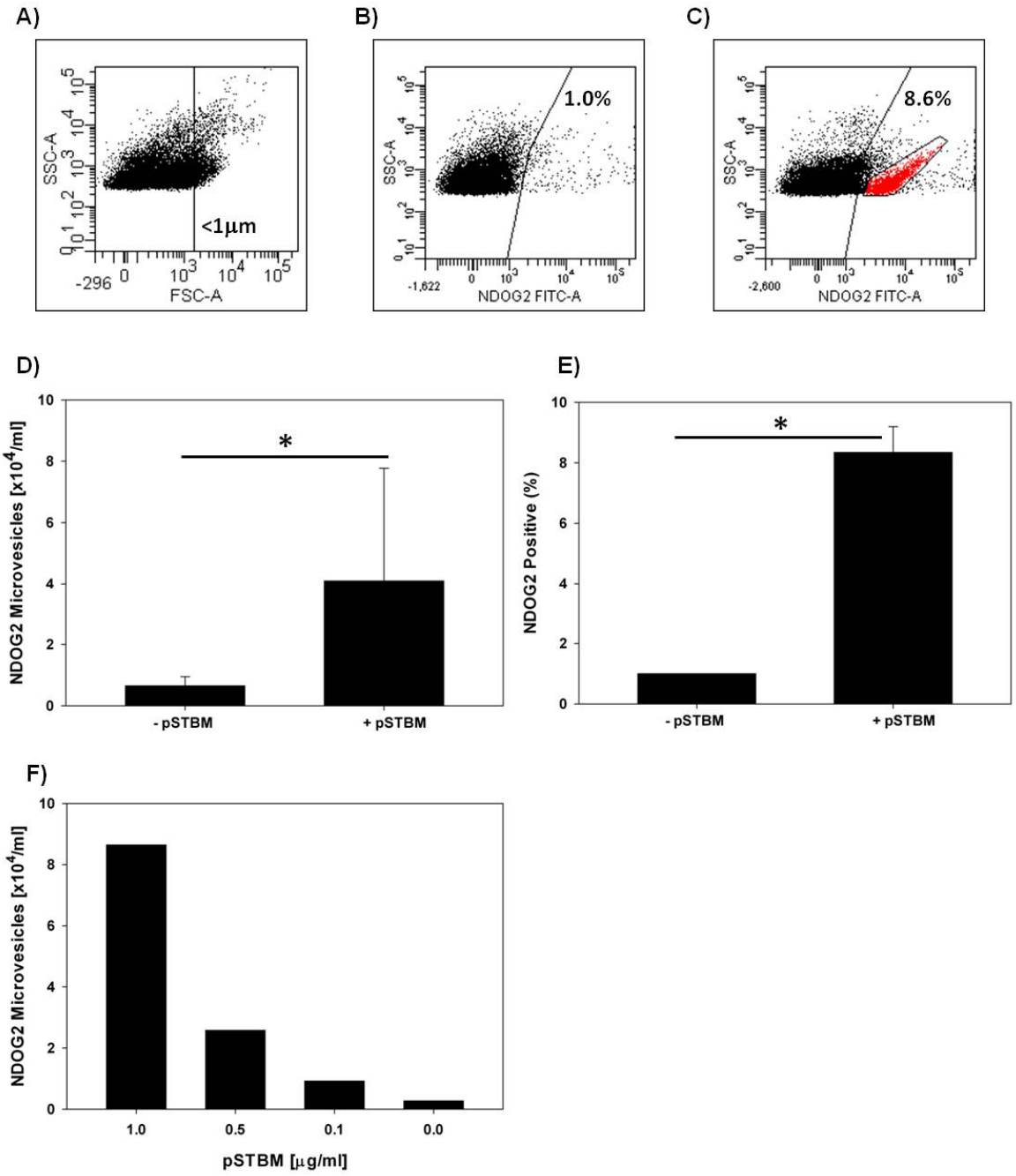

Figure 54. Spiking pSTBM into whole blood from NonP women. A) FSC vs. SSC dot plot of vesicles in PFP pellet with 1µg/ml pSTBM, **B)** Percentage of positive labelling of vesicles with NDOG2 antibody in PFP pellet alone, **C)** Positive NDOG2 labelling of vesicles in PFP pellet spiked with 1µg/ml pSTBM, **D)** Total vesicles labelled with NDOG2 in the PFP pellet spiked with -/+ 1µg/ml pSTBM, **E)** Percentage of positive vesicles labelled with NDOG2 in the PFP pellet spiked with -/+ 1µg/ml pSTBM, **F)** Total vesicles labelled with NDOG2 in the PFP pellet spiked with a titration of pSTBM [0-1µg/ml] n=1. Bars represent Median with the interquartile range * $p<0.05$. n=3.

4.4.4 Analysis of PFP Vesicles from NonP, NormP and PE Samples

4.4.4.1 Flow Cytometric Analysis: Establishing Antibody Panels

Having established that the NDOG2 antibody could be used to identify pSTBM in a PFP pellet, initial experiments aimed to use six-colour flow cytometry to count and phenotype vesicles in PFP pellets from NonP, NormP and PE women. The earlier experiments in this chapter use Lactadherin to identify vesicles, however in this section of work we chose to use the marker Bio-Maleimide (thiol reactive dye that binds cellular membranes). Unlike Lactadherin, Bio-Maleimide will bind to vesicles irrespective of surface exposed phosphatidylserine (Enjeti *et al.,* 2008a) and would therefore be expected to identify the total number of cellular vesicles in a sample. For example this study has shown in Section 4.4.2 the presence of platelet-derived and RBC-derived vesicles that do not label with Lactadherin, yet these would label positive with Bio-Maleimide. We also chose to switch our platelet marker from CD61 used in earlier experiments in this chapter to CD41. This change was based on experiments in Chapter 2 whereby *in vitro* derived pSTBM were shown to express much higher levels of CD61 compared to CD41 and endothelial *in vitro* derived vesicles were shown to express CD61 but not CD41. Hence, CD41 is a more specific marker of platelet derived vesicles than CD61. PFP pellets were labelled with Bio-Maleimide, CD41, CD235a/b, W6/32, CD146 and NDOG2. Gates were set using FMO with isotype controls (Table 8) as previously explained in Chapter 2 Section 2.3.4.1.

FMO Control	Antibody-Fluorochrome					
	FITC	PE	PECy7	PECy5	APCCy7	Alexa-647
Bio-Maleimide	-	NDOG2	CD41	CD235a/b	W6/32	CD146
NDOG2	Bio-Maleimide	IgG1	CD41	CD235a/b	W6/32	CD146
CD41	Bio-Maleimide	NDOG2	IgG1	CD235a/b	W6/32	CD146
CD235a/b	Bio-Maleimide	NDOG2	CD41	IgG2b	W6/32	CD146
W6/32	Bio-Maleimide	NDOG2	CD41	CD235a/b	IgG2a	CD146
CD146	Bio-Maleimide	NDOG2	CD41	CD235a/b	W6/32	IgG1

Table 8. Six-colour panel showing fluorescence minus one (FMO) with isotype controls.

However, these experiments proved to be problematic and resulted in "false positive" NDOG2 labelled vesicles. An example of this is illustrated in Figure 55. A PFP pellet from a NormP woman was single labelled with NDOG2 and corresponding isotype control and resulted in 1.4% positive labelling with NDOG2 (Figure 55A). But when this same PFP pellet was labelled with NDOG2 in the six-colour panel it resulted in 15.6% positive labelling (Figure 55B). Fluorochrome compensation for the six-colour panel had been set up correctly and was not the source of the "false positive" NDOG2 labelled vesicles. To investigate this problem we compared the percentage of NDOG2 labelling in all of the FMO controls to that observed with the complete antibody panel (i.e. all six-colours). This allowed us to examine the effect of each antibody of interest and to help establish which antibody/s may be the source of the "false positive" NDOG2 labelled vesicles. This technique of antibody elimination is described as using "fidelity controls" (Maecker and Trotter 2011). The percentage of NDOG2 labelled vesicles was notably reduced in the CD41-PECy7 FMO control (Figure 55C) and W6/32-APCCy7 FMO control (Figure 55D), suggesting that these two antibodies in combination were the source of the "false positive" NDOG2 labelled vesicles. Hence, NDOG2-PE, CD41-PECy7 and W6/32-APCCy7 cannot all be used in the same antibody panel.

Taking this into consideration, two separate antibody panels to phenotype the vesicles were designed. The first panel aimed to identify the placental derived vesicles which should be PLAP positive and HLA-Class I negative, therefore this panel consisted of Bio-Maleimide-FITC, NDOG2-PE and W6/32-APCCy7 (Table 9). This combination of markers was tested on a PFP pellet from a NormP woman. The NDOG2-PE FMO control was set at 1% (Figure 55E). The percentage of positive vesicles labelled with NDOG2-PE was the same (3.8%) in the W6/32-APCCy7 FMO control (Figure 55F) and that with Bio-Maleimide-FITC, NDOG2-PE and W6/32-APCCy7 all together (Figure 55G).

FMO Control	**Antibody-Fluorochrome**		
	FITC	**PE**	**APCCy7**
Bio-Maleimide	-	NDOG2	W6/32
NDOG2	Bio-Maleimide	IgG1	W6/32
W6/32	Bio-Maleimide	NDOG2	IgG2a

Table 9. Three-colour panel showing fluorescence minus one (FMO) with isotype controls.

The second panel used five-colour flow cytometry to identify vesicles derived from platelets, red blood cells, leukocytes and endothelial cells. This panel consisted of Bio-Maleimide-FITC, CD41-PECy7, CD235a/b-PECy5, W6/32-APCCy7 and CD146-Alexa-647 (Table 10). Although CD41-PECy7 and W6/32-APCCy7 could not be used in conjunction with NDOG2-PE, they could be used together in this five-colour panel. Figure 55H and Figure 55I show the percentage of vesicles labelled with W6/32-APCCy7 (53.5%) or CD41-PECy7 (89.6%) respectively in a PFP pellet from a NonP woman labelled with all five-colours. The percentage of vesicles labelled with W6/32-APCCy7 (50.8%) in the CD41-PECy7 FMO control or vesicles labelled with CD41-PECy7 (88.5%) in the W6/32-APCCy7 FMO control are both comparable to that labelled with all five-colours (Figure 55J and Figure 55K respectively).

FMO Control	Antibody-Fluorochrome				
	FITC	**PECy7**	**PECy5**	**APCCy7**	**Alexa-647**
Bio-Maleimide	-	CD41	CD235a/b	W6/32	CD146
CD41	Bio-Maleimide	IgG1	CD235a/b	W6/32	CD146
CD235a/b	Bio-Maleimide	CD41	IgG2b	W6/32	CD146
W6/32	Bio-Maleimide	CD41	CD235a/b	IgG2a	CD146
CD146	Bio-Maleimide	CD41	CD235a/b	W6/32	IgG1

Table 10. Five-colour panel showing fluorescence minus one (FMO) with isotype controls.

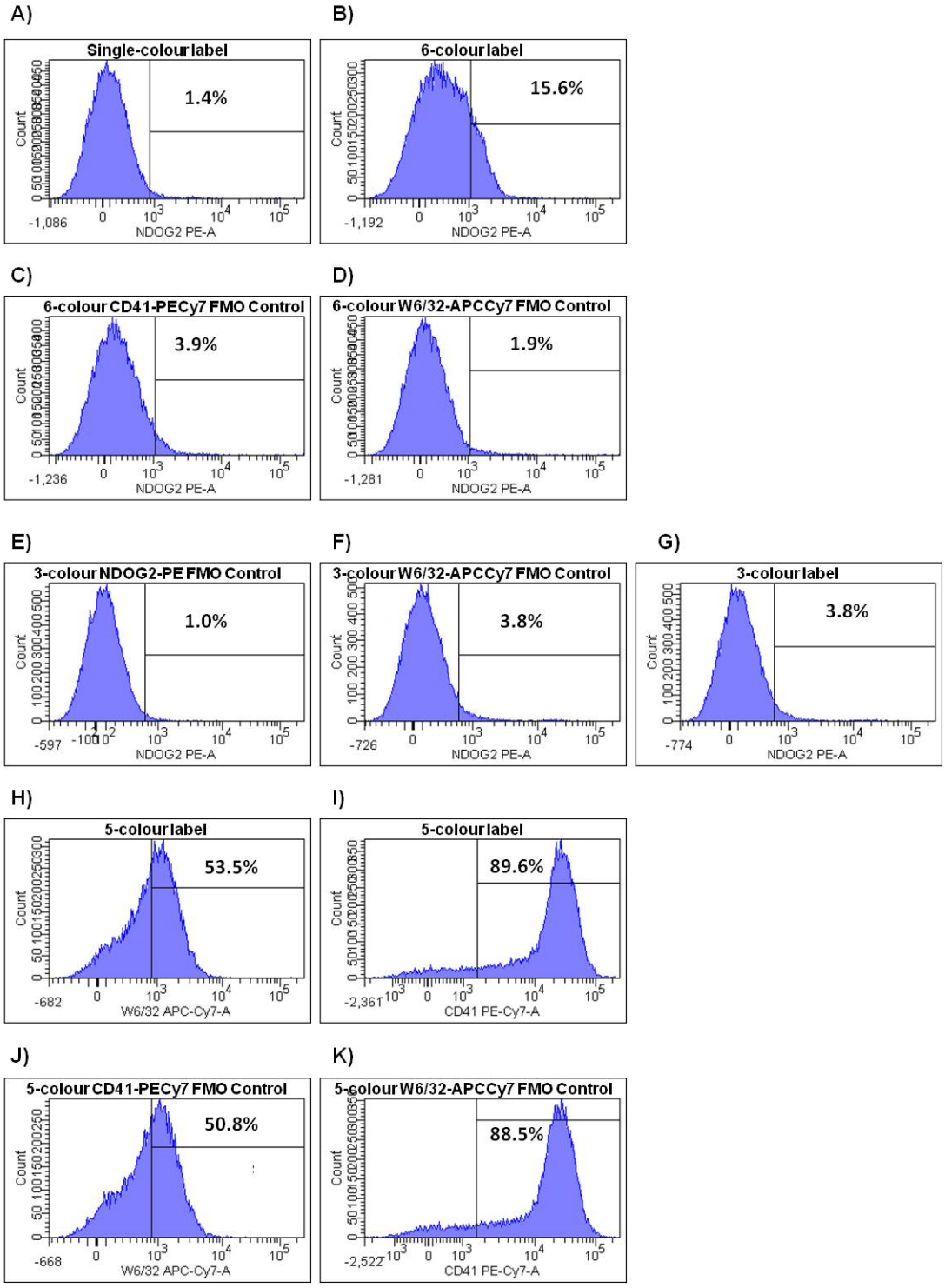

Figure 55. Flow cytometry analysis of PFP vesicles using a six-colour, three-colour and five-colour panel of fluorescent stain/antibodies. A) Single-colour labelling of vesicles with NDOG2 in a PFP pellet from a NormP woman. Percentage of positive labelling with NDOG2 in a PFP pellet from a NormP woman; **B)** six-colour labelling **C)** six-colour labelling; CD41-PECy7 FMO control, **D)** six-colour labelling; W6/32-APCCy7 FMO control, **E)** three-colour labelling; NDOG2 FMO Control set at 1%, **F)** three-colour labelling; W6/32-APCCy7 FMO control, **G)** three-colour labelling; NDOG2-PE, W6/32-APCCy7 and Bio-Maleimide-FITC. PFP pellet from a NonP woman; **H)** five-colour labelling of vesicles showing the percentage of positive labelling with W6/32-APCCy7, **I)** five-colour labelling of vesicles showing the percentage of positive labelling with CD41-PECy7, **J)** five-colour labelling; CD41-PECy7 FMO control showing the percentage of positive labelling with W6/32-APCCy7, **K)** five-colour labelling; W6/32-APCCy7 FMO control showing the percentage of positive labelling with CD41-PECy7.

Figure 56 illustrates the gating strategy used to identify the PFP derived vesicles. Figure 56A shows a representative flow cytometry FSC vs. SSC dot plot of vesicles in a PFP pellet from a NormP woman. A 1μm gate was used to define the vesicle population. The vesicles <1μm were then displayed on a Bio-Maleimide histogram plot to determine the percentage of vesicles that were cellular derived (Figure 56B). The gate was set at 1% using the Bio-Maleimide FMO control and in all thirty PFP pellets (NonP, NormP and PE) analysed ~90% of events labelled positive with Bio-Maleimide. The Bio-Maleimide positive vesicles were then displayed on two-parameter dot plots to determine the phenotype of the vesicles. It is important to note that the Bio-Maleimide negative vesicles did not label with any of the antigens examined in this study (data not shown). STBM were identified as $NDOG2^{+}/W6/32^{-}$ (Figure 56C), RBC vesicles were identified as $CD235a/b^{+}/W6/32^{-}$ (Figure 56D), $CD41^{+}/W6/32^{-}$ and $CD41^{+}/W6/32^{+}$ events were considered to be platelet derived vesicles (Figure 56E), whereas $CD41^{-}/W632^{+}$ events were identified as leukocyte vesicles (Figure 56E) and endothelial vesicles were considered to be $W6/32^{+}/CD146^{+}$ or $W6/32^{-}/CD146^{+}$ (Figure 56F).

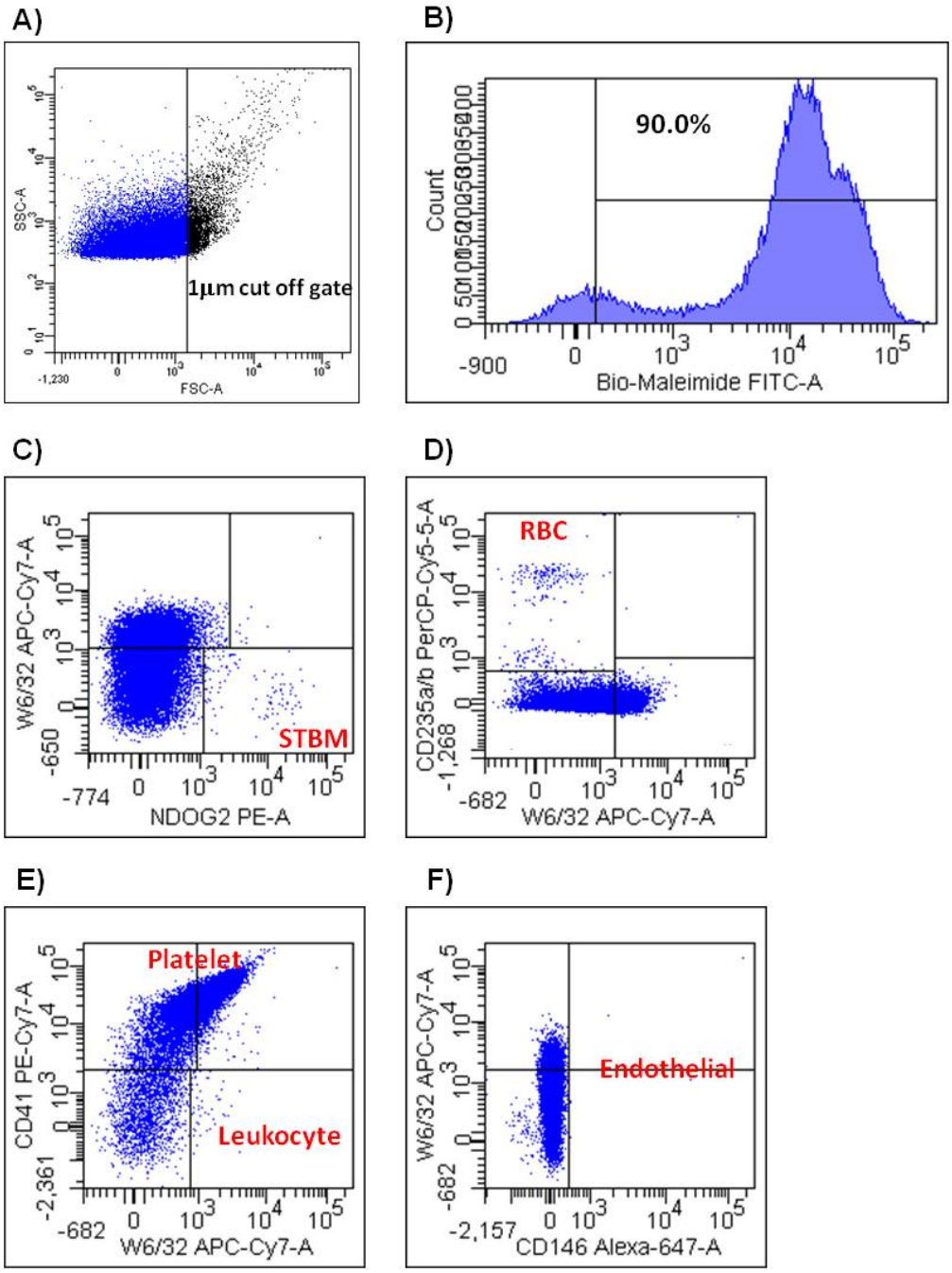

Figure 56. Flow cytometry gating strategy to phenotype PFP vesicles. A) Vesicles displayed on FSC vs. SSC plot with 1µm cut off gate, **B)** <1µm vesicles displayed and gated on Bio-Maleimide histogram. Bio-Maleimide positive vesicles then displayed on 2-parameter plots and phenotype identified, **C)** pSTBM; $NDOG2^{+}/W6/32^{-}$, **D)** RBC; $CD235a/b^{+}/W6/32^{-}$, **E)** platelet; CD41+/W632- or $CD41^{+}/W6/32^{+}$, leukocyte; $W6/32^{+}$/CD41- and **F)** endothelial; CD146+/W6/32- or CD146+/W6/32+.

4.4.4.2 Flow Cytometric Analysis and NTA: Measuring Total Vesicle Counts

PFP pellets from NonP, NormP and PE women were analysed by flow cytometry using the three-colour and five-colour antibody panels and by NTA. Using flow cytometry, total

vesicle counts (both Bio-Maleimide positive and negative) were determined by analysing all vesicles <1µm. No difference in total vesicle counts were found in PFP pellets from NonP, NormP or PE women (Figure 57A). These same samples were also analysed using NTA. A significant increase in the number of vesicles was detected in PFP pellets from NormP and PE women compared to NonP women (Figure 57B). However, there was no difference in vesicle counts in the PFP pellets between NormP vs. PE women (Figure 57B). Vesicle size in the PFP pellets was measured using NTA and compared in NonP, NormP and PE women (Figure 57C). Mean vesicle size was found to be larger in the pellets from NonP women compared to NormP and PE women (Figure 57D). There was no difference in mean vesicle size between PFP pellets from NormP vs. PE women (Figure 57D).

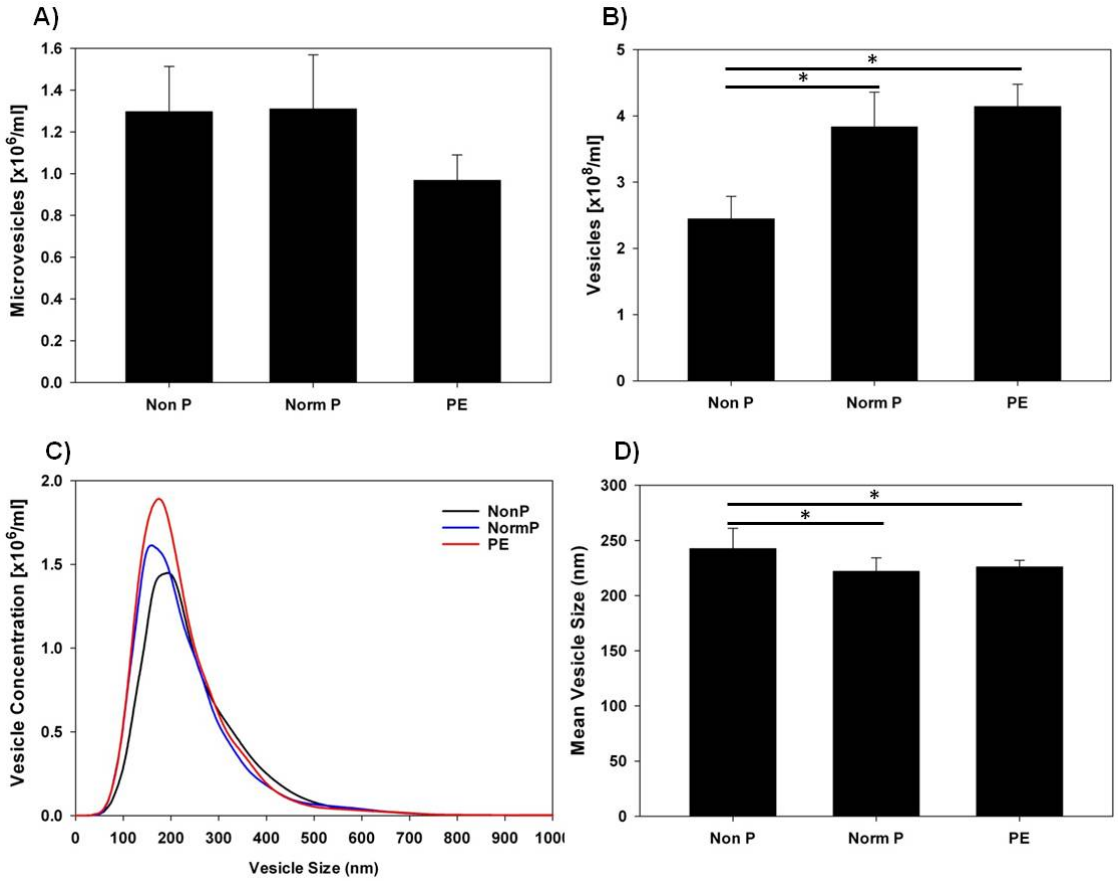

Figure 57. Measurement of total PFP vesicles in NonP, NormP and PE women using flow cytometry and NTA. A) Vesicle counts measured by flow cytometry. Bars represent Mean ± SE, **B)** Total vesicle counts measured by NTA. Bars represent Mean ± SE, **C)** NTA vesicle size vs. concentration profile, **D)** NTA mean vesicle size measurements. Bars represent median with the interquartile range. *p<0.05. n=10 per group.

A comparison of total vesicle counts measured by flow cytometry vs. NTA is shown in Figure 58. NTA counts are shown both as a measurement of the entire population of vesicles (0-1000nm; black bars) and vesicles >290nm (grey bars). This was done so a direct comparison between flow cytometry (only measures vesicles >290nm) and NTA could be made. The change in vesicle concentration measured by NTA (0-1000nm) in comparison to flow cytometry is increased by ~200-, 330- and 440-fold in the pellets from NonP, NormP and PE women respectively. The measurement of vesicle concentration by NTA (>290nm) compared to flow cytometry is ~50-, 70-fold and 100-fold higher in the PFP pellets from NonP, NormP and PE women respectively.

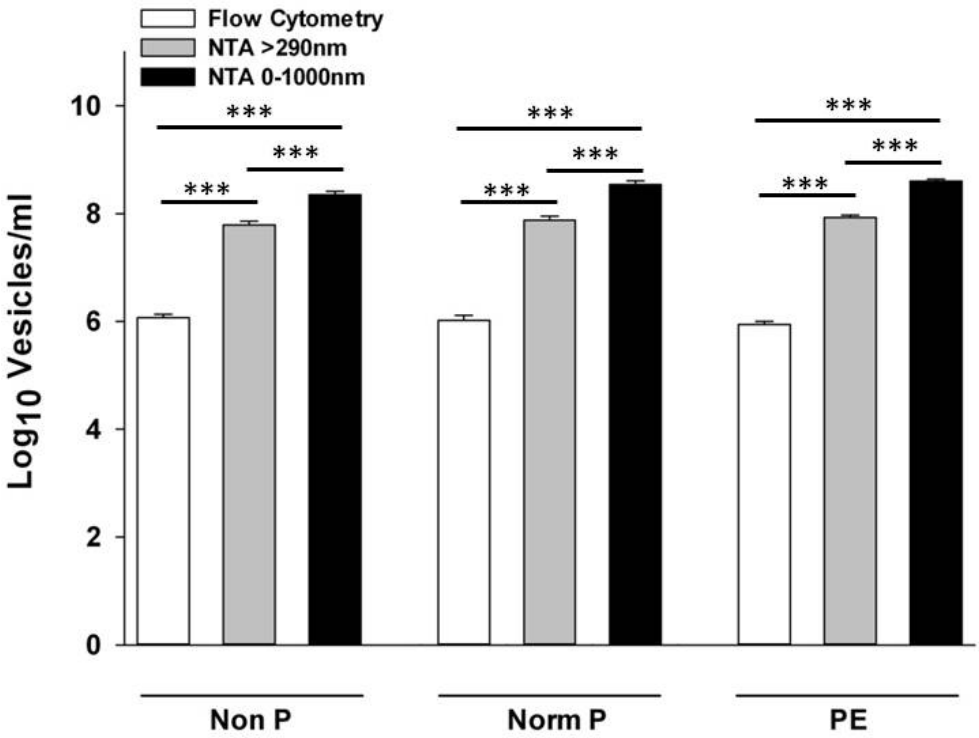

Figure 58. Direct comparison of total PFP derived vesicles in NonP, NormP and PE women measured by flow cytometry and NTA. Total counts measured by; flow cytometry (□), NTA >290nm(▒) and NTA 0-1000nm (■). Data were Log_{10} transformed and bars represent Mean ± SE. ***p<0.001. n=10 per group.

4.4.4.3 Flow Cytometric Analysis: Phenotypic Analysis of Vesicles

Bio-Maleimide vesicle counts were comparable in PFP pellets from NonP, NormP and PE women (Figure 59A). The percentage of vesicles labelling with Bio-Maleimide is shown in Figure 59B and was the same across all three groups. ~90% of all events in the PFP pellets labelled with Bio-Maleimide, thus indicating that the pellet was enriched with cellular vesicles.

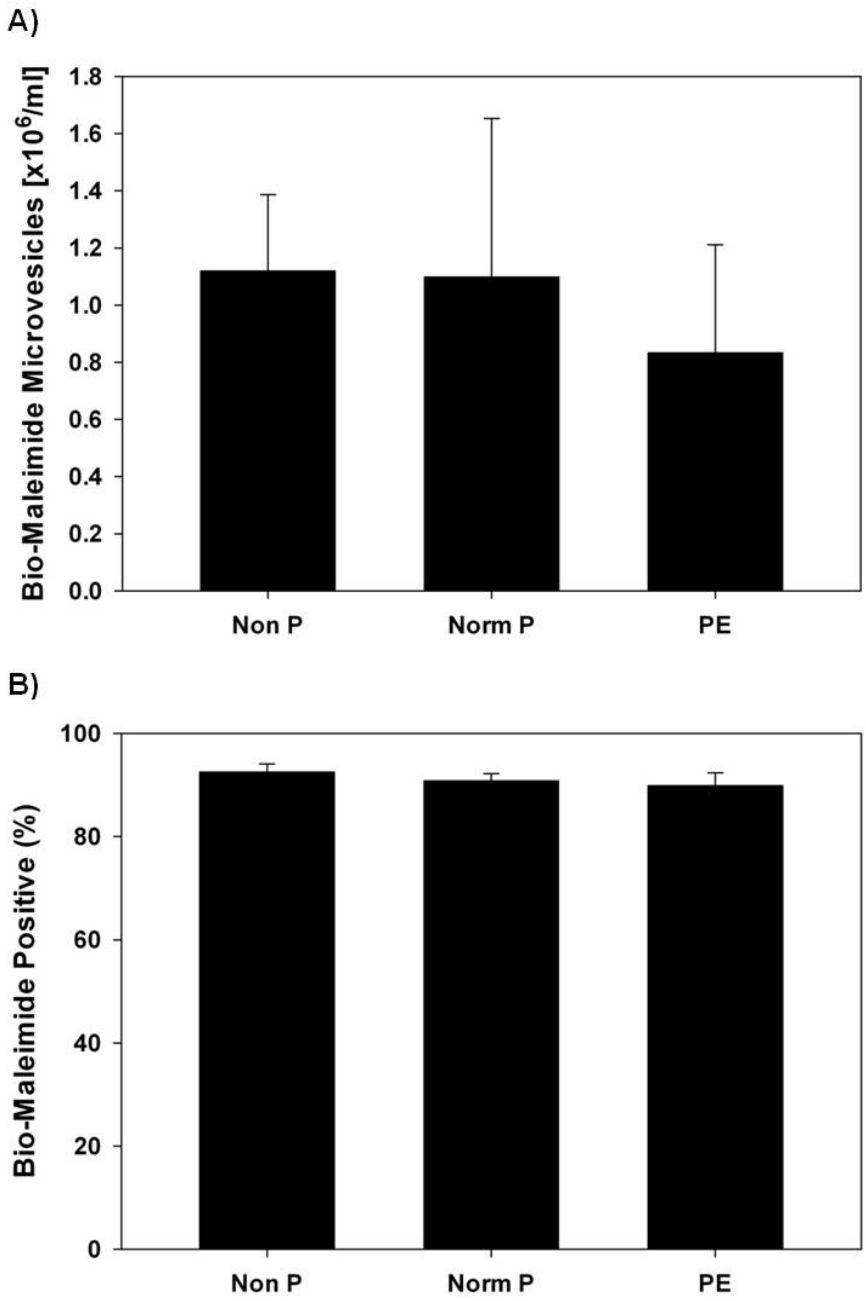

Figure 59. Flow Cytometry Analysis of Bio-Maleimide vesicles in PFP pellets from NonP, NormP and PE women. A) Total Bio-Maleimide vesicle counts, **B)** Percentage positive vesicles labelled with Bio-Maleimide. Bars represent Median with the interquartile range. n=10 per group.

Although vesicles >1μm are not strictly classified as vesicles and are more likely to be apoptotic bodies and other cellular debris it was decided to also analyse this population of Bio-Maleimide vesicles by flow cytometry. Significantly fewer Bio-Maleimide vesicles >1μm were found in the PFP pellet from PE women compared to NonP women (Figure 60A). There was no difference in total Bio-Maleimide vesicles >1μm in NonP vs. NormP women or NormP vs. PE women (Figure 60A). These vesicles were all cellular derived as >99% labelled positive with Bio-Maleimide (Figure 60B). These results suggest there was less apoptotic bodies/cellular debris in PE samples.

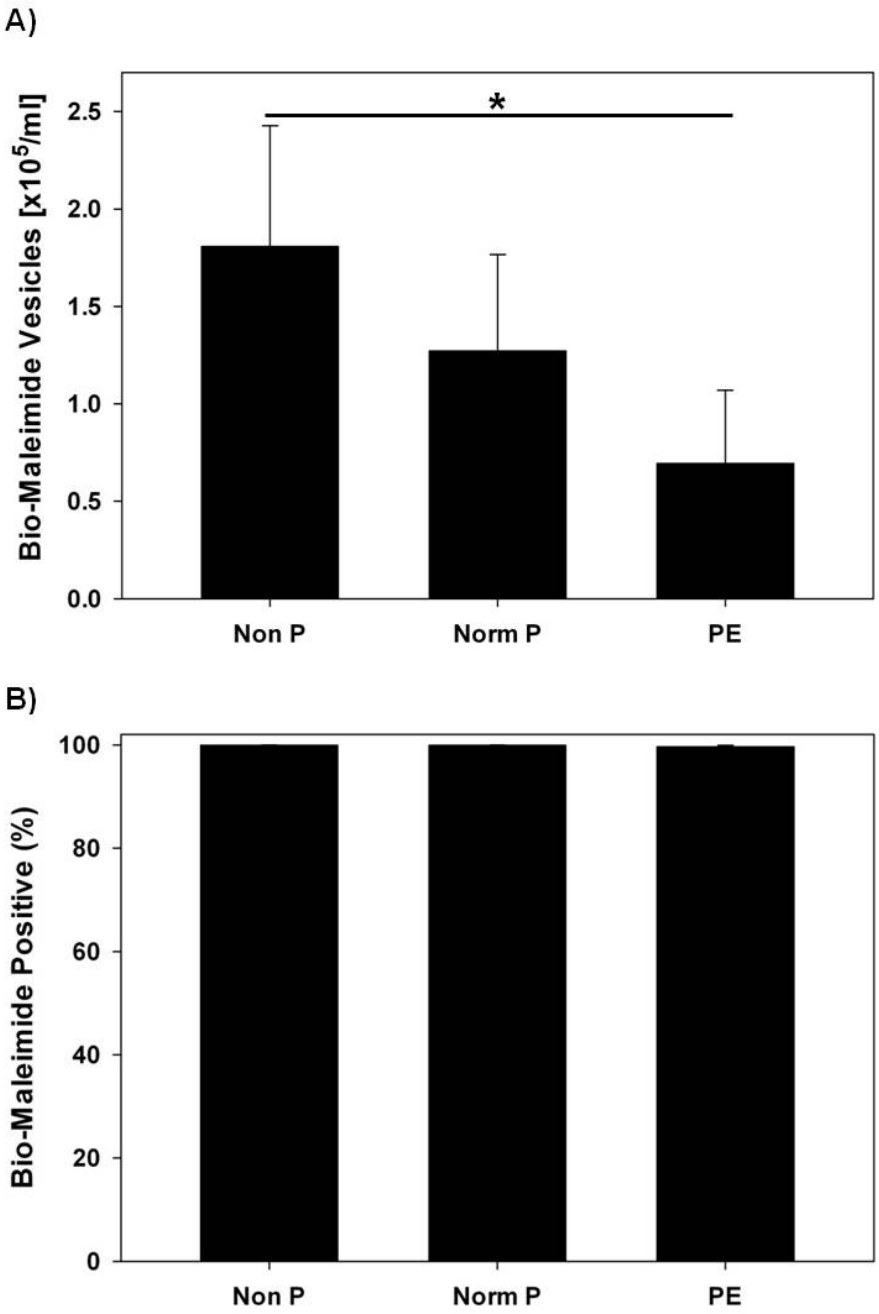

Figure 60. Flow Cytometry Analysis of Bio-Maleimide vesicles >1µm in PFP pellets from NonP, NormP and PE women. A) Total Bio-Maleimide vesicle counts, **B)** Percentage positive vesicles labelled with Bio-Maleimide. Bars represent median with the interquartile range. *p<0.05. n=10 per group.

STBM: STBM (defined as $NDOG2^{+}/W6/32^{-}$) numbers were significantly raised in PFP pellets from PE women compared to background levels observed in NonP women (Figure 61A) and this was also reflected in the percentage of $NDOG2^{+}/W6/32^{-}$ vesicles (Figure 61B). Total STBM counts were also elevated (although not significantly so) in PFP pellets

from NormP women compared to the background levels observed in NonP women (Figure 61A), however there was a significant increase in the percentage of positively labelled $NDOG2^{+}/W6/32^{-}$ vesicles (Figure 61B). No difference in total counts or the percentage of positive vesicles was observed in PFP pellets from NormP women vs. PE women (Figure 61A and Figure 61B respectively). Representative flow cytometry labelling of STBM in PFP pellets from NonP, NormP and PE women is shown in Figure 61C.

The levels of STBM in the same PFP samples from NonP, NormP and PE women were also measured using an in house ELISA (Knight *et al.,* 1998, Goswami *et al.,* 2006, Germain *et al.,* 2007). Unlike flow cytometry which only measures STBM >290nm, the ELISA measures the entire population of vesicles including; nanovesicles, microvesicles and vesicles >1μm. Our study used PFP samples from late-onset PE women (mean gestation; 37.0 weeks) matched to NormP women (mean gestation; 36.3 weeks) and NonP women for age and parity. Consistent with the flow cytometry results, STBM levels were significantly increased in PFP in the samples from NormP and PE women compared to the NonP controls (Figure 62). No difference in STBM levels in PFP between NormP and PE women was found (Figure 62). These findings are in agreement with those observed previously (Goswami *et al.,* 2006) showing no difference in STBM levels in late-onset PE vs. NormP, but did find a significant elevation in early-onset PE.

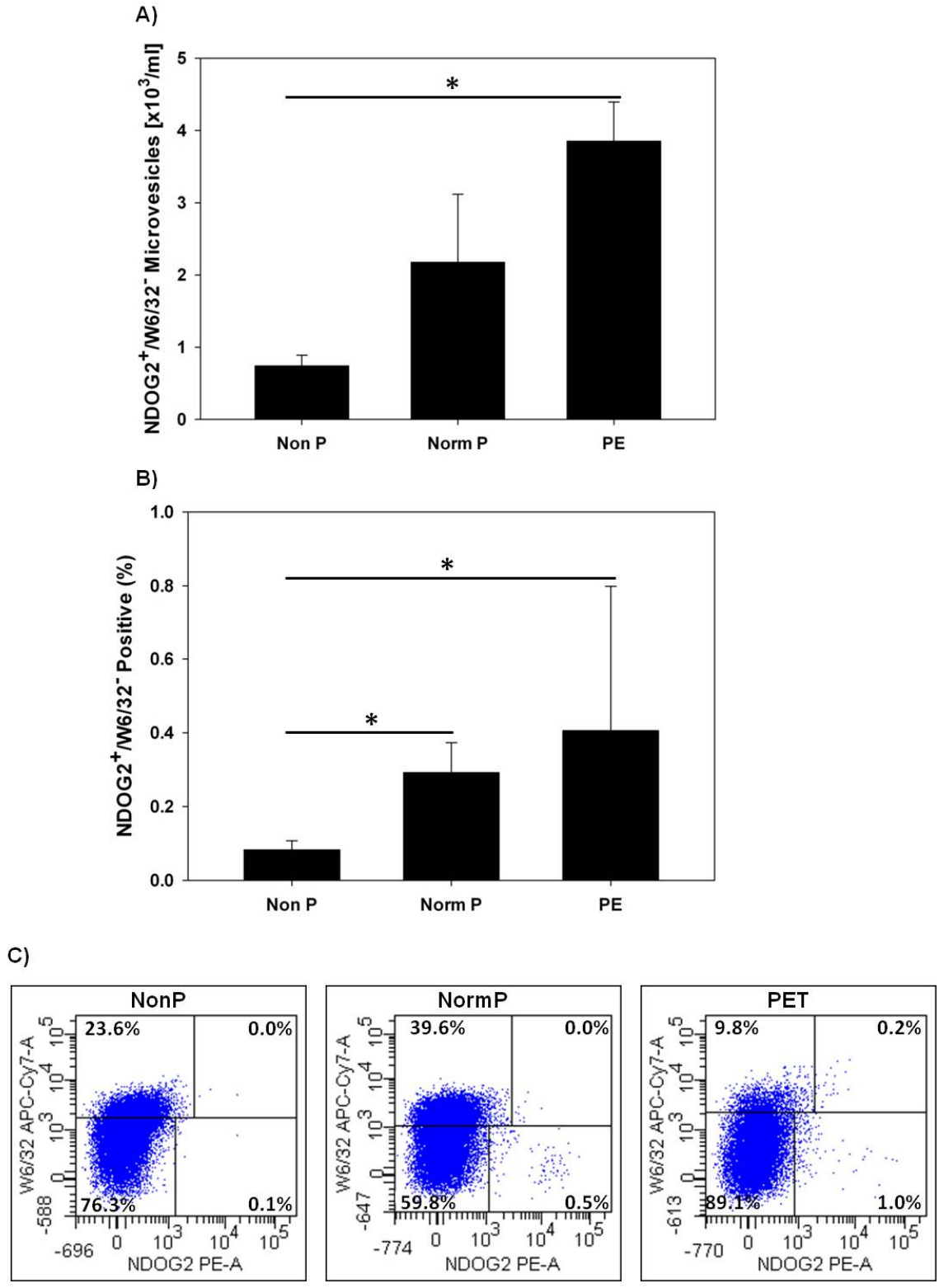

Figure 61. Flow cytometry analysis of STBM in PFP pellets from NonP, NormP and PE women. A) Total STBM counts, **B)** Percentage positive STBM, **C)** Representative 2-parameter plots showing percentage of positive labelling of STBM. Bars represent median with the interquartile range. *p < 0.05. n=10 per group.

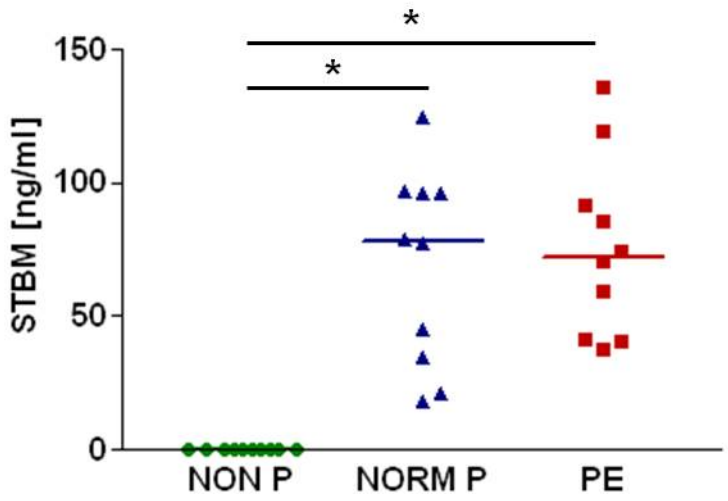

Figure 62. PFP STBM levels in NonP, NormP and PE women measured by ELISA. Bars show median values. *p < 0.05. n=10 per group.

Platelet Vesicles: The majority of vesicles in PFP pellets from NonP, NormP and PE women were found to be derived from platelets. $CD41^+/W632^+$ vesicles were compared between the three groups and were lower in PFP pellets from PE women compared to NonP and NormP women, but not significantly so (Figure 63A). The percentage of $CD41^+/W632^+$ vesicles was lower in the PFP pellets from PE women compared to NormP ($p = 0.087$) women and from PE women compared to NonP ($p = 0.066$) women, however again these differences did not reach statistical significance (Figure 63B). $CD41^+/W6/32^-$ total vesicles numbers and the percentage labelled were also similar in PFP pellets from NonP, NormP and PE women (Figure 63C and Figure 63D respectively). There was a trend showing a decrease in total platelet vesicle counts ($CD41^+/W632^+$ and $CD41^+/W6/32^-$) in PFP pellets from PE women, but this did not reach significance ($p = 0.066$) (Figure 63E). There was however a significant reduction in the percentage of positively labelled total platelet vesicles ($CD41^+/W632^+$ and $CD41^+/W6/32^-$) in PFP pellets from PE vs. NonP women (Figure 63F). Figure 63G shows representative flow cytometry plots of the $CD41^+/W632^+$ and $CD41^+/W6/32^-$ labelled vesicles in PFP pellets from NonP, NormP and PE women.

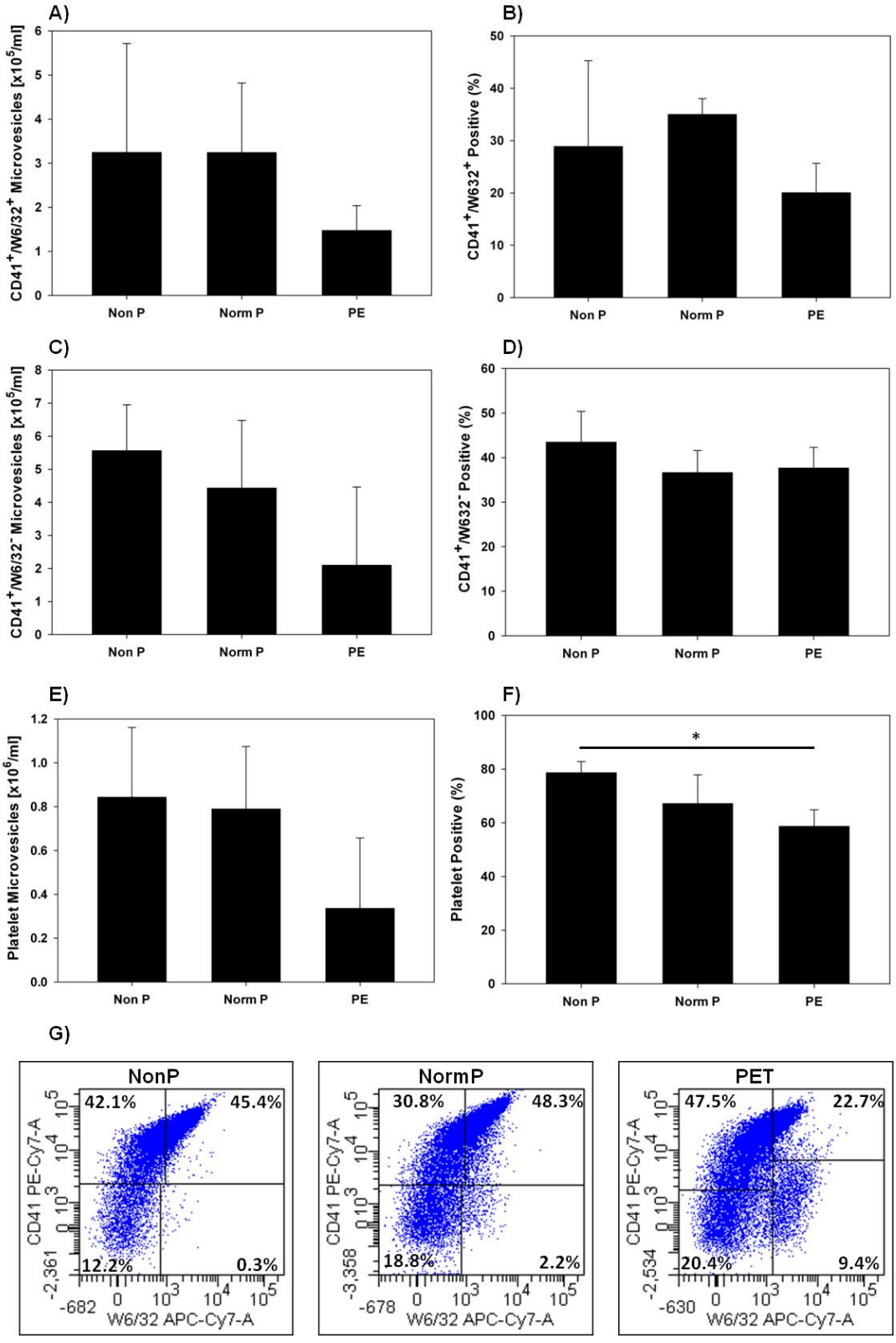

Figure 63. Flow cytometry analysis of platelet vesicles in PFP pellets from NonP, NormP and PE women. A) Total $CD41^+/W6/32^+$ vesicle counts, **B)** Percentage positive vesicles labelled with $CD41^+/W6/32^+$, **C)** Total $CD41^+/W6/32^-$ vesicle counts, **D)** Percentage positive vesicles labelled with $CD41^+/W6/32^-$, **E)** Total platelet ($CD41^+/W6/32^+$ and $CD41^+/W6/32^-$) vesicle counts, **F)** Percentage positive total ($CD41^+/W6/32^+$ and $CD41^+/W6/32^-$) platelet vesicles, **G)** Representative 2-parameter plots showing percentage of positive labelling for platelet vesicles and leukocyte vesicles ($W6/32^+/CD41^-$). Bars represent median with the interquartile range. *$p < 0.05$. n=10 per group.

Leukocyte Vesicles: Leukocyte derived vesicles were defined as W6/32^{+}/CD41^{-}. Representative flow cytometry plots showing W6/32^{+}/CD41^{-} labelling of vesicles in PFP pellets from NonP, NormP and PE women are shown in Figure 63G. These vesicles were found to be significantly elevated in PFP pellets from PE women compared to NonP women (Figure 64A). However, no difference in leukocyte vesicle counts were detected in PFP pellets from NonP vs NormP women or NormP vs. PE women (Figure 64A). Leukocyte derived vesicles accounted for <0.1% of the total vesicle population in PFP pellets from NonP women, <0.8% in NormP women and 2.3% in PE women (Figure 64B).

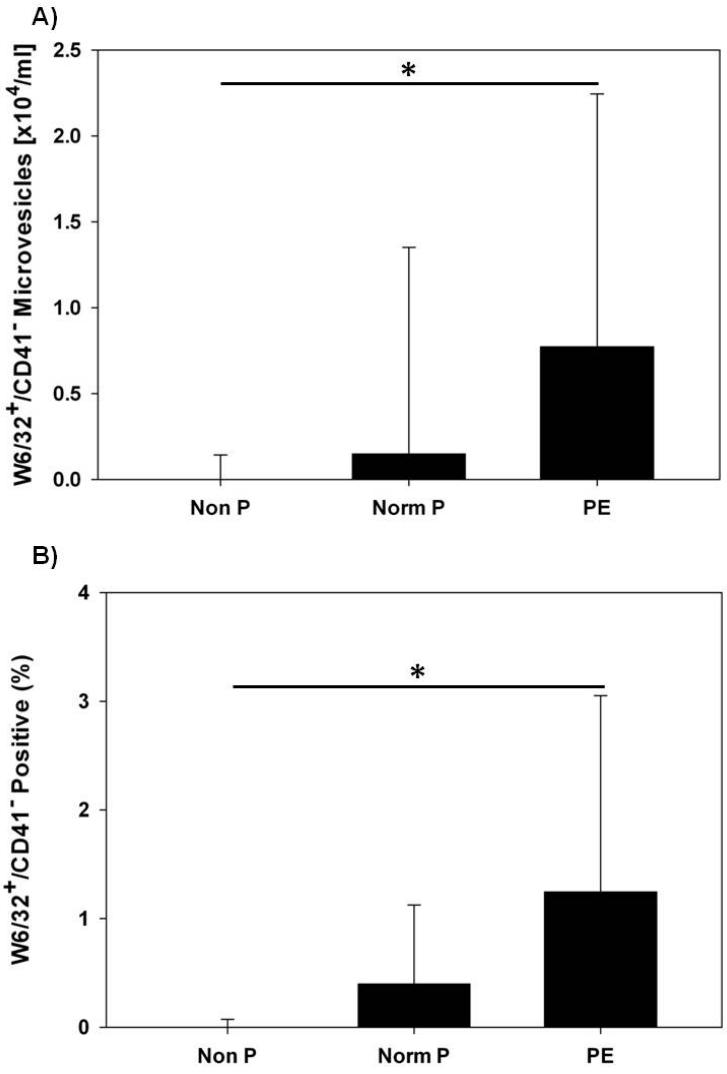

Figure 64. Flow cytometry analysis of leukocyte vesicles in PFP pellets from NonP, NormP and PE women. A) Total leukocyte vesicle counts, **B)** Percentage of positive vesicles labelled W6/32^{+}/CD41^{-}. Bars represent Median with the interquartile range. *p<0.05. n=10 per group.

RBC Vesicles: Total RBC derived vesicles were defined as CD235a/b^{+}/W6/32^{-}. Total counts and the percentage positive CD235a/b^{+}/W6/32^{-} vesicles in PFP pellets from NormP women were significantly elevated in comparison to NonP women (Figure 65A and Figure 65B respectively). There was no difference in total RBC vesicles in PFP pellets from PE women compared to NonP women (Figure 65A), however the percentage of positively labelled vesicles was significantly increased (Figure 65B). Total RBC vesicles and the percentage labelled positive were similar in PFP pellets from NormP and PE women (Figure 65A and Figure 65B respectively). Representative flow cytometry labelling of RBC vesicles in PFP pellets is shown in Figure 65C.

Endothelial Vesicles: Endothelial vesicles defined as CD146^{+}/W6/32^{+} or CD146^{+}/W6/32^{-} were not detected in any of the PFP pellets from NonP, NormP or PE women.

A summary of the total counts (Figure 66A) and percentage (Figure 66B) of all types of derived vesicles in a PFP pellet from NonP, NormP and PE women is shown in Figure 66. This summary figure also includes the total number and percentage of vesicles that were Bio-Maleimide positive, but did not label with any of the markers of interest, these were termed “orphan”. These vesicles accounted for 16-26% of the population.

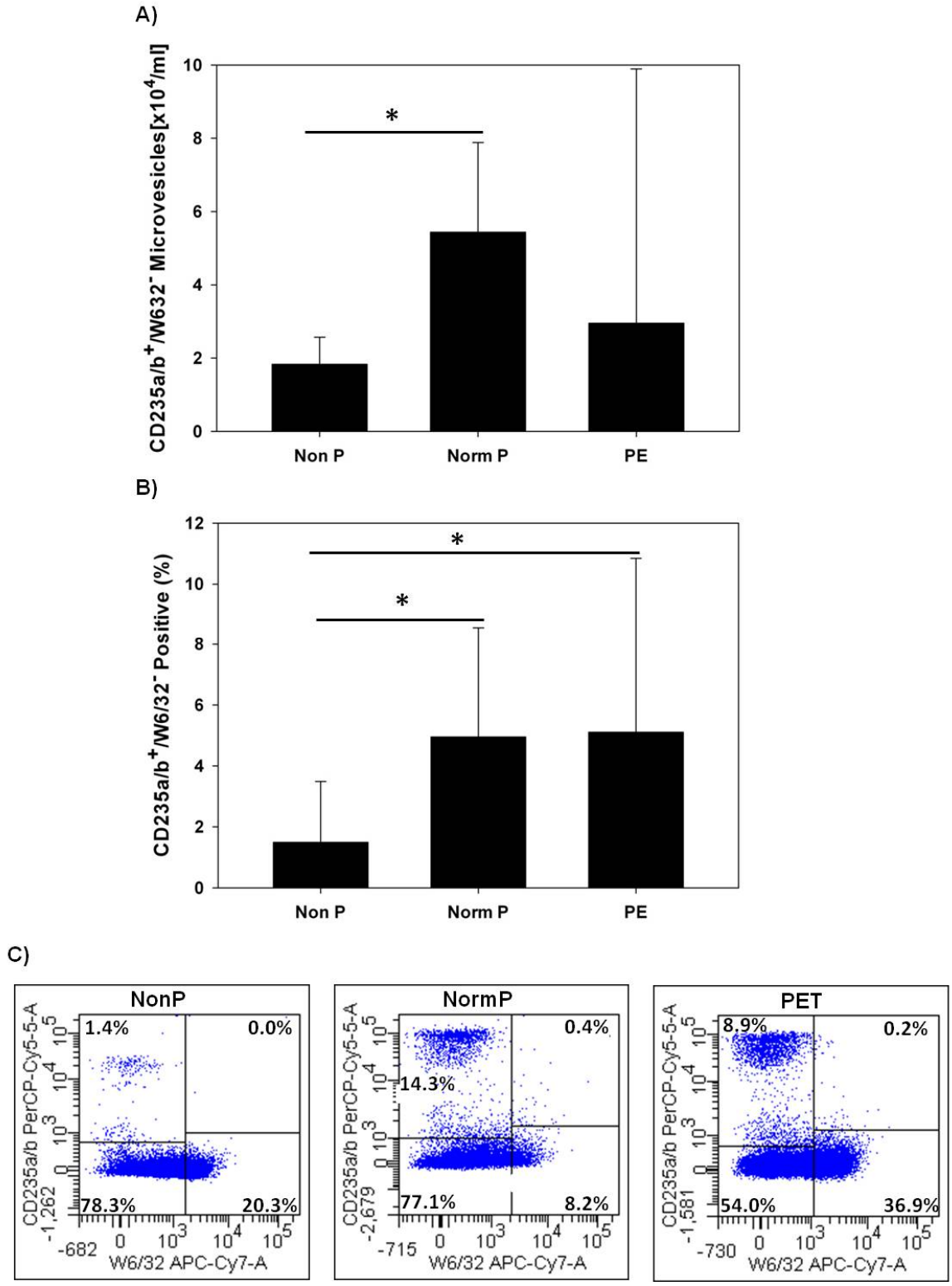

Figure 65. Flow cytometry analysis of RBC vesicles in PFP pellets from NonP, NormP and PE women. **A)** Total RBC vesicle counts, **B)** Percentage positive RBC vesicles, **C)** Representative plots showing percentage of positive labelling of RBC vesicles. Bars represent median with the interquartile range. *p < 0.05. n=10 per group.

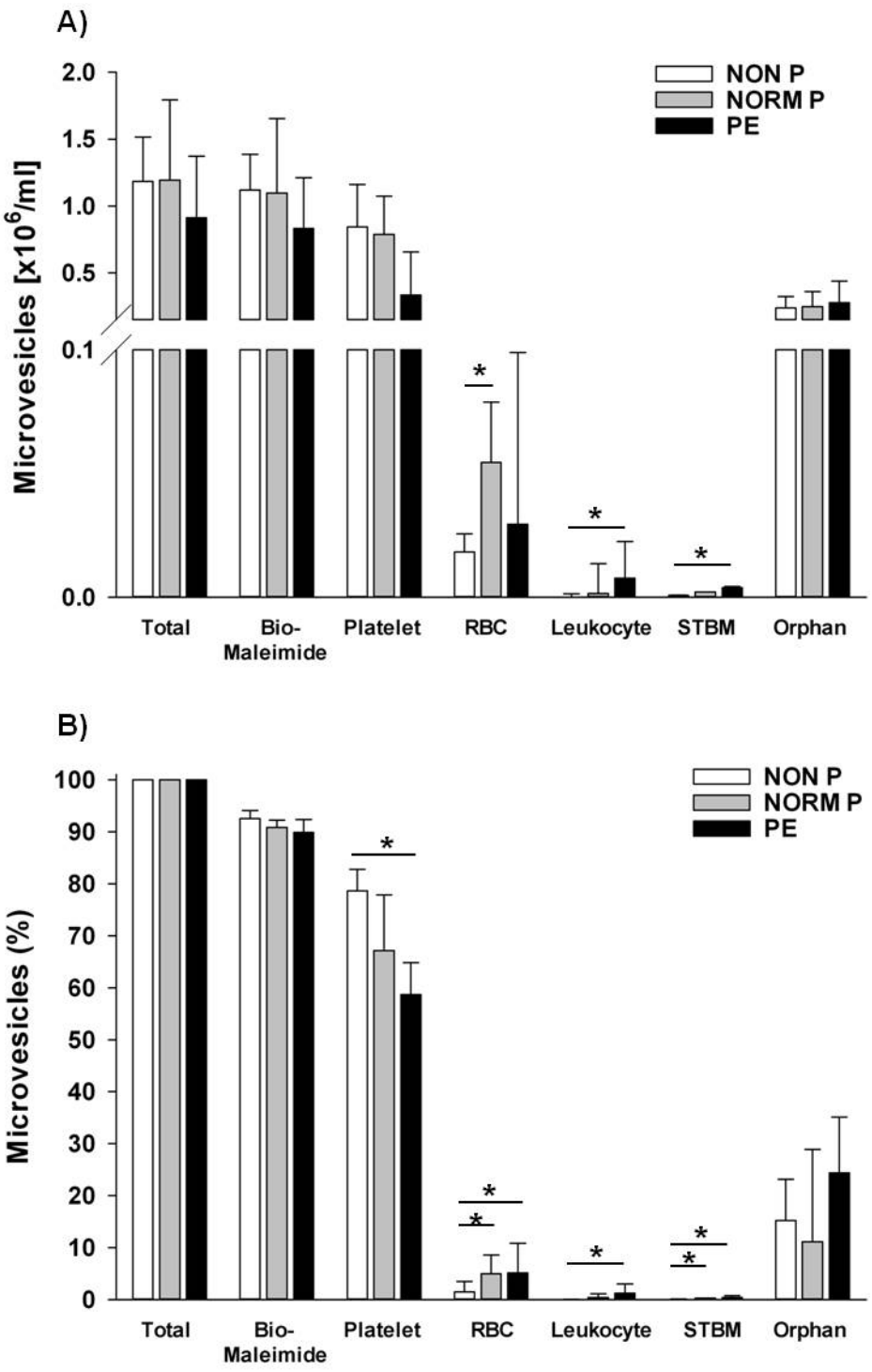

Figure 66. Flow cytometry analysis of vesicles in PFP pellets from NonP, NormP and PE women. A) Total vesicles counts, **B)** Percentage of vesicles. Bars represent median with interquartile range. *p < 0.05. n=10 per group.

4.4.5 Fluorescence NTA

Flow cytometry detects a small number of STBM >290nm in plasma and ELISA will measure vesicles <290nm, but does not provide any information relating to vesicle size. During the scope of this study our group worked with NanoSight Ltd to develop an instrument incorporating a fluorescence capability and therefore making it possible to size, count and phenotype the vesicles. In addition, a more sensitive camera is fitted to this instrument making it possible to track smaller biological vesicles (sub 100nm) than those measured using the LM10 instrument. The NanoSight NS500 instrument uses a 405nm laser and 430nm long-pass fluorescence filter, allowing detection of microvesicles and nanovesicles labelled with Qdot conjugated antibodies.

4.4.5.1 Fluorescence NTA, and Flow Cytometry of pSTBM

Experiments carried out using the NanoSight NS500 and the conjugation of Qdots to antibodies were performed by Dr Chris Gardiner (NDOG, Oxford)

To demonstrate the principle of fluorescence NTA, a mixture of 100nm fluorescent beads and 200nm non-fluorescent beads were analysed (Figure 67A). Both bead populations were resolved using light scatter mode (blue line), however only the 100nm fluorescent beads were tracked when using fluorescence mode (red line). Fluorescence NTA was then used to phenotype a preparation of biological vesicles using pSTBM as a model. pSTBM were labelled with NDOG2-Qdot605 and matching isotype control (IgG1-Qdot605). These custom conjugates were first tested using flow cytometry and were shown to label 93.5% of the pSTBM population (Figure 67B). pSTBM were then analysed using the NanoSight NS500 instrument, first on light scatter (blue line) and then using fluorescence mode (red line; NDOG2-Qdot605, green line; Isotype control IgG1-Qdot605) (Figure 67C). Analysis

using both light scatter and fluorescence modes gave a size distribution of vesicles ranging from 50 – 600nm, with two distinct peaks in the region of 150nm and 200nm. Minimal pSTBM labelling was shown with the IgG1-Qdot605 isotype control. The minor differences between the peak sizes in light scatter mode vs. fluorescence mode are within the observed level of variability (CV 8%) for this assay.

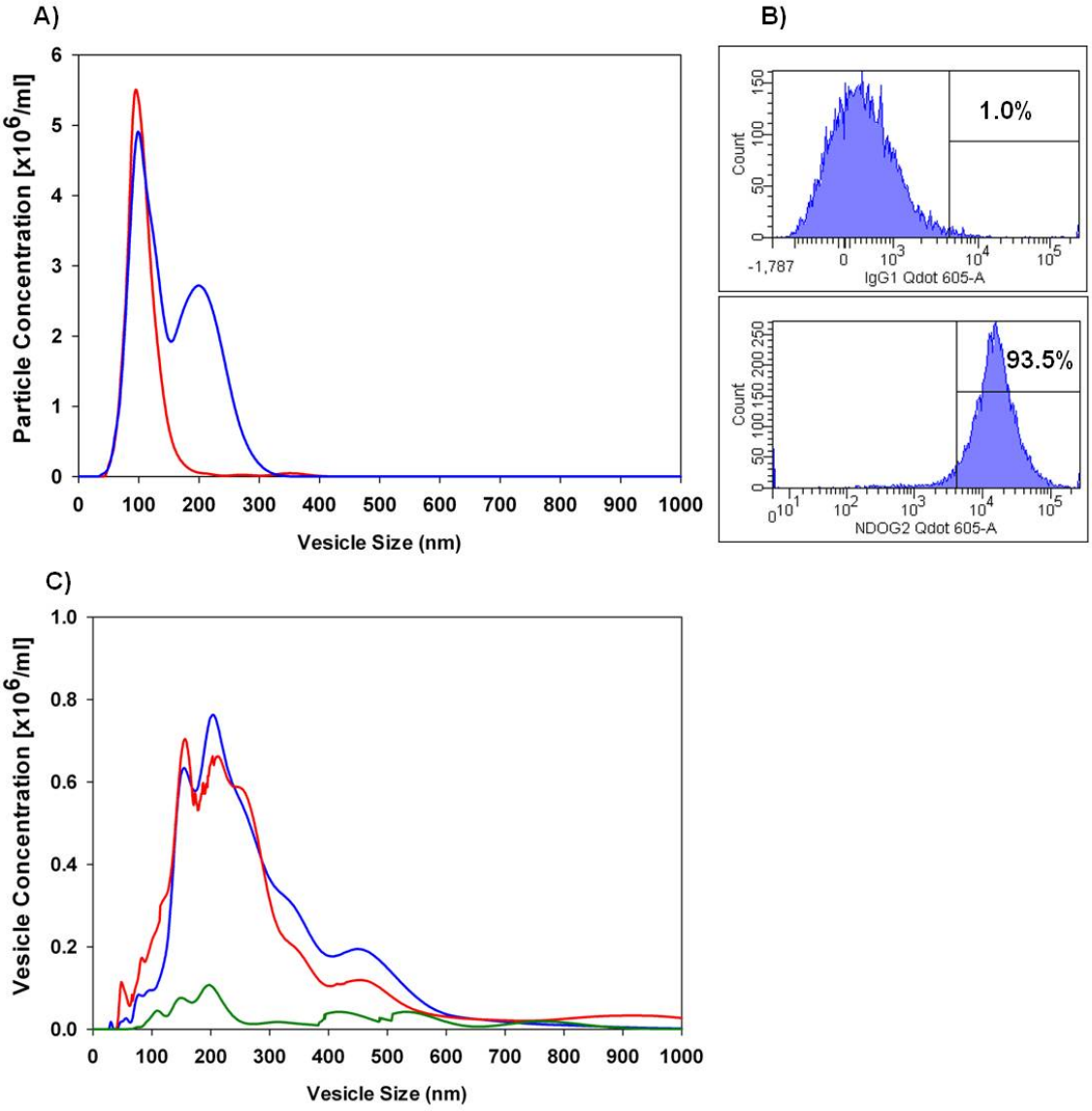

Figure 67. Fluorescence NTA and flow cytometry analysis of pSTBM. A) NTA analysis of a mixture of fluorescent 100nm beads and 200nm non-fluorescent beads analysed using scatter mode (blue line) and fluorescence mode (red line), **B)** pSTBM labelled with IgG1-Qdot605 (control) and NDOG2-Qdot605, **C)** NTA analysis of pSTBM labelled with IgG1-Qdot605 analysed in fluorescence mode (control; green line) and labelled with NDOG2-Qdot 605 analysed in scatter mode (blue line) and fluorescence mode (red line).

4.5 Discussion

4.5.1 Ultracentrifugation of PFP for Vesicle Analysis

In this chapter ultracentrifugation was first investigated as a method to concentrate vesicles in plasma. Currently there is no consensus with regard to centrifugation speeds of plasma for optimal vesicle detection. Some studies analyse PFP directly and others after pelleting the vesicles using low speed (18,000 –20,000 × g) centrifugation or ultracentrifugation (100,000 –150,000 × g). In this study ultracentrifugation was chosen to allow comparison with previous ELISA studies, (Knight *et al.*, 1998, Goswami *et al.*, 2006, Germain *et al.*, 2007). Ultracentrifugation was used to prepare vesicles for analysis using flow cytometry and NTA. It would also be expected to pellet a larger number of the smaller exosome population.

For simplicity, it would be preferable to analyse PFP directly as it requires no further processing of the plasma. However, plasma is a very complex biological fluid containing many different types of proteins, cellular and lipid vesicles. PFP samples can vary between individuals. On average in this study it was necessary to dilute samples by 90-fold prior to analysis by flow cytometry (and greater for analysis using NTA) as undiluted samples contain too many vesicles to achieve a suitable flow rate for analysis (i.e. ~250 events/sec). This large dilution in turn reduces the number of cellular vesicles, making it very difficult to analyse rare populations without having to acquire huge numbers of events. Isolation of vesicles from PFP using centrifugation or ultracentrifugation provides a more concentrated preparation, but will inevitably lead to some vesicle loss. To our knowledge, this is the first study to analyse the PFP, the PFP ultracentrifuge pellet and the SN post

ultracentrifugation. Analysing all three vesicle fractions has formally demonstrated that ultracentrifugation is sufficient to pellet cellular vesicles whilst minimising vesicle loss.

Flow cytometry and NTA were used in parallel to analyse PFP, the PFP ultracentrifuge pellet and the SN. Flow cytometry phenotypic analysis of vesicles was carried out using the platelet marker CD61 and procoagulant marker Lactadherin. Lactadherin binds phosphatidylserine exteriorised on the surface of vesicles and can be used as an alternative to Annexin V (Perez-Pujol *et al.,* 2007, Hou *et al.,* 2011). Lactadherin has two main advantages compared to Annexin V; 1) it has a higher affinity for phosphatidylserine and 2) it binds phosphatidylserine independent of calcium (Shi *et al.,* 2004). Analysis of PFP can be problematic when using buffers that contain calcium as this can cause the plasma to clot. Flow cytometric analysis showed increased numbers of vesicles present in the PFP and SN compared to that of the ultracentrifuge pellet, however many of these vesicles were neither phosphatidylserine positive (Lactadherin negative) nor derived from platelets (CD61 negative). The ultracentrifuge pellet was enriched with cellular derived vesicles as the majority labelled with Lactadherin and CD61. NTA confirmed the results obtained by flow cytometry also showing significantly more vesicles in the PFP and SN compared to that in the ultracentrifuge pellet. Furthermore, NTA showed that the ultracentrifuge pellet was, as might be expected, composed of larger vesicles compared to that in the PFP and SN. Together, flow cytometry and NTA demonstrated the phenotypic and size differences in the vesicles in the ultracentrifuge pellet compared to the PFP and SN.

In order to determine the nature of the vesicles in the PFP which remained in the SN after ultracentrifugation, APOB and triglycerides were measured to determine whether they were chylomicrons and VLDLs. PFP and SN were found to contain comparable concentrations of APOB and triglycerides. Chylomicrons are 80-1000nm in diameter and

contain 90% triglycerides and APOB48. VLDLs are 30-80nm in diameter and contain 65% triglycerides and APOB100 (Frayn 2010). Chylomicrons have previously been shown to be detectable by flow cytometry (Cantero *et al.*, 1998) and DLS (Ruf and Gould 1999) and both chylomicrons and VLDLs are within the size range of vesicles detected using NTA. However, LDL (20-25nm) and HDL (9-15nm) are too small to be detected by flow cytometry or NTA. Together these data provide evidence that the vast majority of vesicles in the PFP and SN are lipoprotein vesicles (chylomicrons and VLDLs) and that techniques to remove these such as ultracentrifugation are an absolute requirement for cellular vesicle enrichment.

4.5.2 Fresh vs. Frozen PFP

In order to carry out large studies of clinical samples to investigate the role of cellular derived vesicles it is simply not practical to analyse fresh PFP. Biobanks containing frozen plasma or serum are being set up world-wide to provide researchers with access to large numbers of samples to study various diseases/clinical conditions. However, if a point-of-care test was to be developed as a predictive or diagnostic tool then freshly isolated PFP would need to be used. Therefore, the effect of freezing PFP on quantification of vesicles in ultracentrifuge pellets is an important issue and this was examined using flow cytometry and NTA. Although only a small number of samples were analysed in a pilot study these data showed some interesting findings.

Total vesicle counts in pellets from fresh and frozen PFP showed no difference when analysed using flow cytometry or NTA. However, the percentage of Lactadherin positive vesicles detected by flow cytometry increased after freezing. This may cause externalisation of phosphatidylserine, resulting in the Lactadherin negative vesicles

becoming positive. However there was no difference in total Lactadherin positive vesicle numbers after freezing. Furthermore, the number of platelet vesicles was comparable in pellets from fresh and frozen PFP. In contrast, freezing had a significant effect on total RBC vesicles as these were reduced in pellets from frozen PFP compared to fresh. $CD235^{+}$/$Lactadherin^{-}$ vesicles were significantly reduced in the pellet from frozen PFP compared to fresh. However, no difference in $CD235^{+}$/$Lactadherin^{+}$ vesicle numbers was detected, suggesting that the $CD235^{+}$/$Lactadherin^{-}$ vesicles had not become $CD235^{+}$/$Lactadherin^{+}$ during the freezing process. These results show that RBC vesicles can be analysed by flow cytometry using frozen PFP, however the numbers were reduced by ~3-fold. This overall reduction could be due to the vesicles being broken down further into smaller vesicles which were not detectable by flow cytometry. However, although only two samples were analysed using NTA there was no evidence of smaller vesicles in pellets from frozen PFP or an increase in total vesicle concentration. More samples would need to be analysed to investigate this further. The other possibility is that the CD235a/b antigen is susceptible to freezing, resulting in its loss from the surface of the vesicle.

4.5.3 Pre-Analytical Variables

There are many pre-analytical variables that may affect vesicle quantification. There is a requirement for all of these to be standardised and this will be discussed in detail in Chapter 5.

When designing this current study to analyse vesicles in pregnancy and PE using flow cytometry, the recommendations that had been made by others who had also looked at pre-analytical variables were taken into account. Blood was collected into the most commonly used anticoagulant, sodium citrate (Jy *et al.,* 2004, Yuana *et al.,* 2011). It was processed

within one hour as delaying the time between venepuncture and centrifugation has been reported to result in an increase in vesicle number (Ayers *et al.,* 2011). A double centrifugation (1500 × g for 15min, followed by 13,000 × g for 2min) was performed to generate PFP, which is absolutely necessary to remove platelets (Mobarrez *et al.,* 2010, Ayers *et al.,* 2011). All PFP samples were obtained from the Oxford Pregnancy Biobank and were stored at -80°C. PFP was thawed at 37°C as there are conflicting reports surrounding thawing samples at room temperature or on ice (Trummer *et al.,* 2009, Ayers *et al.,* 2011). In this study it was shown that ultracentrifugation of PFP was essential for the enrichment of the cellular vesicle populations. All samples were processed using these strict guidelines to ensure that direct comparisons could be made between patient and control groups.

Annexin V is the most widely used marker to measure plasma derived vesicles by flow cytometry. This marker has some drawbacks including that its binding to phosphatidylserine is dependent on the presence of calcium and the availability of phosphatidylserine on the surface of the vesicle. Furthermore, as stated previously, not all vesicles are Annexin V positive yet the majority of studies only analyse these events. There are very few previous studies analysing both Annexin V positive and negative vesicles (Connor *et al.,* 2010, Ayers *et al.,* 2011). The first of these studies (Connor *et al.,* 2010) showed a large number of Annexin V negative platelet derived vesicles and the second study (Ayers *et al.,* 2011) showed both Annexin V negative platelet and endothelial derived vesicles. There are many alternative markers to Annexin V that are now being explored to define vesicles, as previously outlined in Chapter 2. To define PFP vesicles in the current study, the fluorescent membrane stain Bio-Maleimide was used.

4.5.4 Analysis of PFP Vesicles

4.5.4.1 Antibody Panels for Multi-Colour Flow Cytometry

The antibodies used to define the different populations of vesicles were chosen based on the *in vitro* derived vesicle experiments shown in Chapter 2. This study is the first of its kind to use a five-colour antibody panel to phenotype vesicles. six-colour flow cytometry was initially attempted, but this resulted in "false positive" NDOG2 labelled vesicles. Fidelity controls identified W6/32-APCCy7 and CD41-PECy7 as antibodies that could not be reliably used in a panel with NDOG2-PE. The solution adopted was to use two separate antibody panels: 1) a three-colour panel of Bio-Maleimide, NDOG2 and W6/32 to phenotype STBM and, 2) a five-colour panel of Bio-Maleimide, CD41, CD235a/b, W6/32 and CD146 to phenotype total, platelet, RBC, leukocyte and endothelial derived vesicles respectively. Although a six-colour panel would have been preferable and potentially antibody fluorophores could have been interchanged to find a suitable combination, this would have been very time consuming, costly and it is unlikely this would have solved the problem entirely. With each chosen combination "false positive" vesicles would still appear, only effecting a different fluorescent channel each time. Ultimately, this is a limitation of our flow cytometer and is less likely to be a problem with instruments with more available channels (i.e. 3-4 lasers with 8-18 colours).

4.5.4.2 Flow Cytometry vs. NTA: Vesicle Enumeration and Size

In order to directly compare total PFP vesicles using flow cytometry to those measured using NTA, the flow cytometry analysis included both Bio-Maleimide negative and positive vesicles. Total vesicle counts measured by flow cytometry showed no difference between all three groups. In contrast, vesicle counts measured using NTA were significantly elevated in NormP and PE vs. NonP women. The mean vesicle size, as

measured by NTA, revealed that vesicles in NormP and PE were smaller than those in NonP. Furthermore, the mean vesicle size in all three groups was found to be below the detection limit of flow cytometry (≥290nm), indicative that flow cytometry is only analysing a small proportion of the total vesicles. A comparison of total vesicle concentration, as measured by flow cytometry vs. NTA, indicated that up to 443-fold more vesicles were detected using NTA. A further comparison was made whereby total vesicle counts ≥290nm as measured by NTA were directly compared to those measured using flow cytometry and found to be significantly higher. It is however very difficult to directly compare total vesicle counts measured by flow cytometry vs. NTA. As discussed in Chapter 3, NTA can accurately measure the size of polydisperse samples, but always overestimates the concentration. Conversely, flow cytometry may underestimate the concentration of vesicles, as it is possible that vesicles may intercept the laser line simultaneously and therefore be counted as a single vesicle. Furthermore, it has been proposed that using polystyrene beads to set-up the flow cytometer for vesicle analysis may lead to an underestimation of their size (Foladori *et al.,* 2008, Lacroix *et al.,* 2010a, Chandler *et al.,* 2011). It was recently reported that due to differences in refractive index, a 400nm polystyrene bead is equivalent to measuring a 1μm cellular vesicle (Chandler *et al.,* 2011). Hence, our instrument can distinguish a 290nm polystyrene bead population, but this may not directly equate to measuring a 290nm cellular vesicle. This is unlike NTA, which measures vesicle size independent of refractive index. Nevertheless, although vesicle counts by either method may not be an absolute measurement, this does not detract from the principle that NTA extends the power of flow cytometry and, because all three groups have been analysed using identical settings, valid comparisons between groups can still be made.

4.5.4.3 Total Circulating Vesicles

Flow Cytometry

In this study >90% of the vesicles <1μm labelled positive with Bio-Maleimide, thus indicating that ultracentrifugation results in a highly purified preparation of cellular-derived vesicles. Total Bio-Maleimide vesicle (<1μm) counts were comparable between all three groups, although a decrease in total Bio-Maleimide vesicles (>1μm) in PE vs. NonP was observed. This suggests that in PE either fewer large vesicles (including apoptotic bodies/cellular debris) are produced or perhaps these vesicles are cleared from the circulation at a faster rate.

As stated in the introduction to this chapter, previous studies have also analysed total vesicle counts in NormP and PE (Harlow *et al.,* 2002, VanWijk *et al.,* 2002, Bretelle *et al.,* 2003, Biro *et al.,* 2007, Lok *et al.,* 2007, Lok *et al.,* 2008a, Lok *et al.,* 2008b, Lok *et al.,* 2009, Orozco *et al.,* 2009, Alijotas-Reig *et al.,* 2011) all of which analysed Annexin V positive vesicles only, with the exception of one study (Biro *et al.,* 2007) defining total vesicle counts based solely on FSC vs. SSC measurements and another study (Orozco *et al.,* 2009) defining vesicles using the DNA stain PicoGreen. Two studies mention using a 1μm gate to define a cut off for the analysis of vesicles (Bretelle *et al.,* 2003, Alijotas-Reig *et al.,* 2011) and one study (Harlow *et al.,* 2002) defines vesicles as between 200nm – 500nm in size. It is very difficult to make any comparisons between our study and that of the latter (Harlow *et al.,* 2002) as this study analysed vesicles directly in whole blood.

Flow Cytometry vs. NTA

The study presented in this chapter used PFP samples from late-onset PE women (mean gestation; 37.0 weeks) matched to NormP women (mean gestation; 36.3 weeks) and NonP

women for age and parity. Using flow cytometry, these data showed comparable vesicle counts between all three groups. However, as flow cytometry only analyses a portion of the total vesicles in plasma, it was unsurprising that these results were not reflected when using NTA which visualises both nanovesicles and microvesicles. Here, total vesicle counts were elevated and vesicles were found to be smaller in size in NormP and PE women compared to NonP women. Although these counts are probably not an absolute number due to the polydisperse nature of the sample, they do indicate that total vesicle counts are elevated in NormP and PE. This may be a direct reflection of the number of vesicles shed into the maternal circulation as a result of the maternal systemic inflammatory response seen in NormP and PE. These data also suggest that increased activation may lead to the release of smaller vesicles. The inflammatory response is exacerbated in PE and it can be hypothesised that this would result in an increase in circulating vesicles, but total counts were comparable in NormP and PE. However, our results do not take into account the rate at which vesicles are cleared from the circulation. It cannot be ruled out that vesicles in PE women are cleared from the circulation at a faster rate than those from NormP women and for this reason we see no difference.

Throughout this study two questions were addressed: 1) is there a difference in vesicle numbers and size between normal pregnancy and the disease state (NormP and PE)? and, 2) is there a difference in vesicle numbers and size between non-pregnant and pregnant women (NonP vs. NormP and PE)? i.e. does pregnancy itself bring about changes in vesicle populations?

NormP vs. PE

Other studies have also used flow cytometry to measure total vesicle counts from late-onset PE and matched NormP women (Lok *et al.,* 2008b, Orozco *et al.,* 2009). Both of these studies contradict the findings reported in this study. One study (Orozco *et al.,* 2009) reported an increase in total vesicle counts in PE women whereas the other study (Lok *et al.,* 2008b) reported a decrease. Conflicting results were also found in studies looking at early-onset PE. Three studies (Lok *et al.,* 2008a, Lok *et al.,* 2008b, Lok *et al.,* 2009) reported a decrease in vesicle counts in PE vs. NormP women, whereas three other studies (VanWijk *et al.,* 2002, Bretelle *et al.,* 2003, Biro *et al.,* 2007) found no difference. Furthermore, one study (Alijotas-Reig *et al.,* 2011) also reported no difference in total vesicle counts in PE vs. NormP, whereas another study (Meziani *et al.,* 2006) reported an increase in vesicles in PE vs. NormP women, however both these studies were based on samples not matched for gestational age.

NonP vs. Pregnancy (NormP and PE)

The flow cytometry results presented in this chapter showing no difference in total vesicle counts in NonP vs. NormP are in agreement with other reported studies (VanWijk *et al.,* 2002, Biro *et al.,* 2007, Lok *et al.,* 2007, Lok *et al.,* 2008a, Lok *et al.,* 2009, Alijotas-Reig *et al.,* 2011). Only one study (Bretelle *et al.,* 2003) reported an increase in vesicle counts. Total vesicle counts in NonP vs. PE women have also been compared in previous studies. In concurrence with the work presented in this chapter, three studies found no difference in total vesicle counts (VanWijk *et al.,* 2002, Bretelle *et al.,* 2003, Biro *et al.,* 2007) whereas in three separate studies (Lok *et al.,* 2007, Lok *et al.,* 2008a, Lok *et al.,* 2009) lower numbers in PE women were reported.

4.5.4.4 STBM

Currently, STBM can only be measured in PFP on the basis of their phenotype by flow cytometry and not by NTA. Initial experiments spiking *in vitro* derived pSTBM into whole blood showed they could be detected in the PFP pellet after ultracentrifugation using flow cytometry. These data show that PLAP vesicles can be detected down to at least a concentration of 0.1μg/ml, the equivalent of ~10,000 microvesicles/ml. Spiking pSTBM into whole blood using a concentration of pSTBM at 0.1μg/ml was only performed once and concentrations below 0.1μg/ml were not tested in this study. Future experiments are needed to investigate lower concentrations. The *in vivo* STBM counts in NormP and PE women were below the lowest concentration tested in the pSTBM spiking experiments, suggesting that pSTBM concentrations below 0.1μg/ml are measurable. The pSTBM spiking experiments show that the background level of PLAP vesicles (without pSTBM) are actually higher than those detectable in the *in vivo* STBM experiments. There are differences between the *in vitro* STBM and *in vivo* STBM data that may help to explain this difference: 1) Different gating strategies were used and, 2) the *in vitro* STBM experiments were performed using the Lightning Link FITC anti PLAP antibody NDOG2, whereas the *in vivo* STBM experiments used the custom conjugated NDOG2-PE antibody.

Analysis of *in vivo* STBM were found to be elevated in NormP and PE women compared to NonP women. Total STBM counts were significantly increased in PE vs. NonP women, but the increase observed in NormP vs. NonP women did not reach significance. Furthermore, it was shown that the percentage of NDOG2 labelled vesicles was significantly elevated in NormP and PE women compared to NonP women. However, contrary to previous findings in our laboratory using the STBM ELISA (Knight *et al.,* 1998, Germain *et al.,* 2007) no difference in the total number of STBM or the percentage

labelled positive with NDOG2 was evident in NormP vs. PE women. These results were confirmed by the ELISA, showing significantly elevated STBM in NormP and PE women vs. NonP women but no difference when comparing NormP vs. PE women. The reason for this discrepancy is that in this current study all PFP samples were obtained from the Oxford Pregnancy Biobank, which had a drawback in that the majority of samples were from late-onset PE. The results obtained here were similar to those reported previously (Goswami *et al.,* 2006) showing elevated STBM in PE vs. NormP women in early-onset PE, but no difference in late-onset PE. There are currently very few early-onset PFP samples in the Biobank, of which there were insufficient volumes to carry out flow cytometry, NTA and ELISA in parallel. Although it is possible to collect early-onset samples, within the given time-frame of this study it was not feasible and therefore the Biobank samples were used. This is an issue that will need to be addressed in the future.

Circulating STBM have been characterised in four other studies (VanWijk *et al.,* 2002, Lok *et al.,* 2008a, Lok *et al.,* 2008b, Orozco *et al.,* 2009). In agreement with the current study a previous report (Orozco *et al.,* 2009) found a significant increase in total STBM counts in NormP vs. NonP and no difference in STBM counts in late-onset PE vs. matched NormP controls. However, the total number of STBM reported in the previous study (Orozco *et al.,* 2009) was extremely high (NormP; median value $3.5x10^6$/ml and PE; median value $5.0x10^6$/ml). These numbers actually exceed the total vesicle counts observed in the present study by ~3-fold in NormP and ~6-fold in PE and are also much higher than those previously reported (VanWijk *et al.,* 2002, Lok *et al.,* 2008a, Lok *et al.,* 2008b). Moreover, as mentioned in the introduction to this chapter, one study (VanWijk *et al.,* 2002) showed a higher number of circulating STBM in the NonP controls compared to NormP and PE women. This could be a reflection of the indirect staining protocol that was

used to label the plasma vesicles in both these studies. There is a much greater chance of non-specific binding when using indirect labelling, especially when no wash step is included in the procedure.

In an initial study (Lok *et al.,* 2008b) it was reported that total STBM counts and percentages of STBM were comparable in PE vs. NormP women at 28, 32 (early-onset) and 36 (late-onset) weeks gestation. However, contradictory to this finding, in a subsequent study, an increase in STBM in PE vs. NormP women at 30 weeks gestation was reported (Lok *et al.,* 2008a). Also in this same study (Lok *et al.,* 2008a), it was demonstrated that Flt-1, a transmembrane receptor for VEGF was directly associated with STBM. The results from the initial study (Lok *et al.,* 2008b) do not correlate with the STBM ELISA data reported previously (Goswami *et al.,* 2006). One of the major differences between these two studies (Goswami *et al.,* 2006, Lok *et al.,* 2008b) is the antibody used to detect STBM, which may help to explain the discrepancy in the results. In both studies (Lok *et al.,* 2008a, Lok *et al.,* 2008b) the antibody ED822 was used, which is against an unknown antigen expressed on the apical surface of the syncytiotrophoblast layer (Contractor and Sooranna 1986). The specificity of this antibody is uncertain. In our laboratory we have previously shown that ED822 binds to an antigen expressed on pSTBM but also on peripheral blood monocytes (Southcombe *et al.*, unpublished data). Furthermore Flt-1 is expressed on pSTBM (Guller *et al.,* 2011) and it is well documented that it is also expressed on monocytes (Clauss *et al.,* 1996, Waltenberger *et al.,* 2000, Sawano *et al.,* 2001). It is therefore possible that both these studies (Lok *et al.,* 2008a, Lok *et al.,* 2008b) are not solely detecting STBM, but also vesicles derived from monocytes.

4.5.4.5 Platelet Vesicles

The results presented in this chapter confirm previous findings showing that platelet vesicles are the most abundant derived population in plasma (VanWijk *et al.,* 2002, Bretelle *et al.,* 2003, Lok *et al.,* 2008a, Lok *et al.,* 2008b, Alijotas-Reig *et al.,* 2011). The percentage of platelet vesicles was significantly decreased in PE vs. NonP women, however this was not reflected in the total platelet vesicle counts. There was a trend to suggest a reduction, but this was not significant ($p = 0.066$). These results showed that total vesicle counts and the percentage positive were comparable between NonP vs. NormP women and NormP vs. PE women. To our knowledge this is the first study to use CD41 and W6/32 in combination to label platelet vesicles. No difference in CD41 single or CD41/W6/32 double positive platelet vesicles between groups was detected.

NormP vs. PE

There have been two previous studies that have measured circulating platelet vesicles in late-onset PE and matched NormP controls and both reported no difference in total platelet vesicles (Gonzalez-Quintero *et al.,* 2003, Lok *et al.,* 2008b). However, the total platelet vesicle counts (defined using anti-CD42) reported in the first of these two studies (Gonzalez-Quintero *et al.,* 2003) were up to 20-fold higher than those found in this study and the percentage of platelet vesicles (defined using anti-CD61. NormP: 98.1% and PE: 93.2%) reported in the second previous study (Lok *et al.,* 2008b) was also considerably higher than those reported in the present study. An additional study (Macey *et al.,* 2010) measured the percentage of activated platelet vesicles in late-onset PE vs. matched NormP controls and reported an increase in PE women, however this study measured vesicles in whole blood and not plasma. More recently, one study (Alijotas-Reig *et al.,* 2011) also found no difference in platelet vesicles in PE vs. NormP women, but these findings are

based on a non-matched case-control study. The first study to examine platelet vesicles in early-onset PE vs. matched NormP controls found no difference (VanWijk *et al.,* 2002), whereas subsequent studies have all reported a decrease in platelet vesicle counts in PE women (Bretelle *et al.,* 2003, Lok *et al.,* 2007, Lok *et al.,* 2008b, Lok *et al.,* 2009).

Circulating platelet vesicle counts may be a direct reflection of total platelet counts or may be related to the rate at which they are cleared from the circulation. In this study it was not possible to obtain platelet counts for all the NormP and PE women, therefore no comment can be made. Two previous studies have measured total platelet counts and circulating platelet vesicles in parallel, one reporting a positive correlation (Lok *et al.,* 2008b) and the other finding none (Bretelle *et al.,* 2003).

Total platelet vesicle counts observed in this current study and that reported previously (Bretelle *et al.,* 2003) were much lower than those found in two other former studies (Gonzalez-Quintero *et al.,* 2003, Lok *et al.,* 2008b). This is most probably a reflection of the method of preparation of the plasma. The latter studies (Gonzalez-Quintero *et al.,* 2003, Lok *et al.,* 2008b) used plasma which had only undergone a single centrifugation, thus still comprising platelets that during the freezing process may have undergone fragmentation, giving rise to artificial platelet vesicles and hence result in very high counts. This is in contrast to the study presented in this chapter and that reported previously (Bretelle *et al.,* 2003) where double centrifugation was used to remove the platelets and much lower total platelet vesicle counts were shown.

NonP vs. Pregnancy (NormP and PE)

The results presented in this chapter are in agreement with some of those published previously. One study (VanWijk *et al.,* 2002) found no difference in total platelet vesicle counts in NonP controls vs. NormP or PE women. Moreover, in another study (Lok *et al.,* 2007) total platelet vesicle counts were shown to be comparable in NonP vs. NormP women. In a subsequent study (Lok *et al.,* 2008a), total counts were not reported, but the percentage of platelet vesicles between these two groups were found to be similar. In contrast, there are two reports of increased total platelet vesicle counts in NormP women compared to NonP controls (Bretelle *et al.,* 2003, Alijotas-Reig *et al.,* 2011). In this chapter the percentage of platelet vesicles in NonP controls vs. PE women was significantly decreased. This was also reflected in the total platelet vesicle counts, although the difference did not reach significance. A previous study has reported significantly lower platelet vesicle counts in early-onset PE women vs. NonP controls (Lok *et al.,* 2007).

4.5.4.6 Leukocyte Vesicles

In our laboratory we have previously shown that NormP is characterised by activation of leukocytes and this is significantly pronounced in PE (Sacks *et al.,* 1998). Activation of granulocytes, monocytes and lymphocytes may all contribute to the systemic inflammatory responses in pregnancy. Leukocyte activation may in turn reflect the total number of leukocyte derived vesicles found in the circulation. This study used W6/32 as a marker for all HLA Class I leukocyte vesicles. Leukocyte vesicle numbers were very low accounting for <0.1% of the total circulating vesicles in NonP women, <1.0% in NormP women and 2.3% in PE women. Moreover, in Chapter 2 of this thesis it was shown that *in vitro* derived granulocyte vesicles did not label positive with W6/32 and therefore it is likely that these vesicles were excluded from the *in vivo* analysis. However, without including a

specific granulocyte marker (e.g. CD66) in the panel it is impossible to answer this question. Circulating leukocyte vesicles were barely detectable in NonP women, however a significant increase in total leukocyte vesicle counts and the percentage of W6/32 labelled vesicles was apparent in PE vs. NonP women. Total leukocyte vesicle counts and the percentage positive were also raised in PE vs. NormP women and NormP vs. NonP women, but these increases were not significant.

Total leukocyte vesicles have also been measured in other studies. Using anti-CD45 as a marker, which in Chapter 2 was shown not to label all leukocyte vesicles, comparable numbers were found in NormP and PE women in a previous non-matched case-control study (Alijotas-Reig *et al.,* 2011). Whereas when using anti-CD11a as a marker, one study (Meziani *et al.*, 2006) reported elevated leukocyte vesicles in PE women vs. non-matched NormP controls. Another study (Lok *et al.*, 2009) measured leukocyte vesicles in NonP and early-onset PE vs. matched NormP controls and found no difference between all three groups. The total leukocyte vesicle counts in this study (Lok *et al.*, 2009) was determined by measuring different subsets of leukocyte vesicles (i.e. monocytes, lymphocytes and granulocytes). There have been other reports in the literature that have also measured various subsets, which are described below (VanWijk *et al.*, 2002, Lok *et al.*, 2008b). However, in these experiments only single colour or at most double colour labelling was carried out. It was not feasible to analyse the different subsets of leukocyte vesicles in this current study as our flow cytometer only has six available detection parameters.

Monocyte vesicles

Monocyte derived vesicles have been examined in three previous studies. Two studies have shown a significant increase in circulating monocyte vesicles in early-onset PE vs.

matched NormP controls (Lok *et al.,* 2008b, Lok *et al.,* 2009) and in one of these studies an increase was also found in late-onset PE vs. matched NormP controls (Lok *et al.,* 2008b). In contrast, another study (VanWijk *et al.,* 2002) found that the majority of samples had no monocyte derived vesicles and there was no difference between NonP, NormP or PE women.

Granulocyte vesicles

No granulocyte vesicles were detected in early-onset PE women, late-onset PE women, or matched NormP controls in one former study (Lok *et al.,* 2008b). Surprisingly, using the same granulocyte maker (CD66e) in a subsequent study (Lok *et al.,* 2009), granulocyte vesicles were detected and were reported to be elevated in early-onset PE vs. NonP women and NormP vs. NonP women. No difference in granulocyte vesicle counts was observed when comparing early-onset PE vs. matched NormP controls. Granulocyte vesicles (defined using CD66e) were also examined in another previous study (VanWijk *et al.,* 2002). Vesicle counts were comparable in NonP vs. NormP women and elevated granulocyte vesicles were evident in early-onset PE women compared to matched NormP controls or NonP women.

Lymphocyte vesicles

Circulating B-Cell vesicles (defined using CD20), cytotoxic T Cell vesicles (defined using CD8) and helper T Cell vesicles (defined using CD4) have previously been measured in three separate studies (VanWijk *et al.,* 2002, Lok *et al.,* 2008b, Lok *et al.,* 2009).

***B-Cell* Vesicles.** The number of B-Cell derived vesicles did not differ in early-onset PE vs. matched NormP controls (VanWijk *et al.,* 2002, Lok *et al.,* 2008b, Lok *et al.,* 2009).

However, one study (Lok *et al.,* 2008b) reported a significant increase in the number of circulating B-Cell vesicles in PE women at 36 weeks gestation compared to NormP controls.

Cytotoxic T Cell **Vesicles.** There is conflicting data in all three studies (VanWijk *et al.,* 2002, Lok *et al.,* 2008b, Lok *et al.,* 2009) with regard to the numbers of circulating cytotoxic T Cell vesicles. One study (Lok *et al.,* 2008b) only found significantly elevated CD8 positive vesicles in PE women at 28 weeks gestation and thereafter no CD8 positive vesicles were found in NormP or PE women. Another study (VanWijk *et al.,* 2002) reported significantly higher numbers of cytotoxic T Cell vesicles in NonP women compared to NormP women and showed numbers to be significantly increased in PE women compared to NormP controls. In contrast, one study (Lok *et al.,* 2009) only found a significant increase in cytotoxic T Cell vesicles when comparing PE to NonP women, there was no difference in NonP vs. NormP women or PE vs. NormP women.

Helper T Cell **Vesicles.** No difference in circulating numbers of helper T Cell vesicles in PE vs. NormP women were reported in two former studies (Lok *et al.,* 2008b, Lok *et al.,* 2009), whereas in another study (VanWijk *et al.,* 2002) numbers were shown to be significantly elevated in PE vs. NormP controls.

In general, there appears to be huge variation between studies with regard to reported circulating numbers of leukocyte vesicles in NormP and PE. The number of leukocyte vesicles in PE has been reported to account for between 1.4-11.5% of the total number, whereas in NormP this ranges from <0.1-3.1% (VanWijk *et al.,* 2002, Lok *et al.,* 2008b, Lok *et al.,* 2009). One study (Lok *et al.,* 2009) found that the majority of circulating

leukocyte-derived vesicles were from lymphocytes (CD4, CD8 and CD20), followed by monocytes and the smallest group was derived from granulocytes, whereas another study (VanWijk *et al.,* 2002) reported that the majority of leukocyte vesicles were derived from granulocytes, followed by lymphocytes and monocytes. Based on these findings, it is difficult to speculate on the cellular origin(s) that accounts for the elevated number of vesicles observed in PE, presented in this chapter. Experiments using multiple markers for each individual leukocyte population subset would need to be carried out to investigate this further.

At present it is unclear if the observed elevation in leukocyte derived vesicles in PE is a direct consequence of leukocyte cell activation or may possibly play a role in inducing endothelial dysfunction. One previous study (Martin *et al.,* 2004) showed that T-lymphocyte vesicles produced from a T Cell line impaired endothelial function of mouse aortic rings *in vitro*. Furthermore, *in vitro* derived lymphocyte vesicles from diabetic patients were found to decrease the expression of endothelial nitric oxide, a critical component in maintaining normal endothelial function. It is therefore probable that the exacerbated vascular damage observed in PE, may in part be due to an increase in leukocyte derived vesicles.

4.5.4.7 RBC Vesicles

Total circulating RBC vesicles were found to be elevated in NormP vs. NonP women. A significant increase in the percentage of CD235a/b positively labelled vesicles in NormP and PE women vs. NonP controls was also observed. No difference in total RBC vesicle counts or the percentage labelled CD235a/b positive was found in NormP vs. PE women. To date, there have been only two other studies that have examined RBC vesicles in

NormP and PE (VanWijk *et al.,* 2002, Lok *et al.,* 2008b). The first study (VanWijk *et al.,* 2002) examined total counts in NonP controls and early-onset PE vs. matched NormP women (29.9 vs. 30.4 weeks mean gestation respectively) and showed no difference in total RBC vesicle counts between the groups. Whereas the second study (Lok *et al.,* 2008b) found RBC vesicle counts to be significantly elevated at 28 weeks gestation and thereafter (32 and 36 weeks gestation) were comparable to NormP matched controls. It is well established that RBC counts, hemoglobin and hematocrit all decrease in NormP due to an expansion in plasma volume, however levels in PE are comparable with NormP (Dordevic *et al.,* 2008). It has been shown that during NormP the osmotic fragility of RBCs is increased compared to NonP (Rebelo *et al.,* 1995), hence making the RBCs more susceptible to hemolysis and fragmentation which may in turn result in the production of RBC vesicles. RBCs may also be triggered to release vesicles as a result of oxidative stress. Several studies have shown that activated leukocytes release reactive oxygen species (ROS) and reactive nitrogen species (RNS) into the maternal circulation which induces oxidative damage of the RBC membranes (Lynch and Fridovich 1978, Denicola *et al.,* 1998, Tsukimori *et al.,* 2005).

RBC vesicles are comprised of large quantities of hemoglobin (Greenwalt *et al.,* 1991, Lee and Gladwin 2010) and it has also been proposed that RBC vesicles may scavenge nitric oxide from the endothelium, thus reducing its bioavailability (Gladwin and Kim-Shapiro 2009). Nitric oxide is crucial to regulating normal vasodilatation, inhibiting platelet aggregation and endothelial adhesion all of which are impaired in PE. Recently, a study reported reduced nitric oxide bioavailability in PE (Sandrim *et al.,* 2010). Our results show that total RBC vesicle counts are comparable in late-onset PE and matched NormP controls, but functionally they may be very different. This raises the question as to whether

RBC vesicles in PE scavenge more nitric oxide than those in NormP. The expression level of the hemoglobin scavenger receptor (CD163) may be up-regulated on RBC derived vesicles in PE compared to NormP. Moreover, our laboratory has recently carried out proteomic analysis on pSTBM pools from PE and NormP placentas using multi-dimensional protein identification technology (MudPIT) and ultra-performance liquid chromatography tandem mass spectrometry analysis (UPLC-MSE) (Tannetta et al., unpublished data). Preliminary analysis has shown that the hemoglobin scavenger receptor (CD163) is associated with STBM and is common to both preparations, but is highly up-regulated in PE STBM vs. NormP STBM. This suggests that along with RBC vesicles which may scavenge nitric oxide from the endothelium, STBM may also play a role. More experiments are required to investigate this further.

4.5.4.8 Endothelial Vesicles

In this study the endothelial cell marker CD146 was used to examine circulating endothelial derived vesicles in NonP, NormP and PE women. This marker was chosen as it showed no cross-reactivity with any of the other vesicle cell types. However, no vesicles were detected in any of the samples examined. CD146 has been used to measure circulating endothelial vesicles in many other studies (Mallat *et al.,* 2000, Faure *et al.,* 2006, Duval *et al.,* 2010), but this is the first time it has been used to measure endothelial derived vesicles in NormP and PE.

Endothelial vesicles have been investigated in many other studies measuring vesicles in NormP and PE, but these studies have used different endothelial markers including E-Selectin (CD62E), (VanWijk *et al.,* 2002, Gonzalez-Quintero *et al.,* 2004, Lok *et al.,* 2008a), PECAM (CD31) (Gonzalez-Quintero *et al.,* 2003, Meziani *et al.,* 2006, Alijotas-

Reig *et al.,* 2011), VE-Cadherin (CD144) (VanWijk *et al.,* 2002, Alijotas-Reig *et al.,* 2011) and CD51 (Bretelle *et al.,* 2003). The range of circulating endothelial vesicles reported in the literature varies considerably between studies. For example, using the same endothelial marker (CD31) counts range from 13-8406/µl in NormP and 9-14723/µl in PE (Bretelle *et al.,* 2003, Gonzalez-Quintero *et al.,* 2003).

NormP vs. PE

Aside from this current study there is only one other report in which no endothelial derived vesicles were found in PE women vs. non-matched NormP controls (Meziani *et al.,* 2006). Three studies have reported an increase in endothelial vesicle counts in PE vs. NormP. One study was based on not matched for gestational age samples (Alijotas-Reig *et al.,* 2011) and two of the studies were conducted by the same author using plasma from late-onset PE vs. matched NormP controls (Gonzalez-Quintero *et al.,* 2003, Gonzalez-Quintero *et al.,* 2004). In contrast, one former study (Lok *et al.,* 2008b) found no difference in the percentage positive endothelial vesicles in late-onset PE or early-onset PE compared to matched NormP controls and this was also supported by another independent study (VanWijk *et al.,* 2002) who reported comparable endothelial vesicle counts in early-onset PE vs. matched NormP women.

NonP vs NormP and PE

Two studies have reported endothelial vesicle counts to be significantly elevated in NormP women compared to NonP controls (Bretelle *et al.,* 2003, Alijotas-Reig *et al.,* 2011). Very low numbers were found in the NonP control women.

Aside from the studies which have used CD62E to detect circulating endothelial vesicles in plasma, one of the major concerns in the other studies is the choice of markers used. In Chapter 2 of this thesis the endothelial marker CD144 was shown to be weakly expressed on pSTBM, but a recent study using immunohistochemistry staining of placental sections has shown CD144 to be strongly expressed on the syncytiotrophoblast (Groten *et al.,* 2010). It is therefore possible that the CD144 positive vesicles analysed in these previous studies may not be entirely derived from the endothelium, but may also include STBM. Similarly, CD31 is not endothelial specific and is also found on the surface of platelets, monocytes, granulocytes and some lymphocyte subsets. Moreover, it has also been shown to be expressed on the syncytiotrophoblast (Coukos *et al.,* 1998). As a marker of endothelial vesicles CD31 is often used in combination with a platelet marker (i.e. CD41, CD42 or CD61) and those vesicles which label $CD31^{+}$/CD(41,42 or 61)$^{-}$ are deemed endothelial derived vesicles, however they may in reality be vesicles derived from monocytes, granulocytes, lymphocytes or even STBM. In a recent study (Alijotas-Reig *et al.,* 2011) circulating vesicles were measured in PE women and non-matched NormP controls, using two separate endothelial markers (CD144 and $CD31^{+}$/$CD41^{-}$). Using CD144 there was no difference in circulating numbers in PE vs. NormP controls, however counts were significantly elevated in PE women when using the markers $CD31^{+}$/$CD41^{-}$. These data suggest that either these vesicles have a lower copy number of CD144 on their surface compared to CD31 or the vesicles are not entirely derived from the same cellular origin. One former study (Bretelle *et al.,* 2003) used CD51 to examine endothelial vesicles, however the pSTBM MudPIT data (Tannetta et a., unpublished data) suggest that CD51 is associated with STBM and therefore may also include these in the analysis.

It is difficult to explain why no endothelial derived vesicles were detected in any of the samples used in this study with the marker CD146. This same marker has been used previously to investigate endothelial derived vesicles in other disease states and there are reports of elevated numbers compared to normal healthy controls (Mallat *et al.,* 2000, Faure *et al.,* 2006, Duval *et al.,* 2010). There are a few possible explanations. As shown in Chapter 2, CD146 bound to the endothelial derived vesicles produced *in vitro*, but perhaps the mechanism by which the vesicles are produced *in vivo* in NormP and PE is very different such that they don't express this antigen on their surface. It is also possible that the copy number of CD146 on the endothelial derived vesicles is too low to be detected by flow cytometry and as mentioned previously when discussing STBM, clearance rates of vesicles in the circulation are not taken into account. Moreover, a recent study showed that flow cytometric detection of endothelial derived vesicles varies depending on the centrifugation protocol of the plasma and the storage conditions (4ºC or -80ºC) (van Ierssel *et al.,* 2010). Endothelial vesicles were labelled using different markers including $CD31^{+}/CD41^{-}$, CD62E and CD144. Examination of vesicle counts in plasma stored at 4ºC was comparable using all three markers, however freezing resulted in an increase of CD31+/CD41- and CD62E vesicle counts, whereas CD144 vesicle counts were significantly lower (van Ierssel *et al.,* 2010). Endothelial vesicles defined by CD146 may also be effected by freezing, as was shown in previous data in this thesis when examining RBC vesicles in fresh vs. frozen plasma. Future experiments will need to be carried out to examine this further.

4.5.4.9 Orphan Vesicles

In this study there were a significant population of "orphan" vesicles, which accounted for ~16-26% of the total population and did not label with any of the markers of interest.

These vesicles have not previously been reported as the majority of other studies only examine Annexin V positive vesicles, rather than vesicles defined by FSC vs. SSC and Bio-Maleimide. The origin of these vesicles is still likely to be the different cell types investigated in this study (i.e. STBM, platelet, RBC, endothelial and leukocyte), however the antigen copy number on the surface of the vesicle might be too low to be detected by flow cytometry. Different markers may be required to identify these vesicles. In Chapter 2 of this thesis, using *in vitro* derived vesicles, it was demonstrated that some antigens are not expressed on all vesicles and that some markers are also dependent on the stimulation method. This may also apply to the *in vivo* derived vesicles, whereby during their formation certain markers are excluded from their surface. The mechanism by which vesicles are produced *in vivo* may influence the antigens they express.

4.5.4.10 Fluorescence NTA

Although flow cytometry can phenotype vesicles, one of its limitations is that it cannot analyse exosomes and small microvesicles ≤ 290nm. The NanoSight LM10 instrument has shown that it can analyse microvesicles and nanovesicles the size of exosomes, however it cannot phenotype them. As mentioned previously, during the course of this study our group worked with NanoSight Ltd to develop an instrument incorporating a fluorescence capability and therefore it was now possible to not only size and estimate vesicle concentration, but also phenotype the vesicles. In addition, a more sensitive camera was fitted to this instrument making it possible to track smaller celluar vesicles (sub 100nm) than those measured using the LM10 instrument. Using fluorescent 100nm beads in both scatter and fluorescence mode gave accurate sizing and concentration measurements. To test the system on biological vesicles a preparation of pSTBM were then labelled with an NDOG2-Qdot605 antibody and respective IgG1-Qdot605 isotype control antibody.

Analysed in scatter and fluorescence mode, the size distributions of the NDOG2-labelled pSTBM were very similar. These experiments show a population of NDOG2 positively labelled pSTBM never before identified as they are too small to be detected by flow cytometry. This development in the technology while too late to be utilised in this thesis opens up new possibilities to phenotype vesicles in plasma. Using specific markers this would allow plasma derived STBM and other circulating vesicles to be enumerated, accurately sized and phenotyped all in a single assay. The impact that fluorescence NTA could have to the future research into cellular vesicles as potential biomarkers will be discussed in more detail in Chapter 5.

4.6 Summary

In this chapter the final aim of this thesis was addressed, which was to use flow cytometry and NTA to determine the number, size and phenotype of STBM and other cellular derived vesicles in NormP and PE. Cellular derived vesicles were obtained from PFP by ultracentrifugation, which was shown to be an important requirement as it separates the cellular derived vesicles from lipid vesicles in plasma.

An initial attempt using six-colour flow cytometry to quantitate and phenotype the cellular vesicles demonstrated problems with the antibody panel. Subsequently, two separate panels were designed: a three-colour panel for STBM and a five-colour panel for the other vesicle types in NonP, NormP and PE women. Flow cytometric analysis showed no difference in total vesicle numbers between groups, whereas NTA revealed smaller vesicles in significantly elevated numbers in NormP and PE women compared to NonP controls.

Phenotypic analysis of the vesicles larger than 290nm showed that the majority were platelet derived, followed by RBC and leukocyte vesicles with the smallest population being STBM. Differences between non-pregnancy and pregnancy were observed, supporting the hypothesis that during pregnancy vesicle numbers change. Total STBM and leukocyte vesicle numbers were significantly elevated in PE women compared to NonP women and RBC vesicles were increased in NormP women compared to NonP controls. The percentage of platelet vesicles was significantly decreased in PE compared to NonP controls, which may be a reflection of their activation status. Furthermore, the percentages of STBM and RBC vesicles were significantly elevated in NormP and PE women compared to NonP controls and the percentage of leukocyte vesicles was increased in PE vs. NonP control women. There was no significant difference in the numbers or percentage of STBM or any of the other vesicles between NormP and PE women, probably due to the samples being from late rather than early-onset PE women, matched to NormP controls.

Finally, measuring pSTBM using the advanced NanoSight NS500 instrument with fluorescent labelled NDOG2 antibody revealed a population of sub 290nm vesicles never analysed before and opens up new possibilities for the phenotypic analysis of cellular derived vesicles in the future.

Chapter 5

Final Discussion

5.1 Final Discussion

In this thesis it was hypothesised that circulating vesicles in the maternal circulation may be present at a size too small previously to have been detected and individually characterised. Circulating STBM in PE may be altered and therefore may have the potential to be used as a predictive biomarker. Moreover, the other circulating derived vesicles may also change in PE and might be useful as diagnostic biomarkers. To test these hypotheses, blood samples from NonP, NormP and PE women, all recruited to the Oxford Pregnancy Biobank, were used. Circulating vesicles derived from STBM, platelets, RBCs, endothelium and leukocytes were analysed in late-onset PE women matched to NormP and NonP women. The two main techniques used to measure and characterise the cellular derived vesicles in this study were flow cytometry and NTA. This study is the first of its kind to use these two techniques in parallel to measure vesicles in NormP and PE. This has resulted in many interesting findings between these groups and also given rise to several questions which are discussed below.

5.1.1 Measuring Cellular Derived Vesicles Using Flow Cytometry

Flow cytometry is the most common technique used to characterise cellular derived vesicles and has been used in a wide range of studies examining a variety of different diseases. From the literature it was evident that analogue flow cytometers can measure vesicles ≥500nm, whereas newer digital flow cytometers have an increased sensitivity and measure vesicles ≥300nm. Therefore, prior to analysing the clinical samples, first it was necessary to optimise our digital flow cytometer for the detection and counting of vesicles. As shown in Chapter 2 of this thesis, it proved capable of analysing vesicles ≥290nm. In the past year a new generation of digital flow cytometers has been released onto the market with improved light scatter detection performance, resulting in enhanced signal:noise ratio,

enabling the detection of smaller vesicles (Lacroix *et al.,* 2010a). The Apogee A40 flow cytometer is reported to measure 200nm polystyrene beads (Chandler *et al.,* 2011) while the Apogee A50 flow cytometer can clearly distinguish polystyrene beads of 100nm and can discriminate these from 300nm beads in a mixture (Lacroix *et al.,* 2010a). It was also recently reported that the BD Influx flow cytometer can distinguish beads of 100nm from 200nm when used in combination (Hoen *et al.,* 2011). Furthermore, the Millipore easyCyte Guava flow cytometer is claimed to measure beads as small as 40nm, however no formal demonstration of this has yet been published.

Having established that our flow cytometer could analyse vesicles ≥290nm, next panels of antibodies were tested on *in vitro* derived vesicles from all the different cell types that were to be examined in the *in vivo* clinical plasma samples. The results of this study were somewhat surprising as it was not expected that many of the antigens expressed on the parent cells were not expressed on all of the vesicles. Moreover, the expression of some of the antigens was dependent on the stimulation method. As previously mentioned in Chapter 2, the reasons for this are unknown, but can be speculated upon. During formation of the vesicle, selective exclusion of the antigen from the vesicle surface may occur or the antigen copy number on the surface of the vesicle may be too low to be detected by flow cytometry. Currently it is not possible to establish whether these *in vitro* derived vesicles are a true reflection of the *in vivo* situation and whether these same processes occur. Nonetheless, this study shows that this may well be a possibility and markers should therefore be chosen accordingly.

Using the *in vitro* derived vesicles also allowed the specificity of markers to be examined. Many markers were shown to bind more than one cell type and this was crucial in

selecting a panel of markers to use in the multi-colour flow cytometry assay for the analysis of clinical samples. It is clear that many researchers may not have taken this into consideration when selecting markers to examine *in vivo* derived circulating vesicles. Many studies assume that the chosen marker will only label one specific cell type, where in fact it may label several. Examples of this include the analysis of STBM using the anti trophoblast antibody ED822 (Lok *et al*., 2008a, Lok *et al*., 2008b) and endothelial derived vesicles using markers such as CD144 (Van Wijk *et al*., 2002, Alijotas-Reig *et al*., 2011) or CD31 (Gonzalez-Quintero *et al.,* 2003, Meziani *et al.,* 2006, Alijotas-Reig *et al.*, 2011).

5.1.2 Measuring Cellular Derived Vesicles Using NTA

In Chapter 3 of this thesis it was established that one of the major limitations to analysing cellular derived vesicles by flow cytometry is that only a very small fraction of the total population is detected by this technique. This was formally demonstrated by using NTA, which can detect vesicles as small as 70nm, greatly exceeding the resolution of flow cytometry. The evaluation of NTA carried out in Chapter 3 of this thesis clearly showed for the first time that it can be used to estimate vesicle size and concentration in biological samples, although as with many experimental systems there are certain limitations.

Although the smallest size of vesicles that can be detected using NTA is somewhat dependent on their refractive index, the measurement of vesicle size is completely independent of this factor. This is a major advantage over flow cytometry as with the latter technique sizing is very dependent on vesicle refractive index (Chandler *et al.,* 2011). Recently, the standard practice of using polystyrene or latex beads to calibrate flow cytometers for vesicle detection has come into question. How these bead measurements relate to the size of cellular vesicles is not clear. Cellular vesicles have a lower refractive

index than latex or polystyrene beads, which could lead to an underestimation of their size (Foladori *et al.,* 2008, Lacroix *et al.,* 2010a). Using one of the new generation flow cytometers (Apogee A40 instrument) it was recently shown that a 400nm polystyrene bead has a refractive index equivalent to a 1μm lipid or cellular vesicle (Chandler *et al.,* 2011). Hence, flow cytometry may be analysing much larger vesicles than first thought. Even though this is a significant drawback to using beads, currently no uniform, easily obtainable, cross laboratory biological standard exists. The need for a biological standard was recently discussed at the 3rd Flow Cytometry UK meeting in York, 2011. It was suggested that liposomes could be used as an alternative approach to polystyrene beads as these can be manufactured in various sizes, are highly monodisperse and would have an appropriate refractive index. However these are not yet commercially available.

5.1.3 Detection of Vesicles in Plasma – A Need for Standardisation

Within the last year or so there has been a growing literature published on various pre-analytical issues that are thought to effect the quantification of circulating derived vesicles in plasma (Trummer *et al.,* 2009, Hind *et al.,* 2010, Mobarrez *et al.,* 2010, van Ierssel *et al.,* 2010, Ayers *et al.,* 2011, Yuana *et al.,* 2011, Lee *et al.,* 2012). In Chapter 4 Section 4.4.2 of this thesis a small pilot study examined one of these pre-analytical variables, the effect of freezing PFP on quantification of total, platelet and RBC derived vesicles. These data showed that freezing had no effect on the total number of circulating vesicles or those derived from platelets, whereas RBC vesicles were significantly decreased after PFP had been frozen. Three other studies have also used flow cytometry to examine the effect that freezing has on vesicle quantification (Trummer *et al.,* 2009, Mobarrez *et al.,* 2010, Ayers *et al.,* 2011). The results shown in this thesis are in agreement with a former study (Mobarrez *et al.,* 2010) reporting that platelet vesicles are not affected by freezing. The

findings of another study (Trummer *et al.*, 2009) also support these data showing that total Annexin V and platelet derived vesicle numbers were the same after freezing. In contrast, a recent report showed that total Annexin V vesicles and platelet vesicles were increased after freezing (Ayers *et al.*, 2011). This is only one of many pre-analytical variables that have been investigated. Although each of these studies is looking at the same variable, there must be other variables between studies that affect vesicle quantification and account for the observed differences. This makes it increasingly difficult to compare between studies.

There are many other variables, some of which have been investigated that are likely to impact on quantification of vesicles. These include: **1.** Blood collection (needle gauge and anticoagulant); **2.** Plasma preparation (single or double centrifugation of blood and time between venepuncture and centrifugation); **3.** Plasma storage (fresh, 4ºC, frozen or snap frozen); **4.** Thawing temperature of plasma if stored frozen (on ice, at room temperature or at 37°C); **5.** Vesicle isolation (centrifugation speed/time to concentrate vesicles from plasma); **6.** Flow cytometer instrumentation (manufacturer and whether it is an analogue or digital instrument); **7.** Flow cytometry analysis (setting the lower and upper gates to define the vesicles and the choice of threshold (FSC, SSC or fluorescence)) and **8.** Fluorescent markers and antibodies (choice of antigen, clone and fluorophores). In order to directly compare between studies all of these need to be standardised. This is a very difficult task and one that the Vascular Biology group of the Scientific and Standardisation Committee (SSC) of the International Society on Thrombosis and Haemostasis (ISTH) is working toward.

To investigate vesicles as biomarkers in a clinical setting it is essential to understand the impact that these pre-analytical variables may have on the development of a point-of-care test. This is not only applicable to the diagnosis and treatment of PE, but is applicable to a wide range of diseases in which vesicles have been shown to play a potential role (e.g. cardiovascular disease, cancer). A point-of-care test needs to be high-throughput and require as little processing to the sample as possible. It also needs to be designed in a way which has little impact on other clinical tests that might be carried out in parallel. For example it would important to establish whether the anticoagulants used for current clinical assays are also suitable for analysis of vesicles. Samples would be analysed fresh opposed to frozen and in a clinical setting it would be desirable to move away from high-speed ultracentrifugation to purify the cellular vesicles, therefore both of these aspects need to be addressed. Universal assay instrumentation, reagents and protocols would need to be in place.

5.1.4 Measuring Cellular Derived Vesicles in NonP, NormP and PE Women

In Chapter 4 of this thesis, circulating vesicles were investigated in late-onset PE women, NormP and NonP women. As previously stated in Chapter 4 Section 4.5.3, this study was carried out using recommendations that had been made by others regarding pre-analytical variables that could impact on vesicle quantification. Differences in many of the pre-analytical variables discussed above made comparing this current study with those done previously all the more difficult. The reason for using ultracentrifugation to pellet vesicles has been discussed in Chapter 4 Section 4.5.1. Ultracentrifugation of PFP was shown to be an absolute requirement to separate cellular from lipid derived vesicles, whilst minimising vesicle loss. Many researchers use a lower centrifugation speed of ~20,000 × g to isolate vesicles as opposed to the 100,000 (average) × g spin used in this study. No formal

experiments have been done to compare these different centrifugation speeds to establish whether they pellet the same number or size of vesicles, however this comparison will be made in the near future using the techniques developed in this thesis.

Using flow cytometry, a five-colour panel was established to phenotype platelet, RBC, endothelial and leukocyte derived vesicles and a separate three-colour panel was designed to investigate STBM. There is only one other published study investigating plasma derived vesicles by flow cytometry using a three-colour panel (Gelderman and Simak 2008). Hence, this is the first ever study to analyse cellular derived vesicles using both a three-colour and five-colour panel. Furthermore, this is also the first time flow cytometry and NTA have been used together to investigate cellular vesicles.

In this study, changes in vesicle number and percentage for a number of different subtypes were found in pregnancy compared to non-pregnancy. Flow cytometric analysis revealed that total numbers of circulating STBM and leukocyte vesicles were increased in PE vs. NonP women and RBC vesicles were significantly elevated in NormP vs. NonP women. The percentage of platelet vesicles in PE was reduced compared to NonP controls, whereas percentages of STBM and RBC vesicles were significantly increased in PE and NormP women compared to NonP controls. The percentage of leukocyte vesicles was also significantly elevated in PE women compared to NonP controls. These data show that there were clear differences in circulating cellular derived vesicles in pregnancy (NormP and PE) compared to NonP, but there were no differences between NormP and PE. This study used a total of six markers to examine the different vesicle subtypes, however it is possible that other markers may establish differences between PE and NormP not seen with the current panels. It is unclear at which point in pregnancy (1^{st}, 2^{nd} or 3^{rd} trimester)

these changes begin to occur and whether these are seen throughout pregnancy gestation. As previously discussed the lack of differences between NormP and PE is most likely due to the samples being from late- rather than early-onset PE. This is supported by a previous study showing STBM, as measured by ELISA, to be elevated in early-onset but not late-onset PE vs. NormP women (Goswami *et al.*, 2006). However, due to constraints of the Oxford Pregnancy Biobank these samples were not available to analyse in this present study. Investigations into STBM and other cellular derived vesicles throughout pregnancy and in a group of early-onset PE women will be explored in future studies. The use of STBM and the other cellular vesicles as predictive or diagnostic biomarkers in PE therefore remains an open question and will continue to be investigated.

As demonstrated in Chapter 4, the use of NTA has shown that flow cytometry is only analysing a very small proportion of the total cellular derived vesicles in NonP, NormP and PE women. No change in total vesicle number was detected by flow cytometry, however changes were evident using NTA. Total vesicle counts were increased in NormP and PE and the vesicle size was also smaller when compared to NonP controls. Whether or not these changes in concentration and size also relate to the phenotype and potential functions of the vesicles cannot be elucidated in this current study. There is however scope for this as shown by the development of the NanoSight NS500 instrument which has a fluorescence capability and could therefore be used to phenotype vesicles using fluorescent antibodies. As shown in Chapter 4 Section 4.4.5 of this thesis, proof of principle was demonstrated on the NanoSight NS500 instrument by labelling pSTBM with NDOG2-Qdot605 Antibody (Dragovic *et al.*, 2011).

Although next generation flow cytometers are now being claimed to analyse vesicles in the same size range as those analysed using the NanoSight NS500 instrument, fluorescence NTA still has some distinct advantages. As previously mentioned in this chapter, these claims are based on using polystyrene or latex beads which have a higher refractive index than cellular vesicles and therefore may result in vesicles being under-sized. Although at present only single-colour labelling is possible using fluorescence NTA, the vesicle sizing measurement is made entirely independent of their refractive index and therefore sizing is indeed more accurate. Also, the cost of the NanoSight NS500 instrument is considerably more affordable in terms of the initial outlay and running costs in comparison to next generation flow cytometers. At present, further developments are being made to the NS500 instrument to allow the use of conventional fluorophores (i.e. those excited using a 488nm laser) to facilitate phenotyping. This also includes the development of a colour camera and filter system for multi-colour analysis of vesicles. In addition the instrument now incorporates the measurement of surface charge (zeta potential) which is important as there may be charge differences between microvesicles and exosomes or between NormP and PE STBM in relation to phosphatidylserine expression or oxidised proteins which may be generated in the disease state. Differences in charge between subtypes of vesicles could aid in their identification and ultimately their separation.

To develop STBM as a predictive biomarker, one of the ultimate aims would be to identify and isolate this population from blood and determine their composition and function in PE. Isolation of STBM from plasma could be achieved by using immunomagnetic beads coupled to the NDOG2 antibody, to positively select the STBM. It may also be possible to further fractionate the STBM into microvesicles and exosomes which may be important in helping to understand their function. This could be achieved by various methods,

including: filtration through nanofilters of different pore size; differential and density gradient centrifugation and gel filtration chromatography. STBM may also be fractioned using microfluidic separation and currently our laboratory is working with Dr Steven Sheard (Engineering Science, Oxford) and Professor Jeung Sang (Pusan University, Korea) to develop such a device. Fluorescence NTA would be used to verify the separation of the two vesicle subtypes, but would obviously be dependent on the availability of appropriate markers (Raimondo *et al.*, 2011).

Fractionation of STBM into microvesicles and exosomes would allow proteomic and miRNA analysis to determine whether their profiles differ between NormP and PE (Redman *et al.*, 2012). Ultimately, this would facilitate the identification of the molecules that cause the maternal syndrome of PE and eventually help produce a therapy.

References

Abid Hussein MN, Meesters EW, Osmanovic N, Romijn FP, Nieuwland R, Sturk A (2003). Antigenic characterization of endothelial cell-derived microparticles and their detection ex vivo. *J Thromb Haemost* **1:** 2434-2443.

Aharon A, Tamari T, Brenner B (2008). Monocyte-derived microparticles and exosomes induce procoagulant and apoptotic effects on endothelial cells. *J Thromb Haemost* **100:** 878-885.

Alijotas-Reig J, Palacio-Garcia C, Farran-Codina I, Ruiz-Romance M, Llurba E, Vilardell-Tarres M (2011). Circulating Cell-Derived Microparticles in Severe Preeclampsia and in Fetal Growth Restriction. *Am J Reprod Immunol*.

Aly AS, Khandelwal M, Zhao J, Mehmet AH, Sammel MD, Parry S (2004). Neutrophils are stimulated by syncytiotrophoblast microvillous membranes to generate superoxide radicals in women with preeclampsia. *Am J Obstet Gynecol* **190:** 252-258.

Aras O, Shet A, Bach RR, Hysjulien JL, Slungaard A, Hebbel RP, Escolar G, Jilma B, Key NS (2004). Induction of microparticle- and cell-associated intravascular tissue factor in human endotoxemia. *Blood* **103:** 4545-4553.

Ardoin SP, Shanahan JC, Pisetsky DS (2007). The role of microparticles in inflammation and thrombosis. *Scand J Immunol* **66:** 159-165.

Attwood HD, Park WW (1961). Embolism to the lungs by trophoblast. *J Obstet Gynaecol Br Commonw* **68:** 611-617.

Ayers L, Kohler M, Harrison P, Sargent I, Dragovic R, Schaap M, Nieuwland R, Brooks SA, Ferry B (2011). Measurement of circulating cell-derived microparticles by flow cytometry: sources of variability within the assay. *Thromb Res* **127:** 370-377.

Baj-Krzyworzeka M, Szatanek R, Weglarczyk K, Baran J, Urbanowicz B, Branski P, Ratajczak MZ, Zembala M (2006). Tumour-derived microvesicles carry several surface determinants and mRNA of tumour cells and transfer some of these determinants to monocytes. *Cancer Immunol Immunother* **55:** 808-818.

BD Biosciences Fluoresence Spectrum Viewer. Avaliable at: http://www.bdbiosciences.com/research/multicolor/spectrum_viewer/index.jsp

Bdolah Y, Sukhatme VP, Karumanchi SA (2004). Angiogenic imbalance in the pathophysiology of preeclampsia: newer insights. *Semin Nephrol* **24:** 548-556.

Bernimoulin M, Waters EK, Foy M, Steele BM, Sullivan M, Falet H, Walsh MT, Barteneva N, Geng JG, Hartwig JH, Maguire PB, Wagner DD (2009). Differential stimulation of monocytic cells results in distinct populations of microparticles. *J Thromb Haemost* **7:** 1019-1028.

Biro E, Lok CA, Hack CE, van der Post JA, Schaap MC, Sturk A, Nieuwland R (2007). Cell-derived microparticles and complement activation in preeclampsia versus normal pregnancy. *Placenta* **28:** 928-935.

Bournazos S, Rennie J, Hart SP, Dransfield I (2008). Choice of anticoagulant critically affects measurement of circulating platelet-leukocyte complexes. *Arterioscler Thromb Vasc Biol* **28:** e2-3.

Bowen, JA, Hunt, JS (2000). The role of integrins in reproduction. *Proc Soc Exp Biol Med* **223:** 331-43.

Bretelle F, Sabatier F, Desprez D, Camoin L, Grunebaum L, Combes V, D'Ercole C, Dignat-George F (2003). Circulating microparticles: a marker of procoagulant state in normal pregnancy and pregnancy complicated by preeclampsia or intrauterine growth restriction. *Thromb Haemost* **89:** 486-492.

Burton GJ, Yung HW, Cindrova-Davies T, Charnock-Jones DS (2009). Placental endoplasmic reticulum stress and oxidative stress in the pathophysiology of unexplained intrauterine growth restriction and early onset preeclampsia. *Placenta* **30 Suppl A:** S43-48.

Cantero M, Conejo JR, Parra T, Jiménez A, Carballo F, de Arriba G (1998). Interference of chylomicrons in analysis of platelets by flow cytometry. *Thrombosis Research* **91:** 49-52.

Carr B, Hole P, Malloy A, Nelson P, Wright M, Smtih J (2009). Applictions of nanoparticle tracking analysis in nanoparticle research: a mini review. *Euro J Parenter Pharm Sci* **14:** 45-50.

Chandler WL, Yeung W, Tait JF (2011). A new microparticle size calibration standard for use in measuring smaller microparticles using a new flow cytometer. *J Thromb Haemost* **9:** 1216-1224.

Chen LM, Liu B, Zhao HB, Stone P, Chen Q, Chamley L (2010a). IL-6, TNFalpha and TGFbeta promote nonapoptotic trophoblast deportation and subsequently causes endothelial cell activation. *Placenta* **31:** 75-80.

Chen Q, Stone P, Ching LM, Chamley L (2009a). A role for interleukin-6 in spreading endothelial cell activation after phagocytosis of necrotic trophoblastic material: implications for the pathogenesis of pre-eclampsia. *J Pathol* **217:** 122-130.

Chen Q, Viall C, Kang Y, Liu B, Stone P, Chamley L (2009b). Anti-phospholipid antibodies increase non-apoptotic trophoblast shedding: a contribution to the pathogenesis of pre-eclampsia in affected women? *Placenta* **30:** 767-773.

Chen Q, Chen L, Liu B, Vialli C, Stone P, Ching LM, Chamley L (2010b). The role of autocrine TGFbeta1 in endothelial cell activation induced by phagocytosis of necrotic trophoblasts: a possible role in the pathogenesis of pre-eclampsia. *J Pathol* **221:** 87-95.

Clauss M, Weich H, Breier G, Knies U, Rockl W, Waltenberger J, Risau W (1996). The vascular endothelial growth factor receptor Flt-1 mediates biological activities. Implications for a functional role of placenta growth factor in monocyte activation and chemotaxis. *J Biol Chem* **271:** 17629-17634.

Cockell AP, Learmont JG, Smarason AK, Redman CW, Sargent IL, Poston L (1997). Human placental syncytiotrophoblast microvillous membranes impair maternal vascular endothelial function. *Br J Obstet Gynaecol* **104:** 235-240.

Cocucci E, Racchetti G, Meldolesi J (2009). Shedding microvesicles: artefacts no more. *Trends in Cell Biology* **19:** 43-51.

Combes V, Simon AC, Grau GE, Arnoux D, Camoin L, Sabatier F, Mutin M, Sanmarco M, Sampol J, Dignat-George F (1999). In vitro generation of endothelial microparticles and possible prothrombotic activity in patients with lupus anticoagulant. *J Clin Invest* **104:** 93-102.

Connor DE, Exner T, Ma DD, Joseph JE (2010). The majority of circulating platelet-derived microparticles fail to bind annexin V, lack phospholipid-dependent procoagulant activity and demonstrate greater expression of glycoprotein Ib. *Thromb Haemost* **103:** 1044-1052.

Contractor SF, Sooranna SR (1986). Monoclonal antibodies to cytotrophoblast and syncytiotrophoblast of human placenta. *J Dev Physiol* **8:** 277-282.

Coukos G, Makrigiannakis A, Amin K, Albelda SM, Coutifaris C (1998). Platelet-endothelial cell adhesion molecule-1 is expressed by a subpopulation of human trophoblasts: a possible mechanism for trophoblast-endothelial interaction during haemochorial placentation. *Mol Hum Reprod* **4:** 357-367.

Denicola A, Souza JM, Radi R (1998). Diffusion of peroxynitrite across erythrocyte membranes. *Proc Natl Acad Sci U S A* **95:** 3566-3571.

Denzer K, Kleijmeer MJ, Heijnen HF, Stoorvogel W, Geuze HJ (2000). Exosome: from internal vesicle of the multivesicular body to intercellular signaling device. *J Cell Sci* **113 Pt 19:** 3365-3374.

Distler JH, Jungel A, Huber LC, Seemayer CA, Reich CF, 3rd, Gay RE, Michel BA, Fontana A, Gay S, Pisetsky DS, Distler O (2005). The induction of matrix metalloproteinase and cytokine expression in synovial fibroblasts stimulated with immune cell microparticles. *Proc Natl Acad Sci U S A* **102:** 2892-2897.

Distler JH, Distler O (2010). Inflammation: Microparticles and their roles in inflammatory arthritides. *Nat Rev Rheumatol* **6:** 385-386.

Dordevic NZ, Babic GM, Markovic SD, Ognjanovic BI, Stajn AS, Zikic RV, Saicic ZS (2008). Oxidative stress and changes in antioxidative defense system in erythrocytes of preeclampsia in women. *Reprod Toxicol* **25:** 213-218.

Dragovic RA, Gardiner C, Brooks AS, Tannetta DS, Ferguson DJ, Hole P, Carr B, Redman CW, Harris AL, Dobson PJ, Harrison P, Sargent IL (2011). Sizing and phenotyping of cellular vesicles using Nanoparticle Tracking Analysis. *Nanomedicine* **7:** 780-788.

Duckitt K, Harrington D (2005). Risk factors for pre-eclampsia at antenatal booking: systematic review of controlled studies. *BMJ* **330:** 565.

Duval A, Helley D, Capron L, Youinou P, Renaudineau Y, Dubucquoi S, Fischer AM, Hachulla E (2010). Endothelial dysfunction in systemic lupus patients with low disease activity: evaluation by quantification and characterization of circulating endothelial microparticles, role of anti-endothelial cell antibodies. *Rheumatology (Oxford)* **49:** 1049-1055.

Eastabrook G, Brown M, Sargent I (2011). The origins and end-organ consequence of pre-eclampsia. *Best Pract Res Clin Obstet Gynaecol* **25:** 435-447.

Eken C, Gasser O, Zenhaeusern G, Oehri I, Hess C, Schifferli JA (2008). Polymorphonuclear neutrophil-derived ectosomes interfere with the maturation of monocyte-derived dendritic cells. *J Immunol* **180:** 817-824.

Enjeti AK, Lincz LF, Seldon M (2007). Detection and measurement of microparticles: an evolving research tool for vascular biology. *Semin Thromb Hemost* **33:** 771-779.

Enjeti AK, Lincz L, Seldon M (2008a). Bio-maleimide as a generic stain for detection and quantitation of microparticles. *Int J Lab Hematol* **30:** 196-199.

Enjeti AK, Lincz LF, Seldon M (2008b). Microparticles in health and disease. *Semin Thromb Hemost* **34:** 683-691.

Faure V, Dou L, Sabatier F, Cerini C, Sampol J, Berland Y, Brunet P, Dignat-George F (2006). Elevation of circulating endothelial microparticles in patients with chronic renal failure. *J Thromb Haemost* **4:** 566-573.

Filipe V, Hawe A, Jiskoot W (2010). Critical evaluation of Nanoparticle Tracking Analysis (NTA) by NanoSight for the measurement of nanoparticles and protein aggregates. *Pharmaceutical Research* **27:** 796-810.

Foladori P, Quaranta A, Ziglio G (2008). Use of silica microspheres having refractive index similar to bacteria for conversion of flow cytometric forward light scatter into biovolume. *Water Res* **42:** 3757-3766.

Frayn KN (2010). Metabolic Regulation: A Human Perspective, 3rd edn. Blackwell Publishing. pp 275-281.

Gasser O, Hess C, Miot S, Deon C, Sanchez JC, Schifferli JA (2003). Characterisation and properties of ectosomes released by human polymorphonuclear neutrophils. *Exp Cell Res* **285:** 243-257.

Gasser O, Schifferli JA (2004). Activated polymorphonuclear neutrophils disseminate anti-inflammatory microparticles by ectocytosis. *Blood* **104:** 2543-2548.

Gasser O, Schifferli JA (2005). Microparticles released by human neutrophils adhere to erythrocytes in the presence of complement. *Exp Cell Res* **307:** 381-387.

Gelderman MP, Simak J (2008). Flow cytometric analysis of cell membrane microparticles. *Methods Mol Biol* **484:** 79-93.

Germain SJ, Sacks GP, Sooranna SR, Sargent IL, Redman CW (2007). Systemic inflammatory priming in normal pregnancy and preeclampsia: the role of circulating syncytiotrophoblast microparticles. *Journal of immunology* **178:** 5949-5956.

Gladwin MT, Kim-Shapiro DB (2009). Storage lesion in banked blood due to hemolysis-dependent disruption of nitric oxide homeostasis. *Curr Opin Hematol* **16:** 515-523.

Gonzalez-Quintero VH, Jimenez JJ, Jy W, Mauro LM, Hortman L, O'Sullivan MJ, Ahn Y (2003). Elevated plasma endothelial microparticles in preeclampsia. *Am J Obstet Gynecol* **189:** 589-593.

Gonzalez-Quintero VH, Smarkusky LP, Jimenez JJ, Mauro LM, Jy W, Hortsman LL, O'Sullivan MJ, Ahn YS (2004). Elevated plasma endothelial microparticles: preeclampsia versus gestational hypertension. *Am J Obstet Gynecol* **191:** 1418-1424.

Goswami D, Tannetta DS, Magee LA, Fuchisawa A, Redman CW, Sargent IL, von Dadelszen P (2006). Excess syncytiotrophoblast microparticle shedding is a feature of early-onset pre-eclampsia, but not normotensive intrauterine growth restriction. *Placenta* **27:** 56-61.

Gougos, A, St Jacques S, Greaves A, O'Connell PJ, d'Apice AJ, Buhring HJ, Bernabeu C, van Mourik JA, Letarte M (1992). Identification of distinct epitopes of endoglin, an RGD-containing glycoprotein of endothelial cells, leukemic cells, and syncytiotrophoblasts. *Int Immunol* **4:** 83-92

Gratacos E, Casals E, Deulofeu R, Cararach V, Alonso PL, Fortuny A (1998). Lipid peroxide and vitamin E patterns in pregnant women with different types of hypertension in pregnancy. *Am J Obstet Gynecol* **178:** 1072-1076.

Greenwalt TJ, McGuinness CG, Dumaswala UJ (1991). Studies in red blood cell preservation: 4. Plasma vesicle hemoglobin exceeds free hemoglobin. *Vox Sang* **61:** 14-17.

Groten T, Gebhard N, Kreienberg R, Schleussner E, Reister F, Huppertz B (2010). Differential expression of VE-cadherin and VEGFR2 in placental syncytiotrophoblast during preeclampsia - New perspectives to explain the pathophysiology. *Placenta* **31:** 339-343.

Guller S, Tang Z, Ma YY, Di Santo S, Sager R, Schneider H (2011). Protein composition of microparticles shed from human placenta during placental perfusion: Potential role in angiogenesis and fibrinolysis in preeclampsia. *Placenta* **32:** 63-69.

Gupta AK, Rusterholz C, Holzgreve W, Hahn S (2005a). Syncytiotrophoblast micro-particles do not induce apoptosis in peripheral T lymphocytes, but differ in their activity depending on the mode of preparation. *J Reprod Immunol* **68:** 15-26.

Gupta AK, Rusterholz C, Huppertz B, Malek A, Schneider H, Holzgreve W, Hahn S (2005b). A comparative study of the effect of three different syncytiotrophoblast micro-particles preparations on endothelial cells. *Placenta* **26:** 59-66.

Gyorgy B, Szabo TG, Pasztoi M, Pal Z, Misjak P, Aradi B, Laszlo V, Pallinger E, Pap E, Kittel A, Nagy G, Falus A, Buzas EI (2011). Membrane vesicles, current state-of-the-art: emerging role of extracellular vesicles. *Cell Mol Life Sci* **68:** 2667-2688.

Harding SA, Din JN, Sarma J, Jessop A, Weatherall M, Fox KA, Newby DE (2007). Flow cytometric analysis of circulating platelet-monocyte aggregates in whole blood: methodological considerations. *Thromb Haemost* **98:** 451-456.

Harlow FH, Brown MA, Brighton TA, Smith SL, Trickett AE, Kwan YL, Davis GK (2002). Platelet activation in the hypertensive disorders of pregnancy. *Am J Obstet Gynecol* **187:** 688-695.

Harrison P, Gardiner C (2010). How to detect and measure microparticles. *Hematology Education: the education programme for the annual congress of the European Hematology Association* **4:** 33-39.

Heijnen HF, Schiel AE, Fijnheer R, Geuze HJ, Sixma JJ (1999). Activated platelets release two types of membrane vesicles: microvesicles by surface shedding and exosomes derived from exocytosis of multivesicular bodies and alpha-granules. *Blood* **94:** 3791-3799.

Herzenberg LA, Tung J, Moore WA, Parks DR (2006). Interpreting flow cytometry data: a guide for the perplexed. *Nat Immunol* **7:** 681-685.

Hind E, Heugh S, Ansa-Addo EA, Antwi-Baffour S, Lange S, Inal J (2010). Red cell PMVs, plasma membrane-derived vesicles calling out for standards. *Biochem Biophys Res Commun* **399:** 465-469.

Hoen EN, van der Vlist EJ, Aalberts M, Mertens HC, Bosch BJ, Bartelink W, Mastrobattista E, van Gaal EV, Stoorvogel W, Arkesteijn GJ, Wauben MH (2011). Quantitative and qualitative flow cytometric analysis of nanosized cell-derived membrane vesicles. *Nanomedicine***:** EPub Ahead of Print.

Holder BS, Tower CL, Jones, CJ, Aplin JD, Abrahams VM (2012). Heightened pro-inflammatory effect of pre-eclamptic placental microvesicles on peripheral blood immune cells in humans. *Biol Reprod* **86**: 1-7.

Holthe MR, Lyberg T, Staff AC, Berge LN (2005). Leukocyte-platelet interaction in pregnancies complicated with preeclampsia. *Platelets* **16:** 91-97.

Hoo CM, Starostin N, West P, Mecartney ML (2008). A comparison of atomic force microscopy (AFM) and dynamic light scattering (DLS) methods to characterize nanoparticle size distributions. *J Nanopart Res* **10:** 89-96.

Hou J, Fu Y, Zhou J, Li W, Xie R, Cao F, Gilbert GE, Shi J (2011). Lactadherin functions as a probe for phosphatidylserine exposure and as an anticoagulant in the study of stored platelets. *Vox Sang* **100:** 187-195.

Hristov M, Erl W, Linder S, Weber PC (2004). Apoptotic bodies from endothelial cells enhance the number and initiate the differentiation of human endothelial progenitor cells in vitro. *Blood* **104:** 2761-2766.

Hugel B, Socié G, Vu T, Toti F, Gluckman E, Freyssinet JM, Scrobohaci ML (1999). Elevated levels of circulating procoagulant microparticles in patients with paroxysmal nocturnal hemoglobinuria and aplastic anemia. *Blood* **93:** 3451-3456.

Hugel B, Martinez MC, Kunzelmann C, Freyssinet JM (2005). Membrane microparticles: two sides of the coin. *Physiology (Bethesda)* **20:** 22-27.

Hung TH, Burton GJ (2006). Hypoxia and reoxygenation: a possible mechanism for placental oxidative stress in preeclampsia. *Taiwan J Obstet Gynecol* **45:** 189-200.

Huppertz B, Frank HG, Kingdom JC, Reister F, Kaufmann P (1998). Villous cytotrophoblast regulation of the syncytial apoptotic cascade in the human placenta. *Histochem Cell Biol* **110:** 495-508.

Hussein AA, Bozzi B, Correa M, Capson TL, Kursar TA, Coley PD, Solis PN, Gupta MP (2003). Bioactive constituents from three Vismia species. *J Nat Prod* **66:** 858-860.

Jaffe EA, Nachman RL, Becker CG, Minick CR (1973). Culture of human endothelial cells derived from umbilical veins. Identification by morphologic and immunologic criteria. *J Clin Invest* **52:** 2745-2756.

Jensen OA, Prause JU, Laursen H (1981). Shrinkage in preparatory steps for SEM. A study on rabbit corneal endothelium. *Albrecht Von Graefes Arch Klin Exp Ophthalmol* **215:** 233-242.

Jimenez JJ, Jy W, Mauro LM, Horstman LL, Ahn YS (2001). Elevated endothelial microparticles in thrombotic thrombocytopenic purpura: findings from brain and renal microvascular cell culture and patients with active disease. *Br J Haematol* **112:** 81-90.

Jimenez JJ, Jy W, Mauro LM, Soderland C, Horstman LL, Ahn YS (2003). Endothelial cells release phenotypically and quantitatively distinct microparticles in activation and apoptosis. *Thromb Res* **109:** 175-180.

Jones CJ, Fox, H (1980). An ultrastructural and ultrahistochemical study of the human placenta in maternal pre-eclampsia. *Placenta* **1**: 61-76

Jones CJ, Fox, H (1991). Ultrastructure of the normal human placenta. *Electron Microsc Rev* **4**: 129-78

Jungi TW, Spycher MO, Nydegger UE, Barandun S (1986). Platelet-leukocyte interaction: selective binding of thrombin-stimulated platelets to human monocytes, polymorphonuclear leukocytes, and related cell lines. *Blood* **67:** 629-636.

Jy W, Horstman LL, Jimenez JJ, Ahn YS, Biro E, Nieuwland R, Sturk A, Dignat-George F, Sabatier F, Camoin-Jau L, Sampol J, Hugel B, Zobairi F, Freyssinet JM, Nomura S, Shet AS, Key NS, Hebbel RP (2004). Measuring circulating cell-derived microparticles. *J Thromb Haemost* **2:** 1842-1851.

Karumanchi SA, Bdolah Y (2004). Hypoxia and sFlt-1 in preeclampsia: the "chicken-and-egg" question. *Endocrinology* **145:** 4835-4837.

Knight M, Redman CW, Linton EA, Sargent IL (1998). Shedding of syncytiotrophoblast microvilli into the maternal circulation in pre-eclamptic pregnancies. *British Journal of Obstetrics & Gynaecology* **105:** 632-640.

Kornek M, Popov Y, Libermann TA, Afdhal NH, Schuppan D (2011). Human T cell microparticles circulate in blood of hepatitis patients and induce fibrolytic activation of hepatic stellate cells. *Hepatology* **53:** 230-242.

Lacroix R, Robert S, Poncelet P, Dignat-George F (2010a). Overcoming limitations of microparticle measurement by flow cytometry. *Semin Thromb Hemost* **36:** 807-818.

Lacroix R, Robert S, Poncelet P, Kasthuri RS, Key NS, Dignat-George F (2010b). Standardization of platelet-derived microparticle enumeration by flow cytometry with calibrated beads: results of the International Society on Thrombosis and Haemostasis SSC Collaborative workshop. *J Thromb Haemost* **8:** 2571-2574.

Lawrie AS, Albanyan A, Cardigan RA, Mackie IJ, Harrison P (2009). Microparticle sizing by dynamic light scattering in fresh-frozen plasma. *Vox Sanguinis* **96:** 206-212.

Lee JS, Gladwin MT (2010). Bad blood: the risks of red cell storage. *Nat Med* **16:** 381-382.

Lee RD, Barcel DA, Williams JC, Wang JG, Boles JC, Manly DA, Key NS, Mackman N (2012). Pre-analytical and analytical variables affecting the measurement of plasma-derived microparticle tissue factor activity. *Thromb Res* **129:** 80-85.

Levine RJ, Maynard SE, Qian C, Lim KH, England LJ, Yu KF, Schisterman EF, Thadhani R, Sachs BP, Epstein FH, Sibai BM, Sukhatme VP, Karumanchi SA (2004). Circulating angiogenic factors and the risk of preeclampsia. *N Engl J Med* **350:** 672-683.

Levine RJ, Lam C, Qian C, Yu KF, Maynard SE, Sachs BP, Sibai BM, Epstein FH, Romero R, Thadhani R, Karumanchi SA (2006). Soluble endoglin and other circulating antiangiogenic factors in preeclampsia. *N Engl J Med* **355:** 992-1005.

Lok CA, Nieuwland R, Sturk A, Hau CM, Boer K, Vanbavel E, Vanderpost JA (2007). Microparticle-associated P-selectin reflects platelet activation in preeclampsia. *Platelets* **18:** 68-72.

Lok CA, Boing AN, Sargent IL, Sooranna SR, van der Post JA, Nieuwland R, Sturk A (2008a). Circulating platelet-derived and placenta-derived microparticles expose Flt-1 in preeclampsia. *Reprod Sci* **15:** 1002-1010.

Lok CA, Van Der Post JA, Sargent IL, Hau CM, Sturk A, Boer K, Nieuwland R (2008b). Changes in microparticle numbers and cellular origin during pregnancy and preeclampsia. *Hypertension in Pregnancy* **27:** 344-360.

Lok CA, Jebbink J, Nieuwland R, Faas MM, Boer K, Sturk A, Van Der Post JA (2009). Leukocyte activation and circulating leukocyte-derived microparticles in preeclampsia. *Am J Reprod Immunol* **61:** 346-359.

Losche W, Scholz T, Temmler U, Oberle V, Claus RA (2004). Platelet-derived microvesicles transfer tissue factor to monocytes but not to neutrophils. *Platelets* **15:** 109-115.

Lynch RE, Fridovich I (1978). Permeation of the erythrocyte stroma by superoxide radical. *J Biol Chem* **253:** 4697-4699.

Macey MG, Bevan S, Alam S, Verghese L, Agrawal S, Beski S, Thuraisingham R, MacCallum PK (2010). Platelet activation and endogenous thrombin potential in pre-eclampsia. *Thromb Res* **125:** 76-81.

Maecker H, Trotter J (2011). BD Biosciences Application Note: Selecting Reagents for Multicolor Flow Cytometry**:** 1-8.

Mahnke YD, Roederer M (2007). Optimizing a multicolor immunophenotyping assay. *Clin Lab Med* **27:** 469-485.

Mallat Z, Benamer H, Hugel B, Benessiano J, Steg PG, Freyssinet JM, Tedgui A (2000). Elevated levels of shed membrane microparticles with procoagulant potential in the peripheral circulating blood of patients with acute coronary syndromes. *Circulation* **101:** 841-843.

Martin S, Tesse A, Hugel B, Martinez MC, Morel O, Freyssinet JM, Andriantsitohaina R (2004). Shed membrane particles from T lymphocytes impair endothelial function and regulate endothelial protein expression. *Circulation* **109:** 1653-1659.

Maynard SE, Min JY, Merchan J, Lim KH, Li J, Mondal S, Libermann TA, Morgan JP, Sellke FW, Stillman IE, Epstein FH, Sukhatme VP, Karumanchi SA (2003). Excess placental soluble fms-like tyrosine kinase 1 (sFlt1) may contribute to endothelial dysfunction, hypertension, and proteinuria in preeclampsia. *J Clin Invest* **111:** 649-658.

Messerli M, May K, Hansson SR, Schneider H, Holzgreve W, Hahn S, Rusterholz C (2010). Feto-maternal interactions in pregnancies: placental microparticles activate peripheral blood monocytes. *Placenta* **31:** 106-112.

Meziani F, Tesse A, David E, Martinez MC, Wangesteen R, Schneider F, Andriantsitohaina R (2006). Shed membrane particles from preeclamptic women generate vascular wall inflammation and blunt vascular contractility. *Am J Pathol* **169:** 1473-1483.

Mise H, Sagawa N, Matsumoto T, Yura S, Nanno H, Itoh H, Mori T, Masuzaki H, Hosoda K, Ogawa Y, Nakao K (1998). Augmented placental production of leptin in preeclampsia: possible involvement of placental hypoxia. *J Clin Endocrinol Metab* **83:** 3225-3229.

Mobarrez F, Antovic J, Egberg N, Hansson M, Jorneskog G, Hultenby K, Wallen H (2010). A multicolor flow cytometric assay for measurement of platelet-derived microparticles. *Thromb Res* **125:** 110-116.

Moffett-King A (2002). Natural killer cells and pregnancy. *Nat Rev Immunol* **2**: 656-663.

Morelli AE (2006). The immune regulatory effect of apoptotic cells and exosomes on dendritic cells: its impact on transplantation. *Am J Transplant* **6:** 254-261.

Morris JM, Gopaul NK, Endresen MJ, Knight M, Linton EA, Dhir S, Anggard EE, Redman CW (1998). Circulating markers of oxidative stress are raised in normal pregnancy and pre-eclampsia. *Br J Obstet Gynaecol* **105:** 1195-1199.

Mostefai HA, Andriantsitohaina R, Martinez MC (2008). Plasma membrane microparticles in angiogenesis: role in ischemic diseases and in cancer. *Physiol Res* **57:** 311-320.

Muttukrishna S, Knight PG, Groome NP, Redman CW, Ledger WL (1997). Activin A and inhibin A as possible endocrine markers for pre-eclampsia. *Lancet* **349:** 1285-1288.

Nantakomol D, Palasuwan A, Soogarun S (2011). Atomic force microscope imaging of red cell vesiculation. *Eur J Haematol* **86:** 276.

Nevo O, Soleymanlou N, Wu Y, Xu J, Kingdom J, Many A, Zamudio S, Caniggia I (2006). Increased expression of sFlt-1 in in vivo and in vitro models of human placental hypoxia is mediated by HIF-1. *Am J Physiol Regul Integr Comp Physiol* **291:** 1085-1093.

Olsson MG, Centlow M, Rutardottir S, Stenfors I, Larsson J, Hosseini-Maaf B, Olsson ML, Hansson SR, Akerstrom B (2010). Increased levels of cell-free hemoglobin, oxidation markers, and the antioxidative heme scavenger alpha(1)-microglobulin in preeclampsia. *Free Radic Biol Med* **48:** 284-291.

Orozco AF, Jorgez CJ, Ramos-Perez WD, Popek EJ, Yu X, Kozinetz CA, Bischoff FZ, Lewis DE (2009). Placental release of distinct DNA-associated micro-particles into maternal circulation: reflective of gestation time and preeclampsia. *Placenta* **30:** 891-897.

Perez-Pujol S, Marker PH, Key NS (2007). Platelet microparticles are heterogeneous and highly dependent on the activation mechanism: studies using a new digital flow cytometer. *Cytometry A* **71:** 38-45.

Perkins AV, Linton EA, Eben F, Simpson J, Wolfe CD, Redman CW (1995). Corticotrophin-releasing hormone and corticotrophin-releasing hormone binding protein in normal and pre-eclamptic human pregnancies. *Br J Obstet Gynaecol* **102:** 118-122.

Pijnenborg R, Bland JM, Robertson WB, Brosens, I (1983). Uteroplacental arterial changes related to interstitial trophoblast migration in early human pregnancy. *Placenta* **4**: 397-413.

Pisetsky DS, Gauley J, Ullal AJ (2011). Microparticles as a source of extracellular DNA. *Immunol Res* **49:** 227-234.

Pletz MW, Ioanas M, de Roux A, Burkhardt O, Lode H (2004). Reduced spontaneous apoptosis in peripheral blood neutrophils during exacerbation of COPD. *Eur Respir J* **23:** 532-537.

Raimondo F, Morosi L, Chinello C, Magni F, Pitto M (2011). Advances in membranous vesicle and exosome proteomics improving biological understanding and biomarker discovery. *Proteomics* **11:** 709-720.

Raposo G, Nijman HW, Stoorvogel W, Liejendekker R, Harding CV, Melief CJ, Geuze HJ (1996). B lymphocytes secrete antigen-presenting vesicles. *J Exp Med* **183:** 1161-1172.

Ratajczak J, Wysoczynski M, Hayek F, Janowska-Wieczorek A, Ratajczak MZ (2006). Membrane-derived microvesicles: important and underappreciated mediators of cell-to-cell communication. *Leukemia* **20:** 1487-1495.

Raymond D, Peterson E (2011). A critical review of early-onset and late-onset preeclampsia. *Obstet Gynecol Surv* **66:** 497-506.

Rebelo I, Carvalho-Guerra F, Pereira-Leite L, Quintanilha A (1995). Lactoferrin as a sensitive blood marker of neutrophil activation in normal pregnancies. *Eur J Obstet Gynecol Reprod Biol* **62:** 189-194.

Reddy A, Zhong XY, Rusterholz C, Hahn S, Holzgreve W, Redman CW, Sargent IL (2008). The effect of labour and placental separation on the shedding of syncytiotrophoblast microparticles, cell-free DNA and mRNA in normal pregnancy and pre-eclampsia. *Placenta* **29:** 942-949.

Redman CW (1991). Immunology of preeclampsia. *Semin Perinatol* **15:** 257-262.

Redman CW, Sacks GP, Sargent IL (1999). Preeclampsia: an excessive maternal inflammatory response to pregnancy. *Am J Obstet Gynecol* **180:** 499-506.

Redman CW, Sargent IL (2003). Pre-eclampsia, the placenta and the maternal systemic inflammatory response--a review. *Placenta* **24 Suppl A:** S21-27.

Redman CW, Sargent IL (2005). Latest advances in understanding preeclampsia. *Science* **308:** 1592-1594.

Redman CW, Sargent IL (2009). Placental stress and pre-eclampsia: a revised view. *Placenta* **30 Suppl A:** S38-42.

Redman CW, Tannetta DS, Dragovic RA, Gardiner C, Southcombe JH, Collett GP, Sargent IL (2012). Review: Does size matter? Placental debris and the pathophysiology of pre-eclampsia. *Placenta* **33 Suppl A:** S48-54**.**

Reich CF, 3rd, Pisetsky DS (2009). The content of DNA and RNA in microparticles released by Jurkat and HL-60 cells undergoing in vitro apoptosis. *Exp Cell Res* **315:** 760-768.

Ricci D, Braga PC (2004). How the atomic force microscope works. *Methods Mol Biol* **242:** 3-12.

Rinder HM, Bonan JL, Rinder CS, Ault KA, Smith BR (1991). Activated and unactivated platelet adhesion to monocytes and neutrophils. *Blood* **78:** 1760-1769.

Robert S, Poncelet P, Lacroix R, Arnaud L, Giraudo L, Hauchard A, Sampol J, Dignat-George F (2009). Standardization of platelet-derived microparticle counting using calibrated beads and a Cytomics FC500 routine flow cytometer: a first step towards multicenter studies? *J Thromb Haemost* **7:** 190-197.

Roberts JM, Taylor RN, Musci TJ, Rodgers GM, Hubel CA, McLaughlin MK (1989). Preeclampsia: an endothelial cell disorder. *Am J Obstet Gynecol* **161:** 1200-1204.

Ruf H, Gould BJ (1999). Size distributions of chylomicrons from human lymph from dynamic light scattering measurements. *Eur Biophys J* **28:** 1-11.

Sabatier F, Roux V, Anfosso F, Camoin L, Sampol J, Dignat-George F (2002). Interaction of endothelial microparticles with monocytic cells in vitro induces tissue factor-dependent procoagulant activity. *Blood* **99:** 3962-3970.

Sacks GP, Studena K, Sargent K, Redman CW (1998). Normal pregnancy and preeclampsia both produce inflammatory changes in peripheral blood leukocytes akin to those of sepsis. *Am J Obstet Gynecol* **179:** 80-86.

Salzer U, Hinterdorfer P, Hunger U, Borken C, Prohaska R (2002). Ca(++)-dependent vesicle release from erythrocytes involves stomatin-specific lipid rafts, synexin (annexin VII), and sorcin. *Blood* **99:** 2569-2577.

Sandrim VC, Montenegro MF, Palei AC, Metzger IF, Sertorio JT, Cavalli RC, Tanus-Santos JE (2010). Increased circulating cell-free hemoglobin levels reduce nitric oxide bioavailability in preeclampsia. *Free Radic Biol Med* **49:** 493-500.

Sawano A, Iwai S, Sakurai Y, Ito M, Shitara K, Nakahata T, Shibuya M (2001). Flt-1, vascular endothelial growth factor receptor 1, is a novel cell surface marker for the lineage of monocyte-macrophages in humans. *Blood* **97:** 785-791.

Scanu A, Molnarfi N, Brandt KJ, Gruaz L, Dayer JM, Burger D (2008). Stimulated T cells generate microparticles, which mimic cellular contact activation of human monocytes: differential regulation of pro- and anti-inflammatory cytokine production by high-density lipoproteins. *J Leukoc Biol* **83:** 921-927.

Shet AS, Aras O, Gupta K, Hass MJ, Rausch DJ, Saba N, Koopmeiners L, Key NS, Hebbel RP (2003). Sickle blood contains tissue factor-positive microparticles derived from endothelial cells and monocytes. *Blood* **102:** 2678-2683.

Shi J, Heegaard CW, Rasmussen JT, Gilbert GE (2004). Lactadherin binds selectively to membranes containing phosphatidyl-L-serine and increased curvature. *Biochim Biophys Acta* **1667:** 82-90.

Shorter SC, Starkey PM, Ferry BL, Clover LM, Sargent IL, Redman CW (1993). Antigenic heterogeneity of human cytotrophoblast and evidence for the transient expression of MHC class I antigens distinct from HLA-G. *Placenta* **14:** 571-582.

Siedlecki CA, Wang IW, Higashi JM, Kottke-Marchant K, Marchant RE (1999). Platelet-derived microparticles on synthetic surfaces observed by atomic force microscopy and fluorescence microscopy. *Biomaterials* **20:** 1521-1529.

Simak J, Holada K, Vostal JG (2002). Release of annexin V-binding membrane microparticles from cultured human umbilical vein endothelial cells after treatment with camptothecin. *BMC Cell Biol* **3:** 11.

Simak J, Gelderman MP (2006). Cell membrane microparticles in blood and blood products: potentially pathogenic agents and diagnostic markers. *Transfusion Medicine Reviews* **20:** 1-26.

Smalheiser NR (2007). Exosomal transfer of proteins and RNAs at synapses in the nervous system. *Biol Direct* **2:** 35.

Smarason AK, Sargent IL, Starkey PM, Redman CW (1993). The effect of placental syncytiotrophoblast microvillous membranes from normal and pre-eclamptic women on the growth of endothelial cells in vitro. *Br J Obstet Gynaecol* **100:** 943-949.

Southcombe J, Tannetta D, Redman C, Sargent I (2011). The immunomodulatory role of syncytiotrophoblast microvesicles. *PLoS One* **6:** e20245.

Sunderland CA, Redman CW, Stirrat GM (1981). Monoclonal antibodies to human syncytiotrophoblast. *Immunology* **43:** 541-546.

Thadhani R, Mutter WP, Wolf M, Levine RJ, Taylor RN, Sukhatme VP, Ecker J, Karumanchi SA (2004). First trimester placental growth factor and soluble fms-like tyrosine kinase 1 and risk for preeclampsia. *J Clin Endocrinol Metab* **89:** 770-775.

The Human Protein Atlas. Available at: http://www.proteinatlas.org/ (Accessed throughout 2011).

Thery C, Zitvogel L, Amigorena S (2002). Exosomes: composition, biogenesis and function. *Nat Rev Immunol* **2:** 569-579.

Théry C, Amigorena S, Raposo G, Clayton A (2006). Isolation and characterization of exosomes from cell culture supernatants and biological fluids. *Current Protocols in Cell Biology* **Chapter 3:** Unit 3 22.

Théry C, Ostrowski M, Segura E (2009). Membrane vesicles as conveyors of immune responses. *Nature Reviews Immunology* **9:** 581-593.

Torry DS, Wang HS, Wang TH, Caudle MR, Torry RJ (1998). Preeclampsia is associated with reduced serum levels of placenta growth factor. *Am J Obstet Gynecol* **179:** 1539-1544.

Trummer A, De Rop C, Tiede A, Ganser A, Eisert R (2008). Isotype controls in phenotyping and quantification of microparticles: a major source of error and how to evade it. *Thromb Res* **122:** 691-700.

Trummer A, De Rop C, Tiede A, Ganser A, Eisert R (2009). Recovery and composition of microparticles after snap-freezing depends on thawing temperature. *Blood Coagul Fibrinolysis* **20:** 52-56.

Tsukimori K, Fukushima K, Tsushima A, Nakano H (2005). Generation of reactive oxygen species by neutrophils and endothelial cell injury in normal and preeclamptic pregnancies. *Hypertension* **46:** 696-700.

Ullal AJ, Pisetsky DS, Reich CF, 3rd (2010). Use of SYTO 13, a fluorescent dye binding nucleic acids, for the detection of microparticles in in vitro systems. *Cytometry Part A: The Journal of the International Society for Analytical Cytology* **77:** 294-301.

Valadi H, Ekstrom K, Bossios A, Sjostrand M, Lee JJ, Lotvall JO (2007). Exosome-mediated transfer of mRNAs and microRNAs is a novel mechanism of genetic exchange between cells. *Nat Cell Biol* **9:** 654-659.

van der Pol E, Hoekstra AG, Sturk A, Otto C, van Leeuwen TG, Nieuwland R (2010). Optical and non-optical methods for detection and characterization of microparticles and exosomes. *J Thromb Haemost* **8:** 2596-2607.

van Ierssel SH, Van Craenenbroeck EM, Conraads VM, Van Tendeloo VF, Vrints CJ, Jorens PG, Hoymans VY (2010). Flow cytometric detection of endothelial microparticles (EMP): effects of centrifugation and storage alter with the phenotype studied. *Thromb Res* **125:** 332-339.

VanWijk MJ, Nieuwland R, Boer K, van der Post JA, VanBavel E, Sturk A (2002). Microparticle subpopulations are increased in preeclampsia: possible involvement in vascular dysfunction? *Am J Obstet Gynecol* **187:** 450-456.

VanWijk MJ, VanBavel E, Sturk A, Nieuwland R (2003). Microparticles in cardiovascular diseases. *Cardiovasc Res* **59:** 277-287.

Vatten LJ, Skjaerven R (2004). Is pre-eclampsia more than one disease? *BJOG* **111:** 298-302.

Venkatesha S, Toporsian M, Lam C, Hanai J, Mammoto T, Kim YM, Bdolah Y, Lim KH, Yuan HT, Libermann TA, Stillman IE, Roberts D, D'Amore PA, Epstein FH, Sellke FW,

Romero R, Sukhatme VP, Letarte M, Karumanchi SA (2006). Soluble endoglin contributes to the pathogenesis of preeclampsia. *Nat Med* **12:** 642-649.

von Dadelszen P, Hurst G, Redman CW (1999). Supernatants from co-cultured endothelial cells and syncytiotrophoblast microvillous membranes activate peripheral blood leukocytes in vitro. *Hum Reprod* **14:** 919-924.

von Dadelszen P, Magee LA, Roberts JM (2003). Subclassification of preeclampsia. *Hypertens Pregnancy* **22:** 143-148.

Waltenberger J, Lange J, Kranz A (2000). Vascular endothelial growth factor-A-induced chemotaxis of monocytes is attenuated in patients with diabetes mellitus: A potential predictor for the individual capacity to develop collaterals. *Circulation* **102:** 185-190.

Wang ZL (2011). Picoscale science and nanoscale engineering by electron microscopy. *J Electron Microsc (Tokyo)* **60 Suppl 1:** S269-278.

Yuana Y, Oosterkamp TH, Bahatyrova S, Ashcroft B, Garcia Rodriguez P, Bertina RM, Osanto S (2010). Atomic force microscopy: a novel approach to the detection of nanosized blood microparticles. *J Thromb Haemost* **8:** 315-323.

Yuana Y, Bertina RM, Osanto S (2011). Pre-analytical and analytical issues in the analysis of blood microparticles. *Thromb Haemost* **105:** 396-408.

Zitvogel L, Regnault A, Lozier A, Wolfers J, Flament C, Tenza D, Ricciardi-Castagnoli P, Raposo G, Amigorena S (1998). Eradication of established murine tumors using a novel cell-free vaccine: dendritic cell-derived exosomes. *Nat Med* **4:** 594-600.